Modeling of Groundwater Flow System in Wadi Al-Miyah, Eastern Saudi Arabia

by

Ayaz Hasan

A Thesis Presented to the

FACULTY OF THE COLLEGE OF GRADUATE STUDIES

KING FAHD UNIVERSITY OF PETROLEUM & MINERALS

DHAHRAN, SAUDI ARABIA

In Partial Fulfillment of the
Requirements for the Degree of

MASTER OF SCIENCE

In

GEOLOGY

June, 1995

Modeling of Groundwater Flow System in Wadi Al-Miyah Area, Eastern Saudi Arabia

BY

Ayaz Hasan

A Thesis Presented to the

FACULTY OF THE COLLEGE OF GRADUATE STUDIES

KING FAHD UNIVERSITY OF PETROLEUM & MINERALS

DHAHRAN, SAUDI ARABIA

In Partial Fulfillment of the
Requirements for the Degree of

MASTER OF SCIENCE

In

GEOLOGY

June, 1995

KING FAHD UNIVERSITY OF PETROLEUM AND MINERALS
DHAHRAN, SAUDI ARABIA
COLLEGE OF GRADUATE STUDIES

This thesis, written by

AYAZ HASAN

under the direction of his Thesis Advisor, and approved by his Thesis committee, has been presented to and accepted by the Dean, College of Graduate Studies, in partial fulfillment of the requirements for the degree of

MASTER OF SCIENCE IN GEOLOGY

Thesis Committee :

Dr. Abdel-Latif A. Qahwash (Chairman)

Dr. Rashid Al-Layla (Co-Chairman)

Dr. Tahir Hussain (Member)

Dr. Khattab Al-Hinai (Member)

Department Chairman

Dean, College of Graduate Studies

Date: 1-5-1995

Dedicated to

My beloved late father,

loving mother

and

rest of my family members

Acknowledgments

Praise be to the Lord of the World, the Almighty for having guided me at every stage of my life. I am happy to have had a chance to glorify His name in the sincerest way through this small accomplishment and ask Him to accept my efforts. May He guide us and the whole humanity to the right path *(Aameen)*. Thanks are also to our Prophet Mohammad (pbuh) who encouraged us as Muslims to seek knowledge and stressed that science and Islam are never separable.

My deep appreciation goes to my major thesis advisor Dr. Abdul Latif Qahwash for his constant help, guidance and attention. I extent my thanks to my co-advisor Dr. Rashid Al-layla for his priceless suggestions and comments which made this work interesting and learning for me. I would also like to thank for the cooperation, advice and constructive criticism from my committee members, Dr. Tahir Hussain and Dr. Khattab Al-Hinai.

My thanks to the department chairman Dr. Zaki Al-Harari for providing me every help and facility to carry out this research. Special thanks are due to Mr. Ahmad Al-Sheikh from Computer Graphic Center for computer drafting and plotting the geological map. He devoted more than hundreds of hours during this work.

Acknowledgement is due to King Fahd University of Petroleum and Minerals for providing support to this work.

Gratitudes are due to Mr. Nassir Khondakar for his help and guidance and the countless hours of attention he devoted throughout the course of this work. Special thanks are due to Mr. Rasheeduddin for his valuable suggestions and comments in improving the manuscripts of this thesis.

Special thanks are due to Mr. Abdul Razzak Jawad from Ministry of Agriculture and Water, Riyadh, for his help in collecting data from various technical reports. Thanks to Dr. Abdul Qadir Al-Sari from Remote Sensing Center, KACST, Riyadh, for giving LANDSAT-TM and SPOT data and Mr. Asif and Mr. Muqtadir at the Remote Sensing Center, Research Institute, King Fahd University of Petroleum and Minerals, Dhahran for processing of the satellite data and plotting of the geological map of the study area. Thanks are to Mr. Mohammad, Hassan and Asadullah Khan for their help in doing the field survey for electrical resistivity and geological mapping. Thanks to Mr. Ghulam, Mr. Shahul Hamid, and Mr. Aziz from the Earth Science Department for their help and support.

I wish to thank my friends and colleages at KFUPM for their moral support and understanding. Special thanks and appreciations are due to Mohammad Maroof, Naveed Ahmad, Ikram ul Haq Siddique, Jawad Nizami, Zaka Ahmad, Ummar Isa Magaji, Amir Hashmi who helped me in different ways in completion of this work. I should never forget the support of all graduate students in KFUPM who made my

stay at KFUPM a pleasant and memorable one.

I pay my deep gratitude and respect to my mother and other family members for their love, doowas, support and encouragement throughout my studies. Special thanks to my younger sister who suffered a lot because of my absence at home. May Allah bless them and may they live long for me.

Contents

List of Figures

List of Tables

Abstract

Name: Ayaz Hasan

Title: Modeling of Groundwater Flow System in Wadi Al-Miyah Area, Eastern Saudi Arabia

Major Field: Geology

Date of Degree: June, 1995

A detailed geological map of scale 1:150,000 of Wadi Al-Miyah area was constructed on the basis of LANDSAT-TM images. An electrical resistivity model was constructed to determine the thickness of the various hydrogeologic units. Correlation of the resistivity model with the stratigraphic units displayed a probable boundary of a collapsing structure in the Rus formation. Vertical leakage zones were identified based on estimated leakage rates among different aquifers. The high vertical leakage at certain locations confirmed the interconnection and the lithologic control on the groundwater flow and solute distribution. An areal finite element model for fluid-density-dependent groundwater flow and solute transport was used to simulate the existing and future groundwater and solute distribution patterns in the Neogene, Alat and Khobar aquifers. The constructed model was calibrated in steady state and transient conditions. The calibrated model was used to predict the future trends of groundwater flow and chloride concentration for the period of 1994 - 2010 (16 years). Results have shown that chloride concentration along the Gulf coast was very high in the aquifers. Water quality in the eastern part of the study area was found to be good and at some places the concentration was less than 500 ppm in khobar aquifer. Khobar and Alat aquifers were affected by the high rate of pumping. If the present increasing trend is continued, the water level would decline significantly. If the present conditions of pumping is kept constant, a little change would take place during the next 16 years period.

Master of Science Degree

King Fahd University of Petroleum and Minerals

Dhahran, Saudi Arabia

June, 1995

الخلاصة

الإسم : أياز حسن

العنوان : نمذجة أنظمة إنتقال المياه الجوفية في منطقة وادي المياه,
المنطقة الشرقية-المملكة العربية السعودية

التخصص : علوم الأرض

تاريخ الشهادة: يونيو، ١٩٩٥م

لقد تم رسم خريطة جيولوجية لمنطقة وادي المياه بمقياس ١ الى ١٥٠٠٠٠, وذلك بالإعتماد على الصور المأخوذة بواسطة نظام "LANDSAT-TM", وقد تم أيضا" بناء نموذج للمقاومة الكهربية لتحديد سمك مختلف الوحدات الهيدروجيولوجية, وقد أظهرت المقارنة بين نموذج المقاومة و الوحدات الطبقية الأرضية إحتمال وجود حد فاصل في هيكل متكون ألرس المتداعي, أيضا" تم التعرف على مناطق التسرب العمودي وذلك بالإعتماد على نسب التسرب التقديرية لخزانات مختلفة, هذا التسرب العالي في بعض المواقع أكد وجود الترابط الداخلي و السيطرة لنوعية الصخور على انتقل المياه الجوفية و على توزيع المذاب. لقد تم إستخدام نموذج العنصر المحدود المساحي لحركة المياه الجوفية المعتمدة على كثافة السوائل و إنتقال المذاب, لمحاكاة أشكال توزيع المياه الجوفية و المذاب, الحالي منها و المستقبلي في خزانات العلات و الخبر و النيوجين. أخذ بالاعتبار في تصميم النموذج كلا الحالتين, حالة الإستقرار و حالة الإنتقال و أستخدم هذا النموذج للتنبؤ بحركة المياه الجوفية و تركيز الكلورايد للمدة بين عامي ١٩٩٤م و ٢٠١٠م (١٦ عام). أظهرت النتائج أن تركيز الكلورايد في الخزانات الممتده على ساحل الخليج كانت عالية جدا", وقد وجد أن نوعية المياه كانت جيدة في الجزء الغربي من منطقة الدراسة وأنه في بعض الأماكن من خزان الخبر كان التركيز أقل من ٥٠٠ جزء في المليون وقد أظهر إنتاجية أكبر بالمقارنة.
تأثرت خزانات العلات و النيوجين بنسبة الضخ المرتفعة في مناطق النفاذية المنخفضة, وسوف ينخفض مستوى المياه بشكل كبير إذا تم الإستمرار على هذا المنوال, أما إذا ثبتت نسبة الضخ على المعدل الحالي فإن تغييرا" طفيفا" سيطرأ في فترة الستة عشر عام القادمة.

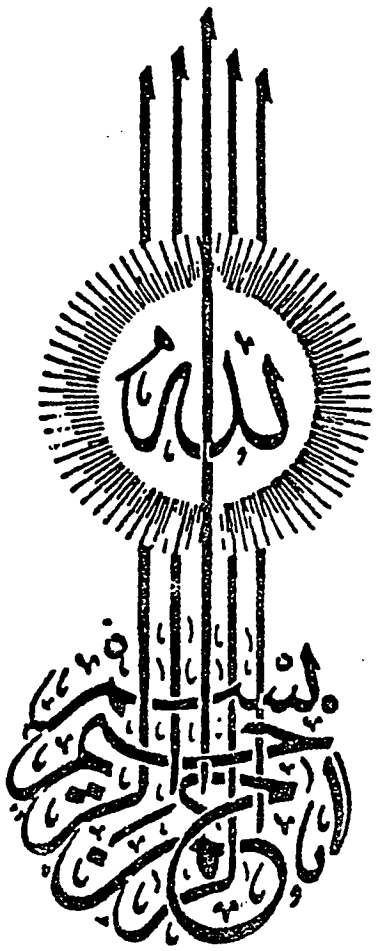
الله
بسم الله الرحمن الرحيم

Chapter 1

Introduction

Water resources are scarce in an arid country like Saudi Arabia. Therefore, all the existing aquifers should be quantitatively assessed and developed to the optimum. The irrigation, municipal and industrial requirements have increased many folds in the Eastern Province which demand a careful evaluation and management of depleting groundwater resources. A large number of wells, tapping water from the Neogene, Alat, Khobar, and Umm Er Radhuma aquifers for many years, have greatly affected the groundwater balance of the region.

Depletion due to over-pumping has occurred and a marked drop in water level is also noted especially in the extraction zones. As a result, the once flowing wells are no longer flowing and many springs (ayns) have been abandoned. Deterioration of water quality and changes of flow patterns are also observed in many places. especially towards the northeast near the coast, where piezometric levels are dropped

appreciably between 1966 and 1994.

The high concentration of chlorides in a number of wells near Abu Hadriya and Manifa area, indicates a possible saltwater intrusion either from the Gulf or from the deep formations. This has been proved by hydrogeochemical studies of Alat and Khobar aquifers by Hassan [1], which indicated a seawater dilution trend in the hydrodynamic equilibrium of the aquifers.

The agricultural developments in recent past, particularly in the 80's, greatly affected the groundwater balance of the area, including areas near As-Sarrar and Mulayjah.

This study is undertaken primarily in order to understand, analyze and predict the physical behavior of the aquifer system through modeling techniques. The simulation of groundwater is helpful in solving complex problems such as depletion of aquifers, rise of shallow water table and deterioration of groundwater quality. The geological control on aquifer geometry and hydrogeological setup also influence the groundwater flow and the salinity distribution patterns.

1.1 Study Area

The study area is located approximately 150 km NW of Dammam city at lattitude 26° 20′−27° 45′N and longitude 48° 00′-49° 20′E, Figure, 1.1. It measures 96 km from west to east and 135 km from south to north, incorporating an area of approximately 10,380 square kilometers. It comprises the Wadi Al-Miyah, along with Hanidh in the southeast and Abu Hadriya and Manifa in the northeast. The arid climate prevails throughout the year with infrequent rainfall. The mean temperature ranges from 41°C to 44°C in summer months (July and August) and from 7°C to 13°C in winter months (December, January and February). The rainy season is December to May. Measurements for the last 20 years indicate an average of less than 150 m.m per annum, Evans, [2]. Mean monthly and annual relative humidity values vary from place to place and from year to year. In coastal areas, relative humidity ranges from 65 to 75% during winter (December through February) as compared to 37 to 63 % during summer (June through August) Evans, [2].

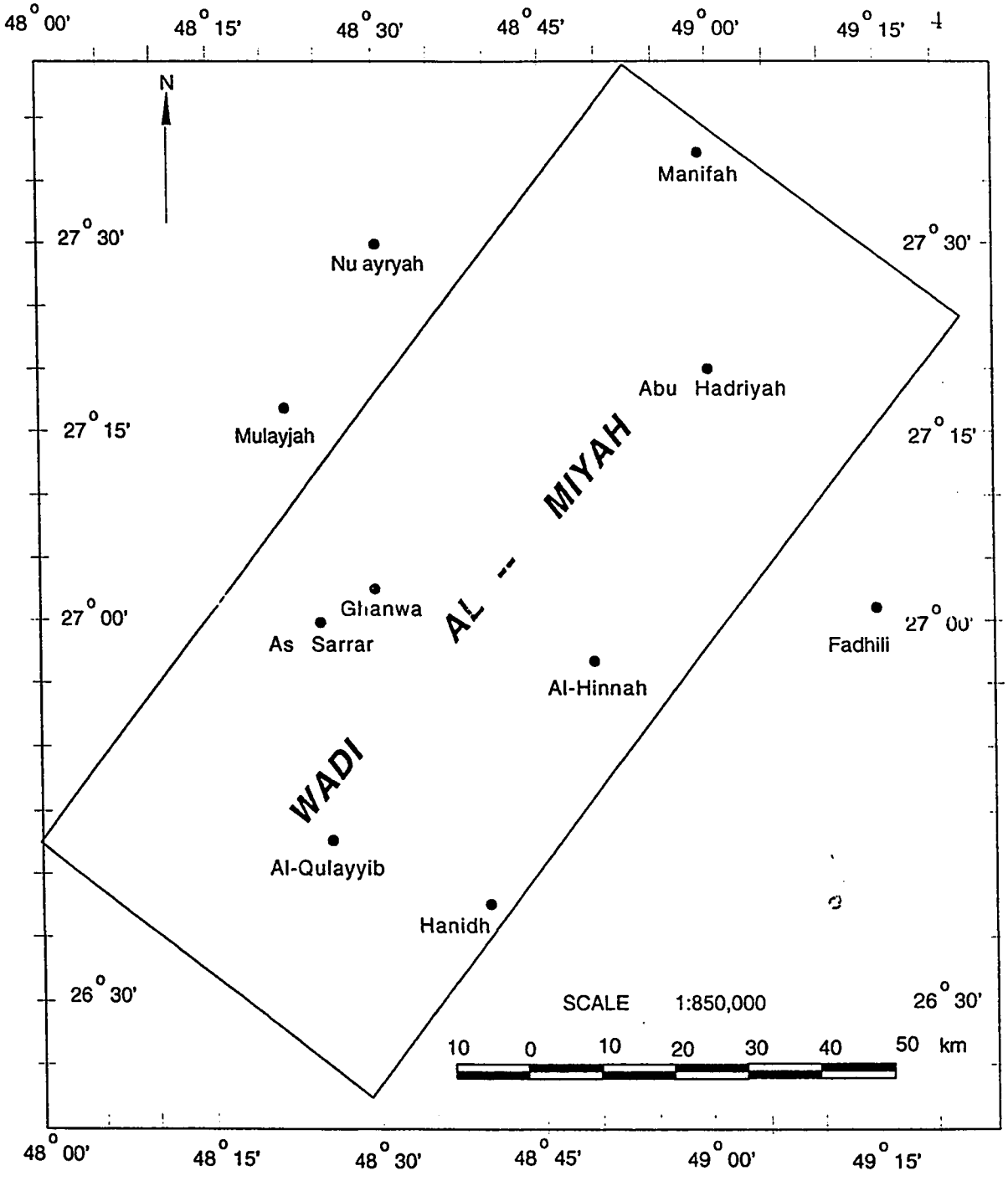

Figure 1.1: Location Map of the Study Area

1.2 Research Objectives

The main objective of the study is to establish the geological and hydrological setting of the study area based on the available information of the shallow aquifer system underlying Wadi Al-Miyah area. It also aims to study the groundwater flow patterns and spatial and temporal variations in groundwater quality within the study area. In summary, the objectives of this research are :

1. To collect and analyze relevant groundwater and hydrogeological data in order to learn the physical behavior of the shallow aquifer system underlying Wadi Al-Miyah area.

2. Modeling of geological, geophysical and hydrogeological data to present an overall groundwater flow and solute distribution pattern through simulation studies.

3. Prediction of long-term changes in regional flow system and the hazardous effects of overpumping which may be used for a better planning and management.

1.3 Literature Review

The present condition and the potential of future development of agricultural base in the Kingdom is a question of great debate. The analysis of agricultural development

potential of the Kingdom showed the dependence of future water supply on fossil groundwater in six major shallow to deep aquifers (a depth of about 300 meters). Burdon and Otkun [4] presented a broad review of geological and hydrogeological conditions controlling the occurrence and development of the groundwater resources in Saudi Arabia. They pointed out the origin of different or mixed groundwaters of different ages found in sedimentary formations. Among them are infiltrated meteoric, residual, connate waters, or waters introduced by past marine transgressions and present-day marine intrusions on and close to the coast. They studied the hydrogeological characteristics of different formations and relations with hydrometeorological conditions (high temperature, high evaporation rates, low humidity) which adversely affected the accumulation and storage of groundwater resources.

Simulation of groundwater system refers to the construction and operation of a model whose behavior assumes the appearance of an actual aquifer behavior (Mercer and Faust [5]). There are a variety of models used to solve diversified and extremely complex hydrological problems throughout the world. Prickett [6] analysed the merits and demerits of groundwater models with emphasis on the development potentials in future.

The mathematical model can be defined as a set of partial differential equations together with appropriate boundary and initial conditions and simplifying assumptions, approximating the field situation and describing the dynamics of the processes active in the aquifer system.

Piggott, et al [7] developed an inverse analysis implementation methodology of the SUTRA model which assists in the estimation of aquifer properties, and ensures its consistent and concurrent development due to its interptetive and predictive capabilites. Inverse analysis formalizes the model calibration procedure as an error function, representing the discrepancy between measured and calculated data, and then minimizes this function through optimazition. Naimi [8] provided hydrological and hydrogeological characteristics of the Umm Er Radhuma, Khobar and Alat aquifers. He approximated regional flow and salinity patterns in the Eastern Province. Italconsult [9] carried out detailed investigations on the geology and hydrogeology of Area IV of the Eastern Province. The study included groundwater flow system and salt distribution patterns within the Eastern Province. The Bureau de Recherches Geologiques et Minieres (BRGM) [10] conducted a reservoir simulation program for groundwater resources assessment and management of the Al-Hassa development project. A quasi-three dimensional flow model was constructed with grid spacing of 10 by 10 km on a regional scale.

Groundwater Development Consultants (GDC) [11] developed a simulation model of the Eastern Province and the Bahrain Island for Umm Er Radhuma, Khobar, Alat and Neogene aquifers. Bakiewicz et al [12] studied the hydrogeology of Umm Er Radhuma aquifer in Saudi Arabia with emphasis on fossil gradients of groundwater flow.

ARAMCO [13] established a regional aquifer observation program to monitor with-

drawal of water from deep aquifers and their effects on shallow aquifers which is causing decline in water levels and deterioration of water quality. The deep aquifers (Wasia and Biyadh) act as source of non-potable water for injection into the underlying oil-bearing reservoirs for pressure maintenance near the coastal region.

Shampine et al. [14] conducted a study for the analysis and interpretation of isotope concentrations in groundwater of Saudi Arabia. The study includes collection and compilation of data of concentrations of O^{18}, deuterium, tritium, S^{34}, C^{13}, and C^{14} throughout the Kingdom. A general assessment of the data is made to evaluate the isotopic characteristics of water in large, regional aquifer systems. The areal distribution of recharge and discharge zones of different aquifers are also delineated. Interpretation indicates that most of the recharge took place about 20,000 years ago and relatively little water has been recharged currently.

Pike [15] presented the division of Eastern Saudi Arabia by an ancient shore line (Sabkha line) of a major marine transgression on the basis of variations in transmissivity values of the Umm Er Radhuma aquifer. These variations changed the flow regime from laminar to turbulent. Marine transgression acted as a major source of saltwater contamination of the coastal aquifer system. The high concentrated water is accumulated into the depressions, causing saline bodies intrude the aquifers.

Al-Layla and deJong [16] presented a conceptual basis of the origin of high salt content in Dammam aquifers near the Arabian Gulf. A review about aquifer dynamics and intrusion mechanisms were also given. An outline of existing and potential

saline water intrusion problem and suggestions for remedies were also mentioned. deJong [17] presented a water balance study of the Eastern segment of Arabian Peninsula, emphasizing on the supply and demand parameters. An outline about regional hydrology, aquifer dynamics and solute distributions was also given. A management strategy for optimization of the use of existing groundwater resources was also presented.

The deteriorating groundwater quality in the coastal region has been reached such an alarming stage which may cause a major constraint in the development of groundwater resources of the region. Abderrahman [18] conducted a study for the evaluation of the adverse effects on groundwater quality in Neogene aquifer at the Al-Hassa oasis due to excessive pumping. The results showed that the continuous increase in groundwater consumption had a detrimental effect on water quality (58% increase in consumption causing an increase of 23% of TDS values) which might severely affect the soil productivity and yield of crops in that region.

Al-Layla [19] conducted a comprehensive study on the groundwater development in the Eastern Province of Saudi Arabia and developed a two-dimensional digital simulation model, a solute transport model and an optimization model. Rasheeduddin [20] constructed a numerical quasi-three dimensional groundwater flow model for a multi-aquifer system in the Eastern Province in order to analyze the flow patterns through various management alternatives. The hydraulic interaction between the aquifers via intervening aquitards were analyzed through steady state and transient

state model calibrations.

Edgell [21] studied the geological framework of groundwater resources of Saudi Arabia and provided a regional structural setting of the various groundwater basins, including Eastern Province. Hasan [1] studied the hydrogeochemistry of Alat and Khobar aquifers in the Eastern Province. The aqueous equilibrium studies which were based on saturation indices pointed out a sea water dilution trend at north of Jubail in the coastal area. Near Abu Hadriya area, the high sulfate, magnesium, sodium and chloride concentrations as well as the increased dolomite and calcite saturation also provide an evidence of sea water intrusions from the Gulf.

Groundwater budgeting is a recent technique which plays a key role in groundwater management. Abderrahman and Rasheeduddin [22] conducted a study to quantify the storage of groundwater in a multiaquifer system in greater Dhahran area by using a detailed water budget analysis. The cell by cell flow volumes of Alat, Khobar and Umm Er Radhuma aquifers were calculated which demonstrated the upward vertical leakage from Umm Er Radhuma to Khobar and Alat aquifers.

Rajai [23] applied a numerical two-dimensional groundwater flow model for Umm Er Radhuma aquifer at the Al-Sharqiyah Agricultural Development Company (SHADCO) Farm. Management alternatives were evaluated after a large number of prediction runs to optimize the use of groundwater for irrigation at different scenarios.

The present study covers the whole Wadi Al-Miyah area in which all the shallow aquifers, (Neogene, Alat and Khobar) were modelled to study the geological and

hydrogeological setting, and the groundwater flow and solute distribution patterns. A solute transport model was constructed using Saturated and Unsaturated Solute Transport (SUTRA), developed by USGS, Voss. [24].

Chapter 2

Geological and Hydrogeological Setting

2.1 Geological Setup of The Area

2.1.1 Geological Mapping

Applications of remote sensing techniques are characterized by an indirect approach which helps in delineation of geological, geomorphological and hydrogeological features through visual interpretation of LANDSAT-TM images. The LANDSAT-TM data acquired over the study area was used to produce a Geological map of scale of 1: 150,000 for identification and detailed analysis of various lithological units, using various image processing techniques. (Plate - A). The satellite image was acquired

by King Abdulaziz City of Science and Technology (KACST) in Riyadh which later was processed at the Remote Sensing Center. Research Institute, King Fahd University of Petroleum and Minerals, Dhahran, Saudi Arabia. The satellite image index comprises:

1. Path/row ... 165/041

2. Date acquired ... May, 27, 1993.

Several field checks, using Global Positioning System (GPS) points as bench marks, were made for groundtruth for the mapping. The lattitudes and longitudes were then drawn on the map. The map includes the anaylsis of landforms and spectral characteristics of the rocks represented by tone or color on the images.

The study includes the identification of major rock types using LANDSAT-TM image through visual interpretation on a false Color Composite image comprising bands 2.4.7 as blue, green and red respectively. The image was then compared with the existing geological map of the area. Lithological contacts were extended and extrapolated for a large distance on the basis of spectral and geomorphologic information which were verified by several field checks. The following geological units are identified and interpreted from the images :

1. Eolian Sand.

2. Sabkhah deposits.

3. Hafuf formation (sandy marl and sandy limestone.)

4. Dam formation (marl and clay)

5. Hadrukh formation (silty sandstone, sandy limestone, sandy marl)

6. Undiffenentiated (marly sandstone, sandy marl, sandstone).

Sand dunes and sabkhah were delineated effectively on the image because of their unique spectral characteristics. Sabkhahs are the natural discharge zones of ground-water from Neogene aquifer. Therefore, their distribution and extent were used in evaluating the amount of discharge from Neogene aquifer. The lineaments are surface expressions of joints, zones of joint concentrations, or faults which are reproduced as conspiceous linear features on satellite imagery. The lineaments in the study area are intermittent which range in length from several hundreds of meters to some tens of kilometers.

2.1.2 Geomorphology

The study area lies at the flank of the desert, ranging in physiography from extensive surfacial sand dune belts to dissected rocky escarpments. Wadi Al-Miyah covers a broad and flat area. It extends upto Arabian Gulf from southwest to northeast. Its rather inconspicuous flanks consist of sandy marls and clays of the Miocene Dam and Hadrukh formations. The wadi fill consists of aeolian and fluviatile sand. Sabkhahs of the wadi floor are found often around spring and well fields where the landforms

prevent the surface runoff. [24]. The landforms are typical for humid climate which are modified into arid landforms, indicating highly fluviatile nature of paleoclimate. The present land surface is a virtual peneplain which slopes very gently towards the Arabian Gulf. Broader relief features rarely exceed 100 meter while local relief seldom exceeds 20 meters.

Sand dunes

These are soft, moving to fixed sands with flat to steep surfaces. These are either in the form of long narrow sand strips or large sand sheets which are partially stabilized by vegetation. The dunes help in recharge of groundwater reservoirs as rainfall perculates rapidly to the subsurface aquifers.

Sabkhahs

They are salty playas or closed evaporation pans, evaporating groundwater either from shallow watertables or from deeper upward leakage from confined aquifers and marked as natural discharge zones. They consist of silts, clays, muddy sands and chalky limestones with encrustations and interbeddings of gypsum and salt, filling shallow depressions. In the study area, these are formed in elongated depressions of structural origin, trending north to northeast. Coastal subkhahs act as a controlling mechanism, allowing a certain amount of groundwater to pass under them to the nearby Gulf but evaporating the rest, so that overall groundwater discharge remains

constant. The distribution of sabkhahs within the study area is shown in Plate - A.

2.1.3 Stratigraphy

The area is underlain dominantly by a thick sequence of carbonate rocks which dip gently NNE towards the Arabian Gulf. They were deposited in a shallow marine environment with frequent intercalations of evaporitic periods as well as continental conditions, causing erosion of previously deposited matarials, (Powers et al. [25]). A generalized lithostratigraphic sequence of the study area is shown in Figure, 2.1.

2.1.4 Dammam Formation

Dammam Formation is mainly a series of marine carbonate rocks interbedded with fine clastics. It lies conformably on the Rus formation. In the middle Eocene, the evaporitic conditions were terminated by a new marine transgression, leading to a widespread deposition of a sequence of mainly carbonate rocks with subordinate shales. The limestones are porous and permeable and form the Alat and Khobar aquifers which are much exploited in the coastal region. The beds dip generally towards east and north which may disturbed locally by positive structure, as near Abu Hadriyah at the right corner of the study area, Figure, 2.2. The thickness varies generally towards east and northeast, ranges from 125 to 200 meters, Figure, 2.3. The Dammam sequence has been divided on the basis of borehole data into five members as follows:

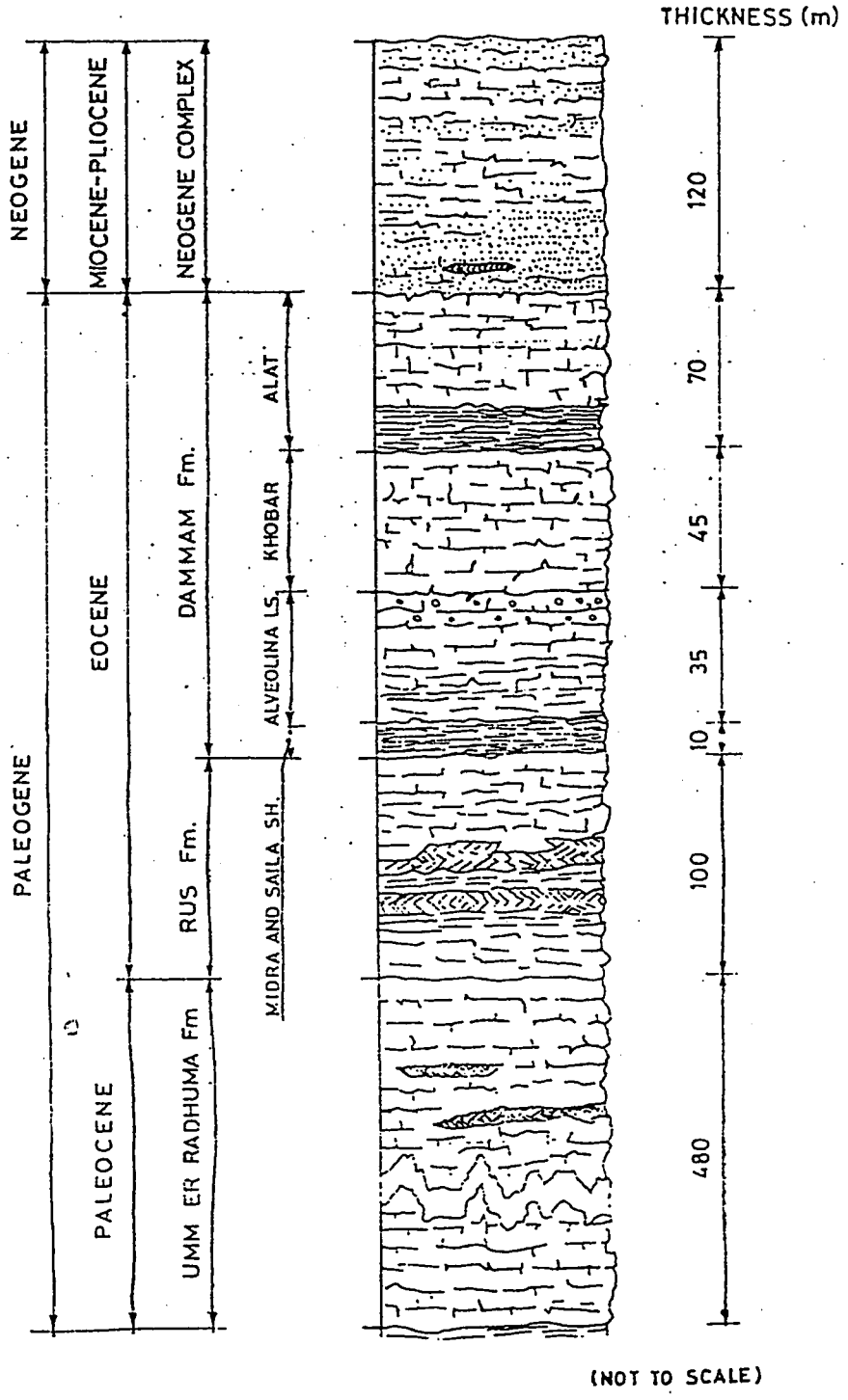

Figure 2.1: A generalized lithostratigraphic section of Wadi Al-Miyah area (after Italconsult, 1967).

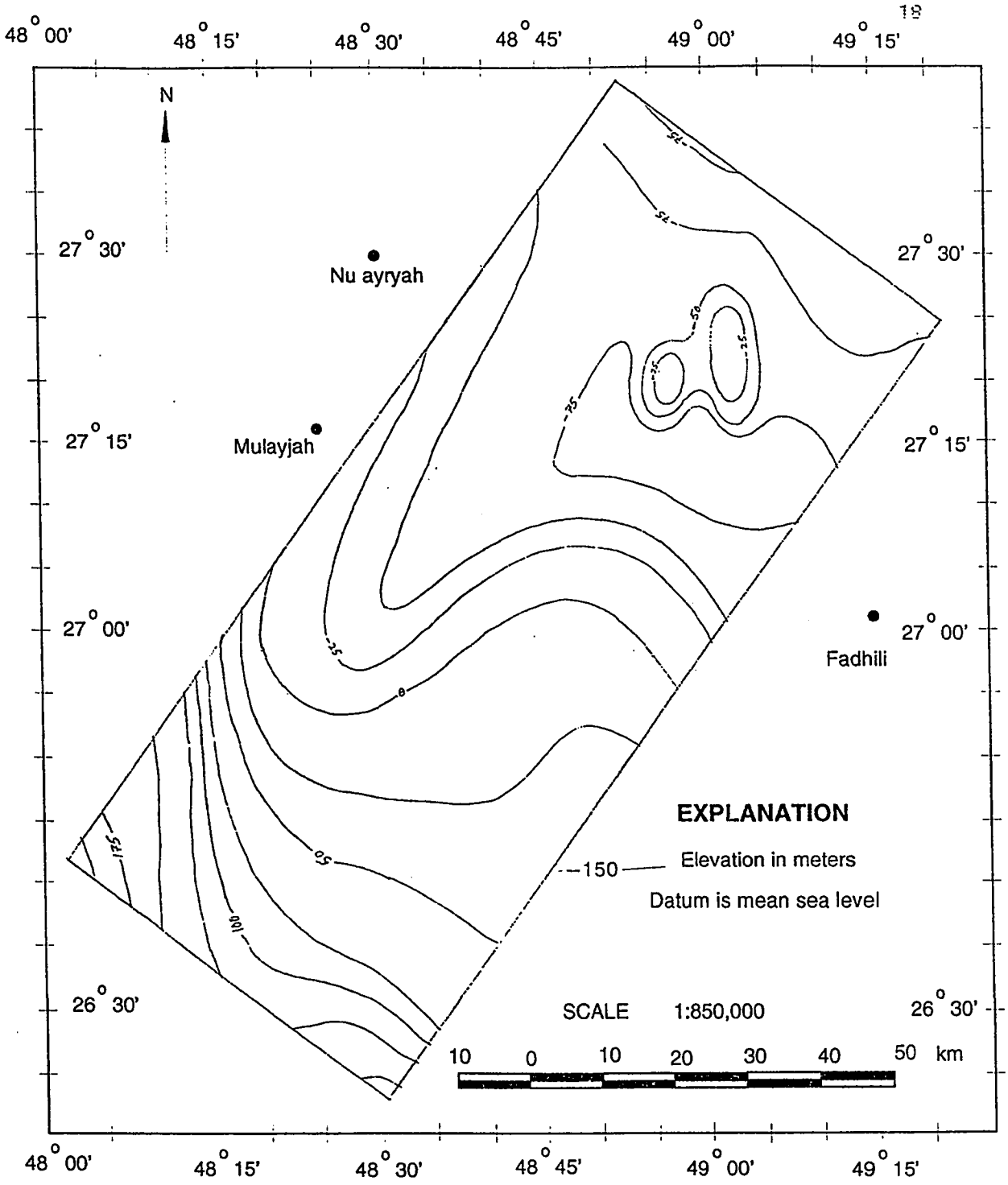

Figure 2.2: Structural Contour Map of the bottom of Dammam Formatiom (after Italconsult, 1967).

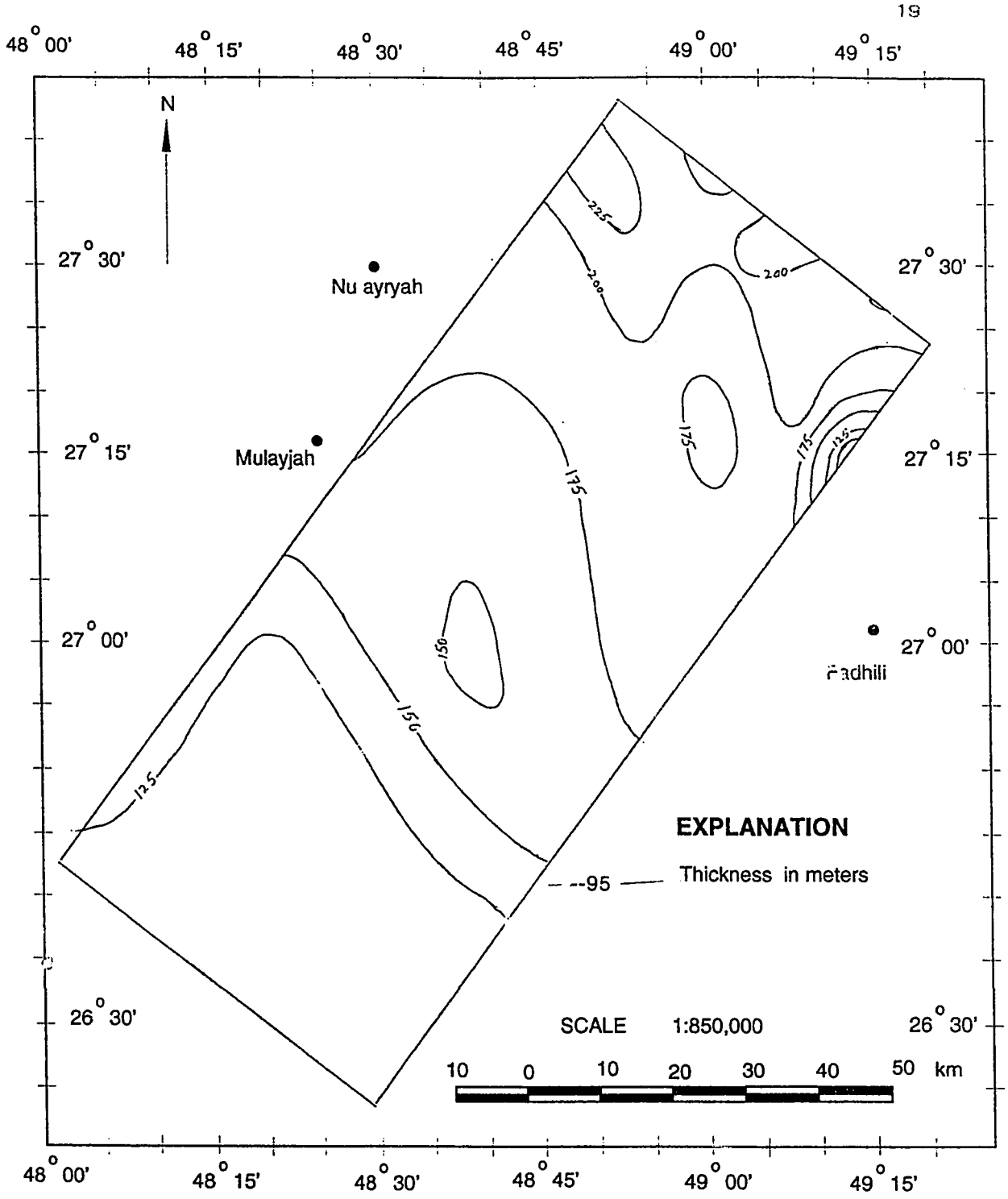

Figure 2.3: Isopach Map of Dammam Formatiom (after Italconsult, 1967).

Midra and Saila Shale Members

The Midra and Saila members form the basal level of the Dammam formation and are bounded at the bottom by the anhydrites and clays of the Rus formation. These members consist mainly of shales. In the study area, they consist of brownish-yellow marls and clays with interbedded dark gray to brown limestones. The thickness varies from 5 to 10 meters. Although, the Midra and Saila members are of limited thickness, their continuity and consistency of facies make them one of the most important marker horizons of the whole studied sequence, Italconsult, [8].

Alveolina Limestone Member

The Alveolina limestone member overlies the Midra and Saila shales and is bounded at the top by the Khobar member. Its lower part consists of gray and gray-blue clays and marls. The upper part consists of colored slightly porous skeletal detrital limestones. The thickness varies from 15 to 20 meters.

Khobar member (Middle Eocene)

It lies on the Alveolina limestone member and is bounded at the top by the orange marls of Alat member. It consists mainly of crystalline tan colored dolomitic limestones to light brown slightly porous limestones with interbedded marls. The thickness is about 45 meters in the study area.

Alat Member: (Middle Eocene)

On the Khobar member lies the Alat member. It is bounded at the top by continental clastics and shales of the Hadrukh formation. It is the uppermost member of the Dammam formation. It consists mainly of a basal light orange, yellow or yellowish gray marls (Orange Marls) followed by cream, white and light tan porous fossiliferous micro crystalline limestones.Alat is much less developed due to selective erosion during post-Dammam orogenic phase. The average thickness is about 70 meters increasing towards the east.

2.1.5 Neogene Formations

All outcrops in the study area are Neogene. They consist of continental clastic deposits with a few marine episodes. They are unconformable on the Eocene formations. These deposits are varicolored fine to medium grain quartzitic sands alternating with sandy marls and chalky limestones with subordinate sandstones and clays. The average thickness is about 120 meters but varies considerably from a few meters at positive structures to a maximum of 130 meters at the Al-Wannan syncline, Figure, 2.4

Hadrukh Formation: (Lower Miocene)

The Hadrukh formation of continental and marine origin lies unconformably on the Eocene formation. Depending on the relationship between marine and continental

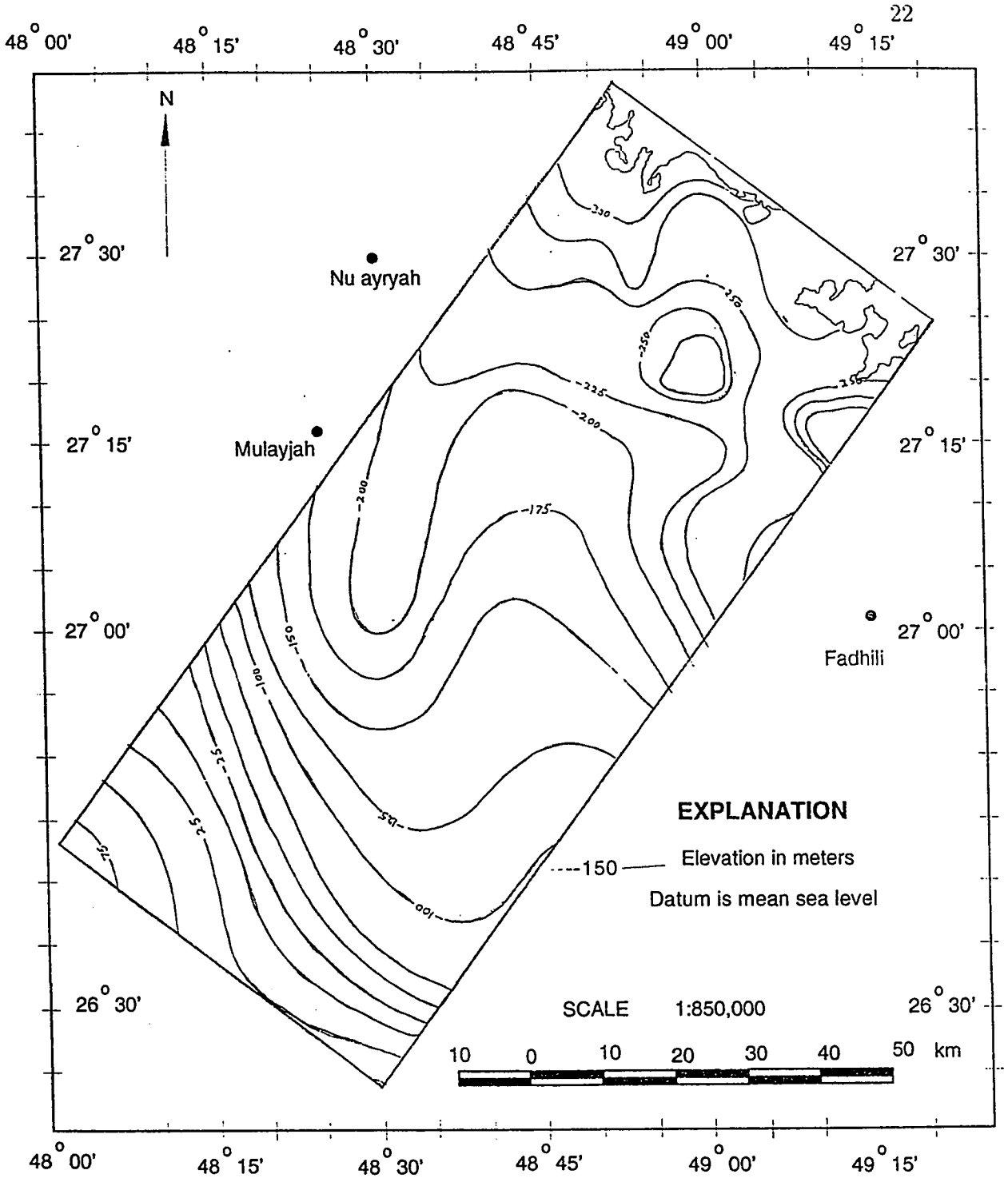

Figure 2.4: Structural Contour Map of the Bottom of Neogene Formatiom (after Italconsult,1967).

sediments, the formation consists of either sandy marls, sandy clays and sandy limestones with interbedded gypsum or of continental clastics generally coarse gray to pink muddy sandstones. The thickness is about 50 m.

Dam Formation: (Lower and Middle Miocene)

It overlies the Hadrukh formation. It consists mainly of red and white marls, red, green and olive-green clays with interbedded sandstones, chalky limestones and skeletal detrital limestones in irregular large lenses.

Hofuf Formation

It represents transitional and continental phase. It consists of white and red conglomerates containing pebbles of limestones, quartz, held in a sandy clayey matrix at the basal part. The middle part consists of soft, white limestone, intercalated with whitish sandy limestones.The upper part is sandy with alternations of red and white sandy marl with flint nodules. The thickness is about 70 meters.

2.1.6 Recent Deposits

These are mainly sabkhahs, calcareous crusts and aeolian sands. They are Pleistocene and Recent unstratified deposits.

2.2 Hydrogeological Framework

The hydrogeology of the basin depends on the hydraulic characteristics of the aquifers which influence the storage and movement of groundwater. The main criteria for differentiation into aquifers and aquitards is permeability and storage capacity. The study area is underlain by a thick sequence of hydraulically connected carbonate rocks with thickness of about 260 meters. The hydraulic characteristics of aquifers are linked with lithology and sedimentation conditions which impose lateral and vertical facies variations in each formation. Aquifers are separated hydraulically on a regional scale, except in those areas where tectonic events or unconformities have brought the formations into contact. So, local facies variations may change an aquiclude into aquifer or vice versa.

2.2.1 Major Aquifers

From the regional point of view, except for local facies variations, the major water-bearing units within the study area are the limestones and dolomitic limestones of Umm ER Radhuma formation, Dammam formation (Khobar and Alat members), the clastics of the Hadrukh formation, and the limestones of Dam formation (Neogene formations). Since the present modeling study is limited to Khobar, Alat, and Neogene aquifers, Umm ER Radhuma aquifer is excluded from the following discussion.

Khobar Aquifer

It is calcarenitic and slightly dolomitic limestone, locally karstified and fissured. It has a moderate yield due to good permeability which provides water for domestic and agricultural purposes in the study area. The aquifer is in artesian condition and it is flowing throughout the area. A great range of permeability values may occur from one area to another. The higher values are connected with highly fractured conditions. The geometry is rather complex because of local facies variations, causing a decrease in aquifer permeability. The matrix shows a less intense fracturing with a pin-point porosity between grains of lime sand. Karstification, dolomitization, secondary solution along joint systems are the major causes of development of secondary porosity within the aquifer, Italconsult [8]. The thickness varies from 55 to 125 meters, Figure,2.5

Alat Aquifer

It is a secondary aquifer of porous, karstified and fissured limestone and dolomitic limestones. It shows erratic productivity due to major variations in thickness and hydraulic properties. At the study area, it shows low matrix porosity due to fine-grained nature. It is relatively a minor aquifer with low transmissivity which increases along the coast and decreases towards the west, Italconsult [8]. The aquifer is hydraulically separated from Neogene by fine clastics and basal clays. The thickness varies from 36 to 57 meters in the study area, Figure, 2.6

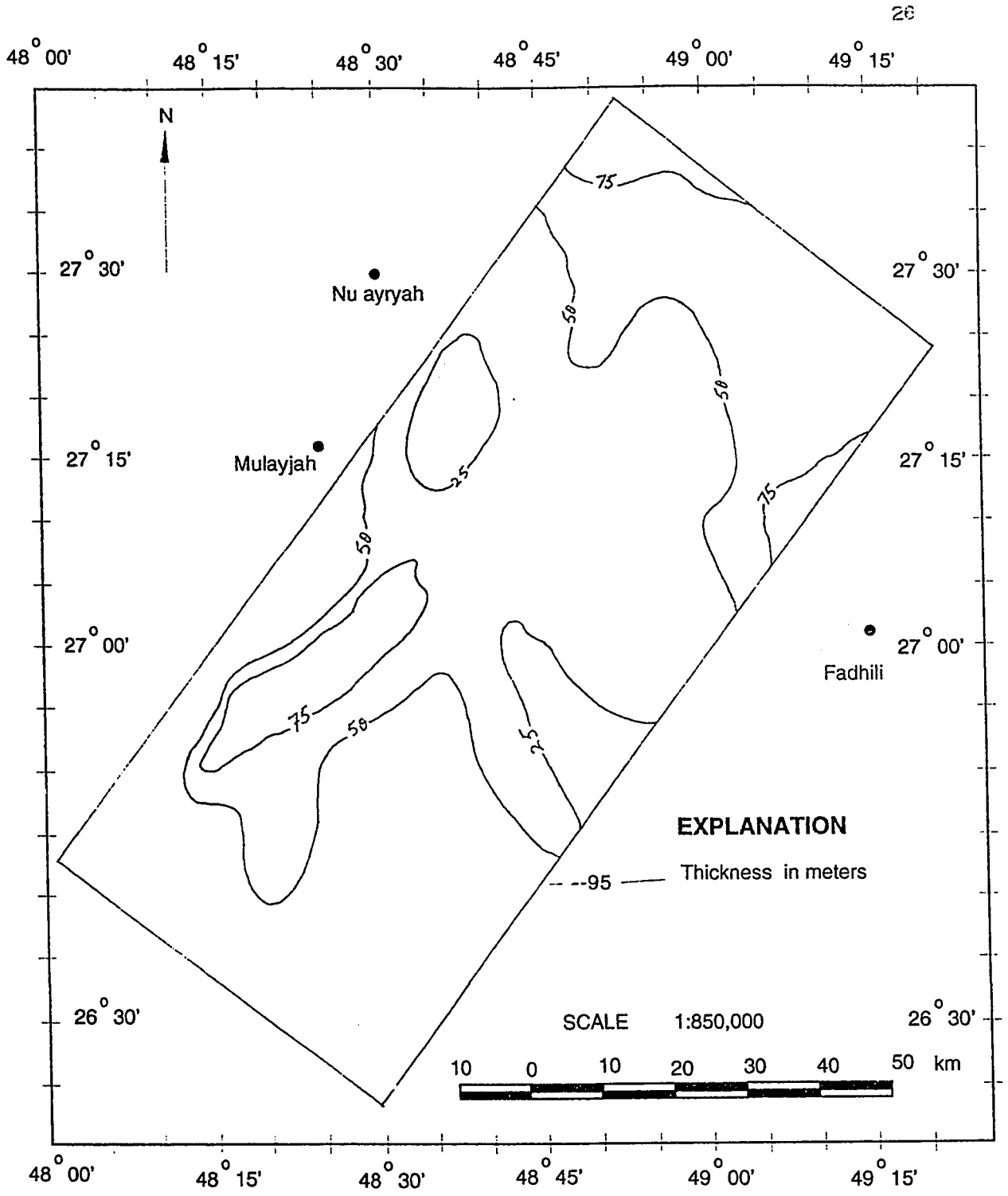

Figure 2.5: Isopach Map of Khobar Aquifer.

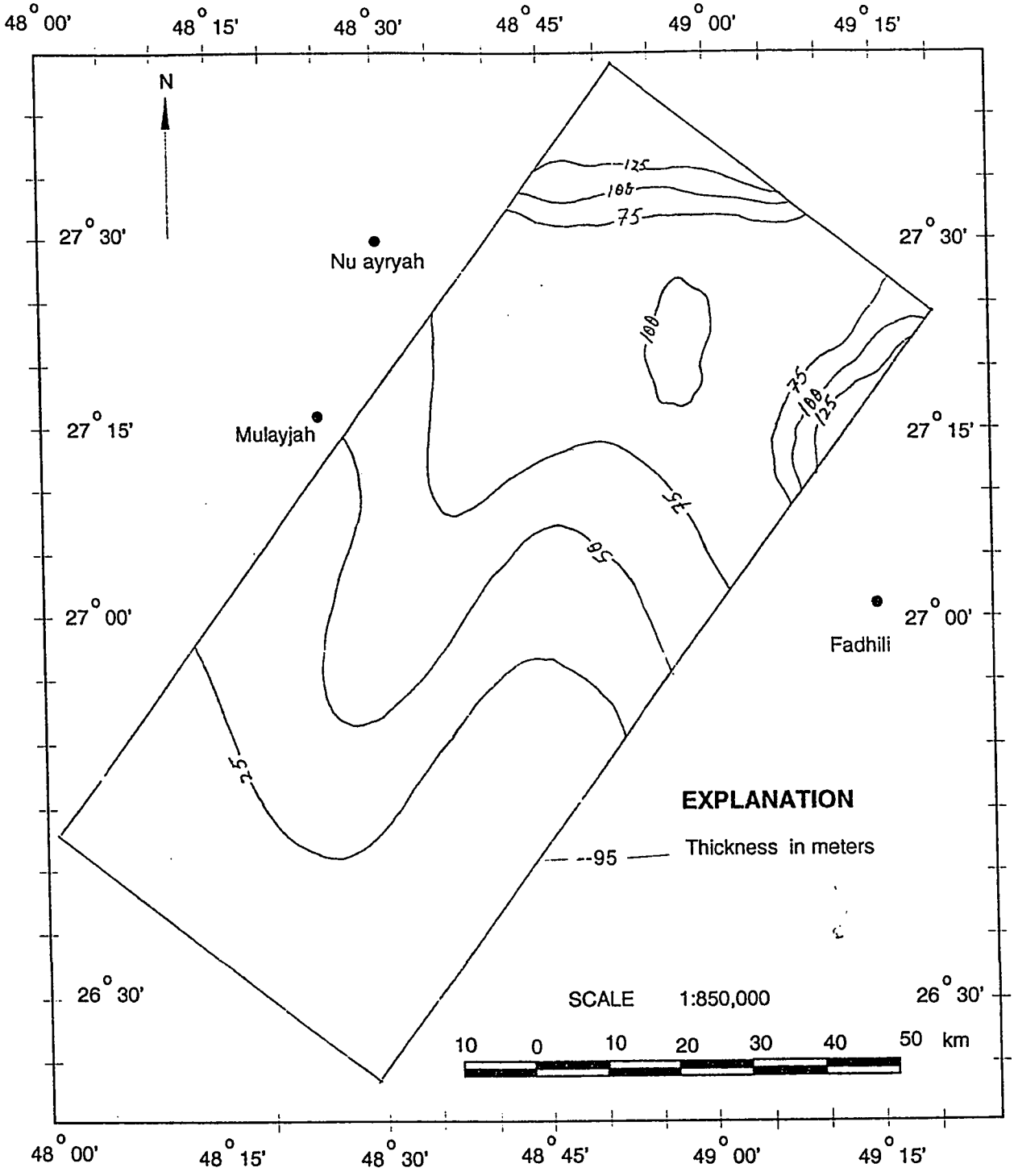

Figure 2.6: Isopach Map of Alat Aquifer.

Neogene Aquifer

The Neogene aquifer, which is one of the most utilized aquifer by the local inhabitants, has limited development potential due to low productivity and higher water salinity. The unit forms an essentially phreatic aquifer throughout the region. Saturated thicknesses vary rapidly and thins out regionally westwards, Figure, 2.7.

The static level of the aquifer is a few meters below ground level, as can be seen in numerous hand dug and drilled wells. The hydraulic properties change rapidly from area to area due to lateral and vertical facies changes as a result of differential weathering. The permeability ranges from 0.1 to 300 meter/day (m/d), Italconsult [8]. The aquifer is hydraulically connected with underlying aquifers, causing downward flow at certain locations due to change in heads. Similarly, the upward leakage of water from aquifer to Sabkhah leads to loss of millions of cubic meters. The thickness ranges from 50 to 125 meters. Figure, 2.7. Lateral and vertical facies change frequently within the Neogene sediments, which currently subdivided into the Dam and Hadrukh aquifers.

Dam Aquifer is fissured and karstified limestone of middle Miocene age with thickness varying from 30 to 100 meters. It has a good permeability and contains good quality of water.

From a hydraulic point of view, Hadrukh formation at the regional level may be considered as an aquiclude. However in the study area, it is basal detrital continen-

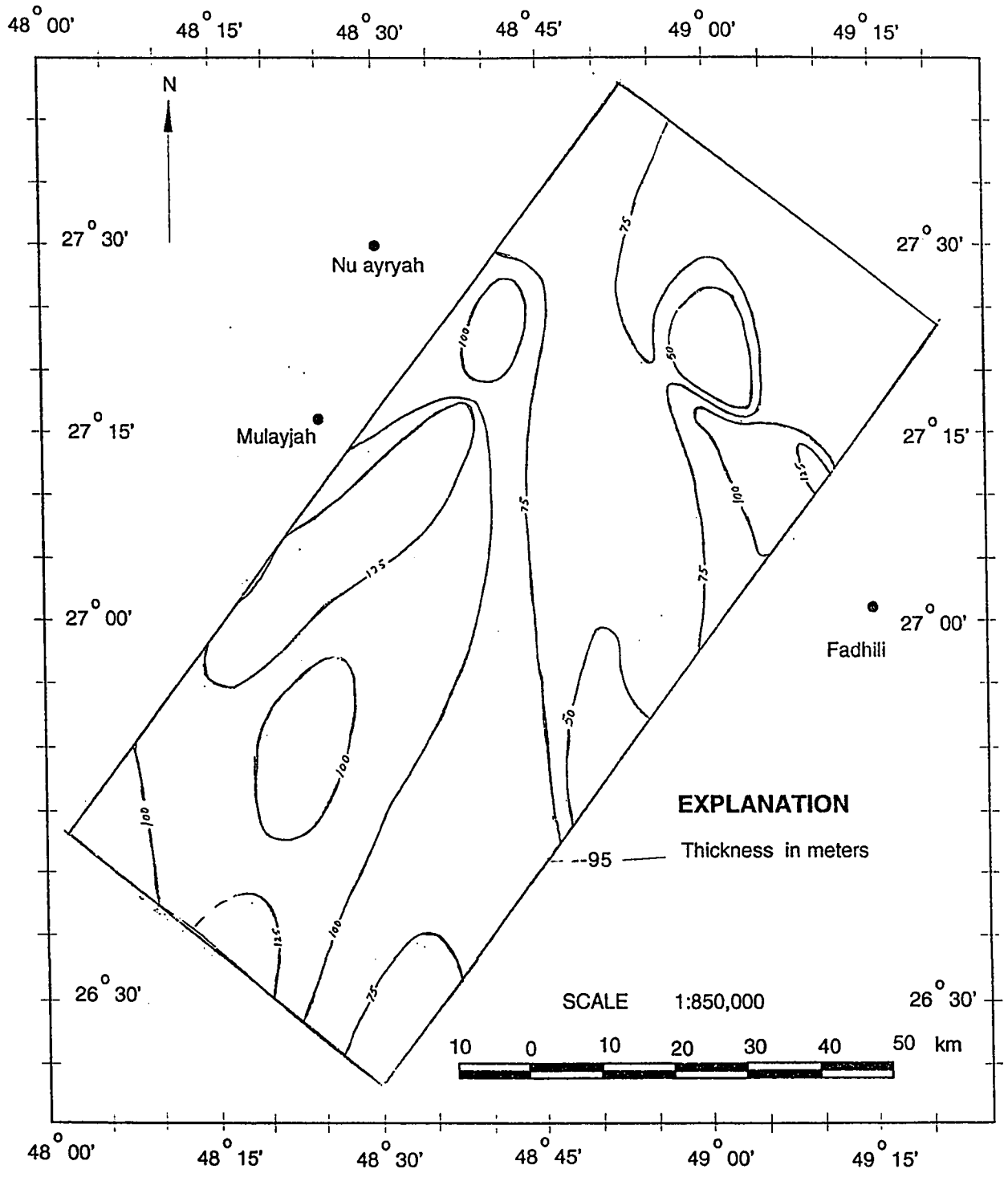

Figure 2.7: Isopach Map of Neogene Aquifer (after Italconsult, 1967).

tal clastics with good hydraulic properties. Its yield is upto 50 lit/sec which is due to high primary intergranular porosities, Italconsult [8].

The Dam and Hadrukh formations constitute a single Neogene aquifer system whose two layers, either alternating or together, have good aquifer characteristics with very similar water qualities and piezometries, BRGM [9].

2.2.2 Major Aquitards

The aquitards are represented by;

1. Fine clastics and evaporites of the Rus formation, Midra and Saila shale, Alveolina marl which separate the Umm Er Radhuma aquifer from Khobar aquifer.

2. Marls and shales at the base of the Alat member, which separate the Khobar aquifer from the Alat aquifer.

3. Shales of the Hadrukh formation, and marls of the Dam formation which separate the Alat aquifer from the Neogene aquifer.

The study area comprises the following aquitards from bottom to top:

Lower Dammam-Rus Aquitard

From hydrogeological point of view, Midra and Saila shales, Alveolina marl and the underlying marl and evaporites of Rus formation, form the basal aquitard (Lower

Dammam-Rus aquitard) which separates the underlying Umm Er Radhuma from Khobar aquifer. The lower Eocene Rus formation consists of interbedded marl, dolomite, anhydrite. It forms an aquitard which generally caps groundwater in Umm Er Radhuma over most of the Eastern province. On structural high, the Rus formation is mainly composed of dolomite and it yields small amounts of poor quality water by upward leakage from Umm Er Radhuma aquifer. In structural troughs, it mostly consists of impermeable anhydrite, gypsum, and marl. The thickness varies from less than 50 meters to 150 meters, Figure,2.8.

The anhydrite-gypsum beds of Rus formation dissolved at certain locations, causing the ground surface to slump in random array, Naimi [7].

Alat Marl Aquitard

Alat Marl (Orange marl) aquitard is relatively uniform in thickness and separates the Alat aquifer from Khobar aquifer throughout the study area. The vertical hydraulic conductivity is about 2.59^{-4} meter/day (m/d), Italconsult [8]. The thickness varies from 10 to 30 meters, Figure, 2.9.

Neogene Leakage Interface Aquitard

It is a slim aquitard, comprising the bottom shales of the Hadrukh formation, and the marls of Dam formation. It separates the Alat aquifer from the Neogene aquifer. The clay beds with very low vertical permeability are dominated and not continuous

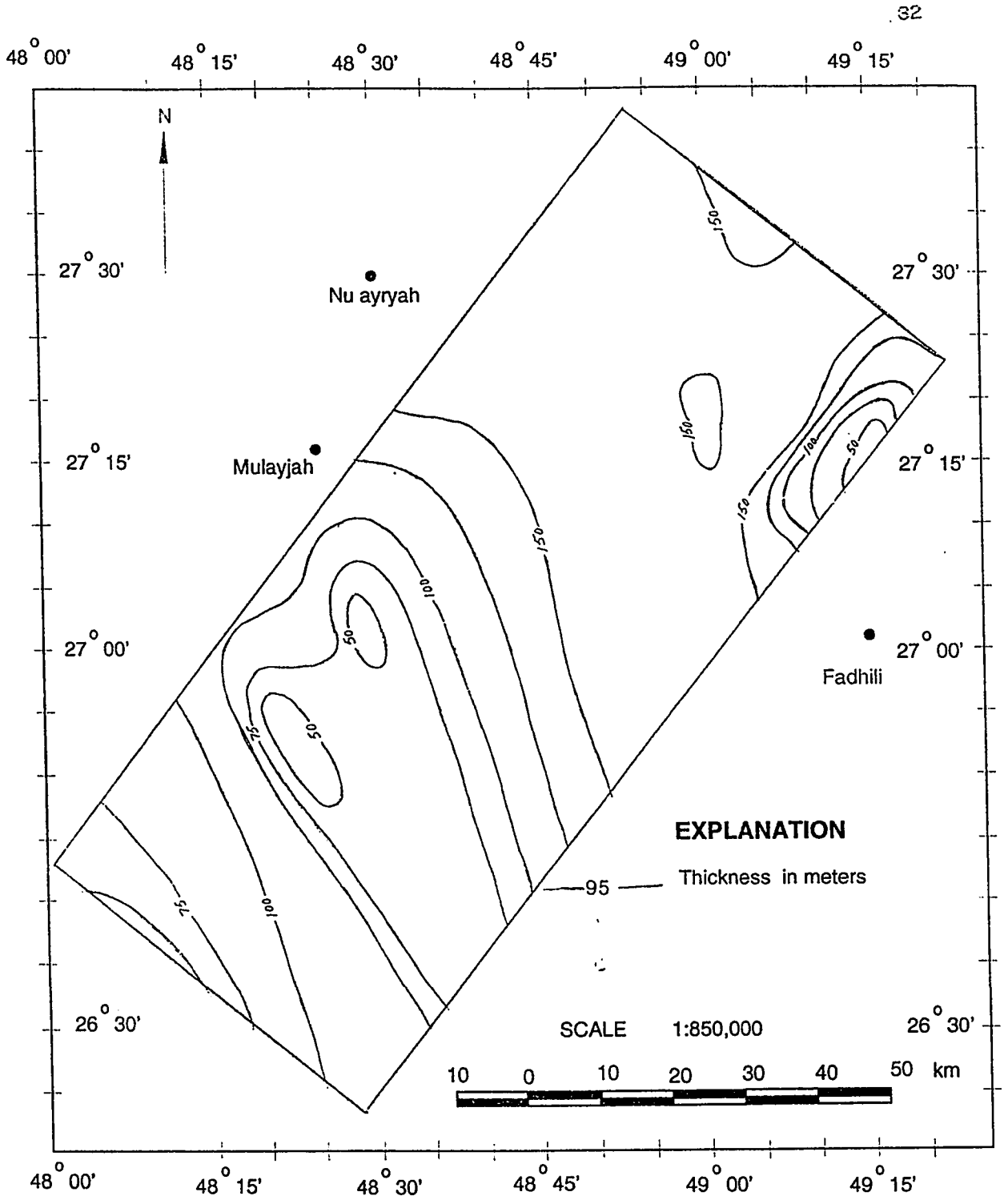

Figure 2.8: Isopach Map of Lower Dammam-Rus Aquitard. (after Italconsult, 1967).

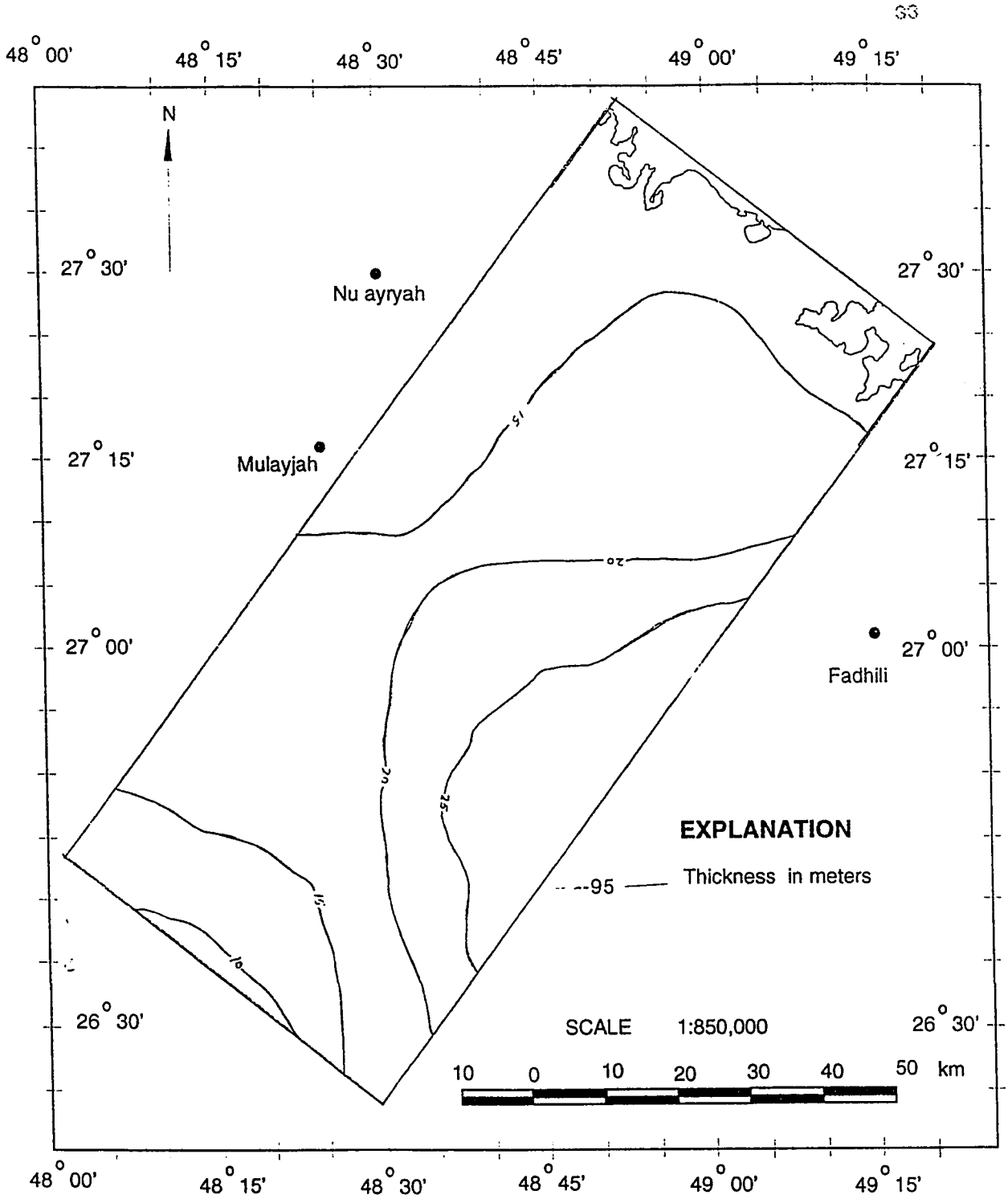

Figure 2.9: Isopach Map of Alat Marl Aquitard.

throughout the study area. It is considered as a conceptual leakage interface. Thus, the integrated effect of vertical permeability over the entire aquifer is equivalent to flow conductance on the interface. The vertical hydraulic conductivity is in the range of 10^{-8} to 2 X 10^{-4} meter/day. G.D.C [10].

Chapter 3

Modeling

3.1 Geophysical Modeling

3.1.1 Introduction

An electrical resistivity survey has been conducted in the Wadi Al-Miyah area to delineate subsurface layers and to determine their thicknesses. Seven vertical electrical soundings by a Schlumberger array were used, Figure,3.1.

The apparatus RESIXIP is used for carrying out the electrical resistivity measurements. The Vertical electrical sounding method (VES) is useful in showing variations of apparent resistivity with depth. The distance between each of the potential electrodes and the current electrodes increases each time for deeper penetration of the ground. In the year 1966, an Italian consultant firm, Italconsult

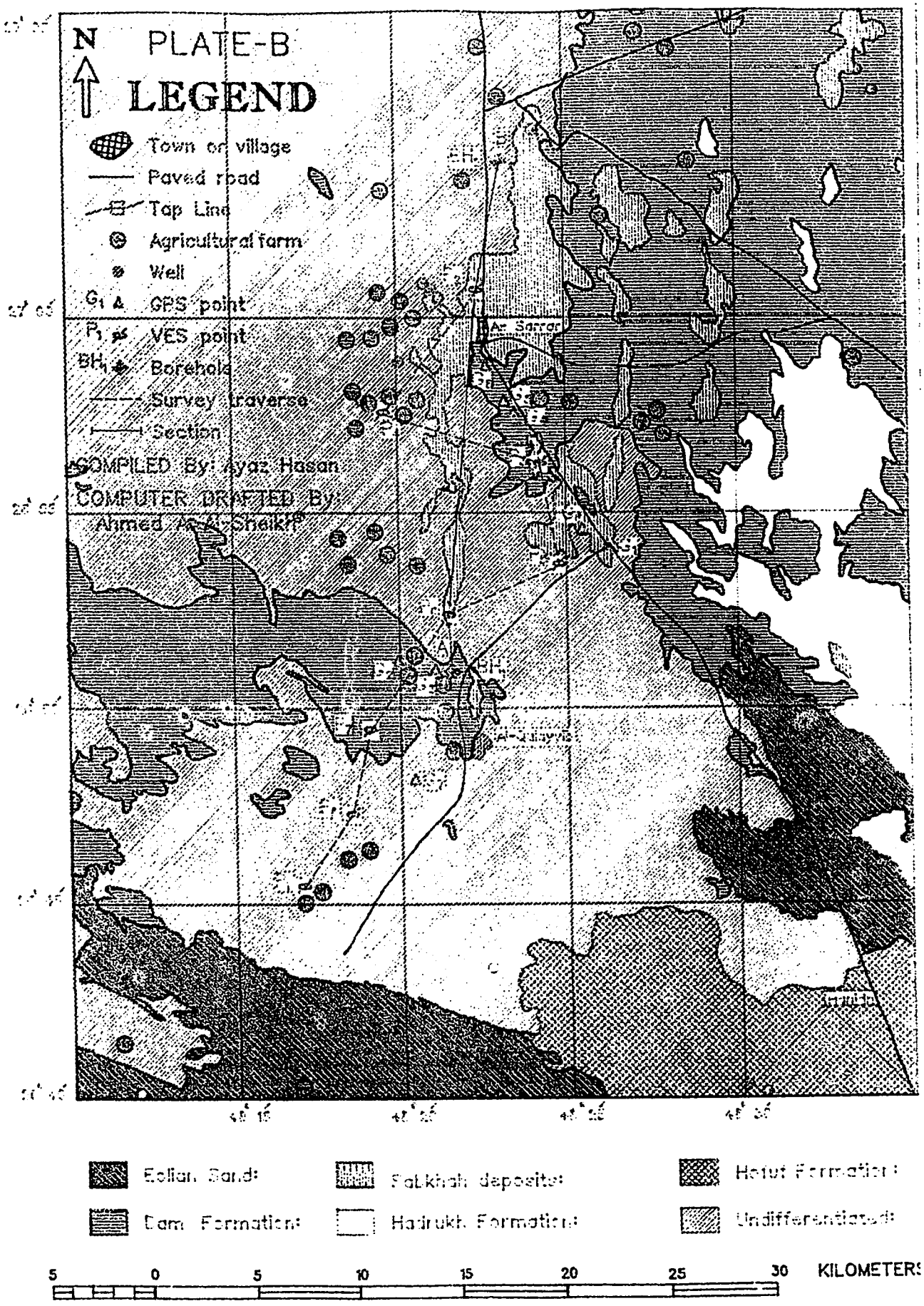

Figure 3.1: Location of VES and GPS points in the study area.

[8], conducted an electrical resistivity survey in order to delineate the deep aquifers within Wadi Al-Miyah area. The work was part of a regional survey of the Eastern Province of Saudi Arabia. The correlations between the electrical logs and the lithostratigraphical logs have revealed the following :

1. The absolute resistivity values for Neogene, Alat and Khobar aquifers.

2. The Alat-Khobar transition coincides with the first conductive-resistive contact.

3. The base of Dammam formation is revealed by an area of lower resistivity. corresponding to the Alveolina and Midra and Saila Shale members.

4. On the basis of surface measurements on outcrops and calibrations carried out in boreholes, the geo-electrical data relevant to the stratigraphic units have been evaluated. Table 3.1.

Absolute Resistivity Values	Stratigraphic Units
200 - 1,500 ohmm layer	Dry sands, calcarenites and sandstones
0.5 - 2 ohmm layer	Sabkhah deposits
5 - 10 ohmm layer	Neogene Complex
10 - 20 ohmm layer	Alat Member
50 - 200 ohmm layer	Khobar Member
10 - 15 ohmm layer	Alveolina Member-Midra and Saila shale member, Rus Formation

Table 3.1: Geoelectric data of the study area (after Italconsult, 1967).

Within the depth (150-200m), the apparent resistivity measured with AB = 800 m is actually a function of the relative thickness of the resistive cover of acolian sands, the highly conductive surfacial saline ground, the conductive Neogene-Alat, and the first resistive horizon of Khobar Member. The areas with resistivity between 5 and 10 ohmm correspond to zones where the resistive cover of aeolian sands and surfacial saline soils are not thick and where the Neogene-Alat has fairly low true resistivities in the range of 5 to 8 ohmm. The areas with resistivity between 10 and 20 ohmm are those where the Neogene-Alat is more calcareous and where the influence of the first deep resistive layer, constituted by Khobar, is more pronounced.(Italconsult, 1967).

The main objectives of the present electrical survey are:

1. To study the distribution of permeable levels in the Neogene cover.
2. To determine the thickness of the surfacial saline layer.
3. To determine the thickness of the Neogene-Alat units, overlying the Khobar aquifer.

3.1.2 Field Survey

The sites were chosen along country and farm roads with no thick sand cover and free from buried cable and pipes. For the selection of sites, it is considered that the estimated depth to the bottom of Khobar aquifer may be within 200 m. The

center point of the spread was located at the middle of the chosen straight stretch of the sounding point. From this point, the following distances (in meters) were measured in each direction: 25, 50, 75, 100, 125, 150, 175, 200, 225, 250, 275, 300, 325, 350, 375, 400 meters. The SYSCAL R2 is an electric resistivity meter with transmission and reception capabilities, Figure, 3.2. It is used as a source of current and a highly sensitive voltmeter. The maximum current supplied to ground is 1.5 ampere and the maximum voltage received is 4 V with resolution up to 10 micro V. The system calculates the resistivity, SP and IP values at the same time and displays them on the screen. The power supply of the instrument is given by six 1.5 V batteries housed at the bottom of the instrument which is enhanced upto 10 to 700 V by a DC-DC converter Figure. 3.2. The unit is supplied by a 10 to 30 V DC voltage provided by a car battery which is a high voltage source for resistivity meter equipment (SYSCAL R2). Three output voltages (110 V, 220 V, 330 V) can be selected through a manual switch. The maximum input current available is 1170 mA for the 110 V output voltage, 390 mA for the 220 V and 390 mA for the 330 V.

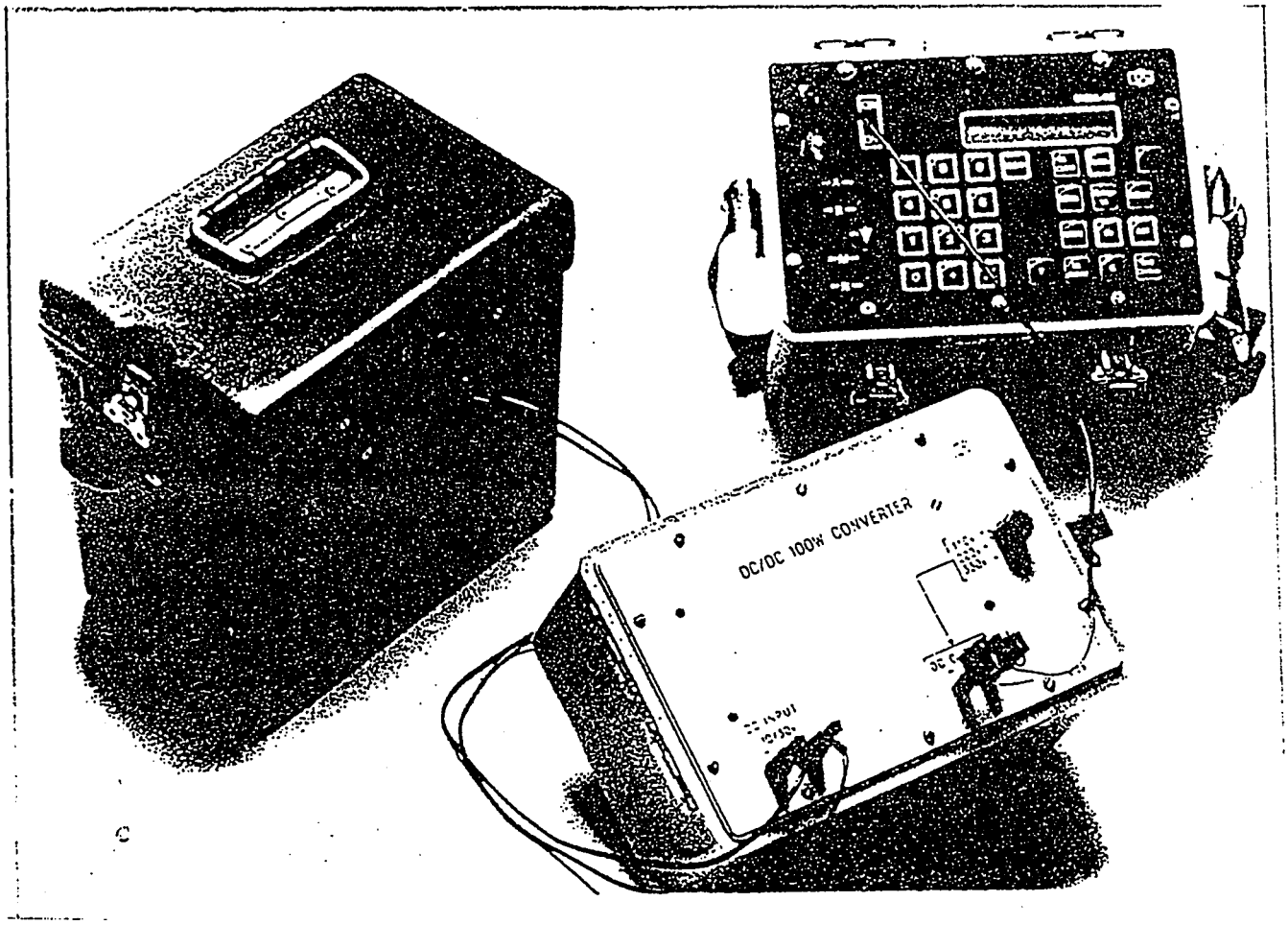

Figure 3.2: SYSCAL R2 Resistivity Meter showing display panel and DC-DC 100 W Converter with battery pack.

A 2-feet electrode of stainless steel was driven into the soil at each end of the spread. Both electrodes A and B, were connected by two 16-gauge cables to the current sender which is located at the center. The potential electrodes M and N were connected to the voltage receiver by two coaxial cables whose shieldings were grounded at the center. The distance MN was kept equal to 2 meters.

The fieldwork required three men. Two men taped the distances, laid the cable, and moved and stood by the two current electrodes. The third man, the observer, remained at the center point; he was responsible for taking the readings. The contact between the three men was established by waving the flags. At each position of A and B, the observer recorded the current sent, the voltage received, and the distances AB and MN. These parameters are used in the calculation of apparent resistivity by the RESIXIP computer processor. Apparent Polarization (IP) and Self Potential (SP) values are also measured at each position. During the field survey, seven sounding points were conducted, which are given in Table 3.2, with the locations of Global Positioning System (GPS) points as bench marks.

Site no.	Latitude	Longitude	GPS/Prof. no.	Location
1	26 54 03N	48 25 53E	G1 (BM)	At road junction
2	26 51 09N	48 20 04E	G2	
3	26 58 05N	48 23 59E	G4	
4	26 58 23N	48 23 53E	G5	
5	26 54 33N	48 25 29E	G6 (BM)	At Wannan
6	26 48 10N	48 20 27E	G7	
7	26 59 08N	48 23 28E	G8	
8	26 45 15N	48 17 17E	P1	At Qullayib
9	27 00 42N	48 23 17E	P2	At Kahafah
10	26 56 46N	48 24 29E	P3	At Sabkhah
11	26 58 03N	48 19 49E	P4	
12	26 53 54N	48 24 50E	P5	
13	26 52 27N	48 21 26E	P6	
14	26 49 34N	48 19 01E	P8	
16	26 50 42N	48 21 05E	BH1	
17	27 04 42N	48 23 57E	BH2	

Table 3.2: Locations of VES Points, GPS Points and Borehole Data.

3.1.3 Interpretation of Resistivity Data

A four-pole vertical electrical sounding (4P-VES) Schlumberger array was used in the field work. This array is designed to analyze the variations in resistivity with depth. The sounding is performed by increasing the length of the AB transmission line while keeping the center O fixed. The current is sent in the ground through two electrodes (denoted A & B), and the potential difference between two electrodes (denoted M & N) is measured. MN is placed symmetrically at the center of AB, and the origin O is their common mid-point. The apparent resistivity is then calculated by the formula:

$$\rho_a = \frac{\pi L^2 \Delta V}{2lI} \tag{3.1}$$

Where

ρ_a	Apparent resistivity.
ΔV	Potential difference across the two electrodes (M & N) in m V.
I	Current sent to the ground in m Amp.
L	Half of the distance between A and B.
l	Half of the distance between M and N.

The data are interpreted by RESIX package for an expected resistivity and thickness model. The RESIXIP is a forward and inverse modeling program for the interpre-

tation of resistivity / IP sounding data in terms of a layered Earth (1-D) model. Sounding curves can be entered as a function of "AB/2" for Schlumberger soundings, "a" for Wenner soundings, "R" for dipole soundings, or "N" for dipole-dipole or pole-dipole soundings. Apparent resistivity data can be interpreted with or without the apparent polarization data. For the forward modeling the package is used for forward and inverse modeling of resistivity data. It uses Anderson style adaptive linear digital filter for most common arrays to provide resistivity contrasts in the range of 1 to 10,000 ohm-m. It calculates a synthetic IP / resistivity sounding curve for a model of up to ten plane layers. Resistivity sounding curves are calculated using linear filters. The IP sounding curves are also calculated with digital filters, using the method of Seara and Granda [26]. For the inverse modeling, the system produced a resistivity model which best fits the recorded data in a non-linear least squares manner. This is done by using a ridge regression, Inman [27], program to adjust the parameters of an initial starting model. The parameters can be either fixed or adjustable. The starting models for inversion can have up to 7 layers if both resistivity and polarization parameters are included, or 10 layers if only resistivity parameters are used. For equivalence analysis, the technique is used to generate a set of equivalent or alternate models, which fit the data nearly as well as the best fit model. This determines the allowable range of each of the model parameters. Resistivity sounding models are designed to be interpreted in terms of a layered earth model. If the earth underneath the sounding site is laterally inhomogenous,

the results of interpretation may not be related to the actual subsurface structure. The seven profiles along with their computer outputs are given in Appendix-A. The interpretation of the electrical resistivity data provides an electrical resistivity model which is correlated with the hydrogeological one. A generalized resistivity model is prepared from the interpretation of resistivity data for the study area, (Table 3.3).

Apparant Resistivities (Ohmm)	Thickness (m)	Geoelectrical Horizons
0.1 - 4	3 - 6	Sabkhah deposits
5 - 10	70 -100	Neogene formations
10 - 20	60 - 90	Mostly Alat member
50 - 100	40 - 62	Khobar member & Alveolina limestone member

Table 3.3: A Representative Resistivity Model of the Study Area .

3.1.4 Stratigraphic Correlation

The resistivity profiles, numbers 2 and 6, are tied up with boreholes 1 and 2 for stratigraphic correlation and resistivity model preparations. An interpretive geo-electrical section is constructed, Figure, 3.3.

The section is bounded from two sides by representative lithologic logs taken from the drilling of test wells for hydrogeological studies done by Italconsult[8] . The resistivity and thickness values of different lithological units were obtained from interpretation of resistivity data which further extended laterally through linear interpolation. The resistivity values are within the range of proposed resistivity model. representing the subsurface geoelectrical horizons of the study area, Table 3.3. The lateral and vertical extent of subkhah deposits are delineated as thin, highly conductive layer near the surface. The resistivity contrast between the first layer (probably Neogene formations) and the second layer (propably Alat member) is clearly marked on the section. The highly resistive horizon of more than 50 ohmm is represented as the top of the Khobar limestone member. The thickness of different units sharply increases towards northeast at a small distance, indicating the boundary of a probable collapse structure. Figure. 3.3.

The resistivity modeling is done to calculate the variations in thicknesses of lithologic units either due to sedimentation and erosion or due to the formation of collapse structures. The boundary of the probable collapse structures can be delineated by

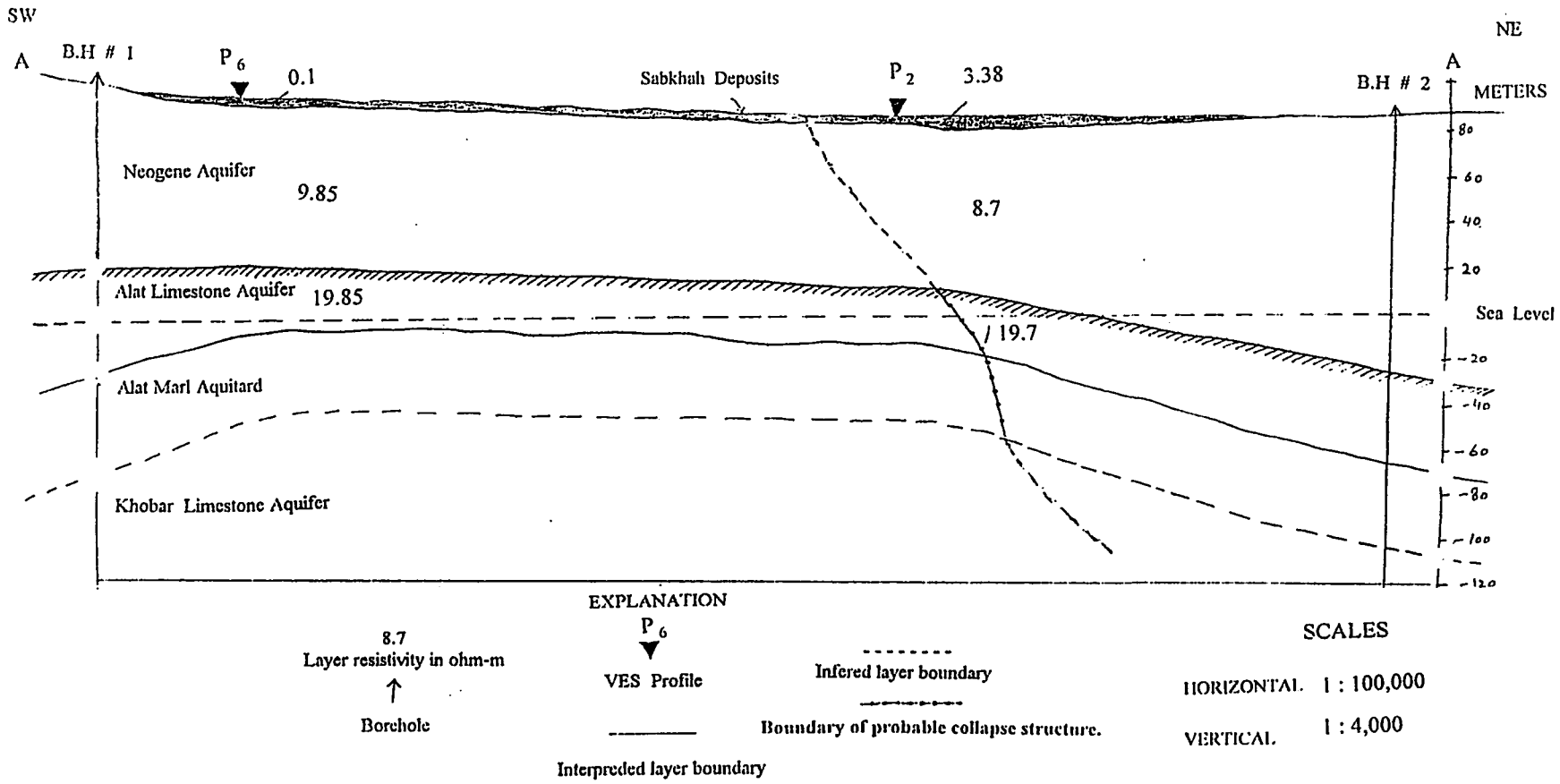

Figure 3.3 : A representative Geoelectrical Section for Wadi Al-Miyah Area, interpreted through Geoelectrical modeling.

sharp change in thickness at a short distance, which is corresponding to the maximum inflexion point of the resistivity layer.

The calculated thickness and depths to various lithologic units from resistivity modeling are used in groundwater simulation model. These values are used as input data for simulation. They provided a control on thickness variations of different hydrogeological units where borehole data are sparse, Tables 3.4 and 3.5.

Profile No	Model Node number	Calculated Thickness (m)
1	207	36 - 40
2	429	70 - 80
3	364	95 - 100
4	368	69 - 70
5	362	79 - 80
6	302	69 - 70
7	336	35 - 40

Table 3.4: Correlation of Resistivity Profiles and Nodes of Groundwater Model for Neogene Formations

Profile No	Model Node number	Calculated Thickness (m)
1	207	greater than 6
2	429	greater than 24
3	364	greater than 32
4	368	30
5	362	52 - 55
6	302	greater than 28
7	336	40 - 50

Table 3.5: Correlation of Resistivity Profiles and Nodes of Groundwater Model for Alat Member

3.2 Groundwater Modeling

The primary goal of groundwater modeling is to evaluate the effects of pumping on water levels and solute distribution patterns and to predict the behavior of flow regime of the aquifer system under these stresses. A great number of wells were drilled to pump irrigation water. High pumping rates over long periods of time from many wells are applied simultaneously without consideration of the hydraulic properties of the aquifers. As a result, great drawdowns and low well-yields are experienced. Detailed hydrogeological data analysis and groundwater modeling are used to understand and predict the effects of these stresses on the aquifer system. The information gained from the electrical resistivity and groundwater models are used to develop a model for the various mechanisms of aquifer dynamics in the study area. Numerical methods such as finite element and finite difference are used to model complex groundwater systems.

A computer simulation model "Saturated-Unsaturated Transport" (SUTRA), Voss, [23], was used to delineate salinity variations due to changes in chemical composition of the groundwater or probable saltwater intrusion. It is a finite-element simulation model for saturated-unsaturated, fluid-density dependent groundwater flow with energy transport or chemically reactive single-species solute transport. It is helpful in solving various problems such as watertable rise, groundwater depletion, high salinity problems at various locations within the study area.

3.2.1 Description of the Model

The SUTRA (Saturated-Unsaturated Transport) model, Voss [23], is a modular computer code written in Fortran-77 that simulates the fluid movement and the transport of either dissolved substances or energy in the subsurface. It uses a two-dimensional, combined finite-element and integrated finite difference method to approximate the equations that describe the above two interdependent processes. SUTRA is based on a general physical, mathematical and numerical structure implemented in the computer code in a modular design. It is primarily a two-dimensional simulation of flow and solute transport model, although a three dimensional quality is provided because the thickness in the third direction may vary from point to point. Simulation may be done in either the aerial plane or in a cross-sectional view. The spatial coordinate system may be either Cartesian (x,y) or radial-cylindrical (r,z). SUTRA tracks the transport of either solute mass or energy in the flowing groundwater through a unified equation. Solute transport is simulated through numerical solution of a solute mass balance equation where solute concentrations may affect fluid density. The main concept of this approach is the discretization of space into elemental volumes and the evaluation of mass balance simultaneously for each element, Voss [23].

3.2.2 Conceptual Model of the Area

The study area is characterized by two main groundwater systems: A shallow water-table system (Neogene), and a deep artesian system (Alat & Khobar). The shallow system is being recharged by precipitation. It is used by local inhabitants through domestic wells. Limestones and marls of Eocene age comprise the deep artesian aquifers which are recharged towards the west where they outcrop. The main hydrogeological units of the study area were modeled on the basis of lithostratigraphic characteristics and hydraulic properties such as permeability and storativities, Figure.3.4. The existing three aquifer units, from top to bottom, are shown in Table 3.6 as:

1. CA1 : The Neogene aquifer, unconfined, limestone unit.
2. CA2 : The Alat limestone aquifer, confined.
3. CA3 : The Khobar limestone aquifer, confined.

The corressponding three confining aquitards are :

1. CB1 : Neogene interface compact horizon, slim aquitard.
2. CB2 : Alat marl (Orange marl)
3. CB3 : Lower Dammam-Rus Aquitard. A composite aquitard includes Midra and Saila shale member, Alveolina marl member, and Rus anhydride formation.

Type	Unit	Formation/Member	Thickness (m)
Unconfined Aquifer (1)	CA1	Neogene/Undifferentiated	50 - 125
Confining Aquitard (1)	CB1	Neogene Interface	5 - 10
Confined Aquifer (2)	CA2	Alat Limestone	36 - 57
Confining Aquitard (2)	CB2	Alat Marl (Orange Marl)	10 - 30
Confined Aquifer (3)	CA3	Khobar Limestone	55 - 125
Confining Aquitard (3)	CB3	Lower Dammam-Rus (Midra-Saila Shale. Alveolina marl. Rus Anhydrite)	25 - 194

Table 3.6: Simulation Model of the Aquifer System.

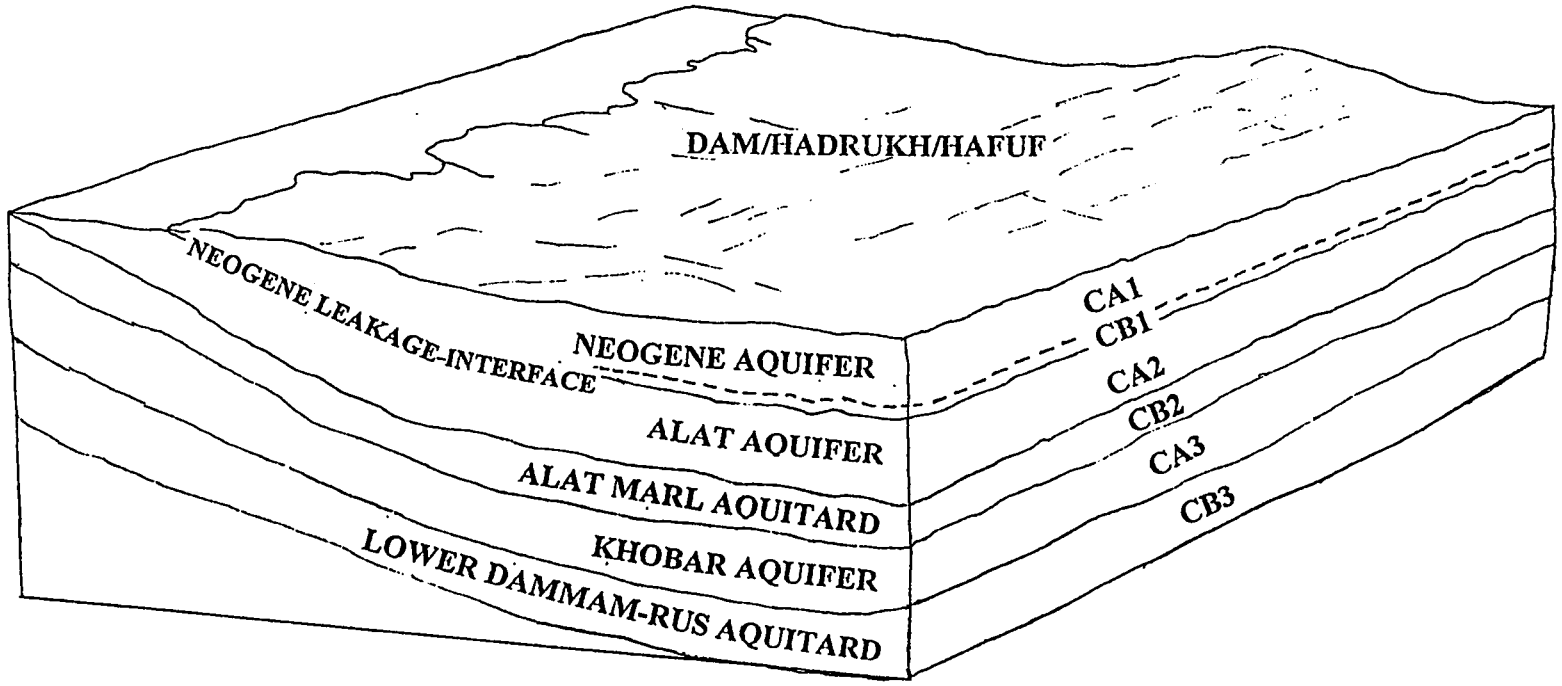

Fig. 3.4 CONCEPTUAL MODEL OF THE AQUIFER SYSTEM

3.2.3 Mathematical Model of the System

The mathematical model comprises a set of partial differential equations together with appropriate boundary and initial conditions, with simplifying assumptions which expresses fluid and solute mass balance and other phenomenological laws that describe continous variables over the model domain. The Darcy equation and the principle of continuity are essentially the major components in development of a generalized equation for the fluid mass balance of the aquifer system. The model simulates the groundwater flow and solute transport, using the fluid and solute mass balance equations and calculates the heads and solute (Chloride) concentrations throughout the model domain. A general form of fluid mass balance equation for two dimensional groundwater flow, as implemented by SUTRA may be written in vector notation as:

$$(S_w \rho S_{op} + \phi\rho\frac{\delta S_w}{\delta_p})\frac{\delta p}{\delta t} + (\phi S_w \frac{\delta p}{\delta c})\frac{\delta c}{\delta t} - \nabla[(\frac{k k_r \rho}{\mu}).(\nabla p - \rho g)] = Q_p \qquad (3.2)$$

p(x,y,t) is the fluid pressure.

c(x,y,t) is the fluid solute mass fraction .

Q_p(x,y,t) is the fluid mass source (including pure water mass + solute mass dissolved in source water).

S_{op}(x,y) is the specific pressure storativity.

S_w(x,y,t) is the water saturation (volume of water/volume of voids).

k(x,y) is the solute matrix permeability (2×2 tensor of values).

k_r(x,y,t) is the relative permeability to fluid flow.

ρ(x,y,t) is the fluid density.

ϕ(x,y,t) is the porosity.

μ is the fluid viscosity.

In SUTRA, the general form of solute mass balance equation for conservative solute (Chloride) in a solution, is written in vector notation as :

$$\frac{\delta(\phi S_w \rho C)}{\delta t} = \nabla[S_w \phi \rho (D_m I + D). \nabla C] - \nabla.(S_w \phi \rho \dot{v} C) + Q_p C' \qquad (3.3)$$

v(x,y,t) is the average two dimensional velocity.

C'(x,y,t) is the solute concentration of fluid source (mass fraction) .

D(x,y,t) is the coefficient of hydrodynamic dispersion.

D_m is the apperent molecular diffusivity of solute in solution in a porous medium.

I is the identity tensor (one on diagonal, 0 elsewhere) (2 × 2).

Assumptions

1. Flow is horizontal and in two dimensions as flow in a single anisotropic layer.

2. Uniform, isotropic and homogeneous hydrogeologic characteristics are assumed of the aquifer within each elemental volume.

3. Fluid density variations due to variations in solute contents of groundwater is negligible.

4. Parameter variations are changing in X-Y directions and uniform in Z-direction as vertically averaged values. (Two-dimensional model)

5. Leakage through the confining bed into the aquifer is vertical and proportional to the difference in the head between aquifer and the head in an overlying or underlying source aquifer.

6. Head in the source aquifer (Umm Er Radhuma aquifer) is invariant with time (no effects of stresses) and storage in the confining bed (aquitard) is neglected.

7. The model boundaries perpendicular to flow lines are assigned as no flow boundaries (northeastern and southwestern).

8. Constant head boundaries are ineaxhaustible source of water during a given simulation time.

9. Variations due to approximation of variables in mass balance equation either elementwise, nodewise or cellwise are neglected.

3.2.4 Numerical Model

The model uses the finite element and integrated difference hybrid method to solve the partial differential equations. Each hydrogeologic unit (aquifer) is divided into

a single layer of rectangular finite elements with finite thickness in third space direction, forming a finite element mesh (grid). The elements are connected with each other by nodal points which lie in the X-Y plane. Thus, each element has a three-dimensional shape, having four nodes, each of which representing the entire Z-axis on which it is located. The variations in aquifer parameter values from point to point in the aquifer are represented by assigning constant values either to individual elements (elementwise) or to each node in the mesh (nodewise, or cellwise).

Numerical solution involves the approximation of the partial differential equations with a set of discrete equations in time and space. The model domain is discretized in required time steps, and spatially into a number of elements and nodes. The set of equations are solved for each element and time step. These discrete equations are combined to form a system of algebraic equations which are solved for each time step.

A generalized model development and solution sequencing employed in SUTRA for solution of the differential equations is given in Figure, 3.5.

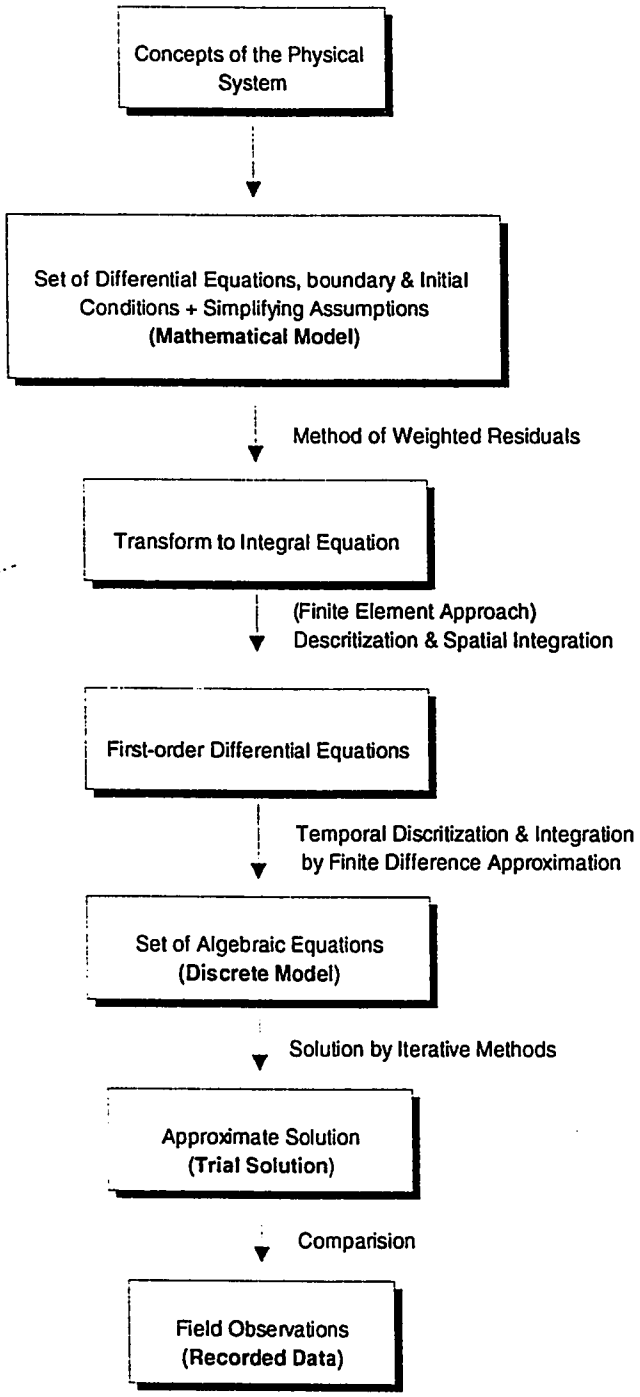

Figure 3.5: Generalized Model Development and Solution Sequencing for Differential Equations

3.2.5 Groundwater Flow System

A complete understanding of a hydrologic system is a prerequisit for the development of the groundwater flow model which includes definition of the system geometry, the natural hydrologic boundaries, the hydrogeologic parameters of major units and the general patterns of the groundwater and solute movement. Each aquifer in our study area has an established hydraulic gradient that decreases towards east and north and a salinity gradient, changing from good quality water in the west to poor quality to the east and north. The gradient follows the regional dip of the sedimentary rocks except where it is modified by local anticlinal structures, lateral and vertical changes in porosity and permeability or by recharge from a large wadi system [8].

Predevelopment Steady State Flow System

A steady state may be defined as a mean and trend-free condition which is represented by an average groundwater surface. A balance exists between inflows and outflows, causing an equilibrium condition between the flow movement and solute distribution pattern in the flow domain. Such conditions often exist in the aquifer system prior to the start of the development schemes. Predevelopment period represents the natural groundwater flow system with no stresses that cause significant changes in the flow and solute distribution pattern of the aquifer. The ideal steady state condition does not exist in reality. So, pseudo steady-state condition is consid-

ered on the basis of collected and published data. As the expansion in agricultural and municipal consumption has been increased after the year 1967, it is reasonable to assume that the predevelopment condition had prevailed before the year 1967.

Groundwater Flow Pattern

The analysis of piezometric surface maps shows an easterly regional hydraulic gradient from southwest to northeast, towards the Arabian Gulf, causing a regional movement of groundwater in the three aquifers, Italconsult [8], Figures, 3.6. 3.7, and 3.8. The present gradients are fossil remnants of conditions created by a wet climatic regime prevailed some thousands of years ago, as determined by isotope studies, Bakiewicz et al. [11]. The piezometric contours generally follow the trend of the outcrop in the west and the coastline in the east. Groundwater movement is influenced by regional hydraulic gradient and by the presence of subsurface structures in which formation permeabilities are generally higher, Italconsult. [8]. The analysis of these maps indicates the differences in the hydraulic gradient at different locations. A considerable variation in the flow regime occurs due to the variations of the hydrogeological characteristics of the aquifers, (Figures 3.6, 3.7, and 3.8).

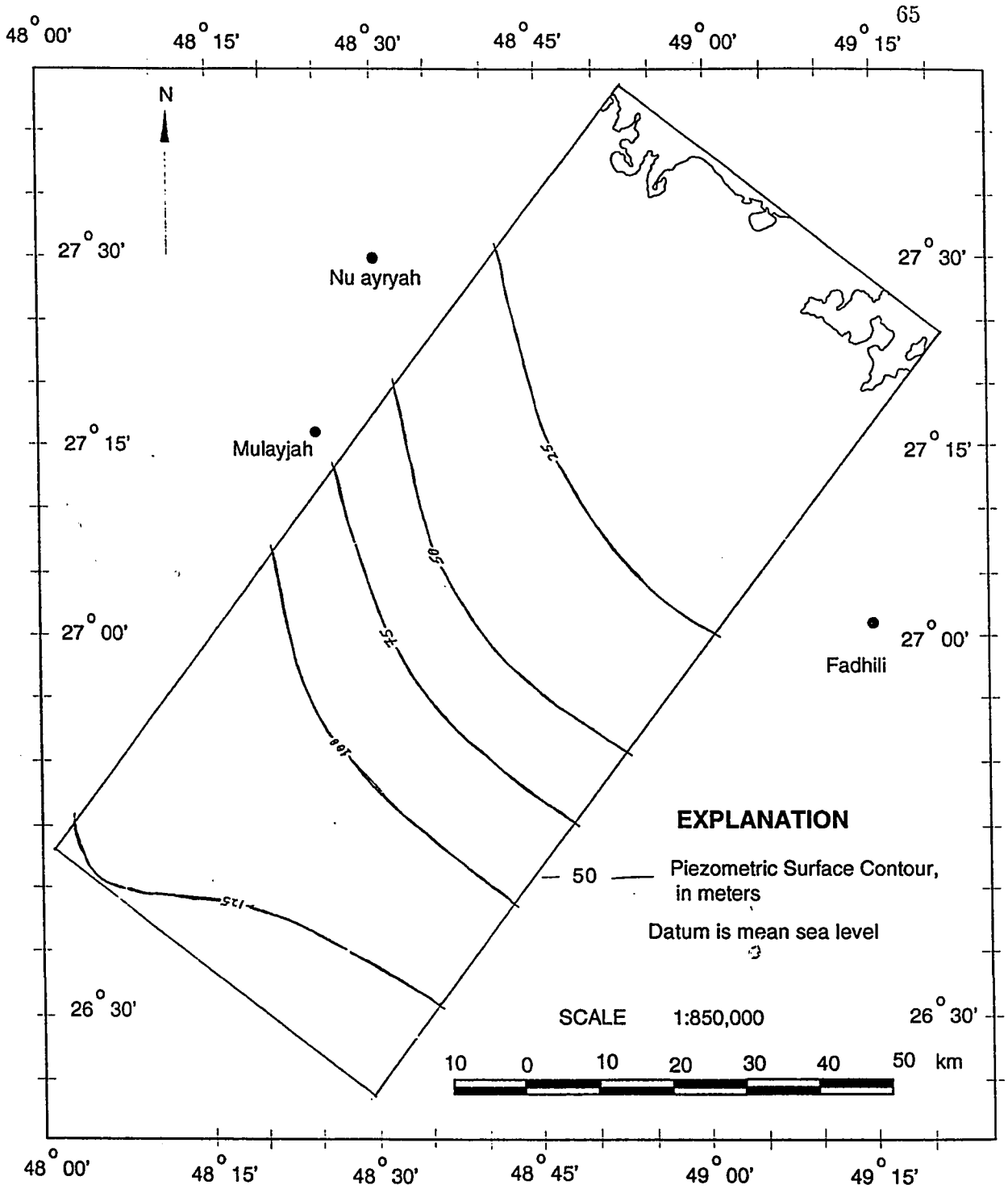

Figure 3.6: Peizometric Surface Map of Khobar Aquifer for the year 1967 (after Italconsult, 1967).

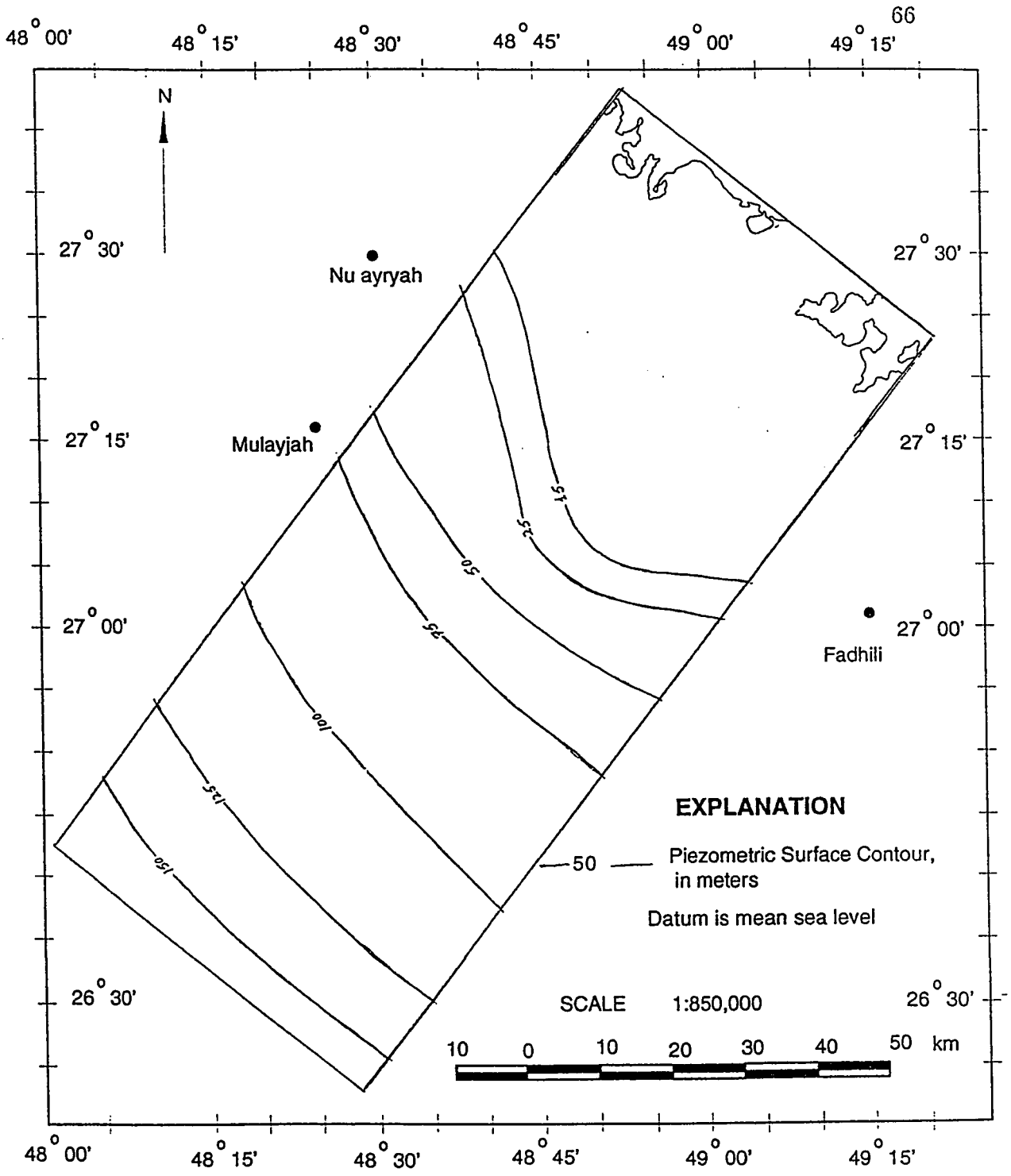

Figure 3.7: Peizometric Surface Map of Alat Aquifer for the year 1967 (after Italconsult, 1967).

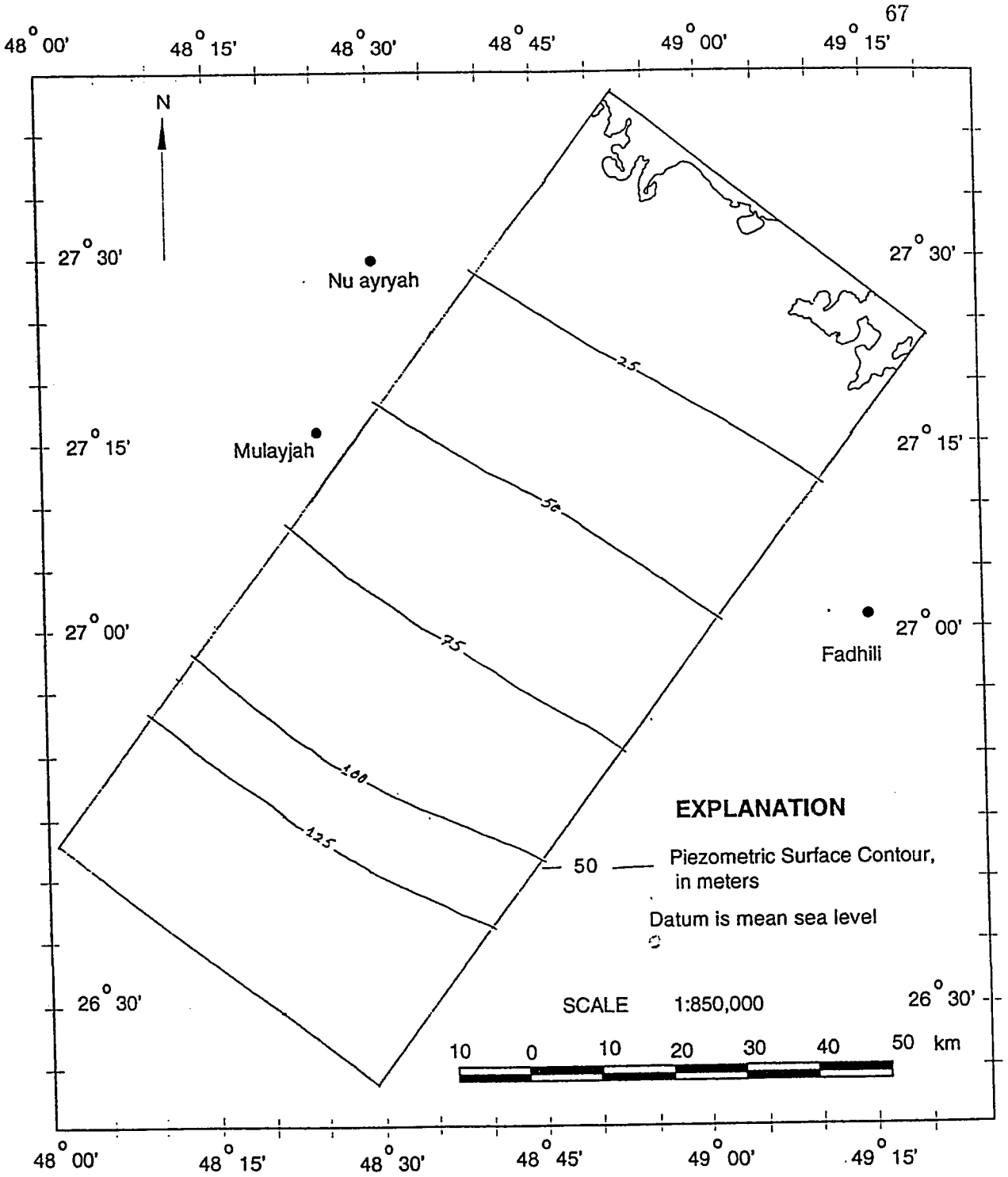

Figure 3.8: Water level Surface Map of Neogene Aquifer for the year 1967 (after Italconsult, 1967).

These patterns indicate the variations in permeabilities due to subsurface structures, local recharge and/or withdrawals from the aquifers. The analysis of piezometric surface map of Khobar aquifer shows a general SW-NE direction of flow, with a uniform hydraulic gradient which is relatively constant with little deviations at the left corner of the study area, Figure, 3.6. The constructed hydraulic gradient section shows relatively steep gradients west of the Coastal line 2.2 m/Km to as much as low 0.3 m/Km near the shoreline. The low gradients near the coast are due to high transmissivities, idicating the existence of a natural discharge area from the Alat-Khobar aquifers. The general groundwater movement in Alat aquifer is also SW-NE, with almost constant regional hydraulic gradient but it flattened between Abu Hadriya and the coast, Figure,3.7.

In Neogene aquifer the freshwater flows with a high velocity towards the Arabian Gulf, causing a flushing action on the salt contents of the aquifer. The flow direction is SW-NE, Figure, 3.8. The local modifications in flow regime may be due to presence of sabkhahs and local extractions.

Vertical Flow of Groundwater

The stable isotope data show that groundwater from Umm Er Radhuma aquifer moves upwards to Khobar and Alat aquifers, Shampine et al. [13]. The vertical flow is controlled by a number of factors, among them are vertical hydraulic conduc-

tivites, nature and thickness of aquitards and head difference across aquifers. The piezometric surface maps of the four aquifers including Umm Er Radhuma, were laid on top of each other and analyzed. The study area was then divided into a number of leakage zones on the basis of the difference in piezometric levels, Figure. 3.9. The zones of different piezometric levels indicate that the aquifers are separated by effective aquicludes or otherwise the aquifers were in hydraulic continuity and a vertical flow is taking place. The distribution of chloride concentration pattern also verifies the vertical leakage from Umm Ur Radhuma aquifer to Neogene aquifer. Figure 3.10 is a vertical section drawn at the middle of the study area to show the major flow directions within the aquifer system.

A detailed analysis of the piezometries and their relationships with the vertical flow patterns has been done and various leakage zones were delineated. Near the coastal region, the static water level in the Neogene is markedly higher than in the Alat and Khobar aquifers, but lower than in Umm Er Radhuma formation. So, downward flow to Alat aquifer is dominant in this region. The low transmissivity values in Umm Er Radhuma aquifer at various locations and the partial interfused nature of Alat and Khobar aquifers due to joint systems forces the water to rise through the Rus anhydride into the overlying Dammam and Neogene aquifers, G.D.C [10].

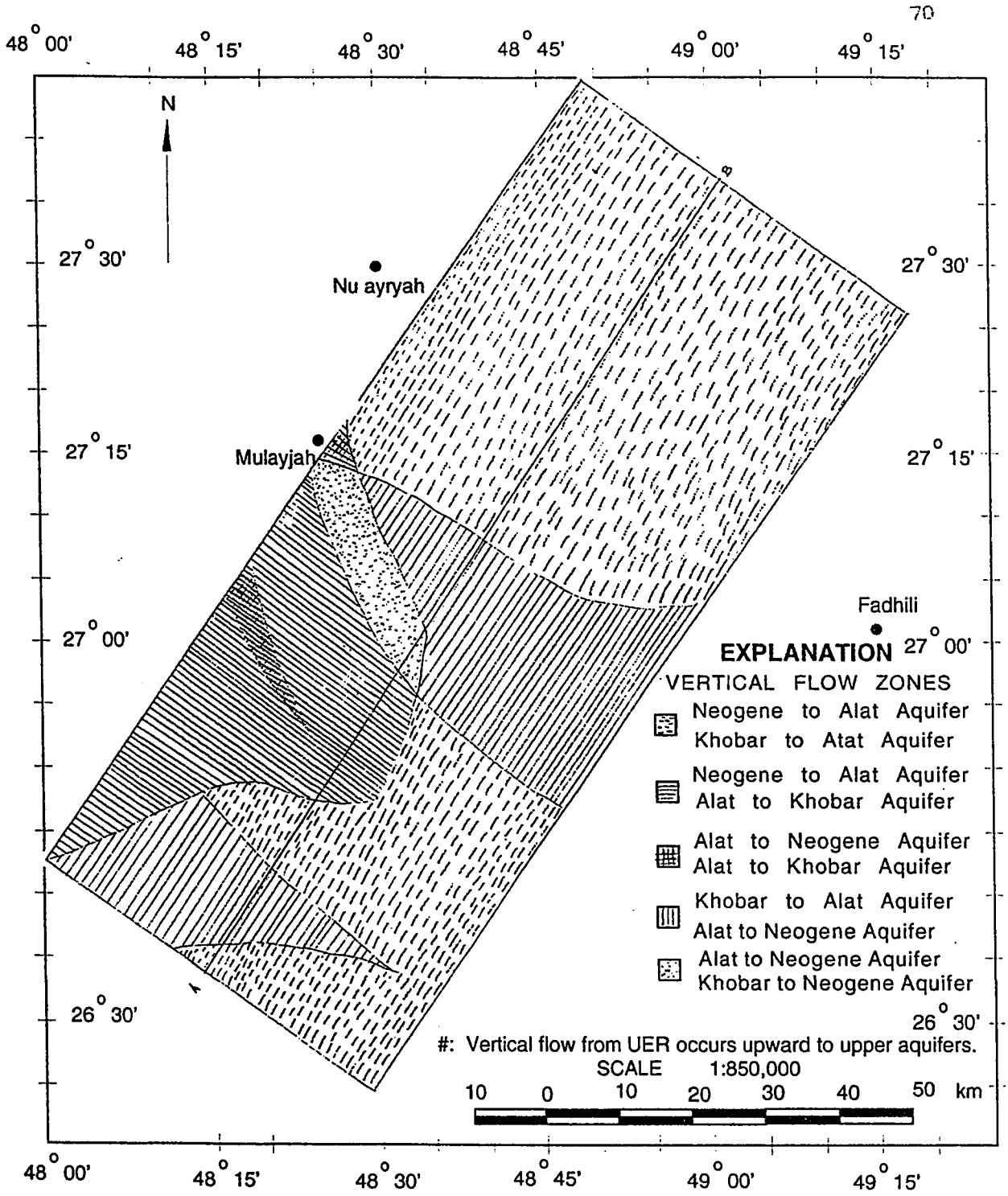

Figure 3.9: Vertical Leakage Zones due to Flow from underlying or overlying Aquifers through Aquitards.

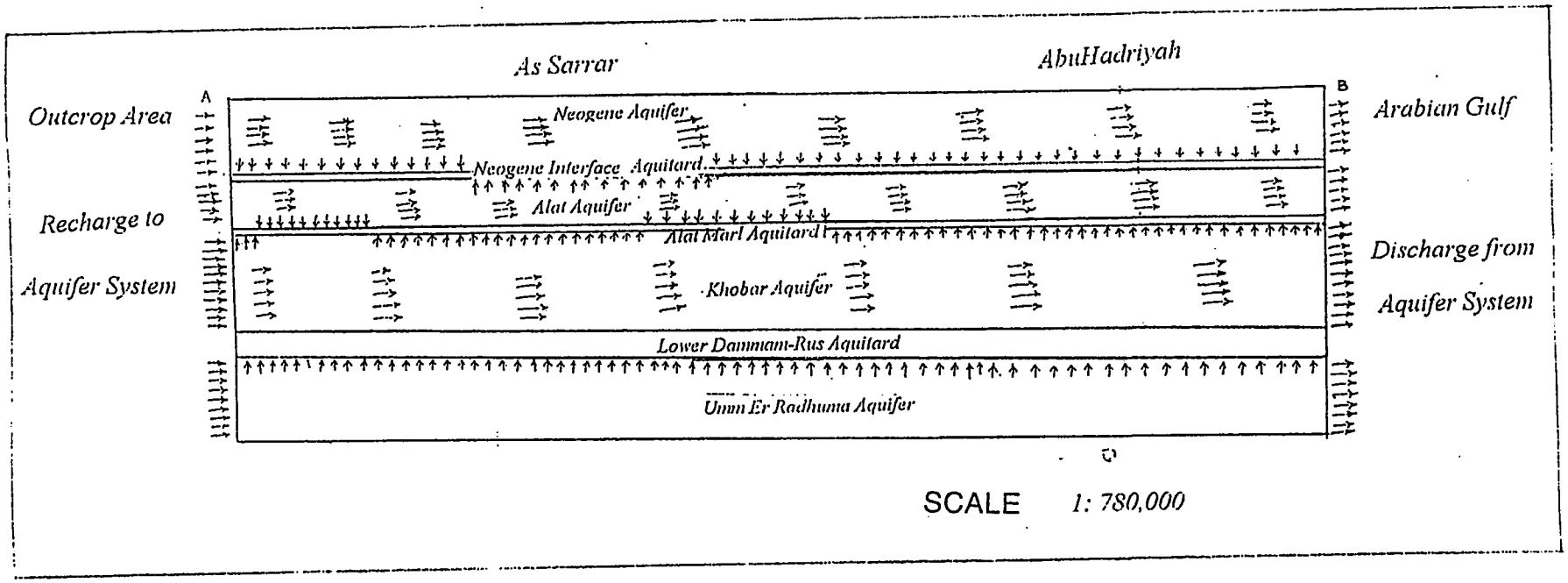

Figure 3.10: A Sectional View of Groundwater Flow Pattern showing Principle Flow Directions.

Solute Distribution Pattern

In the study area the regional salinity gradients for the different aquifers are similar. There is a general increase in salinity towards east, near the coast. These variations in salinity patterns are caused by a number of processes such as flushing action of groundwater as it moves through the saline aquifer matrices, changes in speed of groundwater, leakage from oil-field brine during injection operations, vertical leakage from saline formations due to inperfections in aquicludes, or concentrated centers of extractions. Local variations in porosity and permeability cause minor changes in hydraulic gradients as evident from piezometric surface contour maps of different aquifers.

In the study area, the most obvious chemical changes, taking place as the groundwater moves through the aquifers, are the overall increase in salinity and the change of chemical species from calcium bicarbonate through calcium sulfate to sodium chloride. Bakiewicz et al. [11]. Aquifer matrices are very saline and the flushing action of groundwater causes a gradual quality deterioration such as the accumulation of high concentration near the coast, deJong[16].

During the pluvial periods, precipitation was much heavier, causing high infiltration which was sufficient to flush the aquifers, removing the transgressional marine waters in the upper part of the formations and replacing them by meteoric waters. But during marine transgressions, the meteoric waters would have been replaced by

seawater. This cycle was repeated many times and led to the formation of saline bodies at the bottom of the aquifers, Burdon [28]. This is indicated by the isochlore map of Umm Er Radhuma aquifer which shows very high concentrations in excess of four times the concentrations of seawater (brines) towards the coast close to the major oilfields, Figure, 3.11

Another theory regarding the high salinity suggests that Umm Er Radhuma aquifer should be considered as an aquifer containing highly saline water bodies (brines) at its upper part near the coast (Uqaily M., Personal communication, 1994). These are old trapped lagoons, disconnected intermittently from the sea. Evaporation resulted in a very high salinity up to 70,000 ppm. The pumping operations near the coastal area enhanced the vertical leakage from the saline bodies to Khobar and Alat aquifers.

Other possible source of high salinity is the leakage of oil-field brine, either from surface disposal ponds during the early history of oil and gas development or during injection operation of oil-field brines into the fractured Dammam and Umm Er Radhuma formations.

Imperfection in aquicludes due to collapse structures or solution channels between the aquifers caused the extensive vertical leakages, deJong [16]. This lead to the division of the study area into different leakage zones. The high rate of leakage particularly near Abuhadriya and Manifa area caused a high salinity, indicated by high chloride concentration up to 10,000 ppm, Figures 3.12 and 3.13.

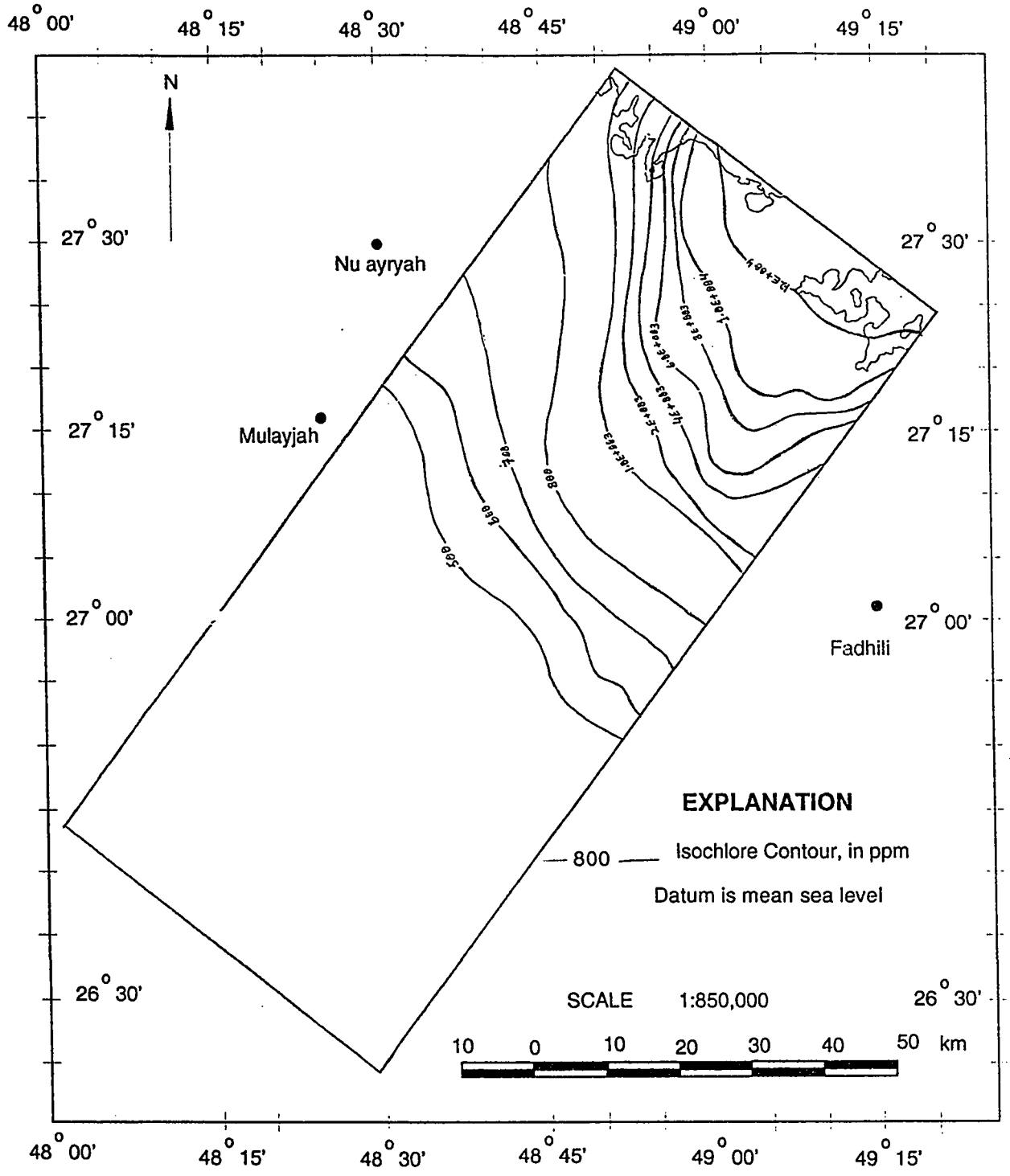

Figure 3.11: Isochlore Map of Umm Er Radhuma Aquifer for the year 1967, (source data collected from Italconsult,1967. G.D.C.,1979)

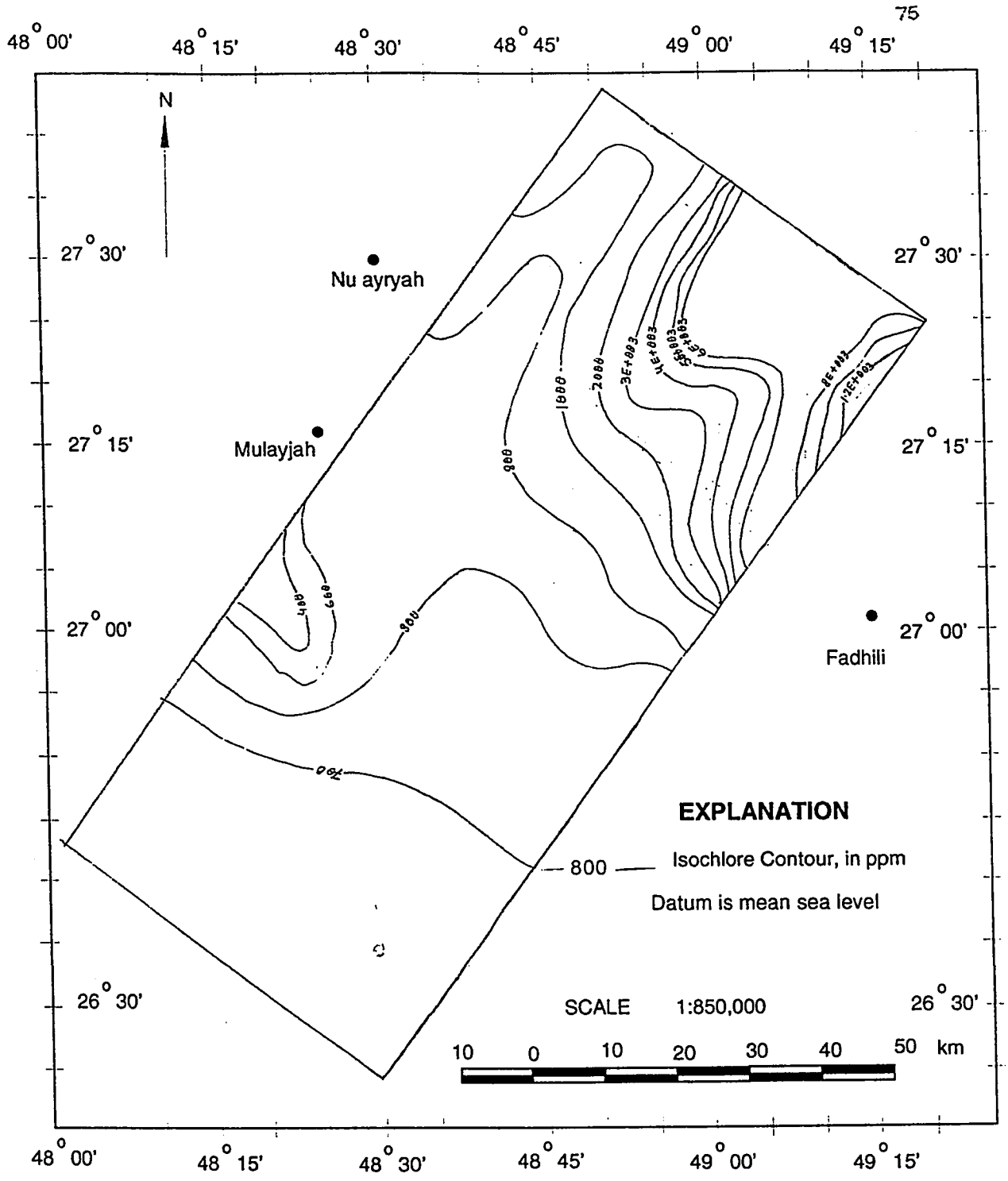

Figure 3.12: Isochlore Map of Khobar Aquifer for the year 1967, (source data collected from Italconsult,1967, G.D.C.,1979)

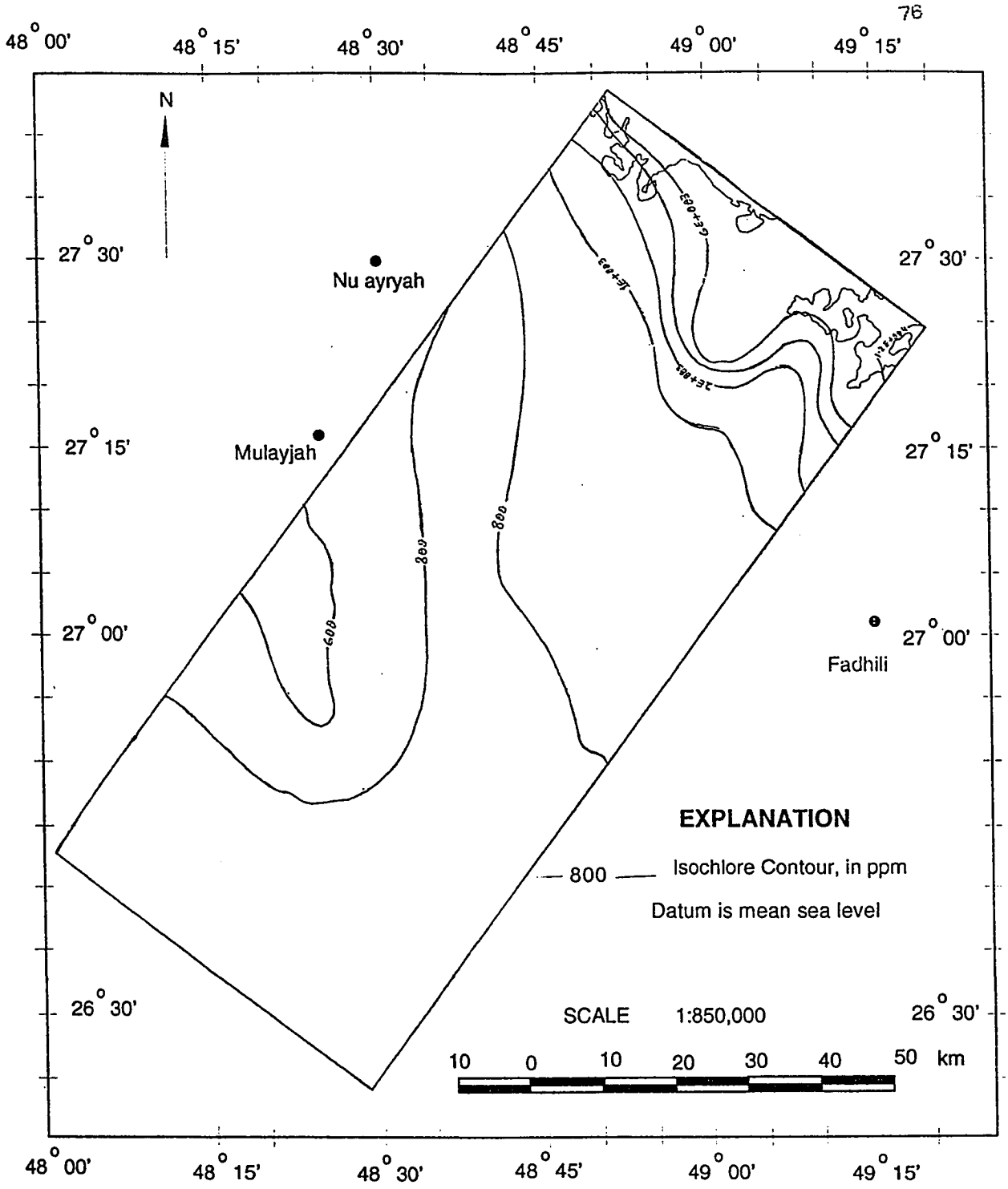

Figure 3.13: Isochlore Map of Alat Aquifer for the year 1967. (source data collected from Italconsult.1967, G.D.C.,1979)

The source data was collected from unpublished reports of Italconsult, [8], G.D.C., [10]. Near As-Sarrar area vertical leakage from Umm Er Radhuma to upper shallow aquifers reached up to Neogene aquifer which is depicted from the low concentration zone at that place, Figure, 3.14. The isochlore maps of the four aquifers, including Umm Er Radhuma, show the major trends in the distribution of chlorides and the interrelationship between flow and salinity distributions. They also provide relative rate and direction of groundwater movement within various aquifers. The low salinities occur where groundwater movement is high while high salinity values are associated with zones of no flow. There is a high amount of leakage between aquifers which also contributed to the variations in salinities at different locations.

Piezometric surface and salinity maps indicate that flow and salinity contours are opposite in direction which may be caused by the complex geometry and by the variations in the hydraulic characteristics of the aquifers.

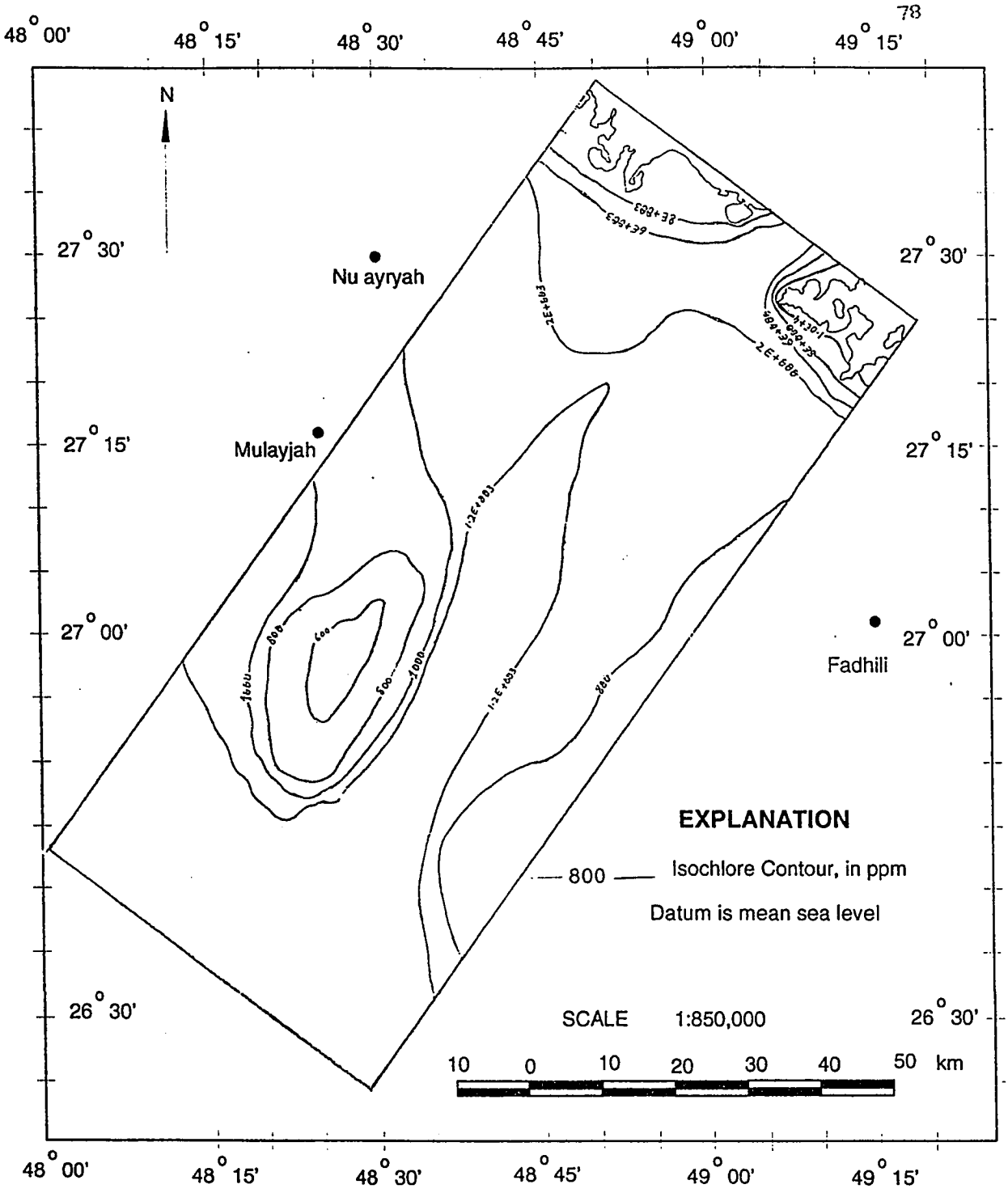

Figure 3.14: Isochlore Map of Neogene Aquifer for the year 1967, (source data, collected from Italconsult.1967, G.D.C..1979)

Transient State Flow System

Recent studies indicate that excessive pumping near the coastal area is greatly deteriorating and even dewatering the shallow aquifers. This is evident from the distribution of pumping wells in the study area, Figure, 3.15. This excessive pumping has caused evasive effects on the groundwater flow system in the study area. The current estimated extraction rate is 360 Mm^3/year for Dammam aquifers. The total extraction is greater than natural recharge [16] which resulted in:

1. Falling of piezometric heads.
2. Reduction in flow from springs.
3. Salinization of shallow aquifers by either seawater invasion or upward migration of deep saline groundwater.

In the study area, the groundwater is continued to be exploited at an increasing rate mainly by agricultural and oil drilling operations, which already have exceeded the aquifer safe yield, Pike [14]. The high pumping rates enhanced the saltwater intrusion either from Arabian Gulf or from deep highly saline formations.

The depositional environment of various hydrogeologic units was shallow marine with frequent episodes of very shallow brakish water, evaporatic periods (shallow lagoons or old coastal sabkhahs) causing the deposition of anhydrite and gypsum with halite associations in Umm Er Radhuma formation, Powers et al. [25].

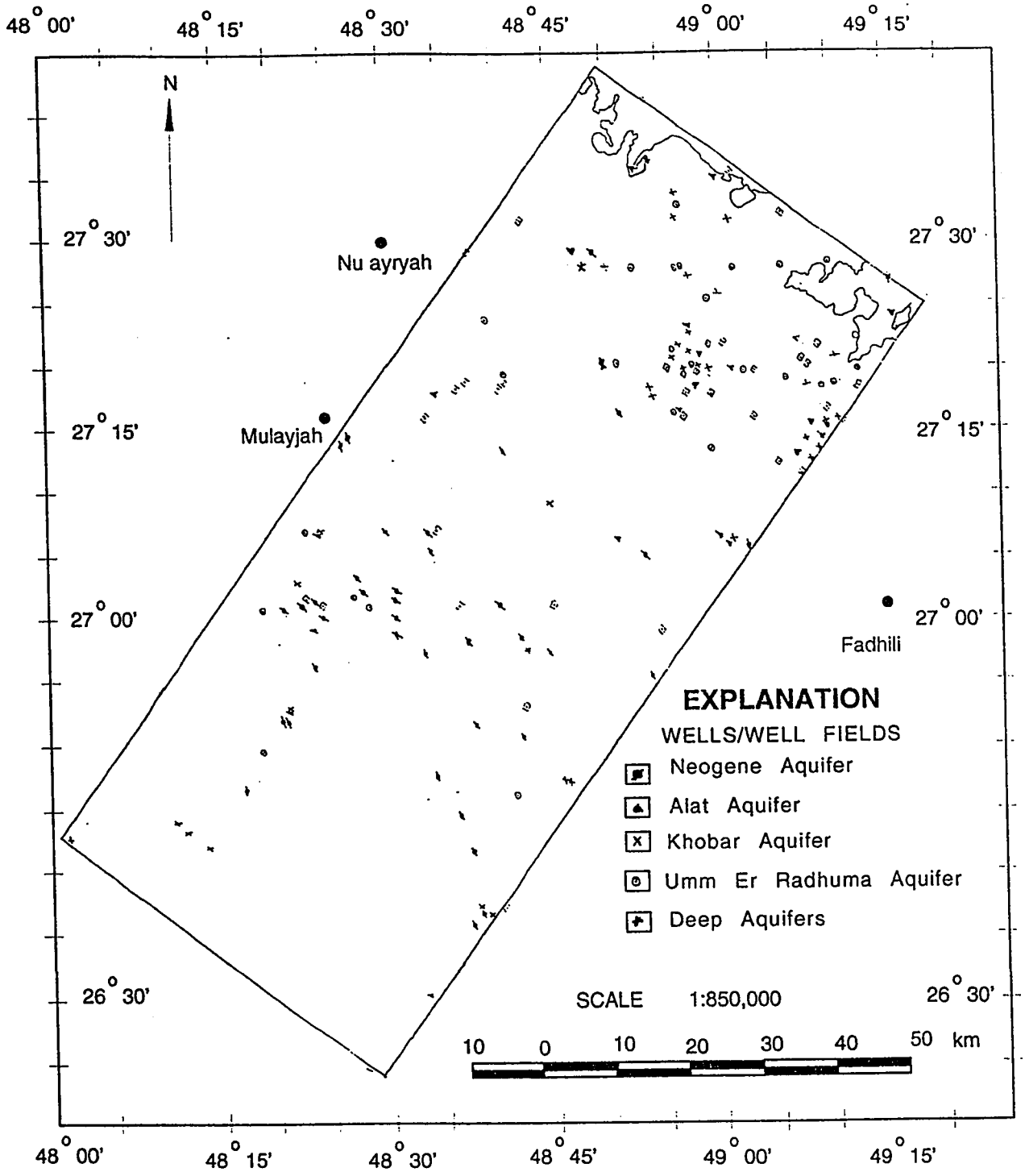

Figure 3.15: The Areal Distribution of Wells/Well fields extracting Water from different Aquifer Horizons within the Study Area, source data collected from Italconsult.1967, G.D.C.,1979

In the coastal region, the salinity of groundwater in Umm Er Radhuma formation increases rapidly from 4000 ppm to 30,000 ppm in the northeast direction. Variable lithological characteristics and the rapid changes in thickness of Rus formation due to collapse structures, greatly influence the groundwater flow system. The eroded anhydrite and gypsum sequence of Rus formation acts as zones (windows) for upward or downward flow of groundwater, if piezometric head difference is high enough. The vertical flow through an aquitard increases with decrease in thickness and increase in vertical permeability. The aquifers and aquitards have relatively uniform thickness and extend below the Arabian Gulf, upto a considerable distance. Figure, 3.16. The seawater seeps downward due to vertical leakage through Alat and Rus-Dammam aquitards. The continued pumping with high rates near the coast enhanced the upward leakage of freshwater through aquitards above. So, a hydrostatic equilibirium condition is established between upward freshwater leakage between aquifers and downward saltwater leakage from sea to aquifers.

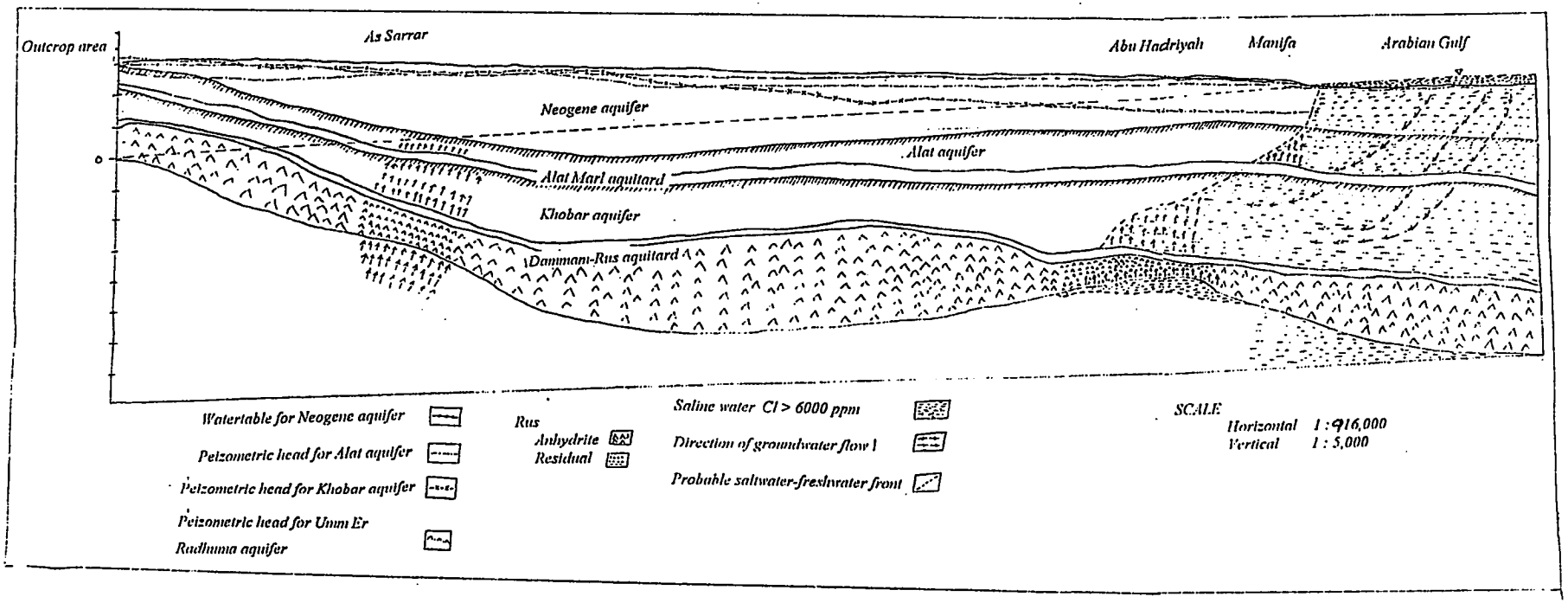

Figure 3.16: A Hydrogeological Section of Aquifer System related with dynamics of Flow Regimes in various Units, showing various Saline Intrusion Mechanisms.

Chapter 4

Computer Simulation

Vertical flow is dominant in all aquifers due to the difference in heads, especially from Umm Er Radhuma to Dammam aquifers, Shampine et al. [13], G.D.C. [10]. All aquitards are leaky in the study area, especially, Rus formation is eroded and thins out due to dissolution processes near As-Sarrar, Fadhli, Manifa and Abuhadriya, causing leakage of high salinity water into Khobar and Alat aquifers. Pumping in these areas enhanced the leakage without causing appreciable decrease in heads in these aquifers. Due to high lateral velocities, the high salinity water moved towards the southeast corner of the model area.

The SUTRA model is used for an areal fluid-density dependent groundwater flow and solute transport of a conservative solute (chloride) to analyze the groundwater flow regime and the salinity variations in the model area Voss[23]. Chloride is used as conservative and highly mobile aqueous species. It moves through aquifers at

similar rates as water molecules and it acts as an ideal tracer for studying intrusion processes. For this reason, high chloride concentration is considered to be the best indicator of possible saltwater intrusion. Hem[29].

Water that enters the model area at a given node as a result of a pressure gradient at the boundary is of specified concentrations: water that exits at such node is of ambient aquifer concentrations. The aquifer system is simulated by six hydrogeological units. Lateral and vertical permeabilities are assumed to vary within each of the six units. Groundwater flow is simulated through numerical solution of fluid mass balance equation. Almost all the aquifer properties which are used in the model varied in values throughout the model area.

4.1 Discretization of the Study Area

In any numerical modeling study, compromises are necessary between detailed analysis and data availability, data handling and computer resources. The model grid should, with a fully three-dimensional perspective, correctly represents the geometry of the groundwater system in a discrete form. The model was discretized into 1170 rectangular elements (39 by 30), each having dimensions of 3.34 by 2 km, resulting in 1240 nodes. Mesh thickness represents the aquifer thickness, varying laterally throughout the model area.

The model grid is oriented 55 degrees towards northeast to achieve the best alignment with the heads of these aquifers which helped in establishing the model boundaries and specifying the input parameters. In the Neogene aquifer, the mesh size of model elements 1050 to 1170 is reduced from 3.6 to one kilometer to avoid numerical spatial oscillation as caused by sharp concentration gradient at the seawater and freshwater interface.

4.2 Boundary Conditions

The boundary conditions are classified as general types such as constant head and constant flux boundaries which are representing the physical boundaries of the aquifer system. The details of each boundary types used in the present modeling study are given in the following sections.

4.2.1 Constant Head & Flux Boundaries

The regional flow is generally from SW to NE towards the Gulf. It is idealized as a flow originating in a constant head boundary at the western side of the model area. The eastern side of the model grid is also assumed as a constant head boundary. It is also assumed that these boundaries are not affected by pumping. During simulation. this is achieved by assigning sufficiently high values of leakage coefficients at the nodes in the flow equation. A single value of constant head is specified

along the western boundary for simulation of sea-level which is assumed as constant throughout the simulation period. This assumption is well supported by results of sea level fluctuation studies by Evans [2] which indicates a rise in sea level of about two meters above the present level during the period of 6000 to 4000 years B.P. The sea level then decreased successively upto present level until 1000 years B.P., which remained constant after that period.

The eastern and western boundaries for the aquifers are assigned as constant flux boundary as the chloride concentration is remained constant throughout the simulation periods.For the Neogene aquifer, the chloride concentration of inflow at the western boundary is assumed as constant (i.e. 1250 ppm) while towards the eastern boundary as an average chloride concentration of sea water (i.e. 25,878 ppm). It is assumed that the saltwater-freshwater transition zone was in equilibrium condition with current sea level.

4.2.2 No-flow Boundaries

The northern and southern boundaries are assumed as no-flow impermeable boundaries along the flow lines (a special case of Neumann type condition). The transmissivities are set equal to zero along the boundary nodes, preventing any flow across the boundary. The discretized mesh with different types of boundaries is shown in Figure. 4.1

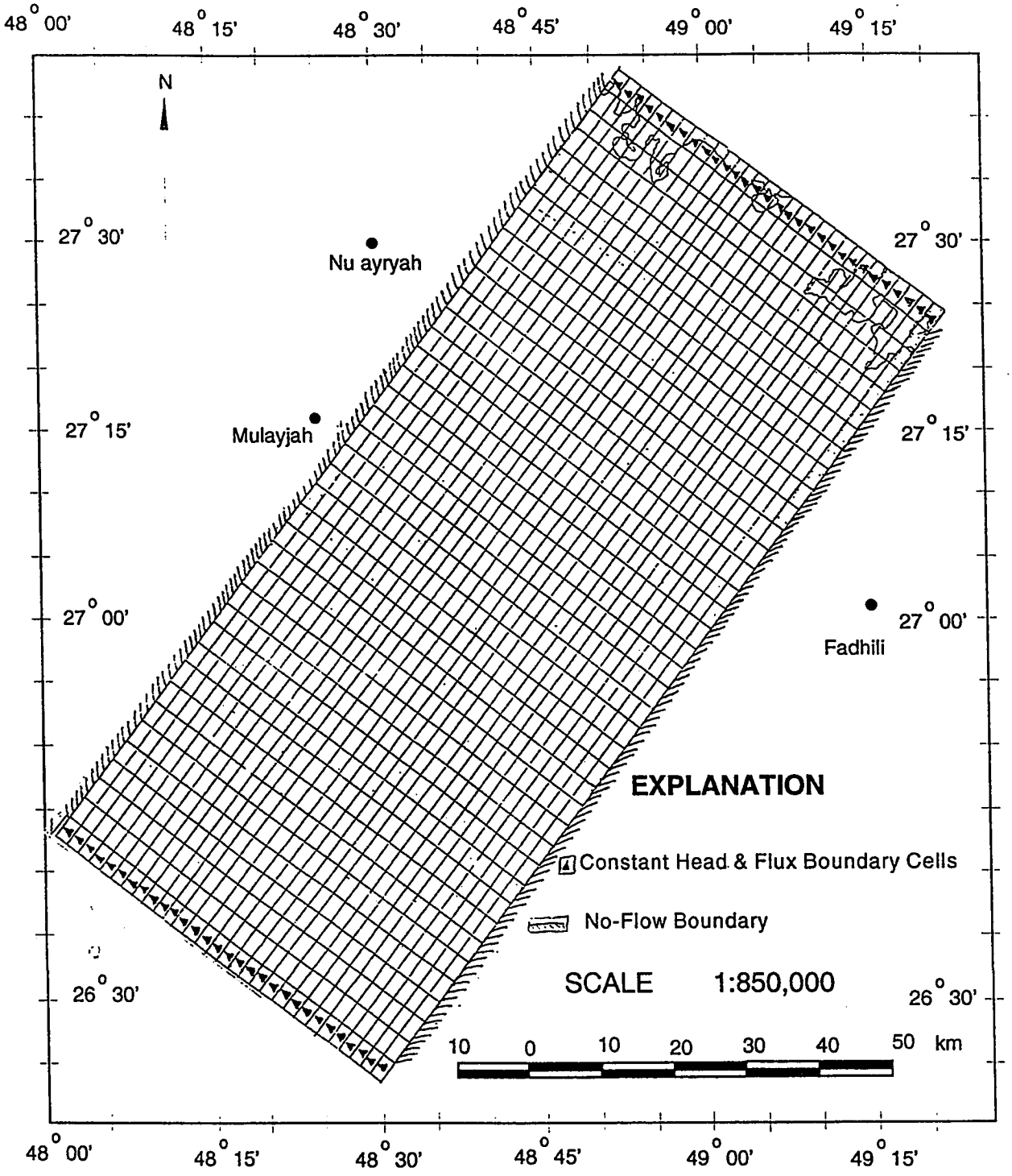

Figure 4.1: Discretization of the Study Area into nodes and elements with simulated boundary conditions.

4.3 Input Data for Simulation

All the input values used for simulation were taken from the published reports. The regional distributions of various aquifer parameters are given in the following sections. The values for solute and fluid properties assumed for simulation are in Tables, 4.1, 4.2 and 4.3.

4.3.1 Permeability

The information regarding regional distribution of horizontal permeability was irregularly distributed over the model area for the three defined aquifer units in which lateral flow was modeled. A considerable amount of data was available in some areas, whereas control was sparse or absent in large areas in the modeled region. For this reason, indirect indicators such as structure, flow patterns and water quality, transmissivity distribution, had to be used to compile regional maps of the permeability patterns in each aquifer unit. The average permeability values are taken from transmissivites at different locations.

Solute properties	Assumed values
Chemical composition	Chloride (Cl.)
Nature	Conservative, highly mobile
Molecular diffusivity in fluid	4.5×10^{-10} m/N [1]
Adsorption parameter	Non-sorbing solute
Rate of solute mass production/decay	0.00
Rate of adsorbate mass production/decay	0.00

Table 4.1: Solute properties assumed for simulation 1. SUTRA update manual [23]

Solid matrix properties	Assumed values
Compressibility of solid matrix (Neogene)	$1.440856 \times 10^{-8} m^2/N$ [2]
Compressibilty of solid matrix (Alat)	$6.3384 \times 10^{-10} m^2/N$
Compressibility of solid matrix (Khobar)	$7.183497 \times 10^{-10} m^2/N$
Density of solid grain	2650 kg/m^3

Table 4.2: Solid matrix properties assumed for simulation 2. From Ground water hydraulics by Lohman [30]

Fluid properties	Assumed values
Temperature	25° C
Fluid compressibility	4.57×10^{-10} m/N ^{3}
Diffusivity	1.35×10^{-10} m/sec
Viscosity (Dynamic)	8.937×10^{-4} paacal.sec

Table 4.3: Fluid properties assumed for simulation 3. The properties of ground water by Matthess and Harvey, [31]

The permeability of Alat and Khobar aquifers caluculated from 78 pumping tests, ranges between 0.05 to 500 m/d, Figure. 4.2. The hydraulic properties of the Neogene aquifer vary from place to place, depending upon the variations in lithologies. The range of permeabilities is very large, from more than 0.1 to 300 m/d, (Bakiewicz, [9]). The wells are of large-diameter, hand-dug type and some having specific capacities of 1 (l/sec)/m.The intensive pumping lead to a rapid lowering of water levels at some locations. The initial assessments of spatial distribution of aquifer transmissivities calculated from test data, compiled mainly from Italconsult.[8], G.D.C.,[10] and B.R.G.M.,[9] are shown in the Figures. 4.3, 4.4 and 4.5.

4.3.2 Porosity

The porosity values for karstified and dolomitic limestone aquifers vary from 20 to 30 %. After considering the facies variations, karstification and dolomitization, the porosity values are assigned as 27%, 20.5% and 22.7% for Neogene, Alat and Khobar aquifers, respectively.

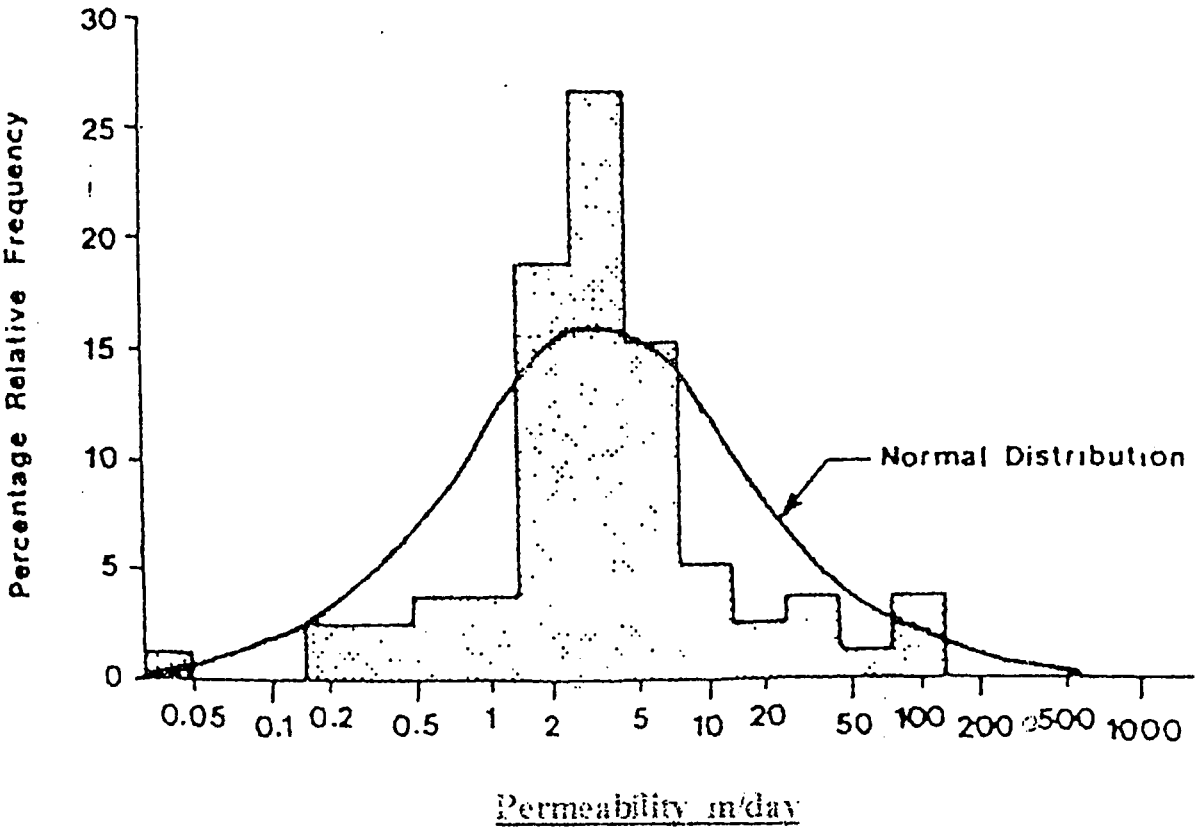

Figure 4.2: Alat and Khobar aquifer permeabilities (m/day), calculated from 78 pumping tests (Bakiewicz et al. 1982).

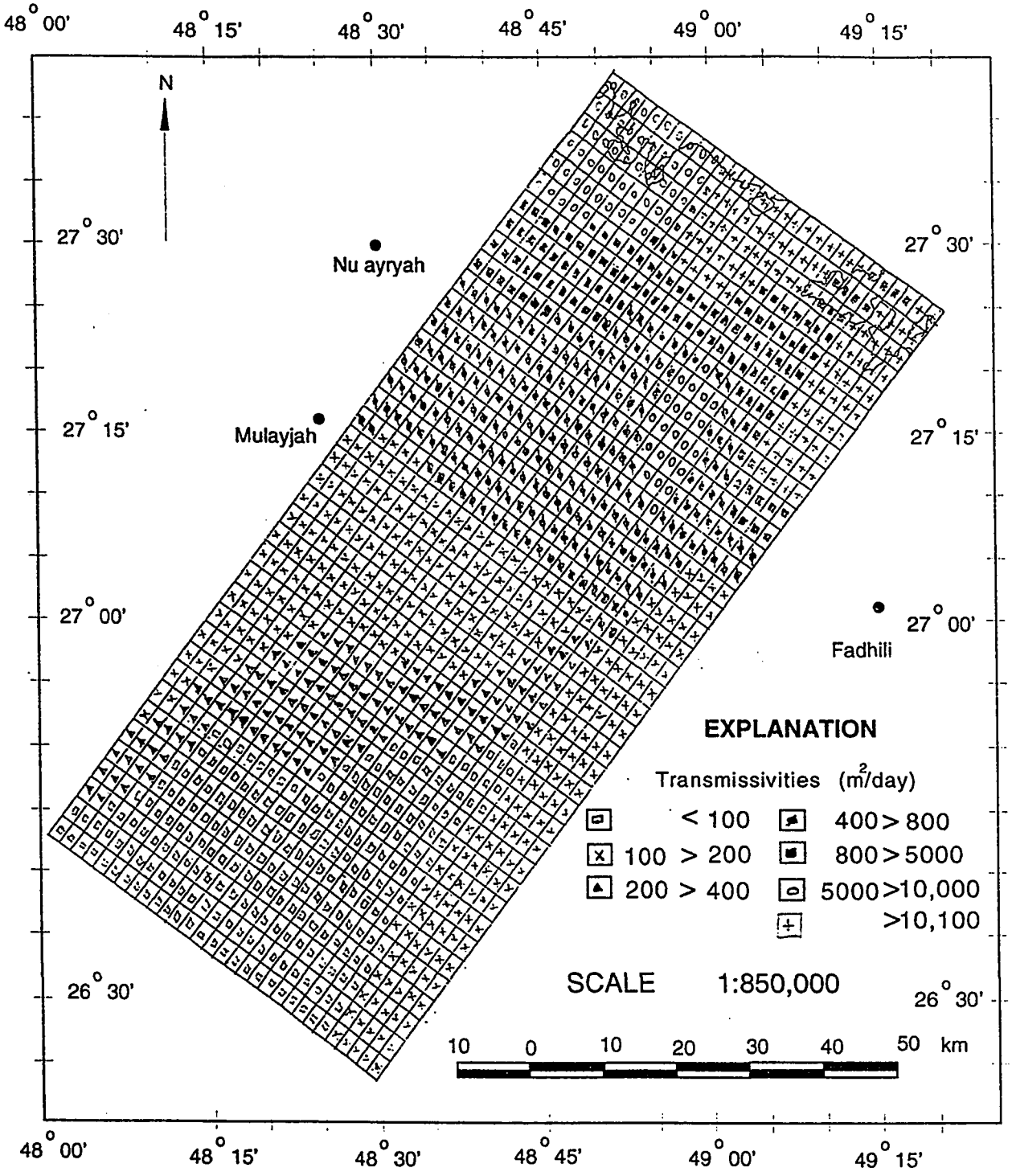

Figure 4.3: Initial Assessment of Khobar Aquifer Transmissivities. (after Italconsult, 1967. BRGM, 1977, GDC, 1980).

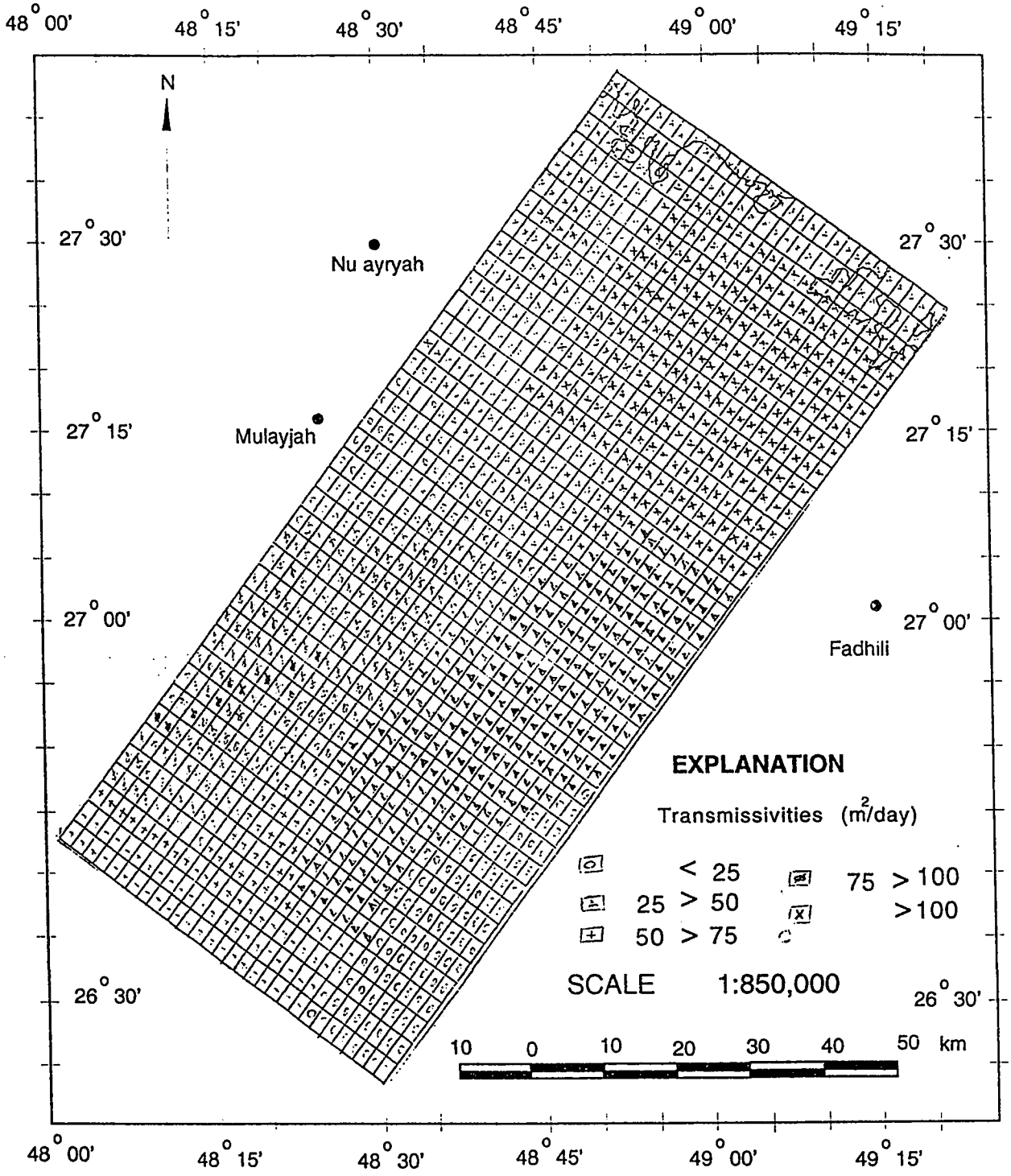

Figure 4.4: Initial Assessment of Alat Aquifer Transmissivities. (after Italconsult, 1967, BRGM, 1977, GDC, 1980).

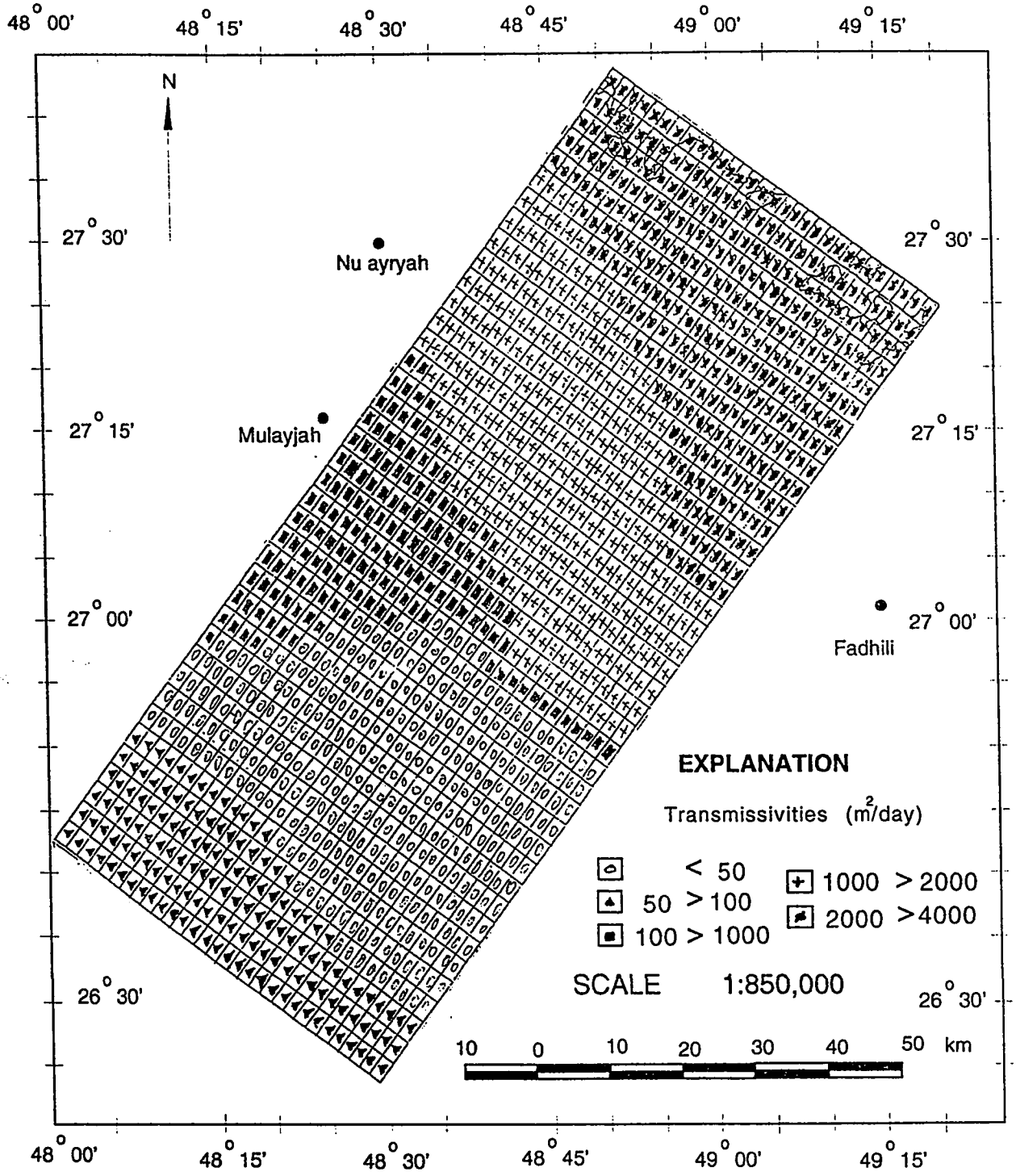

Figure 4.5: Initial Assessment of Neogene Aquifer Transmissivities. (after Italconsult, 1967. BRGM, 1977, GDC. 1980).

4.3.3 Vertical leakage rates

The vertical leakage in the aquifer system is either due to thickness variation of aquicludes because of erosion or fracturing, jointing, solution channels, collapse structures in aquitards. Facies variations from shale to anhydride in Rus Formation also caused vertical leakages into the Khobar aquifer. The vertical permeability is to a large extent dependent on the presence or absence of residual gypsum and zones of argillaceous beds at the base of the Rus Formation (Pike [14]). Anhydride undergoes dissolution, causing solution channels and collapse structures. The Rus Formation is eroded appreciably due to the presence of anhydride beds at different places as depicted from isopachyte map (Figure, 3.4). They act as windows or zones of vertical leakage of high salinity water from underlying Umm Er Radhuma into Khobar aquifer as at Sarrar, AbuHadriya and Manifa area. The aquitard effect of the Neogene is modelled as a conceptual leakage interface at the base of the unit. This is due to the presence of complex interfingered lenses of varying lithologies from clays to limestones.

The vertical leakage through an aquitard is a function of vertical hydraulic conductivity, thickness of the aquitard, and the head difference across it. The excessive pumping during a long period of time enhanced the vertical flow from underlying formations. The data for head difference are extracted by overlapping the potentiometric heads distribution maps of aquifers, taking into account the vertical flow

directions. The thickness of aquitards are calculated from isopachyte maps at different nodal points. The vertical hydraulic conductivity values are taken from G.D.C [10] and B.R.G.M [9]. Then the areal distribution maps of the vertical leakages for the model area were prepared for the three aquifers, Figures, 4.6, 4.7 and 4.8. The vertical leakages were simulated as sources of fluids of specified concentrations injecting fluid with specified rates. The vertical leakage rates range from 1.4 X 10^{-2} to 9.8 X 10^{-5} (m^3/sec) which appears low in terms of unit values, but because of the large area involved, the total vertical flow volumes exceed the water flowing due to lateral hydraulic gradient. The vertical flow (q) through an aquitard of thickness (D) is governed by the following equation:

$$q = \frac{K}{D} \quad or \quad q = \frac{\Delta h}{C} \tag{4.1}$$

Where

q	Vertical flow (m^3/d) for unit area.
K	Vertical permeability (m/d).
Δh	Effective pressure head difference (m).
C	Hydraulic resistance (days).

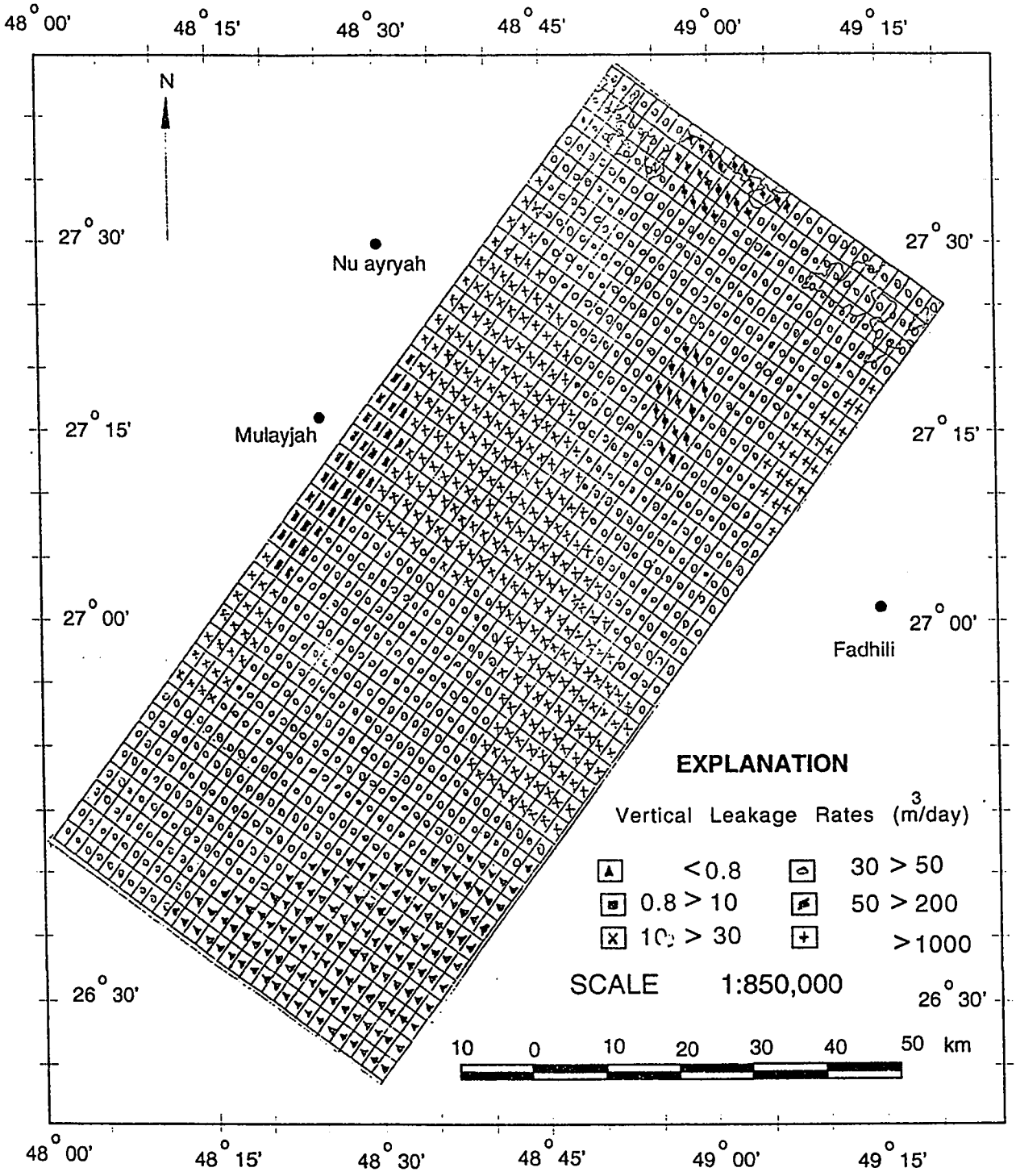

Figure 4.6: Initial Assessment of Vertical Leakages of Lower Dammam-Rus Aquitard. (after Italconsult, 1967, BRGM, 1977, GDC, 1980).

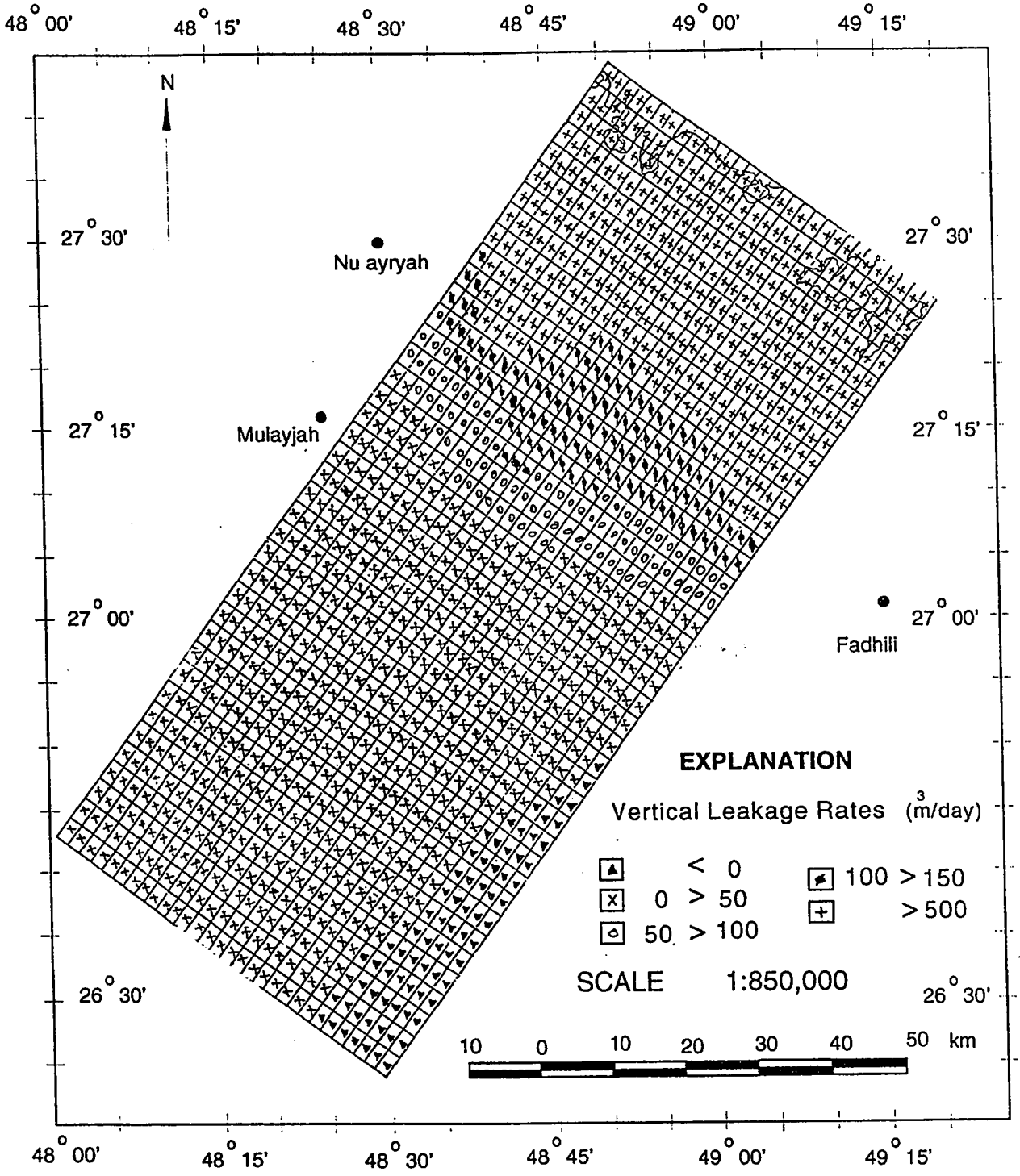

Figure 4.7: Initial Assessment of Vertical Leakages of Alat Marl Aquitard. (after Italconsult, 1967, BRGM, 1977, GDC, 1980).

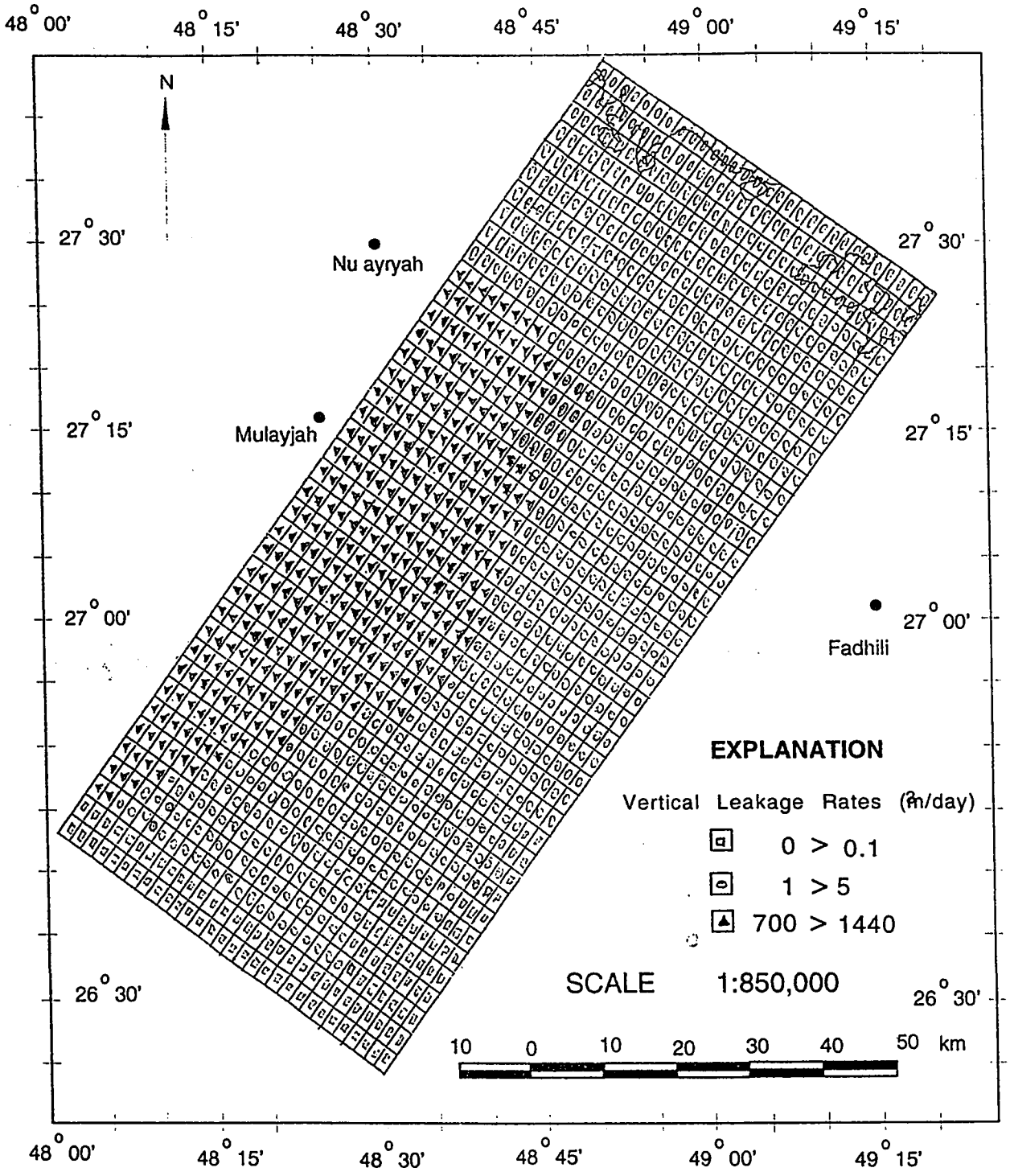

Figure 4.8: Initial Assessment of Vertical Leakages of Neogene Leakage Interface Aquitard. (after Italconsult, 1967, BRGM. 1977, GDC, 1980).

4.3.4 Dispersivity

It is a scale dependent property. It varied throughout the model area. The laboratory measurements of dispersivity for Neogene and Dammam aquifers are not feasible because actual field hydrological condition can not be set up in the laboratory. The dispersivity values are selected on the basis of numerical stability of the model area. The spatial distribution at different nodes is controlled by weighing factor operation during simulations.

In the Neogene aquifer, seawater concentration (25,878 ppm) is assumed at the eastern side of the seafront and freshwater concentrations (1,250 ppm) at the western side. The grid spacing is reduced and assumed as greater than half of the grid spacing to avoid numerical spatial oscillations which may occur near the concentrations front. The values for longitudinal dispersivities are assumed as the same as of the largest hydrogeologic or the flow inhomogeneites along the transport, while transverse dispersivites are taken as one tenth of longitudinal dispersivities.

4.3.5 Recharge Rates

Precipitation generally occurs as convective thunderstorms and it is discontinuous in space and time. Mean annual precipitation ranges from 50 mm to greater than 600 mm per year. The outcrop area covering Dammam formation is about 1200 square kilometers. (deJong, [16]). Recharge is a complex process which is affected by

climatological, geological and hydrogeological factors. Shampine et al. [13] analysed the isotope concentrations in the groundwater of Saudi Arabia. Then collected and compiled data of concentrations of O^{18}, deuterium, tritium, ^{34}, C^{13}, and C^{14} throughout the Kingdom. Interpretation on the basis of this analysis indicates that most of the recharge took place about 20.000 years ago and relatively little water has been recharged currently.

The recharge is conceptualized as water infiltrates and flows laterally from outcrops to the study area. It can be simulated by increasing the leakage rates near the landward boundary. The annual recharge rates at different nodes are calculated from annual recharge rates by rainfall, Table, 4.4, (Bakiewicz et al. [11]).

Year	Neogene Aquifer	Dammam Aquifer
1952	0	0
1953	740	82
1954	0	0
1955	1210	134
1956	0	0
1957	254	28
1958	0	0
1959	122	13
1960	0	0
1961	0	0
1962	0	0
1963	0	0
1964	356	40
1965	0	0
1966	0	0
1967	0	0
1968	39	4
1969	905	100
1970	0	0
1971	74	8
1972	170	19
1973	0	0
1974	141	16
1975	54	6
1976	1346	149
1977	31	3
1978	0	0
Mean	202	22

Table 4.4: Estimates of annual recharge in (Mm^3/year) by rainfall (after Bakiewicz et al. 1982)

4.3.6 Extraction Rates

In recent years, well water irrigation has increased in Wadi Al-Miyah area as well as in other parts of the Eastern province. The extraction rates are approximately equal to replenishment (infiltration) rates in the past which are now exceeded and causing mining of fossil groundwater. (Burdon and Otkun, [3]). The total water consumption in the study area has increased significantly after 1967 due to agricultural, social and industrial developments. The extraction rates from the three aquifers were compiled from two sources: water point inventory, Italconsult[8], and an inventory made by G.D.C [10]. On the basis of the given data for different individual well fields, discharge history for these aquifers is developed which had an acceptable level of credibility, Appendix-B .

In Neogene aquifer, the total number of hand-dug wells is 135. These wells vary in depth from 2 to 10 meters and have a diameter of 1 to 3 m. The exploitation is mainly for irrigation around the sabkhah fringes. The gross extraction estimates for the whole wadi are given in Figure. 4.9. The abstractions for the study area are estimated (72 Mm^3/ Year) which is in close agreement with the gross value.

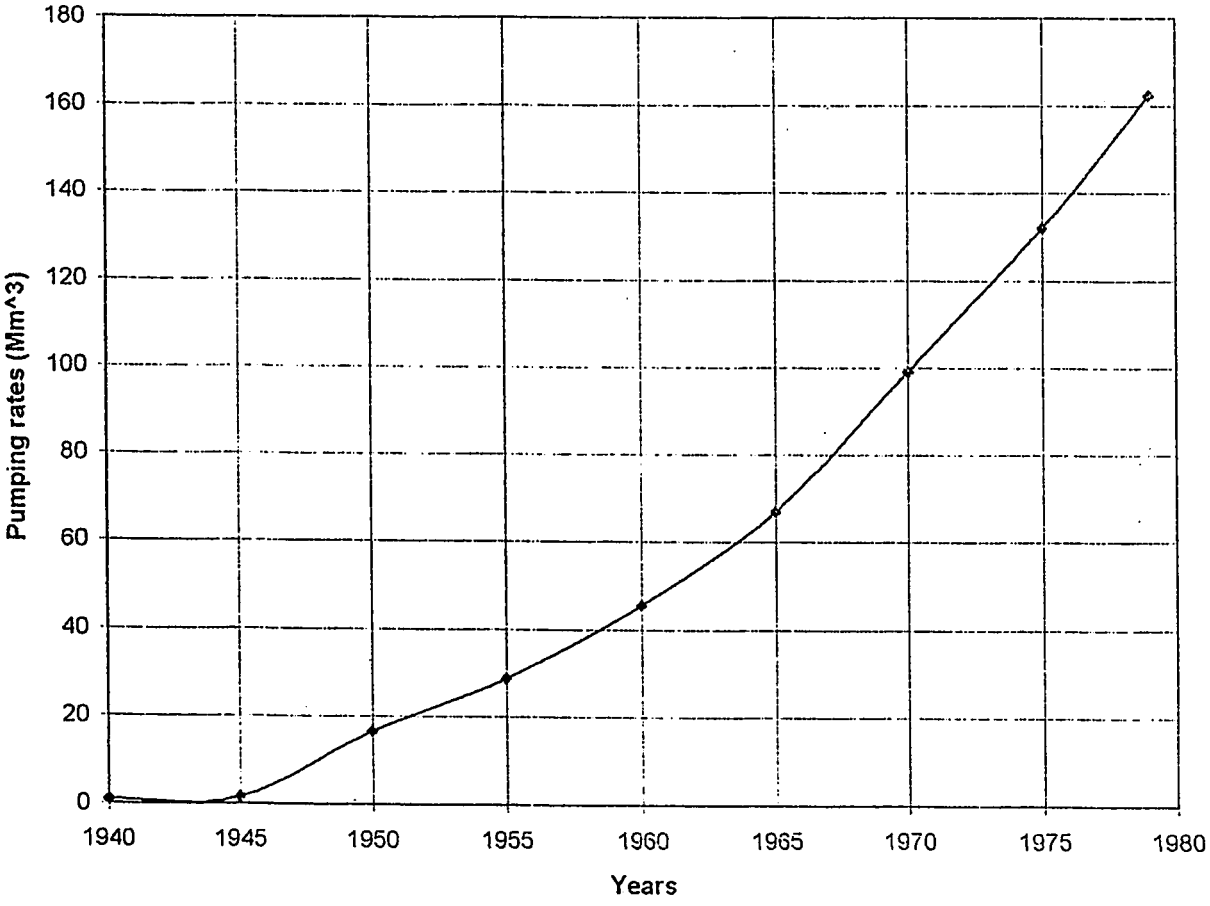

Figure 4.9: Gross Extraction Rates from Neogene Aquifer in Wadi Al-Miyah area. (after G.D.C. 1979, Italconsult, 1966.

It is assumed that before the new development in 1940, extractions from wells (or improved springs) in the Dammam aquifer were about in balance with the water consumed on the cultivated area which was estimated as 70 Mm^3/year. The extraction rates increased significantly as the agricultural and oil field operations increased during the period of 1975 to 1990. The history of increased extractions for agriculture was entered in the model for calibration of transient conditions. Figure. 4.10.

In order to simulate the calibration period, the pumpage from each aquifer was divided into 28 annual pumping periods, begining with 1967. The year 1967 was chosen as the initial starting time since agricultural growth was very limited and it was, therefore, reasonable to assume that there was a steady-state condition existed during that year. The annual pumping periods and associated rates of pumping are shown in Figures. 4.11. 4.12 and 4.13. respectively. The annual values have been further subdivided into the average withdrawal per well per pumping period and assigned to the appropriate node in the model. The distribution of wells or well fields for Khobar. Alat and Neogene aquifers are shown in Figures. 4.14. 4.15 and 4.16. respectively.

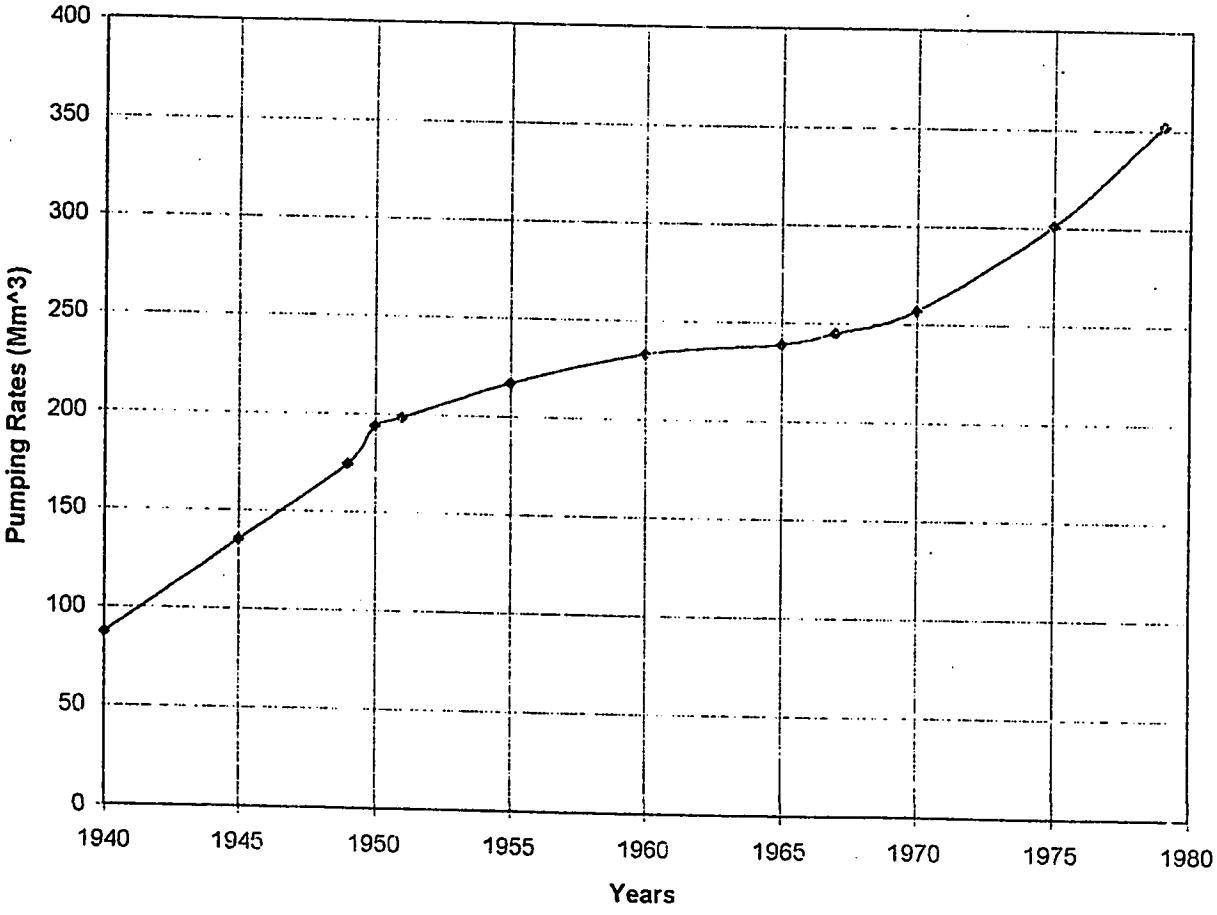

Figure 4.10: Gross Extraction Rates from Dammam Aquifers (Alat & Khobar) in Wadi Al-Miyah area. (after G.D.C. 1979, Italconsult. 1966.)

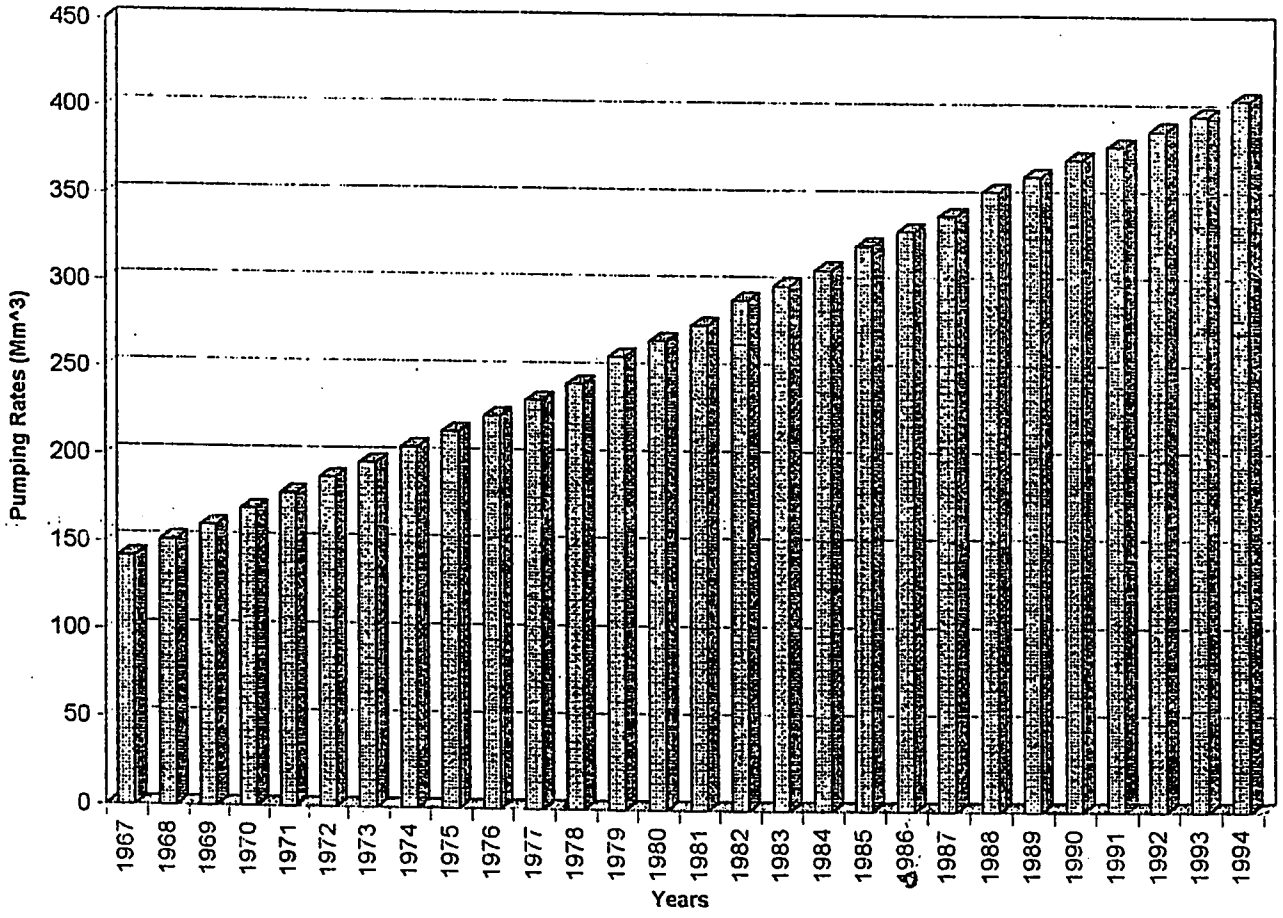

Figure 4.11: Gross Extraction Rates from Khobar Aquifer in Wadi Al-Miyah area. (after Aramco, 1972, G.D.C. 1979, Italconsult, 1966, FAO. 1982.)

Figure 4.12 Gross Extraction Rates from Alat Aquifer in Wadi Al-Miyah area.

(after Aramco, 1972, G.D.C, 1979, Italconsult, 1966, FAO, 1982.)

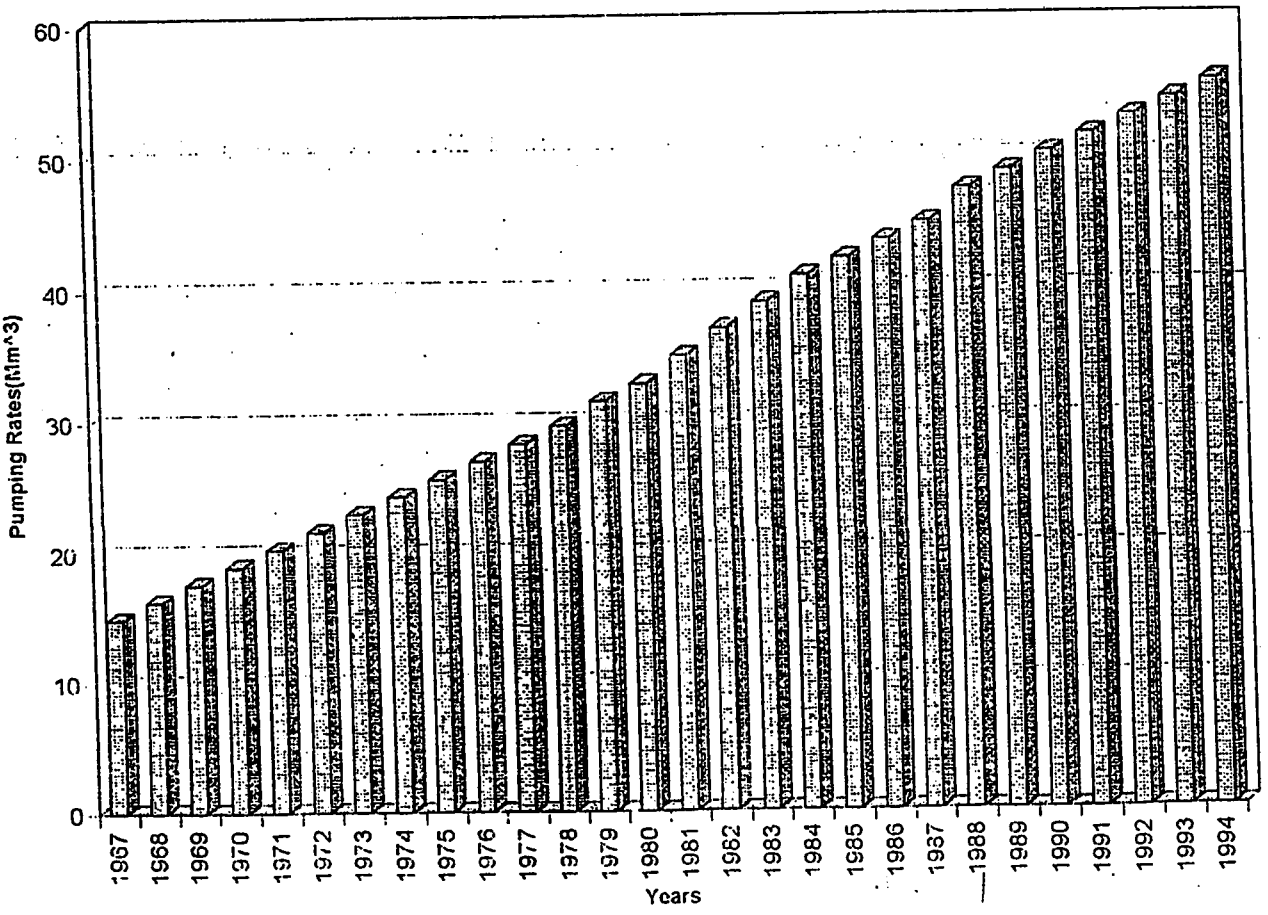

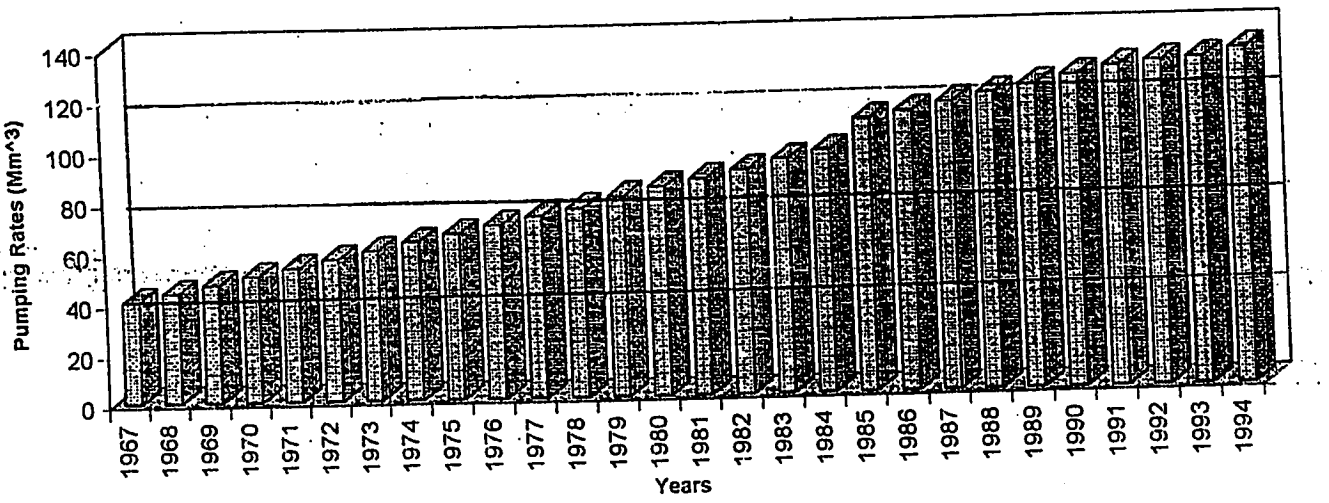

Figure 4.13: Gross Extraction Rates from Neogene Aquifer in Wadi Al-Miyah area. (after Aramco, 1972, G.D.C, 1979, Italconsult, 1966, FAO, 1982.)

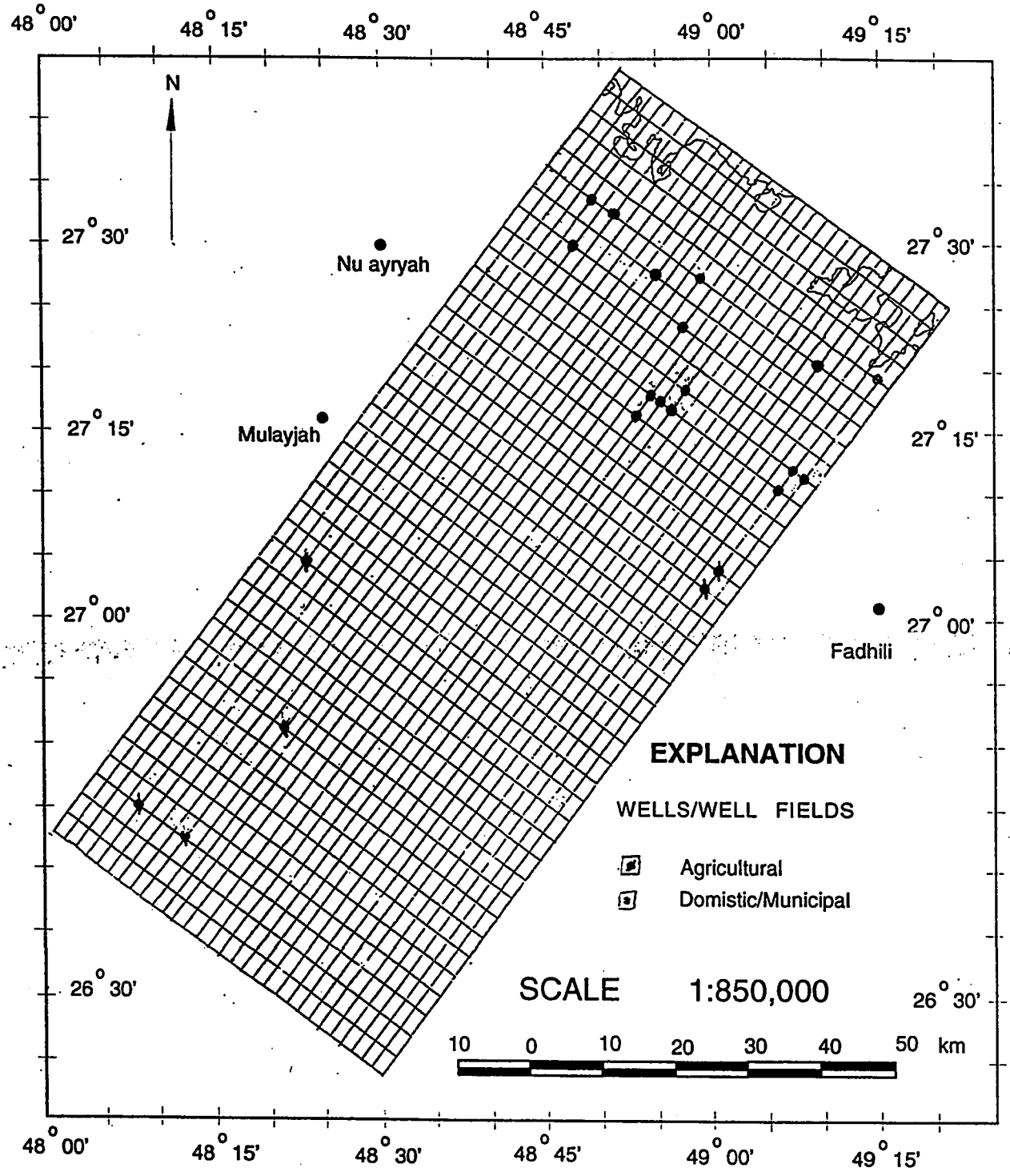

Figure 4.14: Model Grid with locations of Wells/Well Fields in Khobar Aquifer.

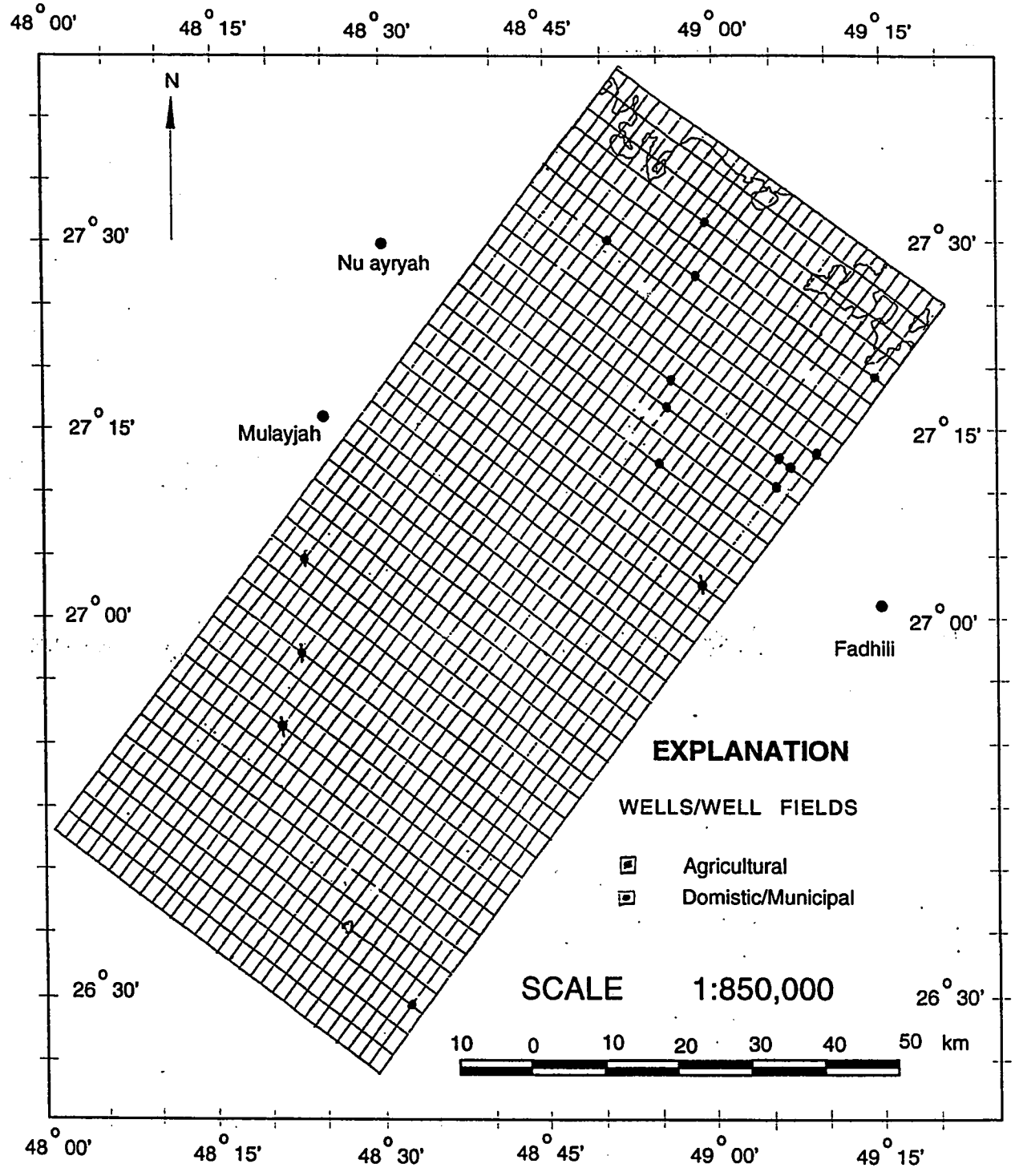

Figure 4.15: Model Grid with locations of Wells/Well Fields in Alat Aquifer

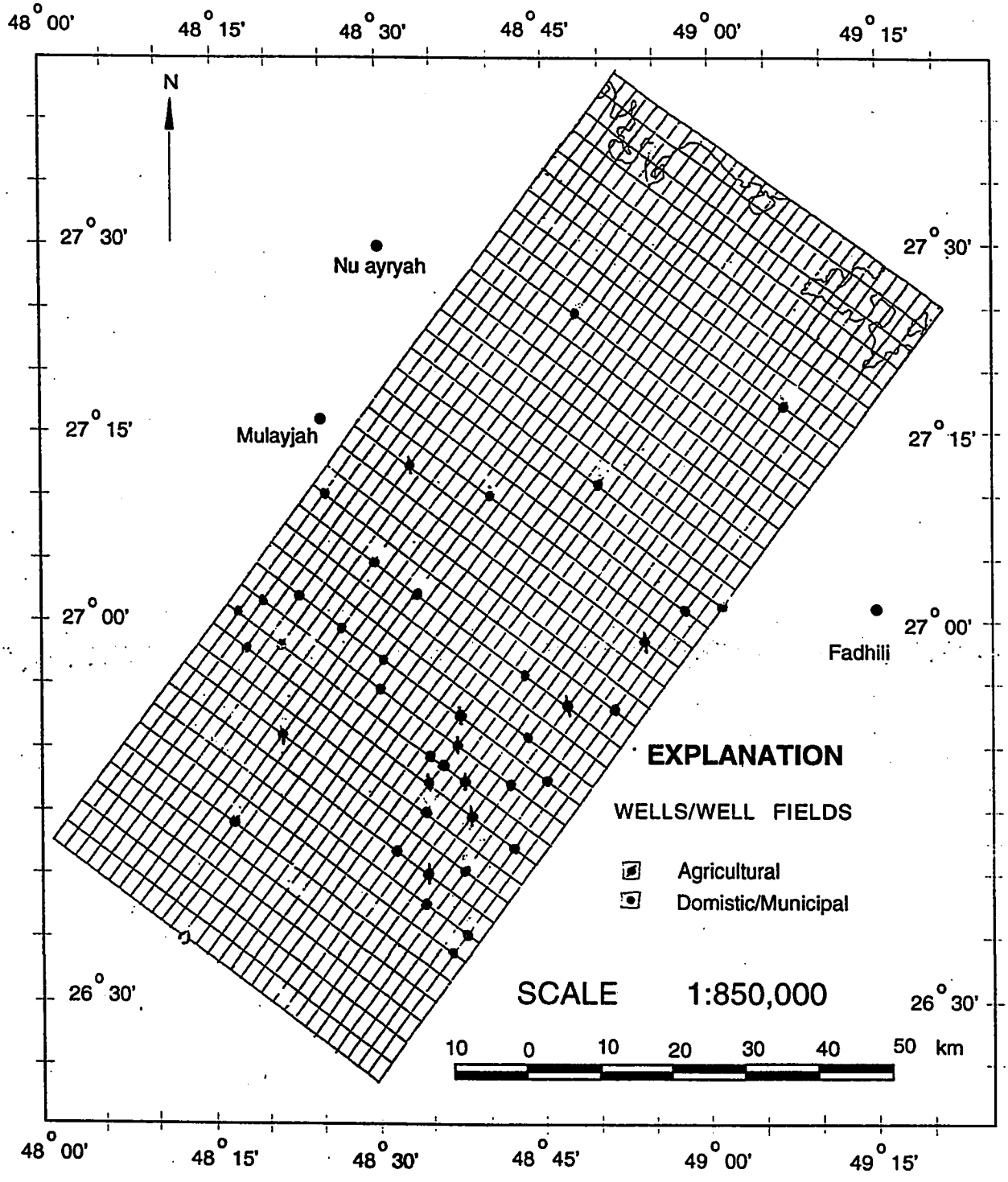

Figure 4.16: Model Grid with locations of Wells/Well Fields in Neogene Aquifer

4.4 Model Calibration and Verification

4.4.1 General Calibration

In any model of a real aquifer system it is unlikely that all the parameters influencing the groundwater and solute balance are known precisely over the whole model region. Uncertainty arises either through a lack of data or because the extrapolation of local data to the regional data base cannot be well defined. For this reason it is necessary for a model to undergo a process of calibration. This calibration involves the comparison of the model's response with the same known response of the real aquifer system. If necessary, input parameter values can be adjusted to make a closer agreement with the two systems. Initial estimates of the hydrogeologic parameters were adjusted during the calibration process. These estimates were varied within reasonable limits dictated by deductions made from the conceptual model and by knowledge of the hydrogeology of the aquifers, and they resulted in the computation of heads and chloride concentrations that compare satisfactorily with available data. The standard method of calibration consists of two stages. The first stage is a steady state calibration in which recorded steady state head and solute concentration values are recreated by the model for the same conditions. This matching is achieved by the adjustment of permeability, dispersivity or other input parameters which affect the flow balance. The second stage is a transient calibration where the model's response to a historical record of recharge, abstraction, head and saltwater movement data

is compared with the observed values of the real aquifer system. Again various input parameters were adjusted to achieve this. In case of poor data, re-run and re-calibration has to be conducted under steady state conditions. The sequence of simulation and calibration operation for the steady and transient conditions are shown in Figure 4.17.

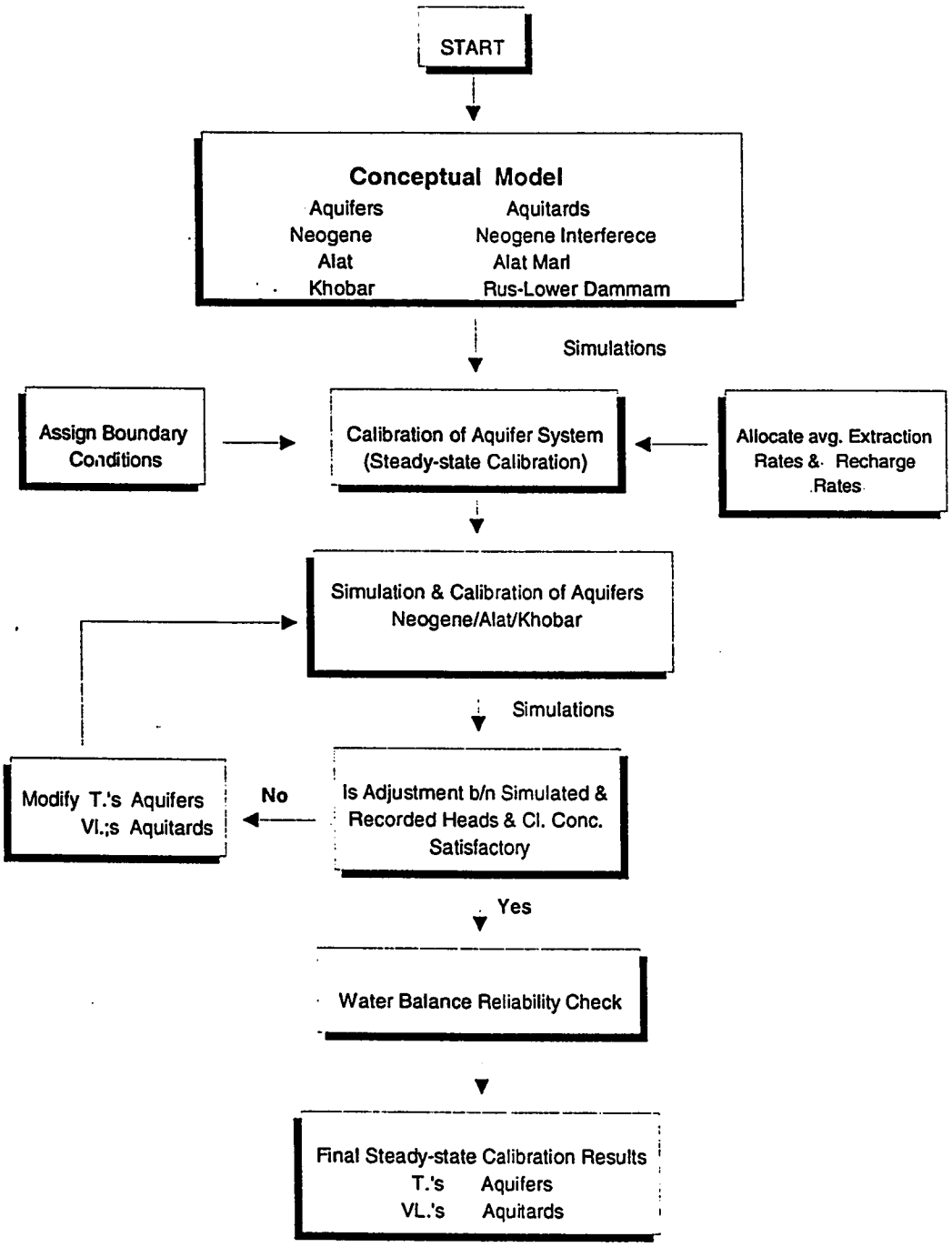
START
Conceptual Model
Aquifers
Neogene
Alat
Khobar
Aquitards
Neogene Interferece
Alat Marl
Rus-Lower Dammam
Simulations
Assign Boundary Conditions
Calibration of Aquifer System (Steady-state Calibration)
Allocate avg. Extraction Rates & Recharge Rates
Simulation & Calibration of Aquifers Neogene/Alat/Khobar
Simulations
Modify T.'s Aquifers Vl.;s Aquitards
No
Is Adjustment b/n Simulated & Recorded Heads & Cl. Conc. Satisfactory
Yes
Water Balance Reliability Check
Final Steady-state Calibration Results
T.'s Aquifers
VL.'s Aquitards
Contd.

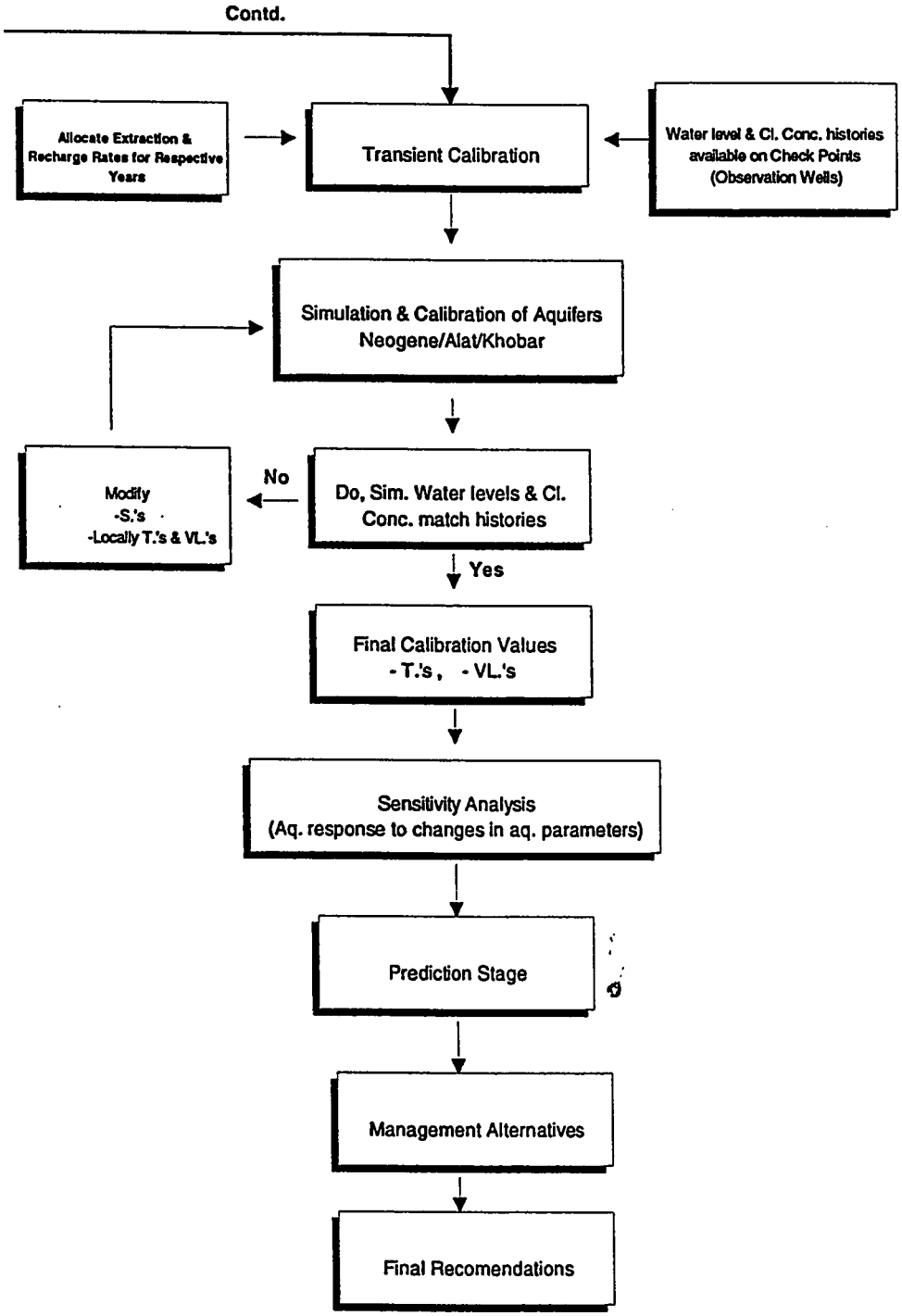

Figure 4.17: Flow chart for Simulation and Calibration Operation

4.4.2 Steady-state Calibration & Simulation

The steady-state calibration has two purposes. The first is to calibrate the model to a selected equilibrium hydrologic condition in which the stress and response characteristics of the system are well documented. The second is to provide the steady-state simulation needed as the initial condition for subsequent transient-state simulations. In this study an areal finite element model for fluid-density-dependent groundwater flow and solute transport is selected to simulate the existing and future groundwater flow and solute distribution patterns in Neogene, Alat and Khobar aquifers. The model simulates mainly the confined conditions of the aquifers. As Khobar and Alat aquifers are confined throughout the model area, so they are simulated as confined aquifers. The Neogene aquifer, because of its unconfined nature, was simulated as unconfined aquifer. To achieve this, the Fortran code has been modified at the necessory location to simulate the unconfined condition of the Neogene aquifer. The option of aquifer type is added into the routine "main.for" at the Input data lines. The modified program uses the aquifer compressibility value from input data for confined aquifer and porosity value for unconfined aquifer in calculation of heads and chloride concentrations.

The initial simulated potentiometric surface of Neogene, Alat and Khobar aquifers corresponds to a pseudo-stabilized state. The general configuration of the flow field is typical of a coastal aquifer having a seaward gradient. The contours show a general

hydraulic gradient from recharge area towards the discharge area (Arabian Gulf). On the basis of published data about extraction, it is assumed that pseudosteady state condition had been established in the year 1967 and afterwards expansion of agricultural activities started in the study area.

Freshwater flows from the outcrop area in the west towards the Arabian Gulf with a high velocity, causing flushing action on salt contents of the aquifer to be carried away into the sea. As the groundwater flows, it dissolves salts due to mechanical mixing (advection) resulting in an increase in salt contents which is mainly controlled by flow velocities. Chloride (Cl) is selected as a transporting solute because of its highly mobile and conservative nature in groundwater regime and it acts as a good indicator of hydrological processes within aquifers. It is assumed that before the pumping started, the saltwater-freshwater transition zone in the northeastern side of the study area was in an equilibrium condition with current sea level.

During steady state simulations, a large number of transient runs were carried out in which boundary condition values and aquifer properties were adjusted by trial and error to simulate steady state condition. Initially, intrinsic permeability and dispersivity values are adjusted. The steady-state heads and concentrations based on boundary conditions and given aquifer properties are simulated, and the results stored in an output file to be used as initial conditions for subsequent runs on a later stage. Initially, heads, based on the boundary conditions and starting concentrations of zero everywhere, were set throughout the study area. Subsequent runs often used

results from the previous runs as initial conditions. Experimentation with space and time discretization helped in the selection of a unique condition which may give realistic lateral distribution of solute concentrations, and prevent numerical spatial oscillations that may occur near the concentration front. A single step of 100 years is used to simulate the steady state conditions. Both pressure and concentrations are computed for the time step.

Steady state calibration is achieved by:

1. Matching simulated heads for the three aquifers with recorded (observed) pre-development heads at various locations.

2. Matching chloride concentrations with existing measured values where these values exist.

3. By keeping appropriate upward/downward leakage from different aquifers as calculated from the vertical hydraulic gradients at different locations.

4. By keeping the values of all aquifer parameters consistent with measured data and known hydrogeologic conditions in the area.

At this stage, a number of calibration runs were repeated until a good agreement is reached between simulated and observed system response of fluid flow and solute movement at steady state condition, Tables, 4.5, 4.6 and 4.7. The simulated predevelopment flow fields were compared with the observed ones for the year 1967 for

Khobar, Alat and Neogene aquifers, Figures, 4.18, 4.19 and 4.20. The distribution of calibrated predevelopment chloride concentrations associated with flow fields of the three aquifers are given in Figures 4.21, 4.22 and 4.23.

Well no	Recorded Head (m)	Simulated Head (m)	Recorded chloride Concentration (ppm)	Simulated chloride Concentration (ppm)
WA - 347	427.9	426.42		1470
WA - 320	419.6	421.6		1475
WA - 327	416.9	415.4		726
WA - 311	408.8	407.94		815
MI - 4N	399.1	398.84	1478	1193
WA - 339	394.9	396.97	-	967
WA - 338	392.9	390.02	1190	1116
WA - 262	-	381.62	1204	1236.5
WA - 282	-	376.6	1704	1238
WA - 296	382	382.81	-	1031
WA -	373.6	370.6	-	431
WA - 277	347.4	349.4	-	859.2
WA -	341.1	342.13	-	699
WA -	337	336.6	-	1209.5

Table 4.5: Comparison of recorded and simulated Data for Neogene Aquifer after Steady State Simulation.

Well no	Recorded Head (m)	Simulated Head (m)	Recorded chloride Concentration (ppm)	Simulated chloride Concentration (ppm)
WA-329	439.9	439.7	–	573.9
MI-25A	388.5	388.02	543	518
MI-3A	413.1	413.43	763	642
AHW-804	–	308.12	1150	974.4
S-222	–	314.9	795.2	776.5
S-505	–	291.3	6486	4165
	340.2	343.87		541.2
HU-35A	313.5	316.1		576.94

Table 4.6: Comparison of recorded and simulated Data for Alat Aquifer after Steady State Simulation.

Well no	Recorded Head (m)	Simulated Head (m)	Recorded chloride Concentration (ppm)	Simulated chloride Concentration (ppm)
MI-2K	407.5	407.43	841.5	822.1
MI-23K	387.5	386.97	706	639.82
TWW-1BX	-	386.3	823	808.51
B-13	306.9	304.25	-	
AHWW6	-	341.6	6690	6410
B - 9	-	340.5	6699	6424.3
S - 505	-	303.2	6493	6526.8

Table 4.7: Comparison of recorded and simulated Data for Khobar Aquifer after Steady State Simulation.

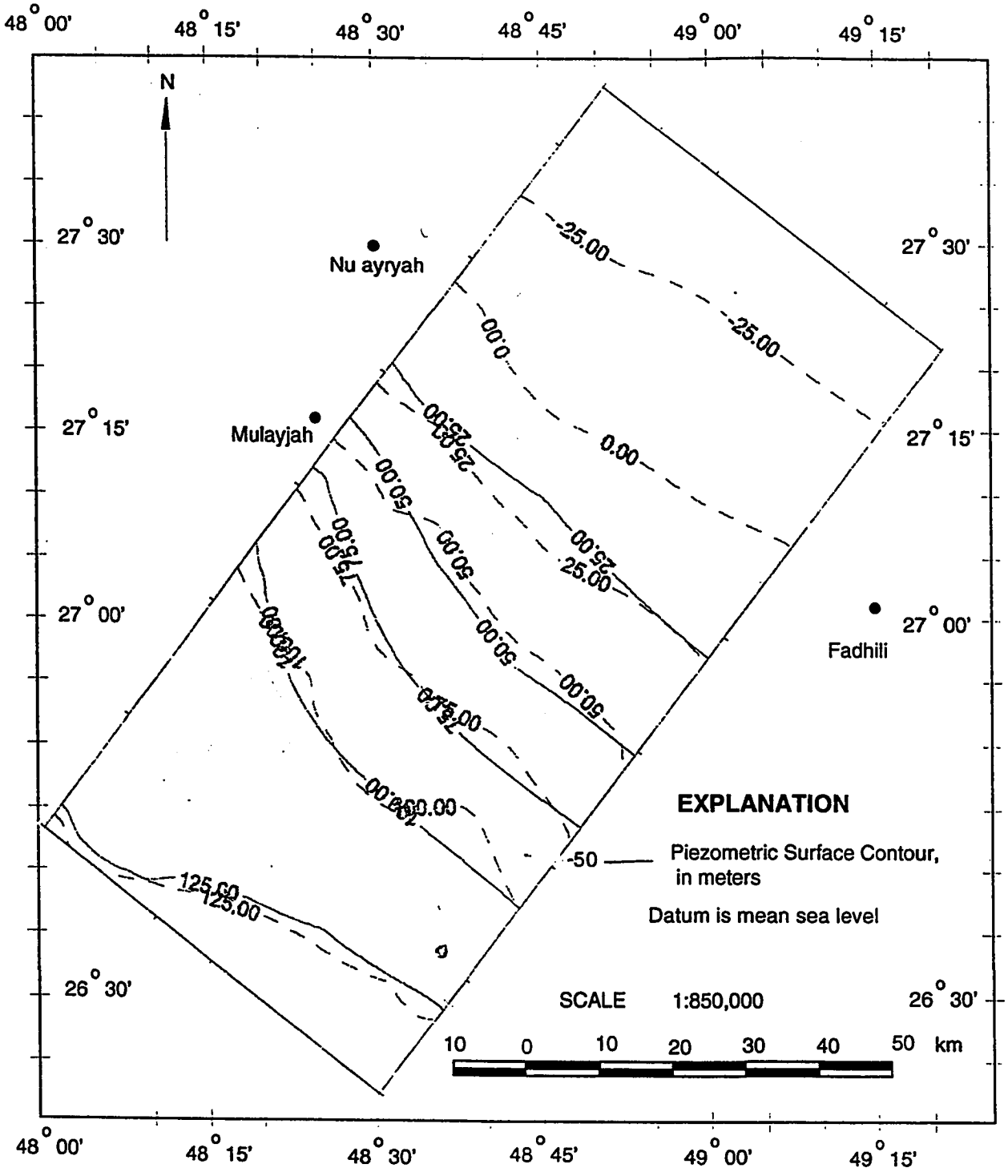

Figure 4.18: Simulated Piezometric Surface Map of Khobar Aquifer (Steady-state Simulation)

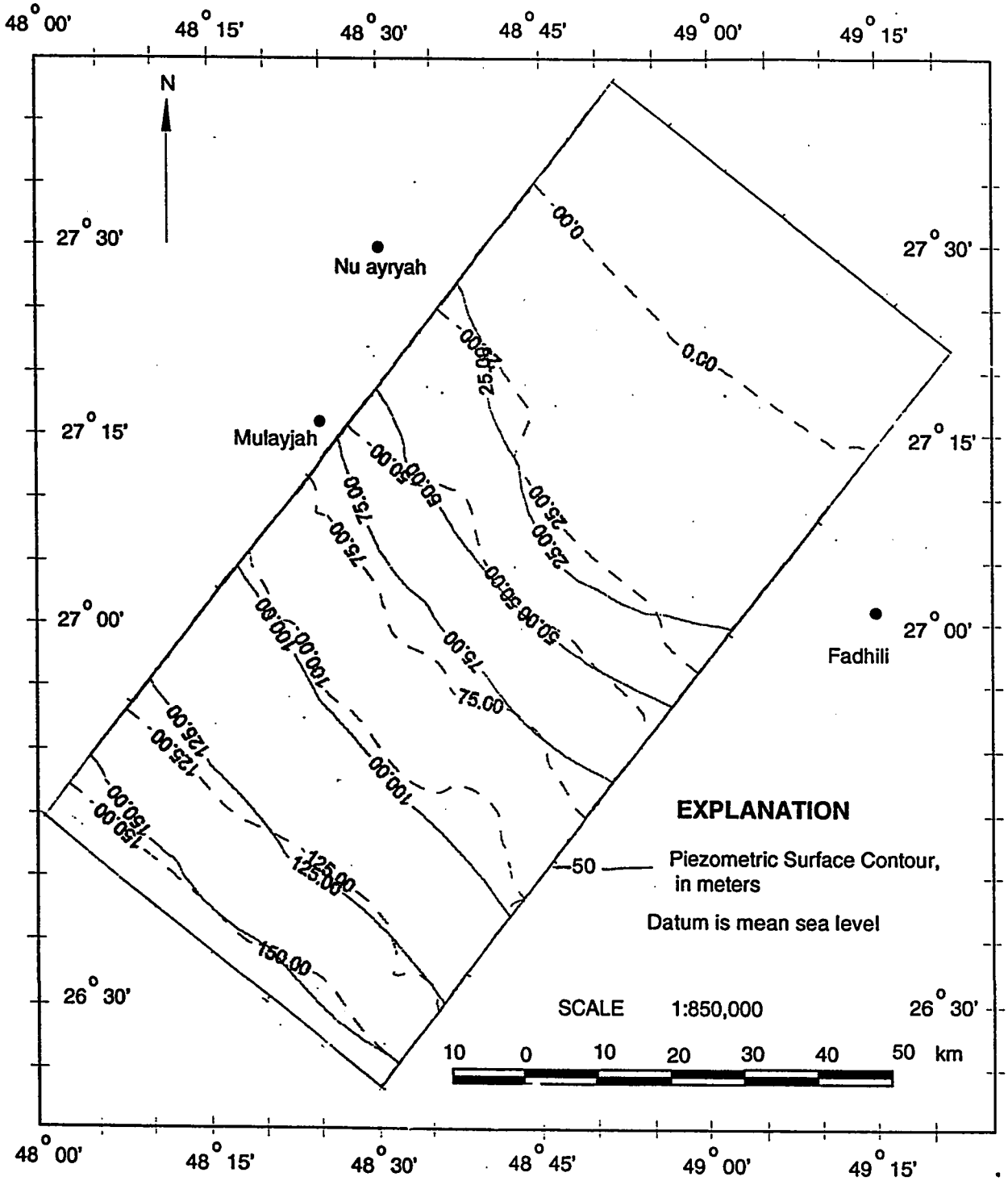

Figure 4.19: Simulated Piezometric Surface Map of Alat Aquifer (Steady-state Simulation)

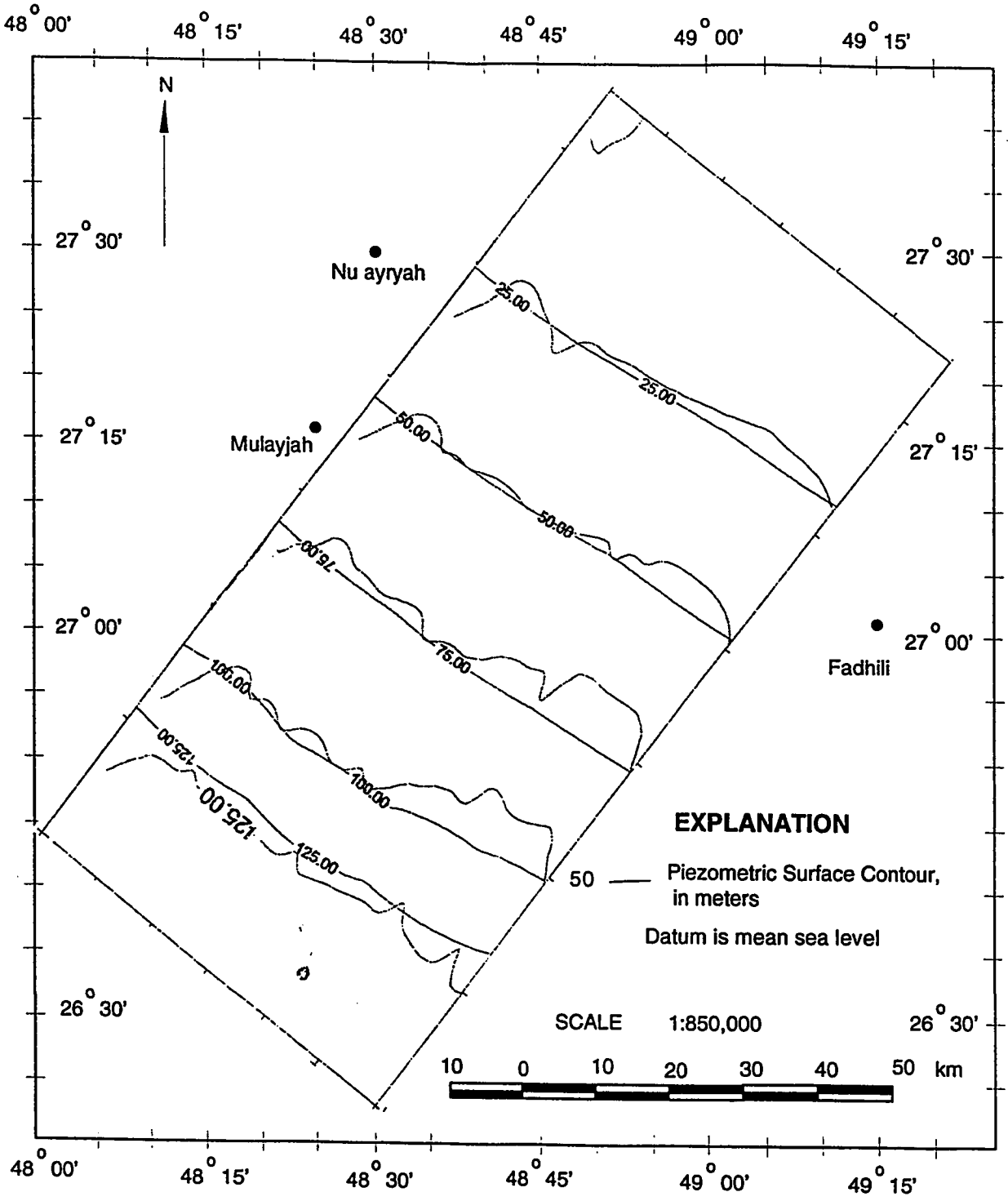

Figure 4.20: Simulated Water level Surface Map of Neogene Aquifer (Steady-state Simulation)

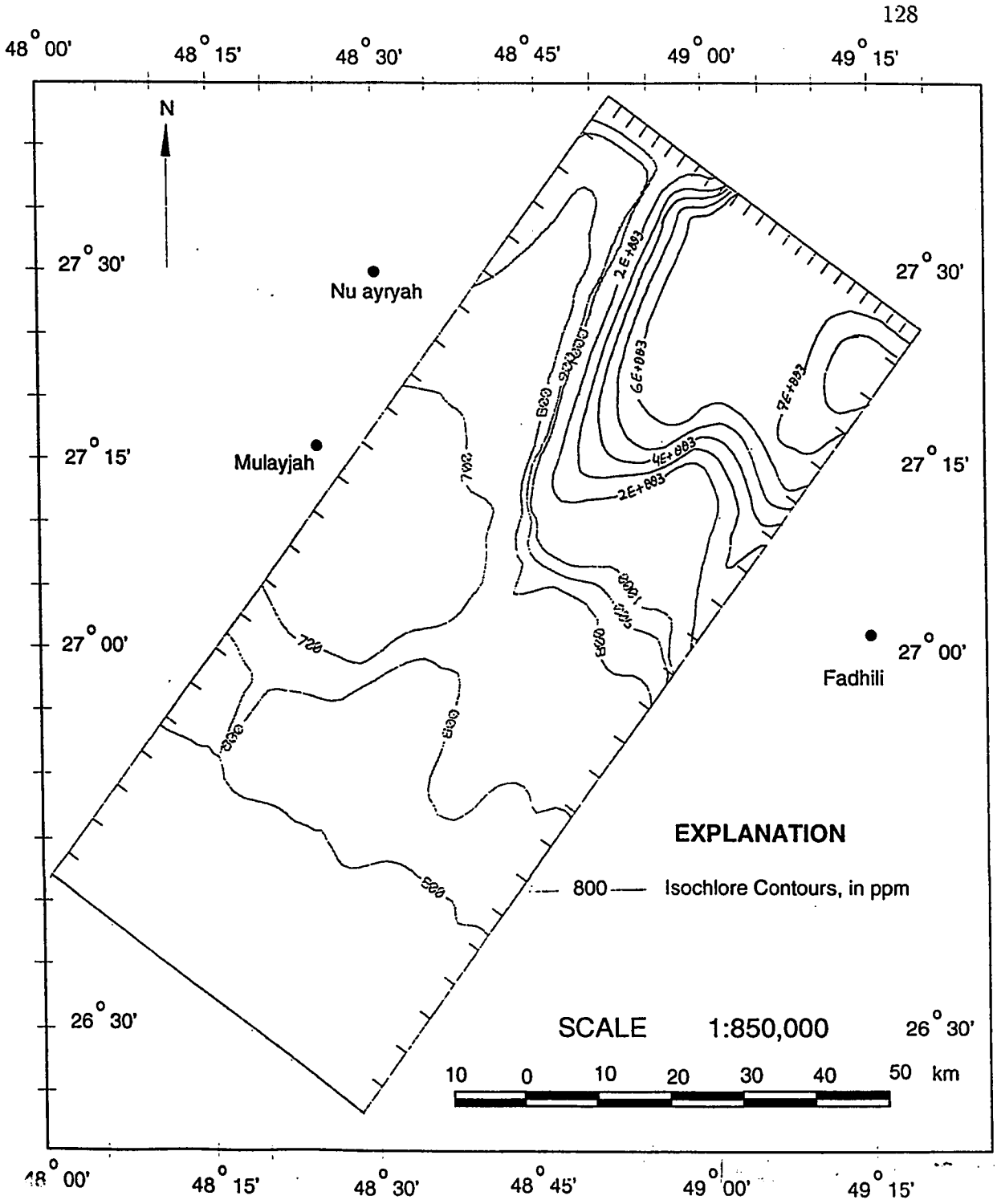

Figure 4.21: Isochlore Map of Khobar Aquifer (Steady-state Simulation)

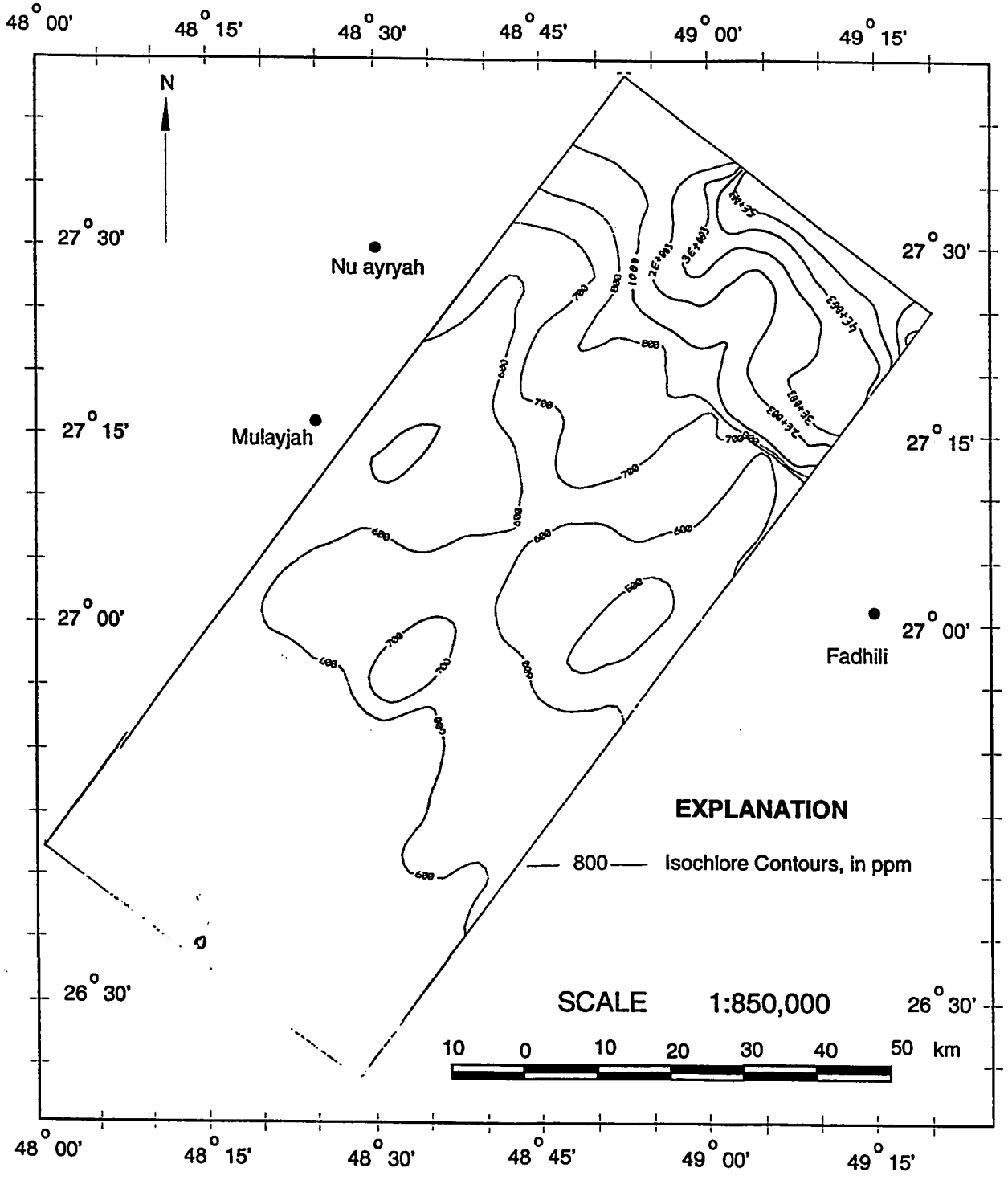

Figure 4.22: Isochlore Map of Alat Aquifer (Steady-state Simulation)

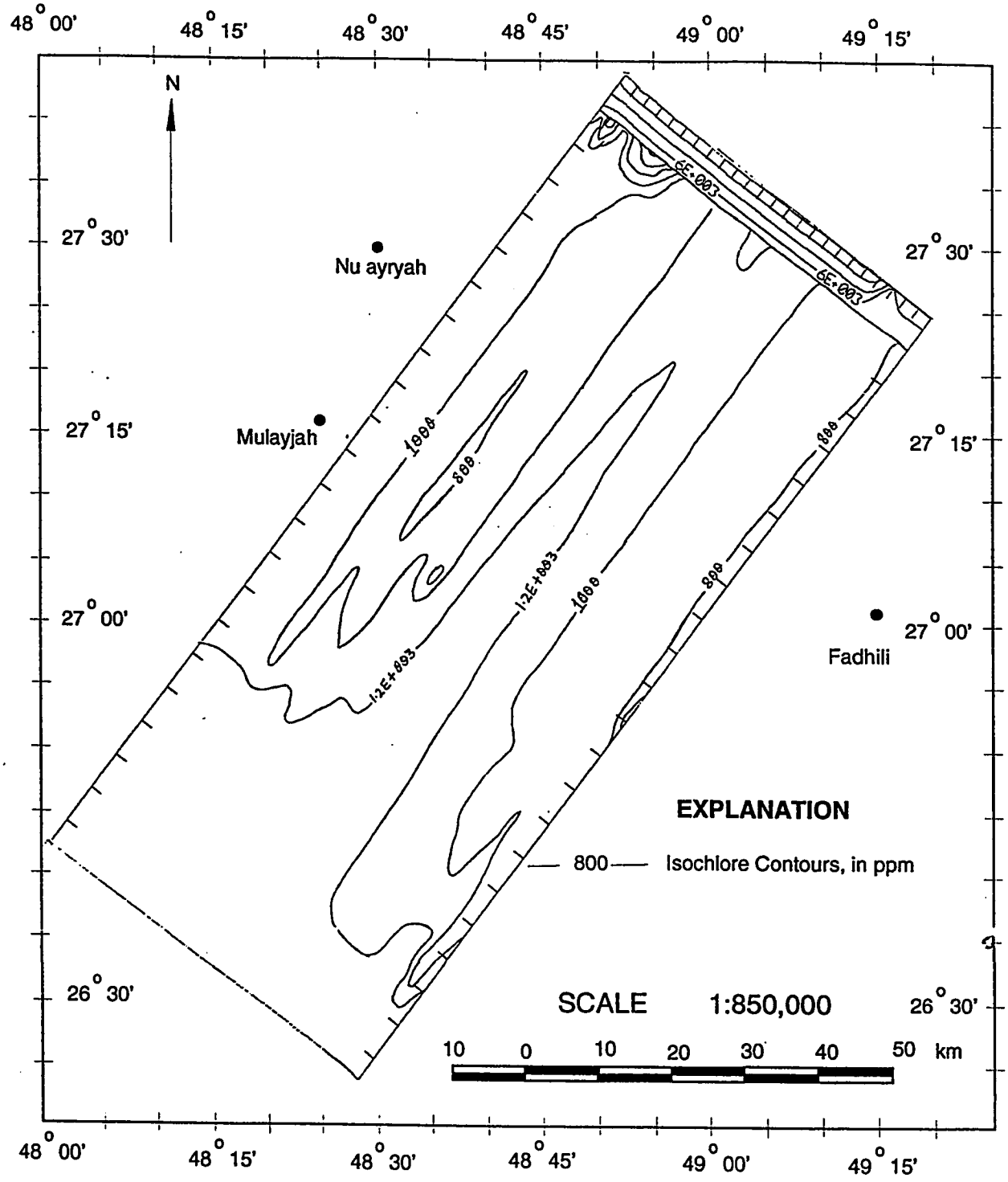

Figure 4.23: Isochlore Map of Neogene Aquifer (Steady-state Simulation)

4.4.3 Transient Calibration & Simulation

Transient calibration is carried out to simulate the effects of groundwater development on the predevelopment flow regime. A number of simulation runs were done in a series of time periods of one year to reproduce varying groundwater conditions from 1967 to 1994. The main purpose was to simulate the drop of heads and variations in Chloride concentrations due to extractions at various locations during that period.

The simulated time for transient runs is discretized into 28 stress periods of one year, each with 4 equal time steps. The aquifer properties and boundary conditions were kept unchanged during simulations. The flow and solute transport equations are solved during each time step for both pressure and Chloride concentrations. During the transient calibration, adjustment of inflow rate is done at the eastward boundary due to recharge and changes in storativity values are done by adjustment of aquifer compressibility values in the input data. The transmissivity and vertical leakage rates generated by the accepted steady-state calibration are changed locally for subsequent transient calibration. The extraction rates calculated for the period of 1967-1994 were used as aquifer stresses which show a steadily increasing trend. The analysis of relevant water balance is done to verify the distribution of computed aquifer parameters particularly close to the boundaries. Piezometric surface and isochlore maps of Khobar, Alat and Neogene aquifers for the year 1994 could

not be constructed because of the sparseness of observed data. The observed data collected consist of discontinous records of water level and Chloride concentration of few monitoring wells of the Ministry of Agriculture and Water (MAW). However, a reasonable comparison has been obtained between observed and simulated results. The simulated piezometric surface maps of Khobar, Alat and Neogene aquifers are shown in Figures 4.24, 4.25 and 4.26 respectively. A slight change in water levels for the three aquifers indicated that a very small portion of the aquifer storage is utilized in pumping during simulation period. The simulated isochlore maps of Khobar, Alat and Neogene aquifers for the 1994 year are shown in Figures 4.27, 4.28 and 4.29 respectively. The changes in storativities have little effect on the results which indicating that a very small fraction of the pumpage is supplied by aquifer storage while the bulk of flow comes either from vertical leakage or lateral flow. The transient calibration results reproduced the changes in water levels due to imposed changes in groundwater withdrawals at different well fields in the study area. It is observed that the pumpage had no significant effect on the regional distribution of groundwater levels except at few places. The transient calibration results also indicated that there is no appreciable change in the chloride distribution pattern which is verified by the field data.

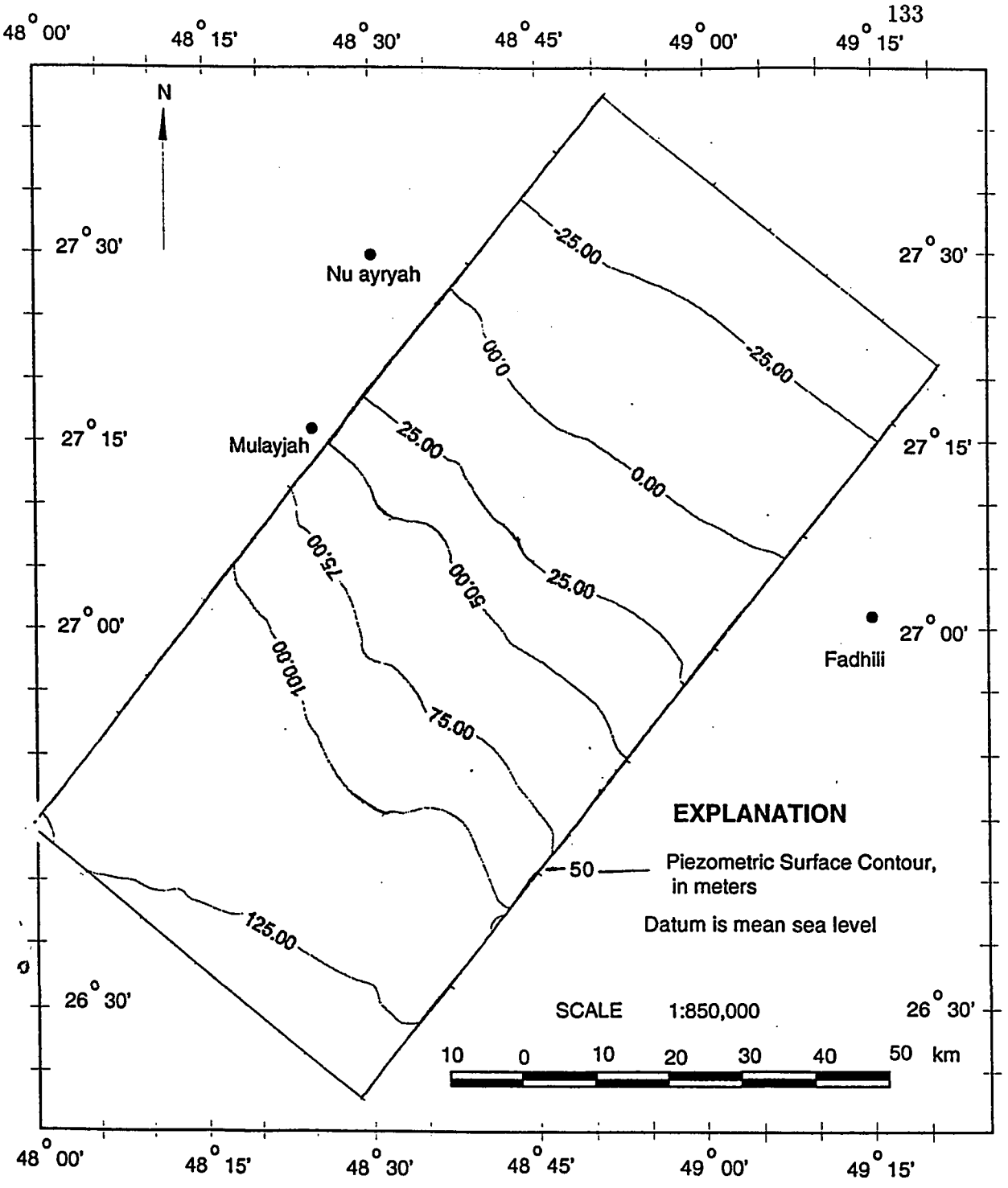

Figure 4.24: Simulated Piezometric Surface Map of Khobar Aquifer for the year 1994 (Transient run)

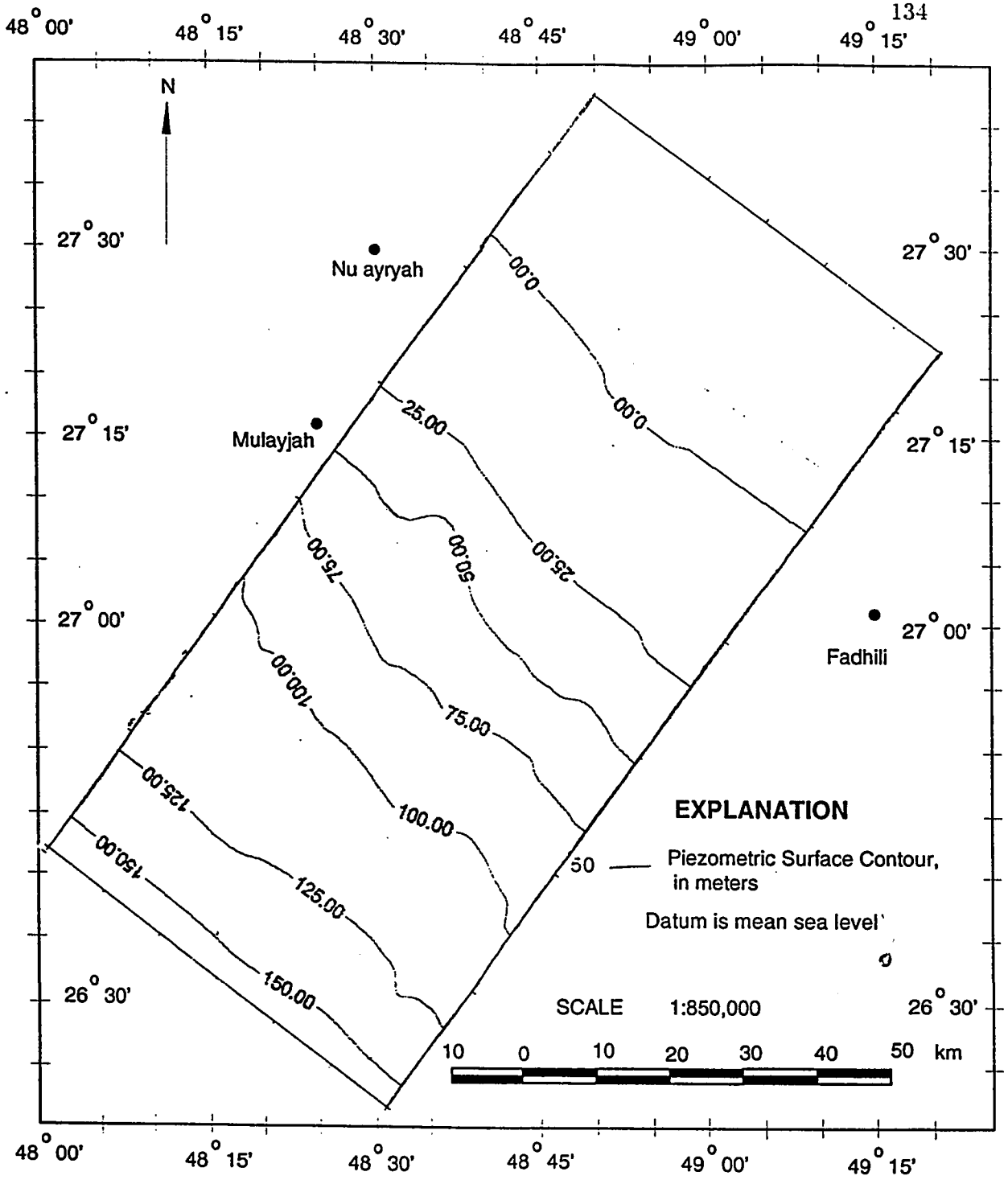

Figure 4.25: Simulated Piezometric Surface Map of Alat Aquifer for the year 1994 (Transient run)

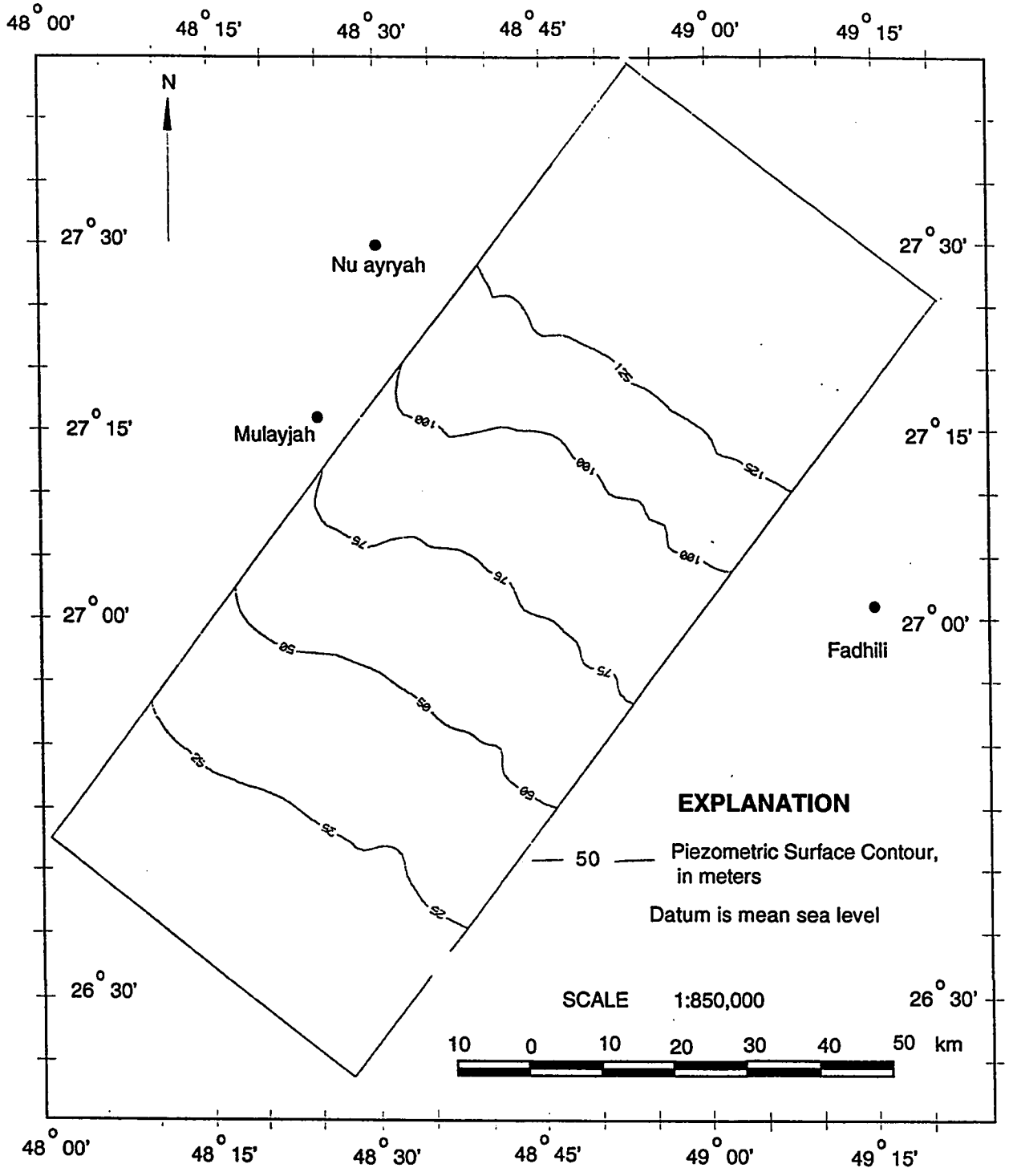

Figure 4.26: Simulated Water Level Surface Map of Neogene Aquifer for the year 1994 (Transient run)

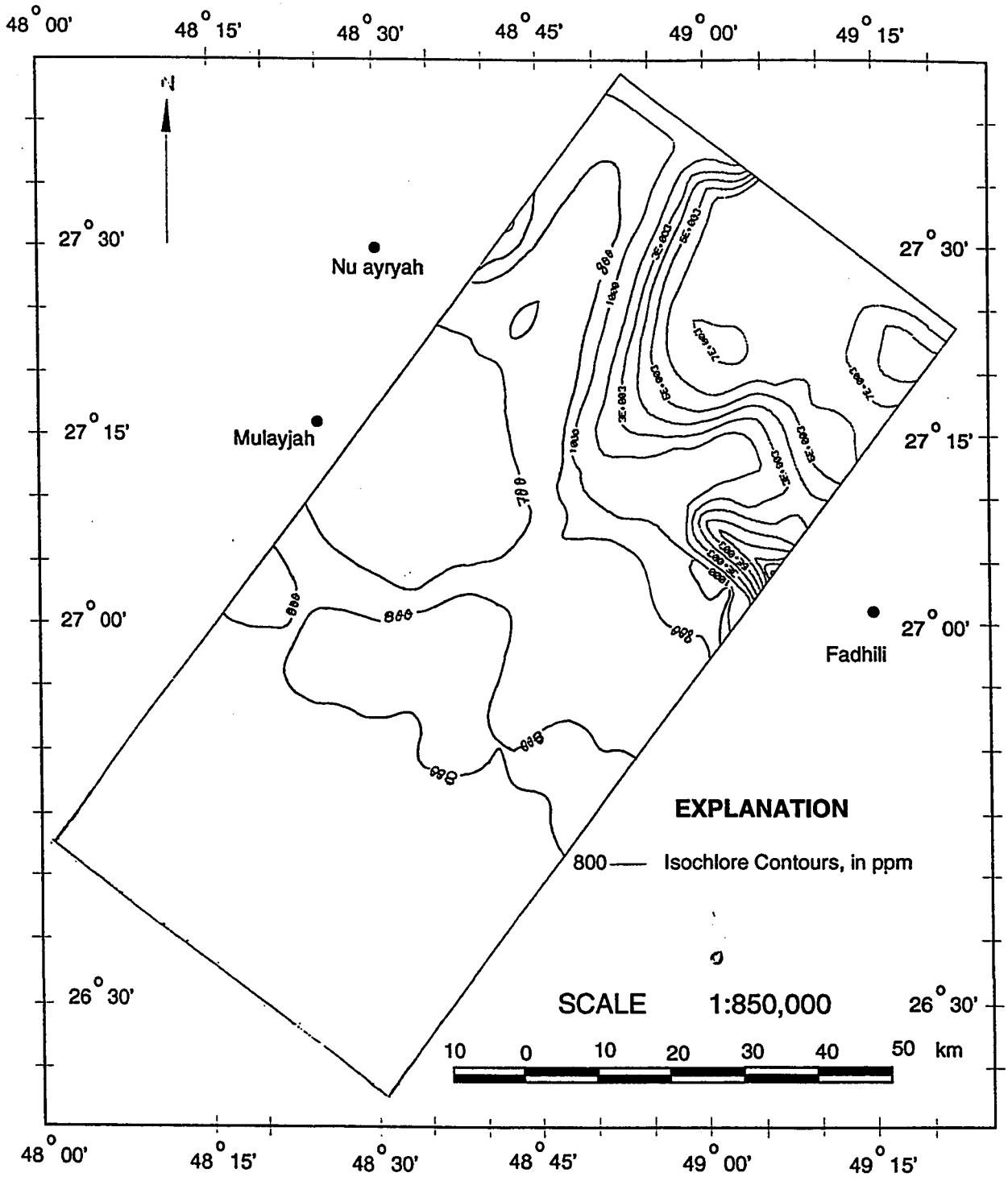

Figure 4.27: Simulated Isochlore Map of Khobar Aquifer for the year 1994 (Transient run)

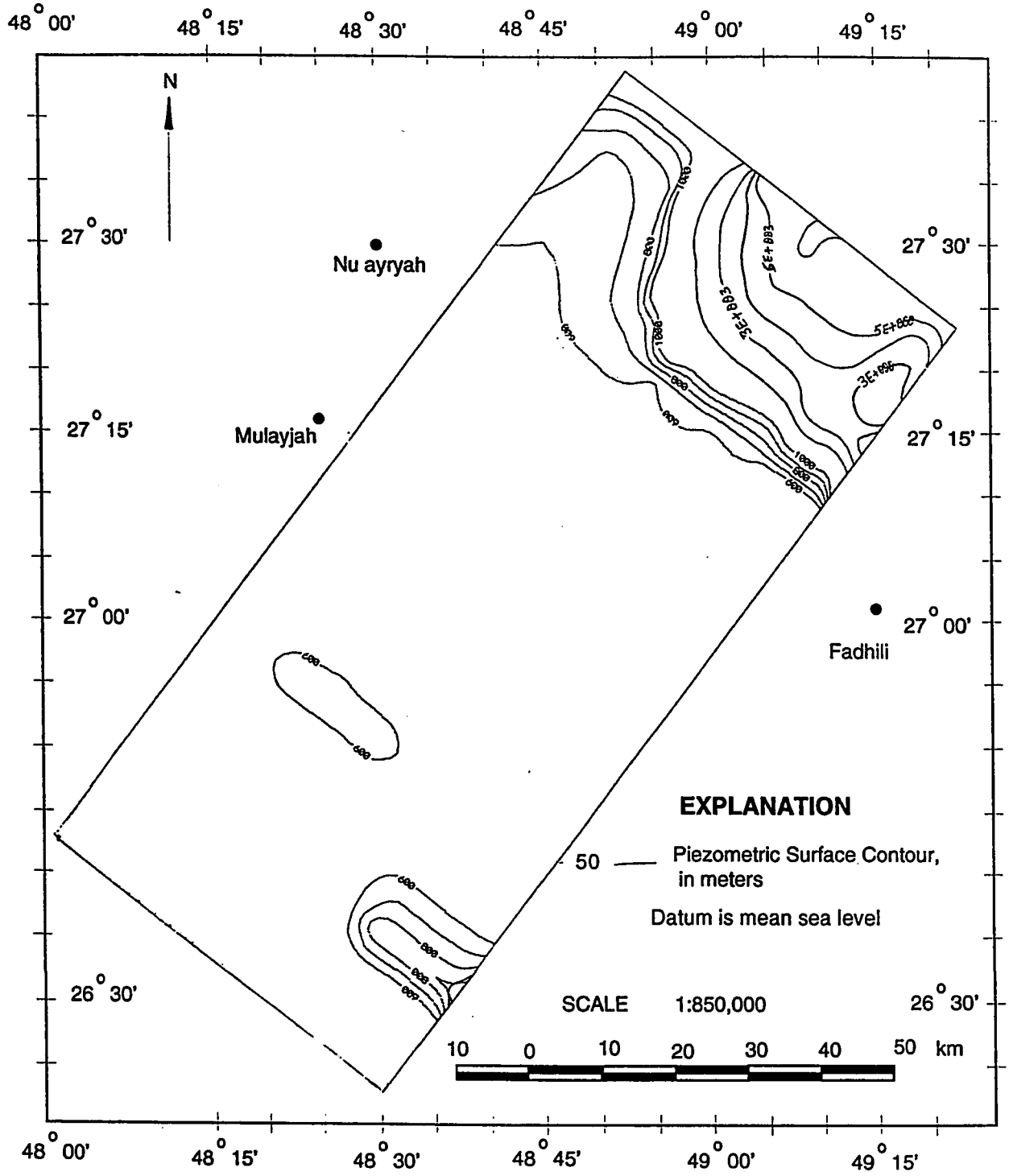

Figure 4.28: Simulated Isochlore Map of Alat Aquifer for the year 1994 (Transient run)

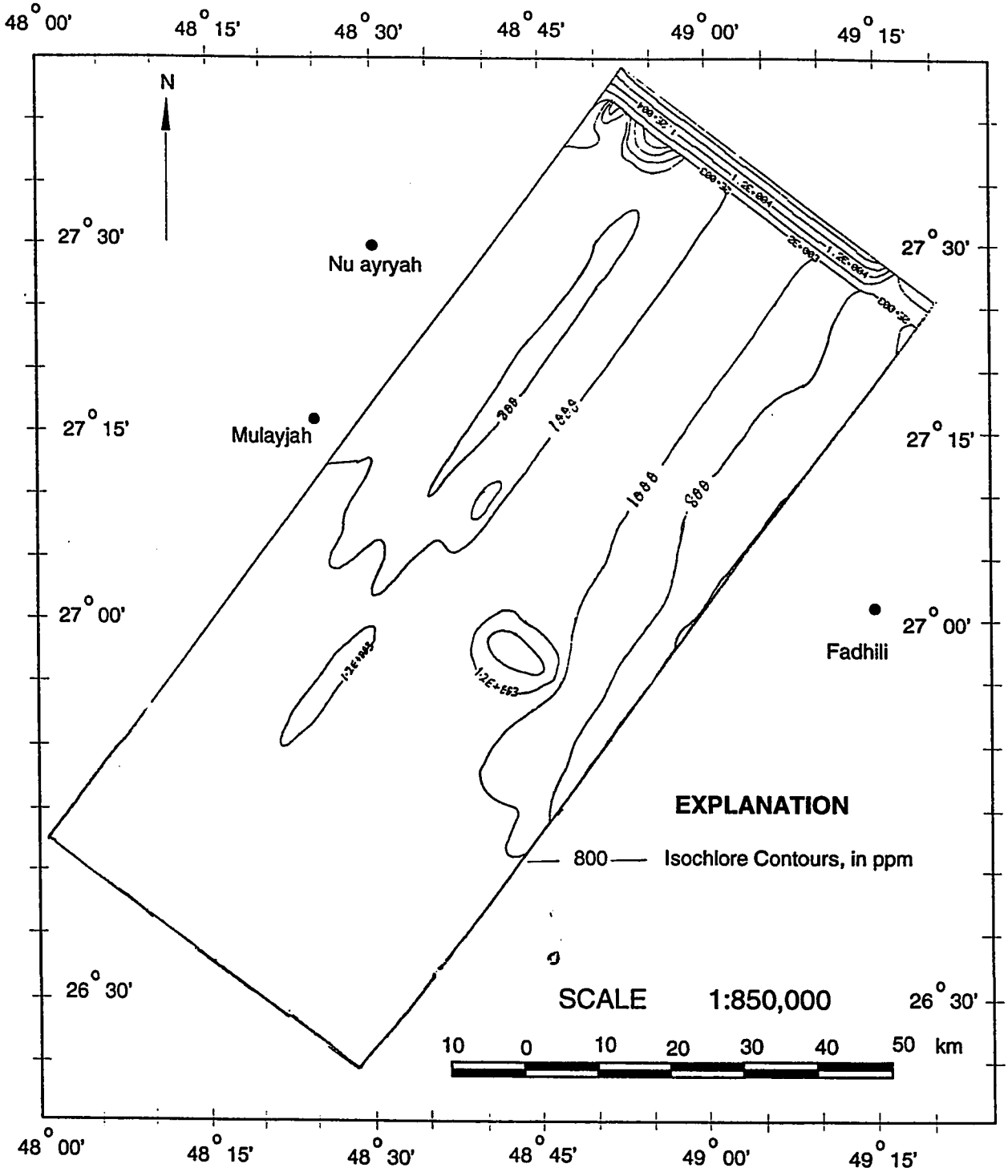

Figure 4.29: Simulated Isochlore Map of Neogene Aquifer for the year 1994 (Transient run)

It is observed that the pumpage had no significant effect on the regional distribution of groundwater levels except at few places. The transient calibration results also indicated that there is no appreciable change in the chloride distribution pattern which is verified by the field data except near Abuhadriya and Manifa areas where the concentrations were changed significantly.

In Khobar aquifer, with the given rates of leakage from Lower-Dammam aquitard at the given nodes , a zone of higher Chloride concentrations (greater than 5000 ppm) is simulated near Fadhli, Abuhadriya and Manifa areas. The pumping enhanced the vertical leakage, causing a sharp concentration gradient in the region. Due to high lateral groundwater velocities, the high concentrated zone in the northeasten corner of the study area is increased in size and moved towards the Arabian Gulf.

Verification

The recorded data available for 18 monitoring wells (Five in Khobar, seven in Alat, and six in Neogene aquifers) of the Ministry of Agriculture and Water (MAW) are used for comparison and verification of the model for transient simulations. The locations of these observation wells, corresponding to the nearest node of the element, are shown in Figures 4.30, 4.31 and 4.32 for Khobar, Alat and Neogene aquifers, respectively.

The results of SUTRA simulation show the distribution of heads and Chloride concentrations throughout the model area as they vary with time. They also show the magnitude and direction of fluid velocities as function of time. A large number of transient simulation runs are done to match the spatial and the temporal variations between observed and simulated head and chloride concentration values at specified locations. A considerable match was observed between the recorded and simulated head and Chloride concentrations at observation points for Khobar, Alat and Neogene aquifers, respectively. in the study area.

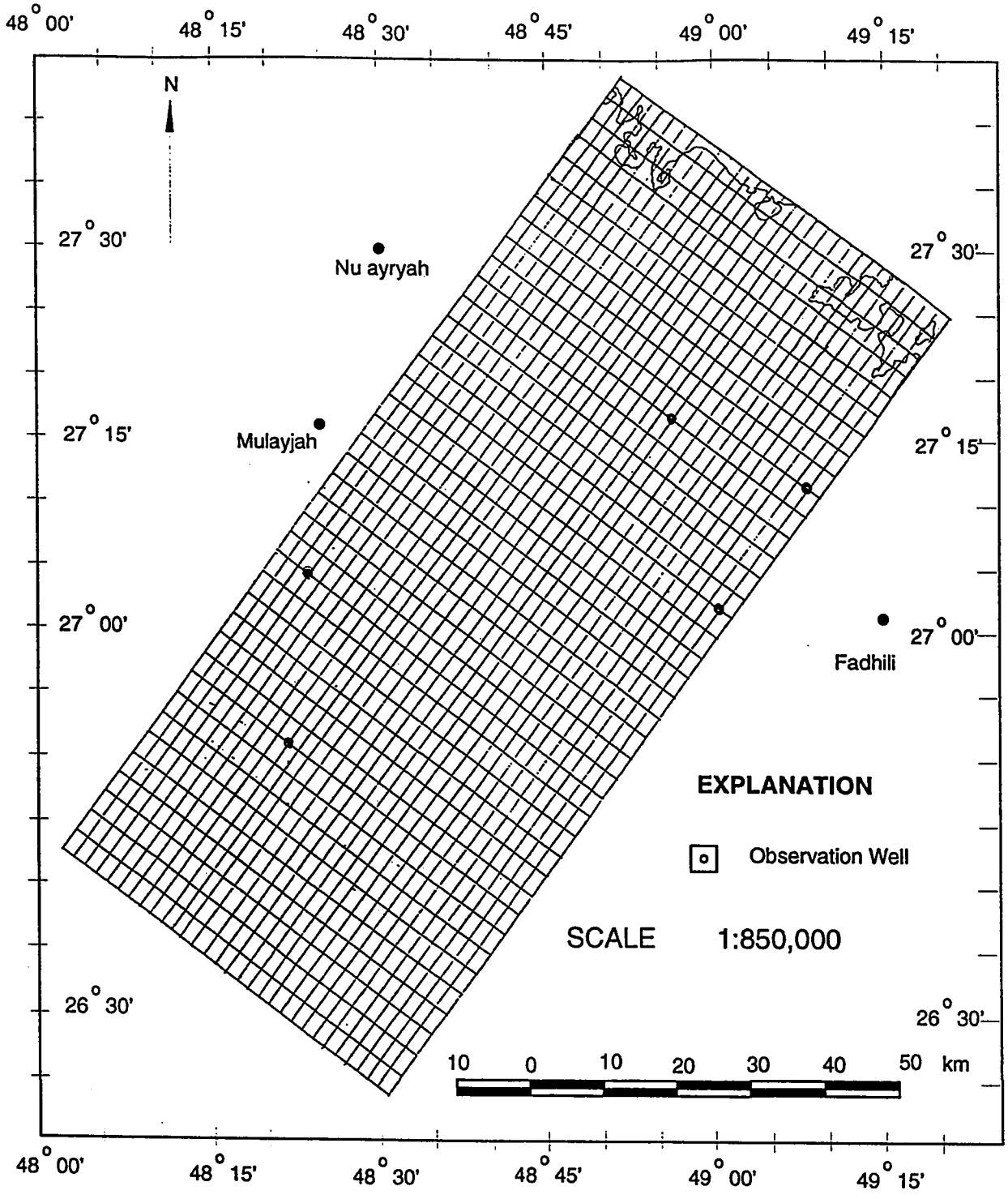

Figure 4.30: Location of Observation Wells for Khobar aquifer in the Study Area.

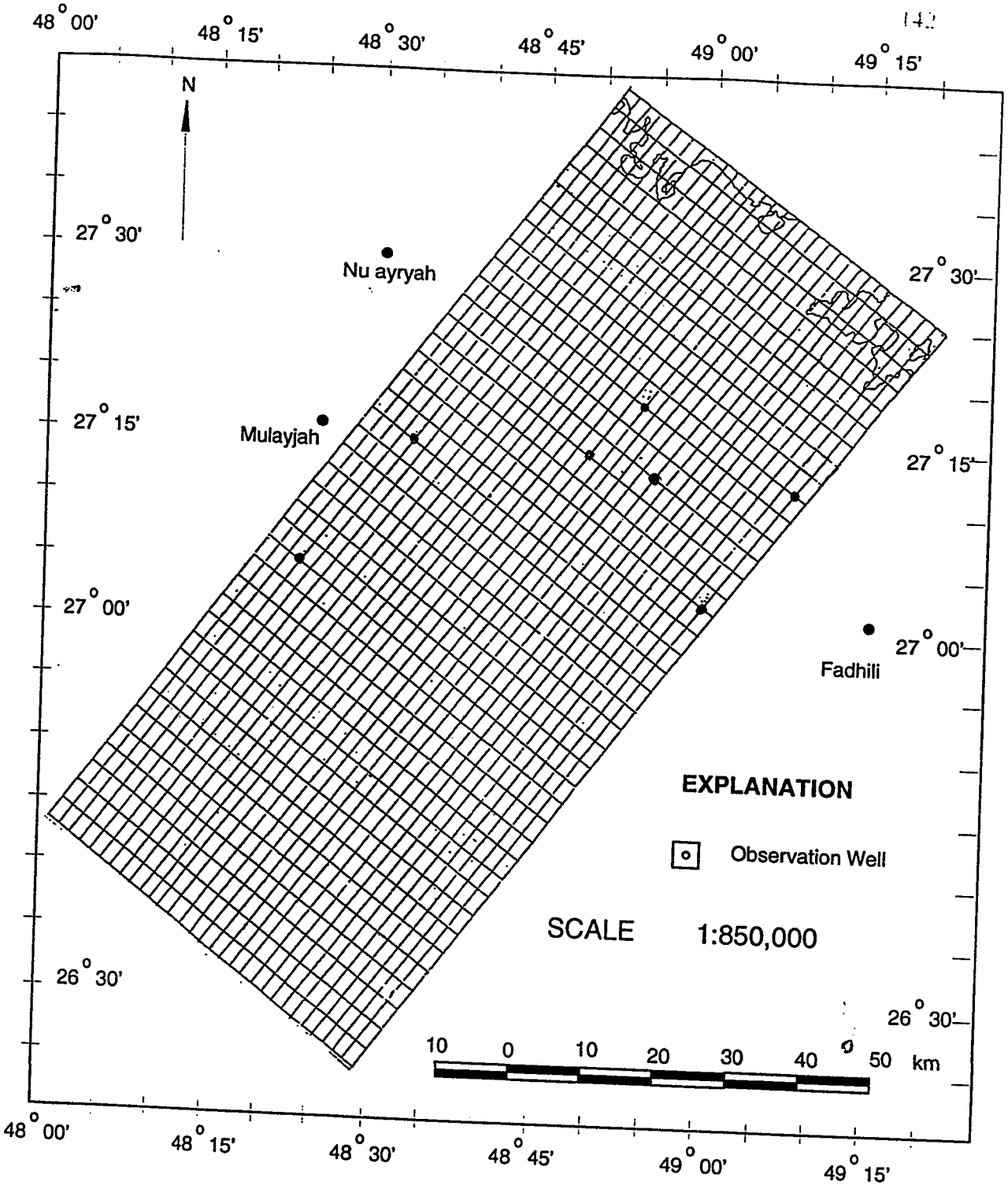

Figure 4.31: Location of Observation Wells for Alat aquifer in the Study Area.

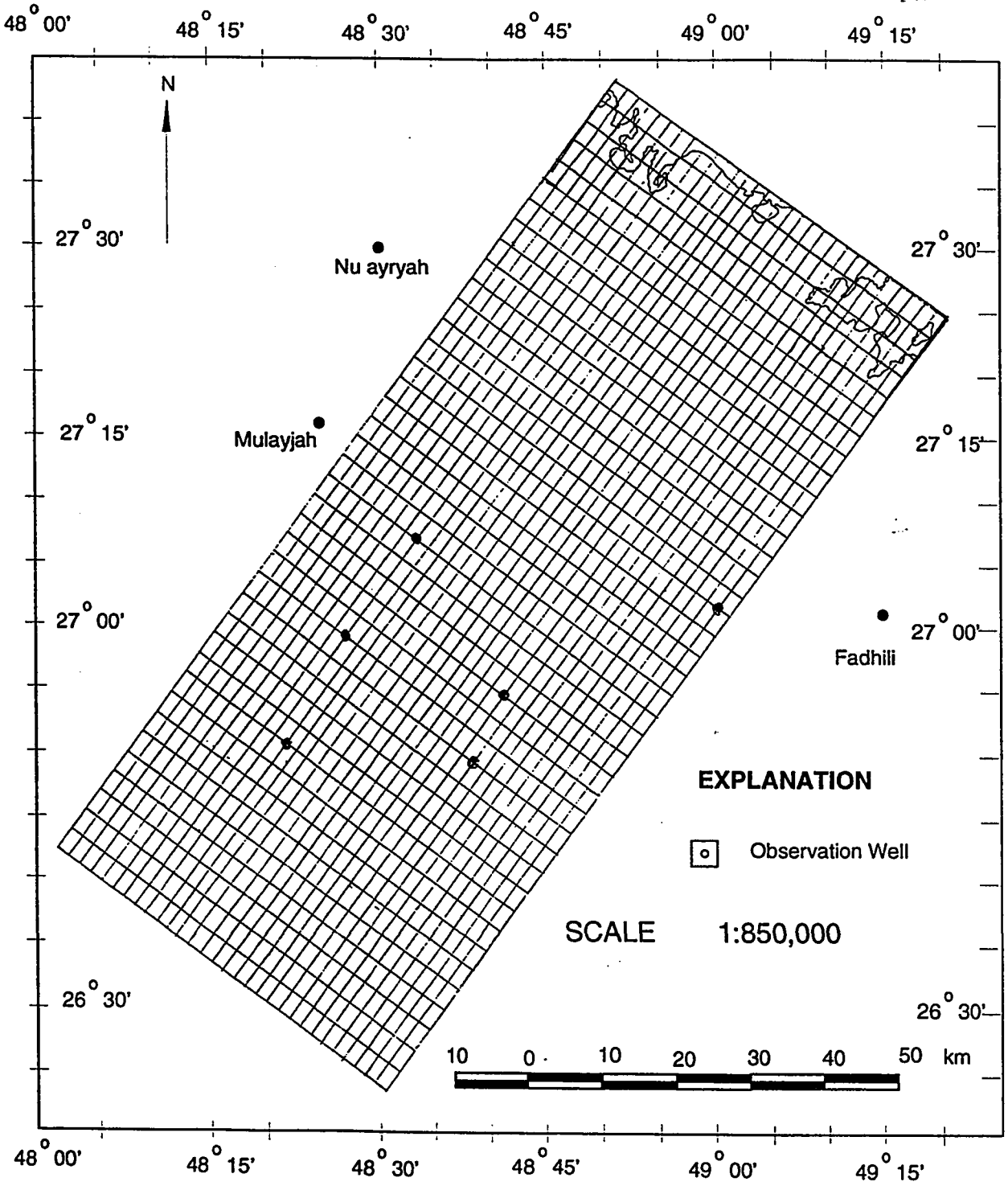

Figure 4.32: Location of Observation Wells for Neogene aquifer in the Study Area.

Khobar Historical Data & Model Results

The observed water level data at two monitoring wells (MI-2K and MI-23K) of the Ministry of Agriculture and Water (MAW) are utilized; their location corresponds to nodes(301) and (493), respectively. The simulated and observed water level data are shown in Figure 4.33. A perfect match is obtained at the nodes. The water level variation trend indicates that there was very little decrease in the water level from 1967 to 1994 which confirms a high vertical upward leakage from Umm Er Radhuma to Khobar aquifer.

The observed data for Chloride concentration were available for the three monitoring wells (HU-36K, ABDH-27 and KRSN-805) of the Ministry of Agriculture and Water (MAW) which are located at the nodes (746, 912 and 932), respectively. The match between observed and simulated chloride concentration variations through time are shown in Figures 4.34 and 4.35. The simulated Chloride concentration results are closely matching the observed ones, showing an increasing trend from less than 4000 ppm to more than 8000 ppm, except in well number ABDH-24, where the rate is rather slow (an increase of only 300 ppm).

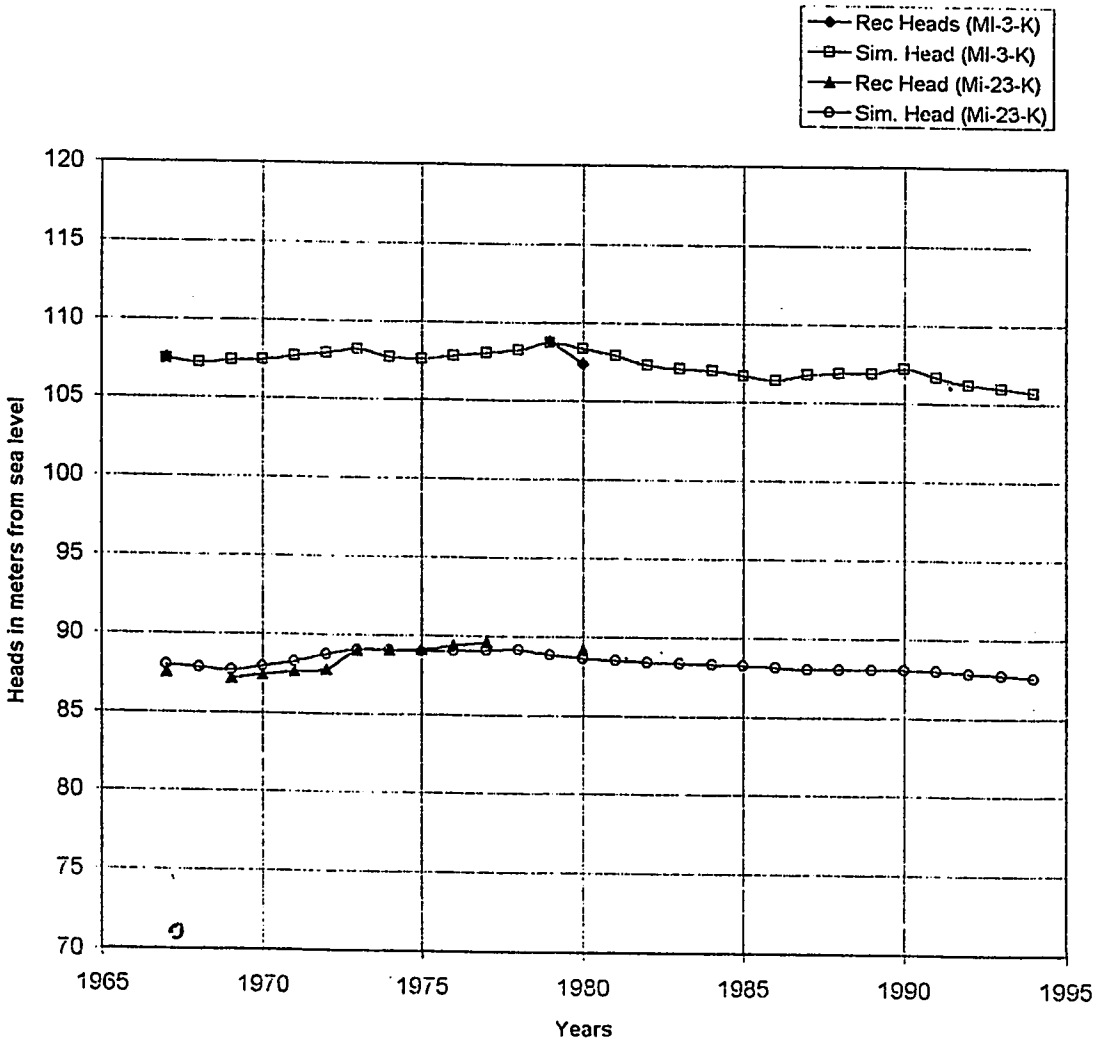

Figure 4.33: Water Level Hydrograph for Khobar Aquifer at nodes (301 & 493).

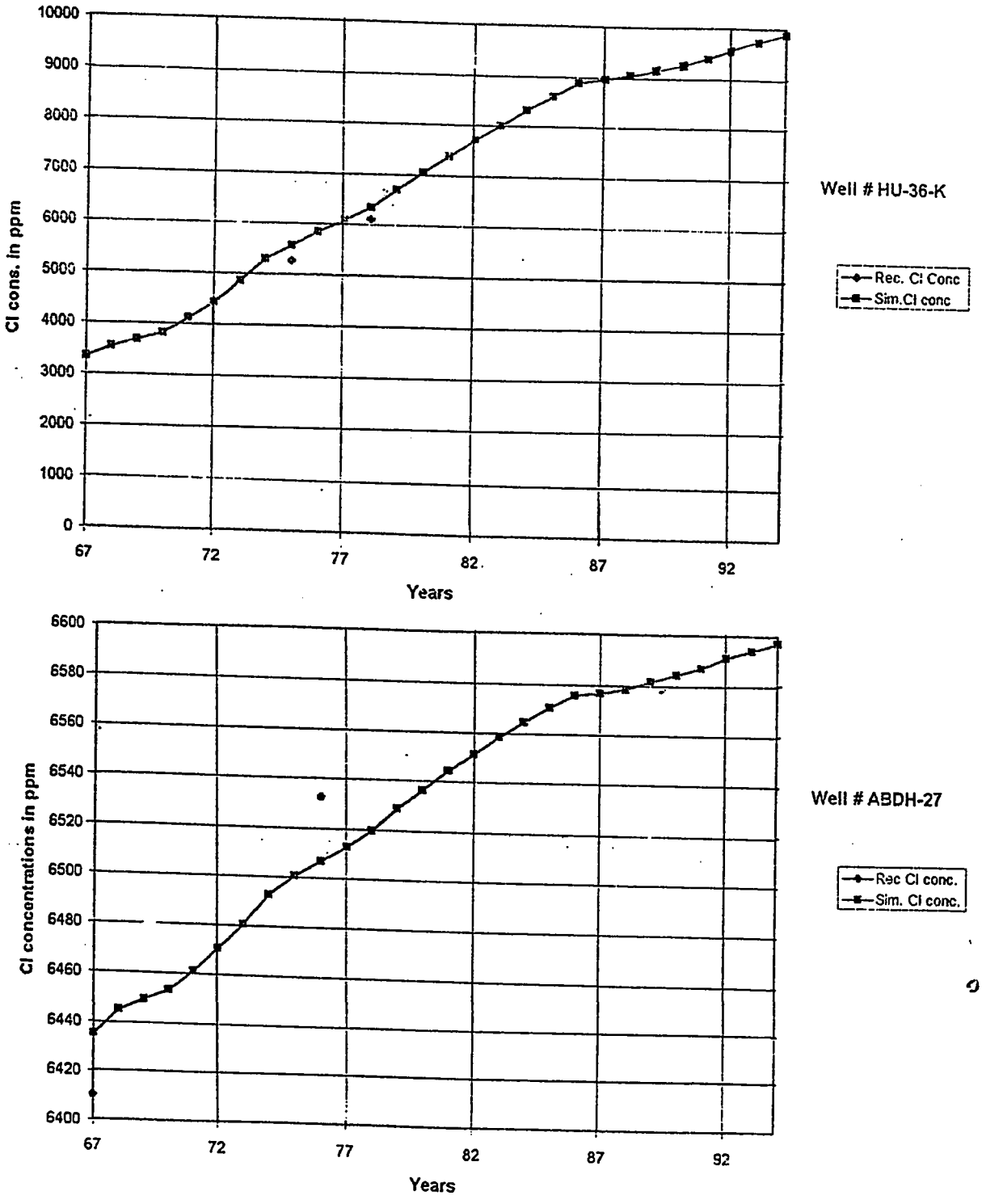

Figure 4.34: Comparison of Temporal variations in Recorded and Simulated Cl. Concentrations for Khobar Aquifer at nodes (746 & 912).

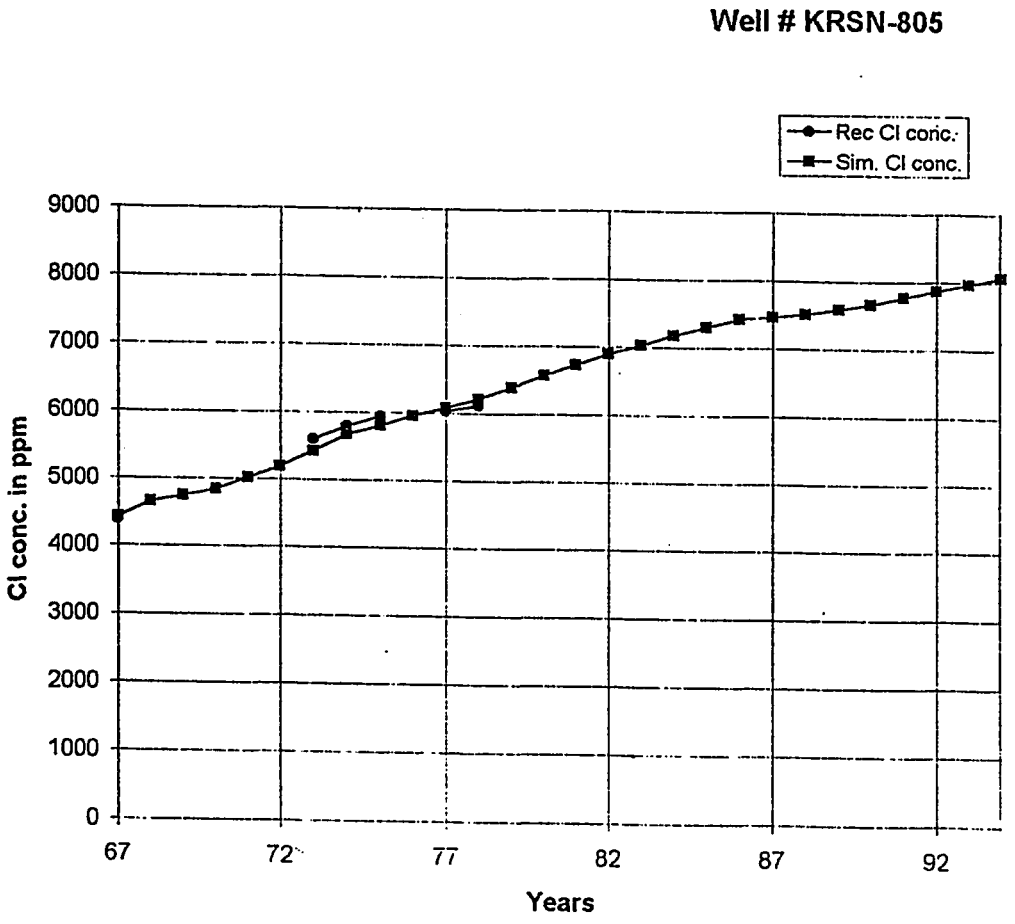

Figure 4.35: Comparison of Temporal variations in Recorded and Simulated chloride Concentrations for Khobar Aquifer at nodes (931).

Alat Historical Data & Model Results

The historical water level data for two monitoring wells (MI-3A and MI-23A) of the Ministry of Agriculture and Water (MAW) are utilized; their location correspond to nodes (301) and (493), respectively, Figure 4.36. Water level hydrographs indicate a slightly decreasing trend, showing the effects of pumping in this region. The chloride concentration variations are calibrated by comparing the recorded water quality data of five monitoring wells (WA-329, MI-3A, S-222, AHW804 and KRSN-803) of the Ministry of Agriculture and Water (MAW) which correspond to the nodes (301, 822, 848, 932, and 914), respectively. The graphs between observed and simulated chloride concentration variation through time are shown in Figures 4.37, 4.38 and 4.39. A general increasing trend is evident from the figures which is due to the high leakage rate of saline water from Khobar into the Alat aquifer through the thin and leaky aquitard.

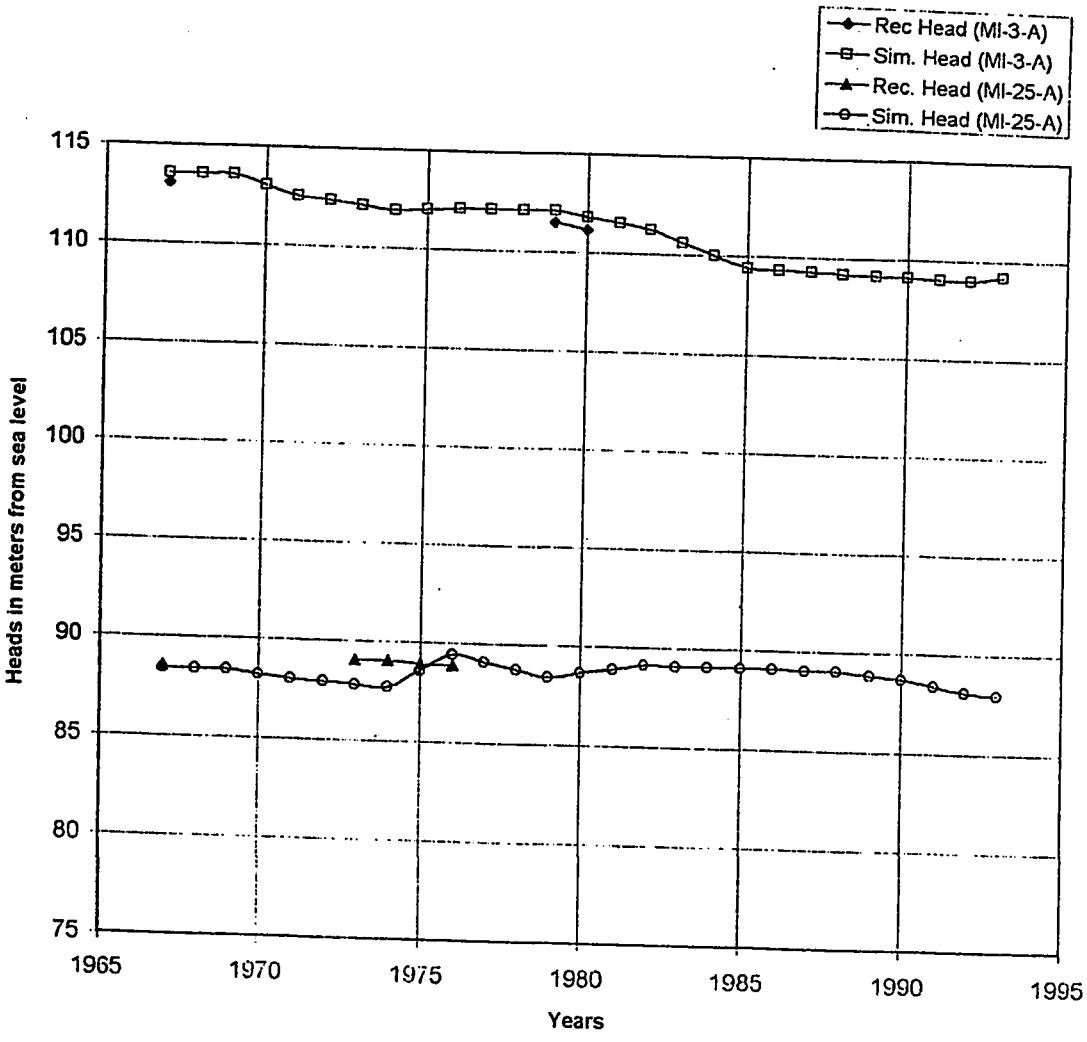

Figure 4.36: Water Level Hydrograph for Alat Aquifer at nodes (301 & 493).

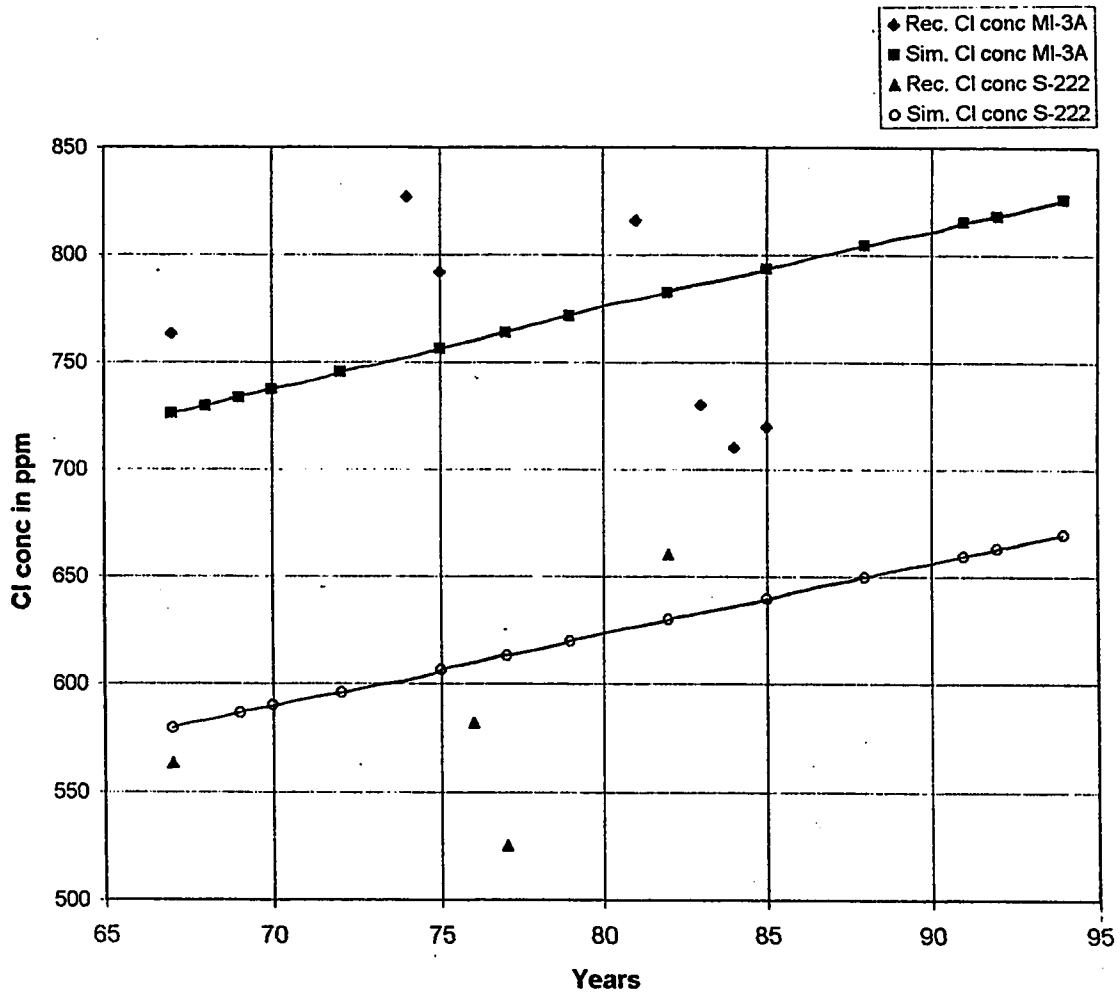

Figure 4.37: Comparison of Temporal variations in Recorded and Simulated chloride Concentraions for Alat Aquifer at nodes (301 & 822).

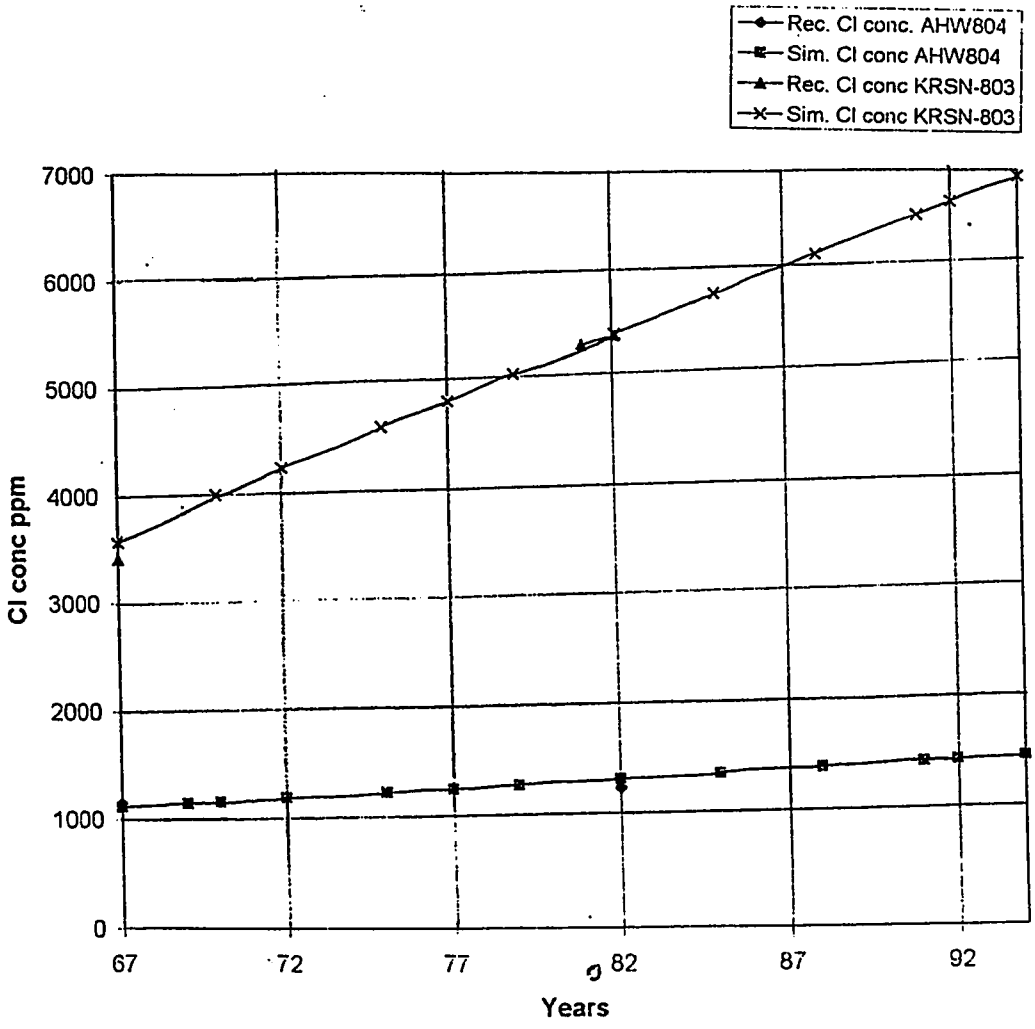

Figure 4.38: Comparison of Temporal variations in Recorded and Simulated chloride Concentrations for Alat Aquifer at nodes (848 & 932).

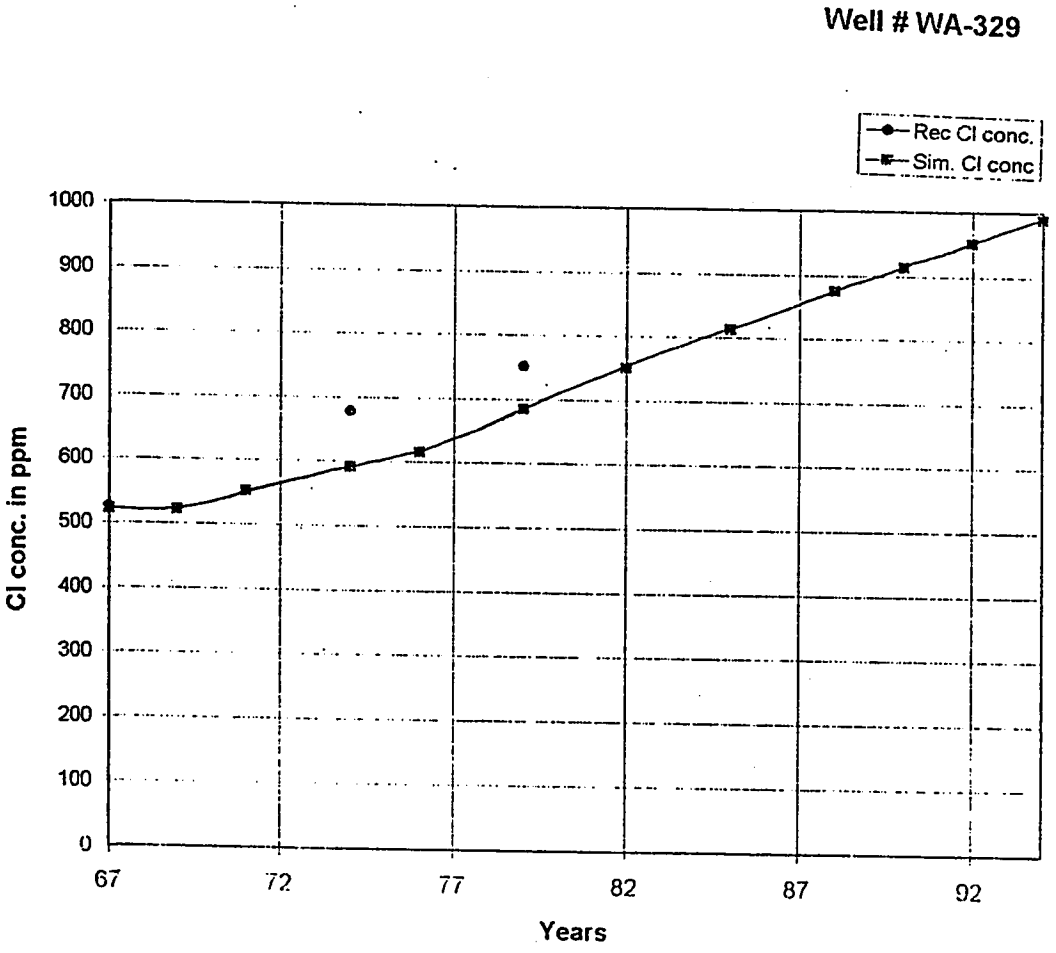

Figure 4.39: Comparison of Temporal variations in Recorded and Simulated chloride Concentrations for Alat Aquifer at nodes (914).

Neogene Historical Data & Model Results

The historical water level data for two monitoring wells (MI-4N and HU-34N) of the Ministry of Agriculture and Water (MAW) are utilized; their locations correspond to nodes (301) and (746), respectively, Figure, 4.40 Water level hydrographs indicate a perfect match of simulated water levels with observed ones. The low extraction rates from Neogene aquifer are evident from the slight variations in the water levels at these check points. Extractions are mainly utilized for irrigation on land immediatly overlying this aquifer. The return flows to the aquifer, which is approximately 50% of the gross abstraction, compensated the effects of the pumping in this region. Transient calibration of model for chloride concentrations is done by comparing the simulated results of four wells (WA338, WA240, WA283 and WA228) of Ministry of Agriculture and Water (MAW) with the observed ones. These wells correspond to the nodes (301, 822, 848, 932, and 914) of the model grid, respectively. The graphs between observed and simulated chloride concentration variation through time are shown in Figures 4.41 and 4.42. A perfect match was obtained at the four nodes. The observed trend in chloride concentration data were satisfactorily reproduced, indicating a gradual increase in concentration due to upward leakage of saline waters from Alat aquifer into Neogene through slim aquitard.

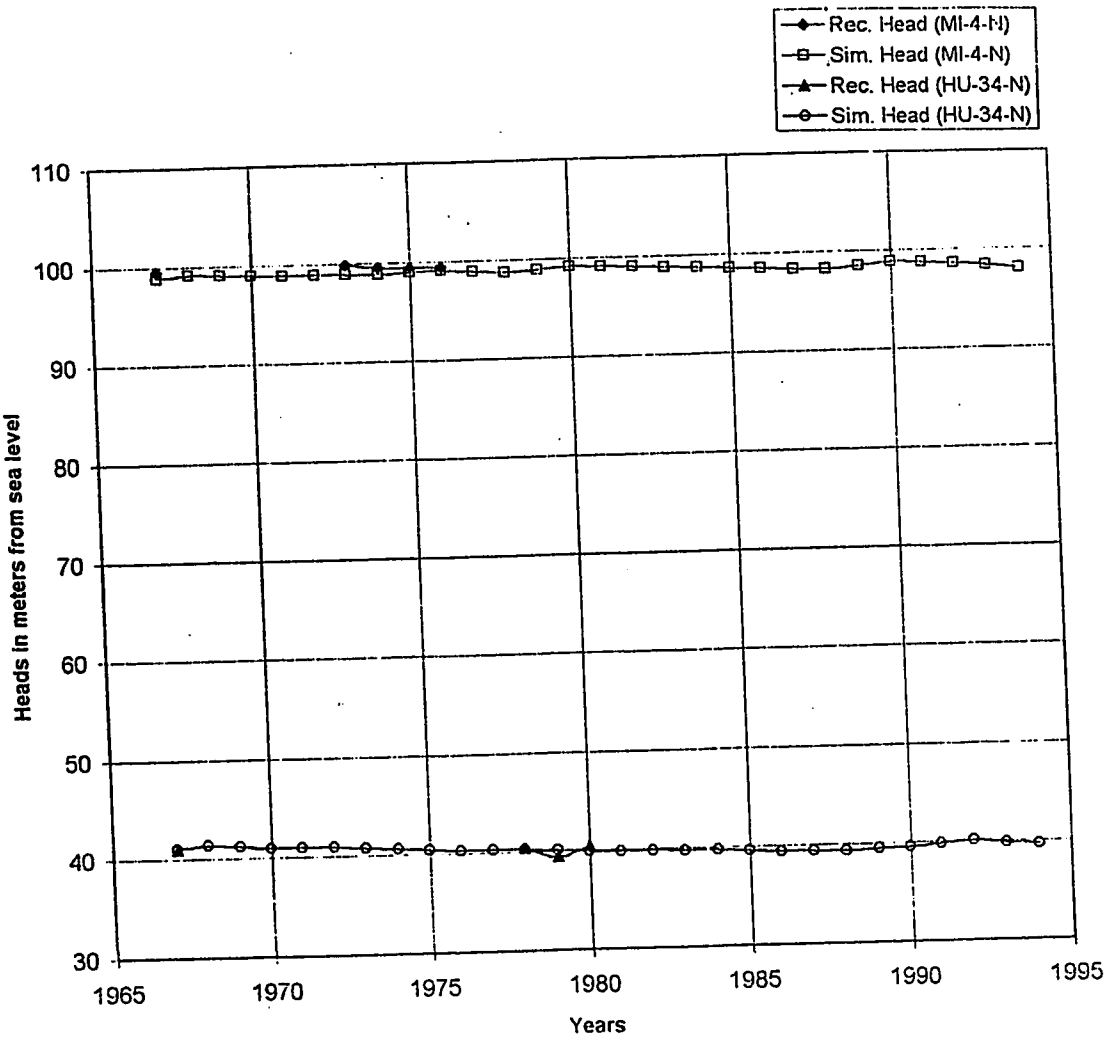

Figure 4.40: Water Level Hydrograph for Neogene Aquifer at nodes (301 & 746).

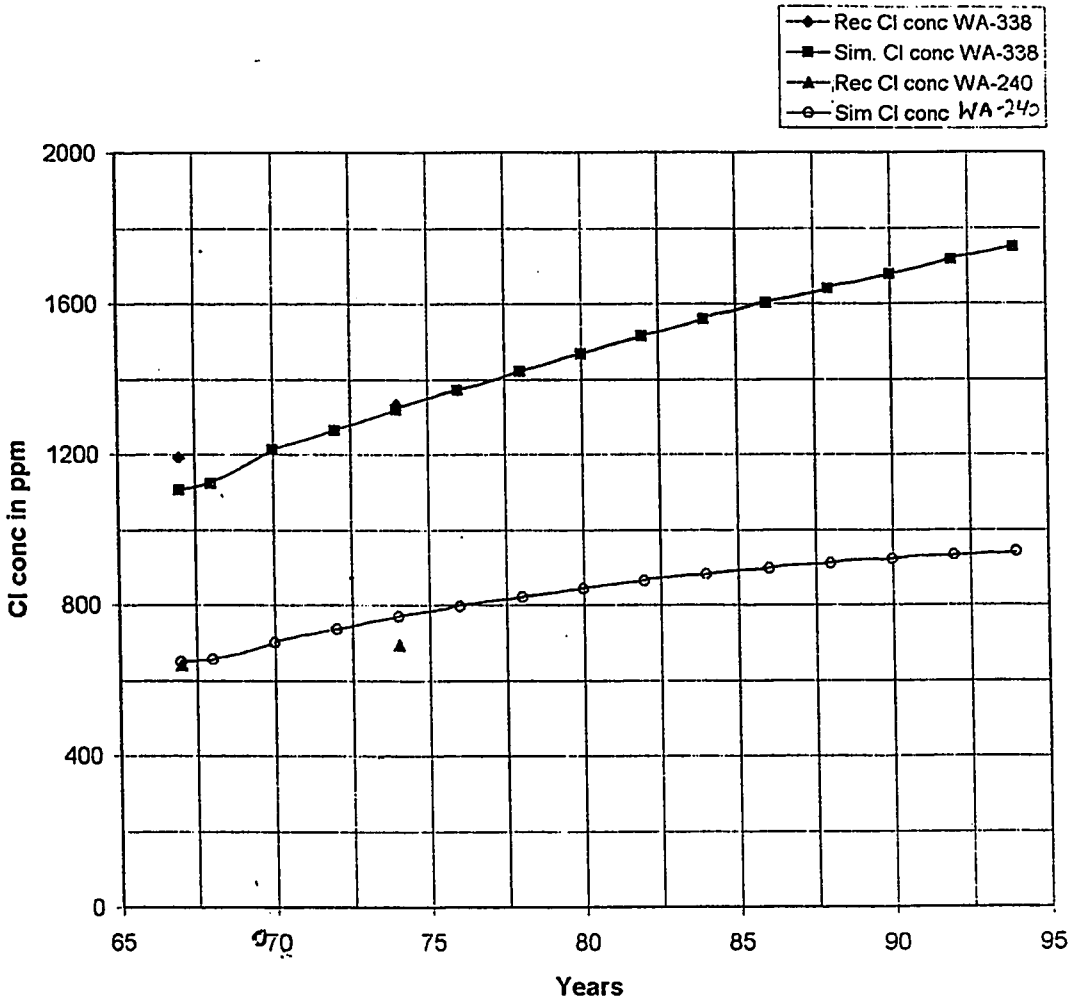

Figure 4.41: Comparison of Temporal variations in Recorded and Simulated chloride Concentrations for Neogene Aquifer at nodes (413 & 457).

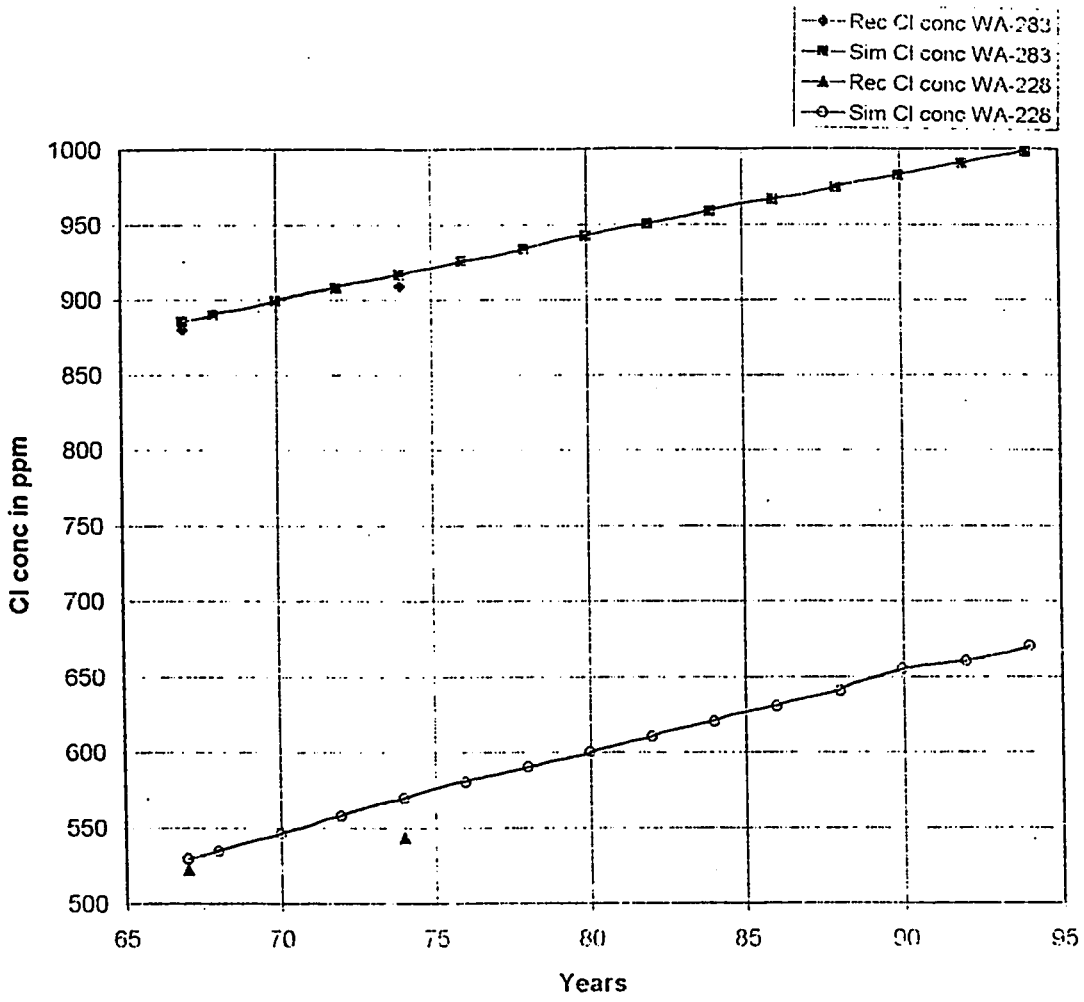

Figure 4.42: Comparison of Temporal variations in Recorded and Simulated chloride Concentrations for Neogene Aquifer at nodes (507 & 612).

4.4.4 Calibrated Aquifer Parameters

The aquifer parameter values that produced the best predevelopment simulation results are shown in Table, 4.8. The lateral permeabilities in the three aquifers are more than 20 times the transverse permeabilities which verifies the anisotropy of the aquifers. This anisotropy caused the major component of flow in lateral direction in the aquifers. A comparison of simulated transmissivites with field ones is given in Table, 4.9. The results show a reasonable match. The slight discrepancy in the results is due to the fact that field transmissivities represent the point values while simulated values indicate the values of the model element of 3.6 by 2 Kms. The regional distribution of calibrated transmissivities and leakage rates in Neogene, Alat and Khobar aquifers are shown in Figures, 4.43, through 4.48, respectively. Figure 4.43 represents the calibrated transmissivity patterns in Khobar aquifer. Low transmissivities (100 to 300 m^2/d) are found along the southwest region of the model. This is confirmed with the steep hydraulic gradients observed in this area. The northeastern part (including Abuhadriyah and Manifa areas) is characterized by very high transmissivities, ranging from 5000 to 10,000 m^2/d. The low hydraulic gradients, observed in this region are due to these high transmissivity values. The calibrated derived transmissivity values of Alat aquifer are illustrated in Figure, 4.44. The high transmissivities are found along the northeast and the low ones along southwest. Figure, 4.45 illustrates the spatial distribution of calibrated

aquifer transmissivities in Neogene aquifer. It shows a relatively uniform pattern of distribution with slightly high values at the northeast corner and low values at the southwest corner.

Aquifer Properties	Neogene	Alat	Khobar
Lateral Intrinsic Permeabilities (m/d)	62.994 - 188.983	0.605 - 58.1	1.749 – 114.9
Transverse Intrinsic Permeabilities (m/d)	0.1987 - 0.5962	0.225 - 21.57	0.864 - 56.85
Transmissivities (m^2/d)	2677.25 - 16063	11.7 - 1789.5	48.1 - 6319.5

Table 4.8: Calibrated Aquifer Parameters after Simulation Runs.

Aquifers	Italconsult Well Number	Corresponding Model Element Number	Aquifer Transmissivities Field Value (Test data)	Calibrated Value
Neogene	Point A	292	12.96	7496.3
Alat	Point A	292	81.216	1771.2
Alat	Point c	478	2.246	96.768
Khobar	Point A	292	14.61 - 777.6	645.73
Khobar	Point c	478	155.52 - 224.64	95.99
Khobar	Hulaysiyah Village	301	40	645.65

Table 4.9: Comparison of Field and Calibrated Transmissivities of Aquifers.

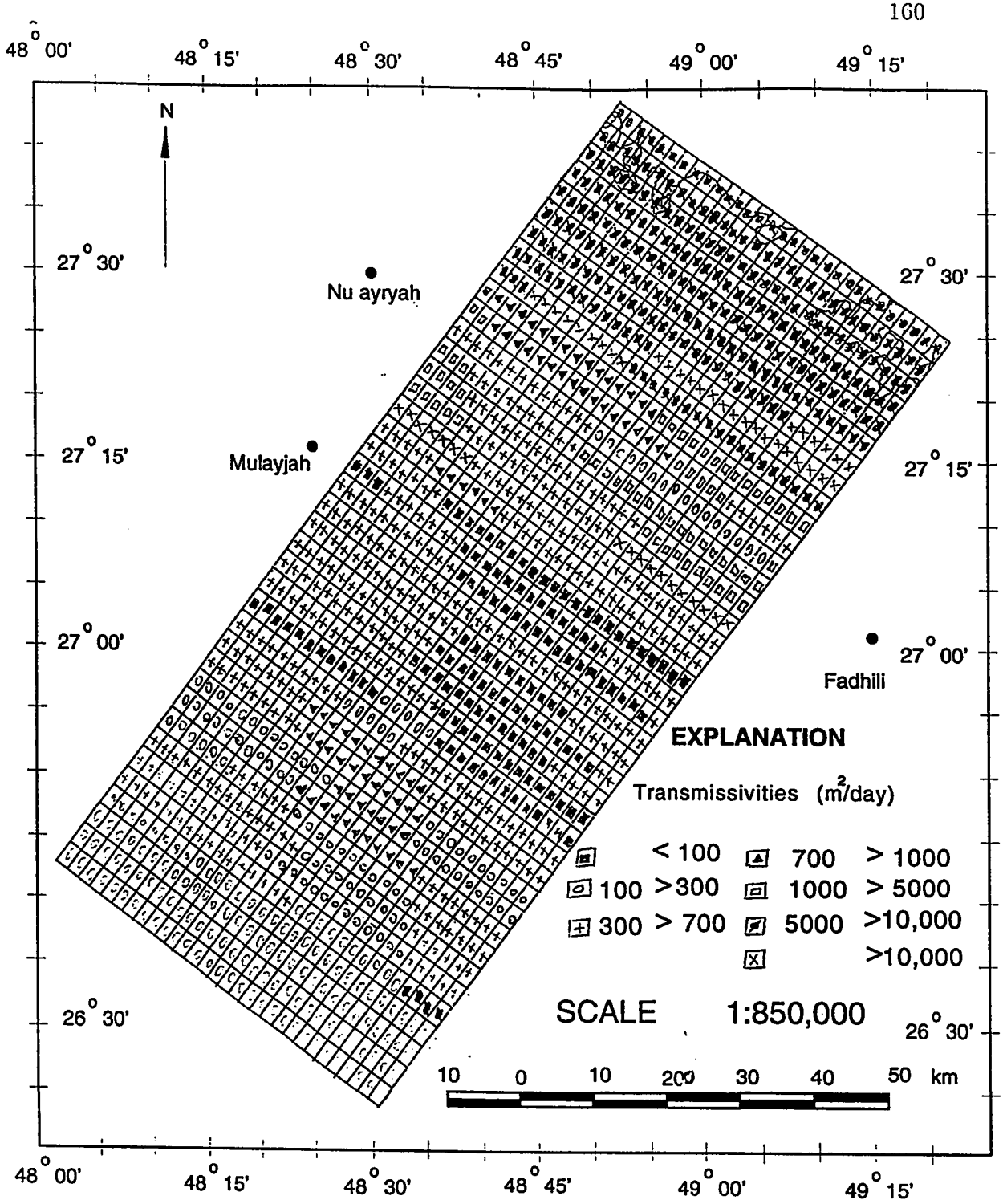

Figure 4.43: Calibrated Transmissivity distribution Map of Khobar Aquifer

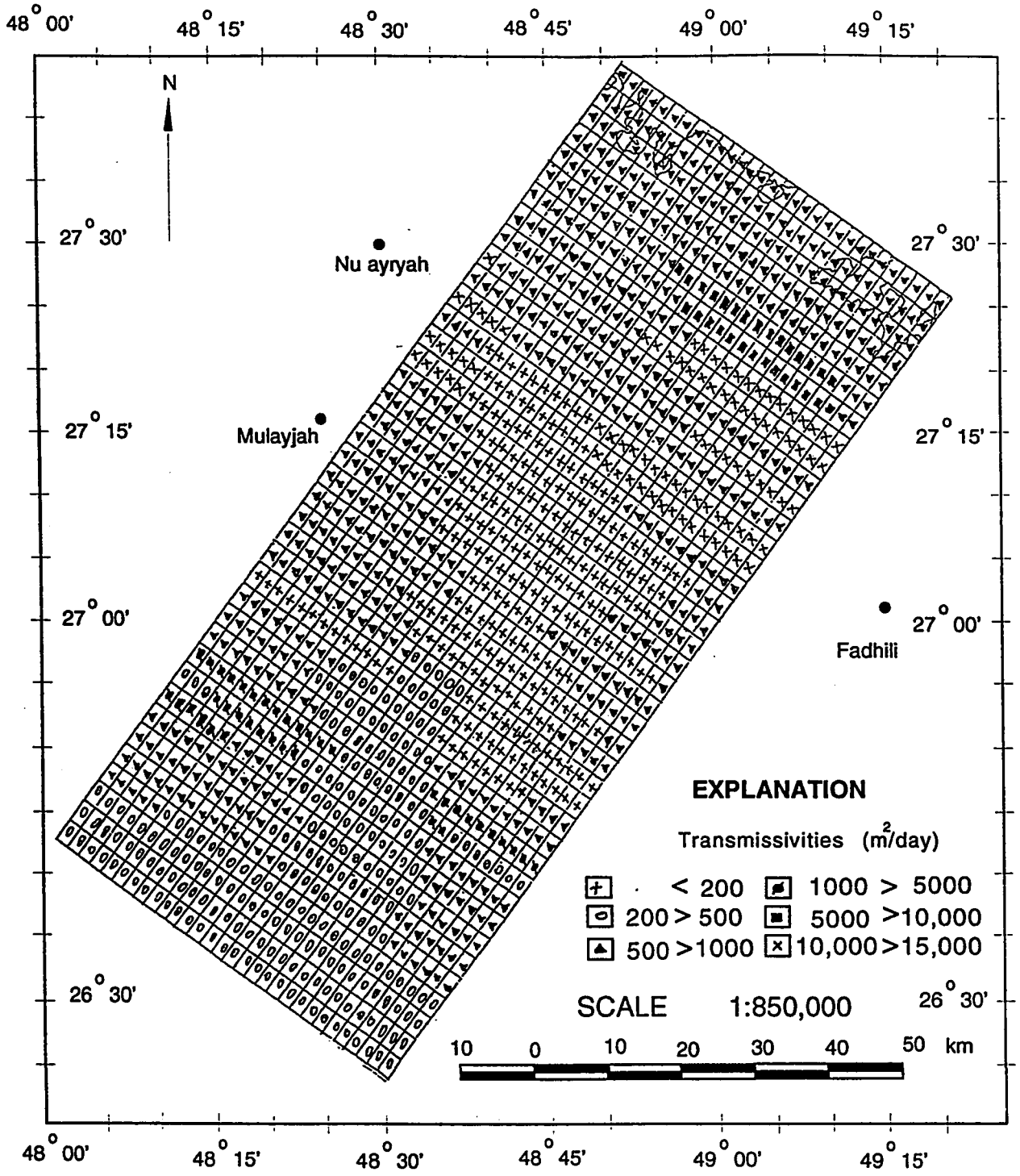

Figure 4.44: Calibrated Transmissivity distribution Map of Alat Aquifer

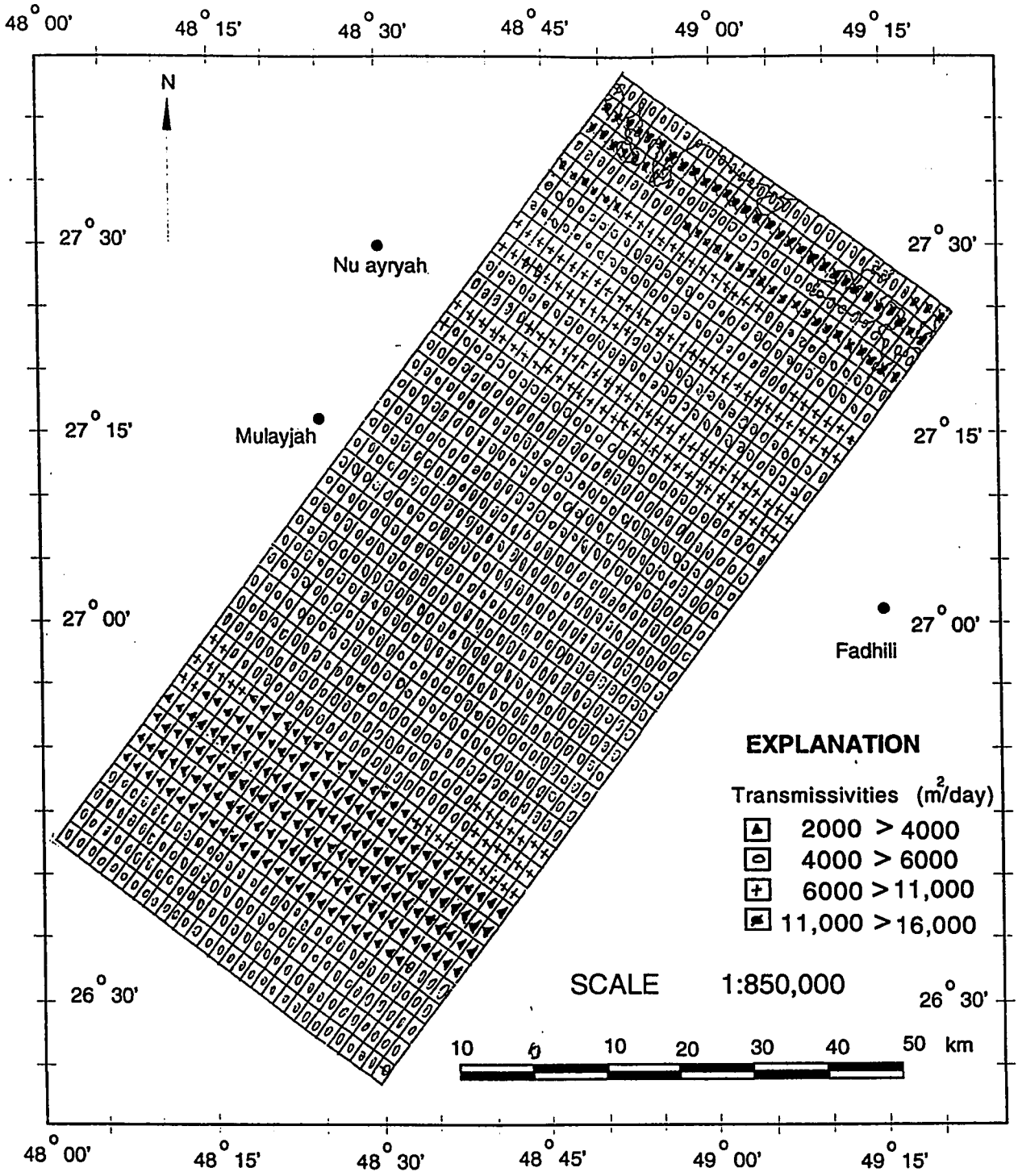

Figure 4.45: Calibrated Transmissivity distribution Map of Neogene Aquifer

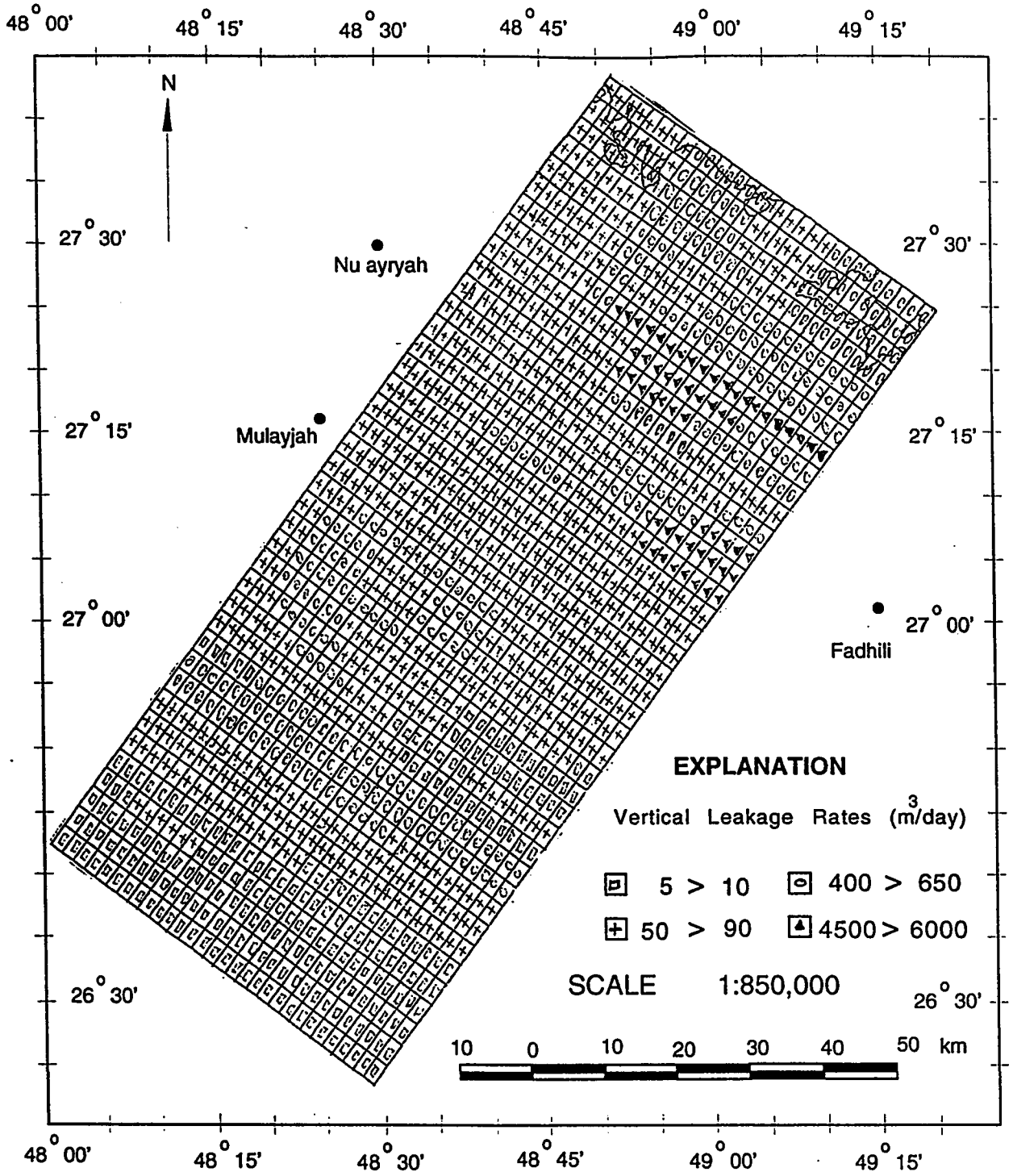

Figure 4.46: Calibrated Vertical Leakage Rates Distribution Map of Khobar Aquifer

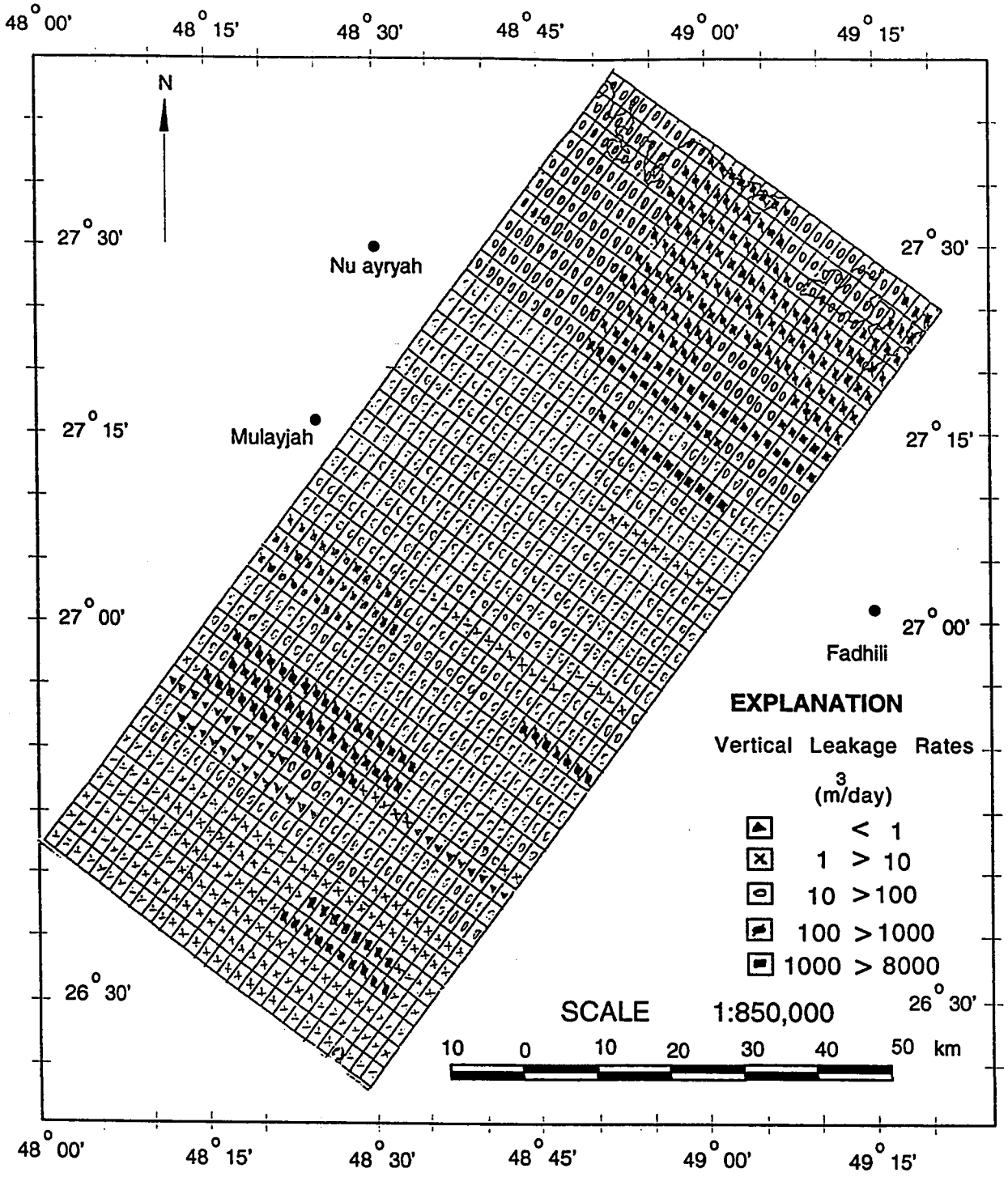

Figure 4.47: Calibrated Vertical Leakage Rates Distribution Map of Alat Aquifer

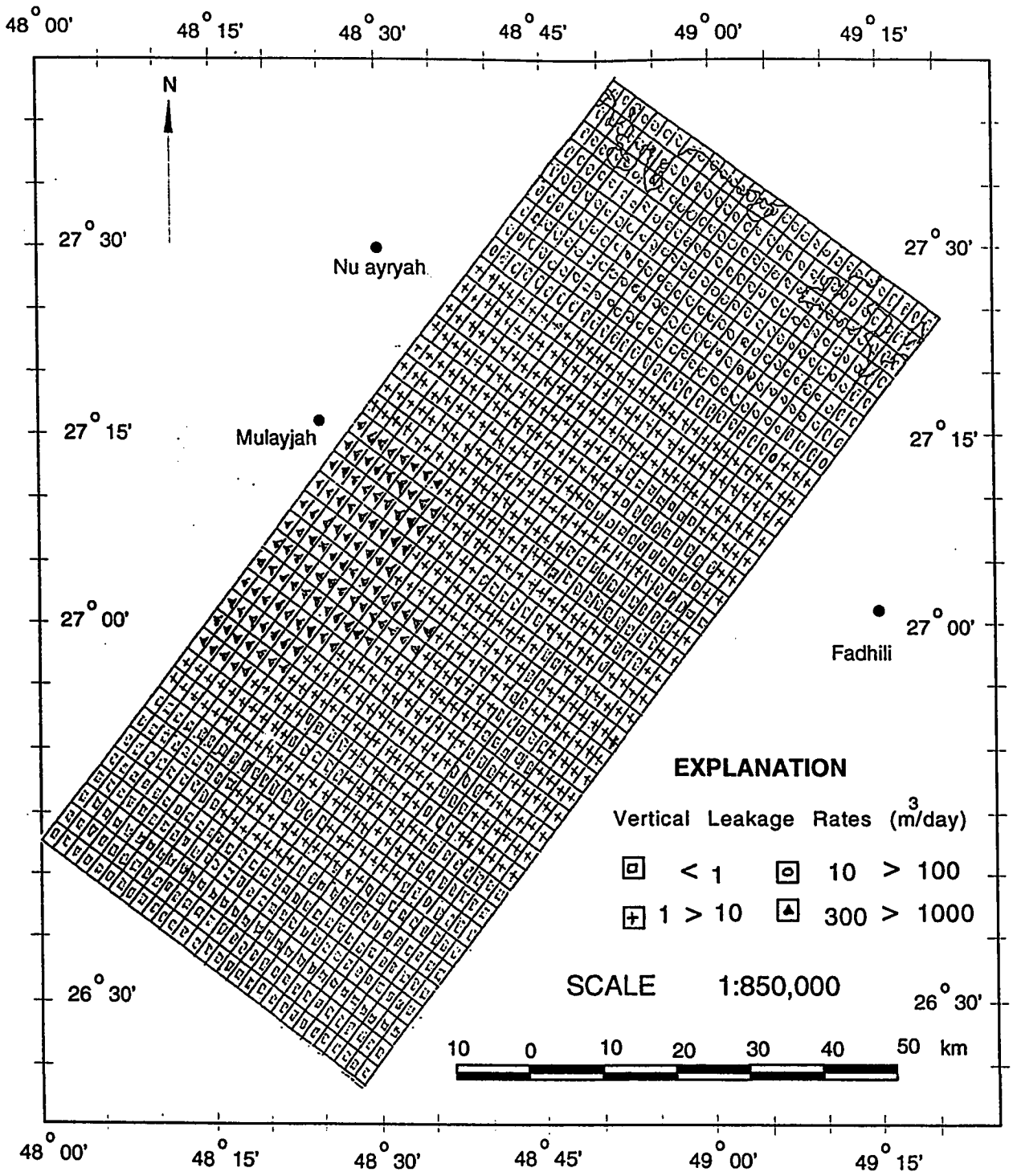

Figure 4.48: Calibrated Vertical Leakage Rates Distribution Map of Neogene Aquifer

4.4.5 Sensitivity Analysis

The main purpose of sensitivity analysis is to measure the uncertainty (inability) in order to define the exact spatial and temporal distribution of parameters in the flow domain. The sensitivity analysis is carried out to analyse the variations in distribution of head and chloride concentrations through steady state simulations for 1000 years, by changing aquifer parameters at selected locations within the model area. Tables, 4.10 through 4.18. It shows the relative importance of various input parameters on the model's response. This was achieved by adjustment of various model parameters. The model results indicate that the head distribution is highly sensitive to any change in longitudinal(lateral) permeability values for all the aquifers. The changes in water levels of (2-6%), (9-10%) and (1-2%) were found for Khobar, Alat and Neogene aquifers, respectively. The model sensitivity for transverse permeability values on water level changes were found to be less than 1% for all the aquifers, Tables, 4.10, 4.11 and 4.12. The model is highly sensitive to any change in lateral permeability values as to their effects on the chloride concentration distribution pattern. A change of (5-9%), (1-29%) and (5-14%) in chloride concentration was measured in Khobar, Alat and Neogene aquifers, Tables 4.13, 4.14 and 4.15. The changes in dispersivity values were found to affect chloride concentration patterns in a smaller degree (less than 1%), Tables, 4.16, 4.17 and 4.18.

Node #	% change in Piezometric Heads			
	% Change in Lateral Permeability (m/d)		% Change in Transverse Permeability (m/d)	
	+ %50	-50%	+50%	-50%
301	-0.5	1.22	-0.2	0.36
493	-0.74	1.66	-0.23	0.42
405	0.05	-0.13	-0.52	0.98
1043	-2.0	5.34	-0.02	0.02

Table 4.10: Sensitivity Analysis of Piezometric heads for Khobar Aquifer versus aquifer permeability.

Node #	% change in Piezometric Heads			
	% Change in Lateral Permeability (m/d)		% Change in Transverse Permeability (m/d)	
	+ %50	-50%	+50%	-50%
95	-0.48	1.23	-0.1	0.23
301	-0.31	0.80	-0.34	0.72
493	-0.75	1.722	-0.27	0.53
709	-1.38	4.4	-0.46	0.83
746	-3.48	9.87	0.044	0.095
913	-3.46	9.74	0.08	-0.28
1071	-2.47	7.175	0.14	-0.28

Table 4.11: Sensitivity Analysis of Piezometric heads for Alat Aquifer versus aquifer permeability.

Node #	% change in Piezometric Heads			
	% Change in Lateral Permeability (m/d)		% Change in Transverse Permeability (m/d)	
	+ %50	-50%	+50%	-50%
301	-0.09	0.34	0.12	-0.24
410	-0.67	1.60	-0.1	0.12
413	-0.36	0.92	-0.05	0.15
450	-0.03	0.20	-0.06	0.15
504	-0.34	1.07	-0.18	0.34
789	-0.21	0.53	-0.03	-0.06

Table 4.12: Sensitivity Analysis of water level surfaces for Neogene Aquifer versus aquifer permeability.

Node #	% change in Cl. Concentrations			
	% Change in Lateral Permeability (m/d)		% Change in Transverse Permeability (m/d)	
	+ %50	-50%	+50%	-50%
301	-0.07	-0.62	-0.1	0.35
493	4.75	-8.91	1.22	-0.41
405	-0.01	0.56	0.1	-0.1
1043	-78.1	5.23	7.91	-29.1

Table 4.13: Sensitivity Analysis of chloride concentrations for Khobar Aquifer versus aquifer permeability.

Node #	% change in Cl. Concentrations			
	% Change in Lateral Permeability (m/d)		% Change in Transverse Permeability (m/d)	
	+ %50	-50%	+50%	-50%
95	-2.58	5.94	-2.2	0.51
301	-4.6	9.0	-1.25	3.33
493	1.02	-3.13	0.23	1.743
709	-1.0	29.1	3.9	0.03
746	2.70	24.2	-1.48	3.165
913	-13.2	8.56	-1.12	0.44
1071	-6.63	6.675	-1.97	1.2

Table 4.14: Sensitivity Analysis of chloride concentrations for Alat Aquifer versus aquifer permeability.

Node #	% change in Cl. Concentrations			
	% Change in Lateral Permeability (m/d)		% Change in Transverse Permeability (m/d)	
	+ %50	-50%	+50%	-50%
301	-0.24	0.60	-0.03	0.02
410	4.24	-11.27	0.1	-0.17
413	3.85	-10.39	0.0	-0.04
450	0.36	-1.1	0.04	-0.01
504	4.95	-13.97	0.1	-0.3
789	1.08	-3.31	-0.03	0.0

Table 4.15: Sensitivity Analysis of chloride concentrations for Neogene Aquifer versus aquifer permeability.

Node #	% change in Cl. Concentrations			
	% Change in Longitudinal Dispersivity (m)		% Change in Transverse Dispersivity (m)	
	+ %50	-50%	+50%	-50%
95	-0.1	-0.1	0.26	-0.334
301	-0.1	0.1	0.0	-0.04
493	-0.02	-0.02	-0.32	0.36
709	0.0	0.01	0.25	-0.26
746	0.01	0.01	0.22	-0.16
913	0.0	0.01	-0.45	1.6
1071	0.0	0.0	2.161	-2.161

Table 4.16: Sensitivity Analysis of chloride concentrations for Alat Aquifer versus aquifer dispersivity.

Node #	% change in Cl. Concentrations			
	% Change in Lateral Dispersivity (m)		% Change in Transverse Dispersivity (m)	
	+ %50	-50%	+50%	-50%
301	0.13	-0.13	0.0	0.0
493	-0.18	0.22	0.04	-0.08
405	0.11	0.16	0.18	-0.27
1043	0.04	-0.06	-1.6	1.8

Table 4.17: Sensitivity Analysis of chloride concentrations for Khobar Aquifer versus aquifer dispersivity.

Node #	% change in Cl. Concentrations			
	% Change in Lateral Dispersivity (m)		% Change in Transverse Dispersivity (m)	
	+ %50	-50%	+50%	-50%
301	3.8	-7.19	0.86	
410	-0.38	0.46	0.75	
413	-0.2	0.45	0.63	
450	-0.04	0.04	0.08	
504	-0.29	0.97	-0.33	
789	-0.05	0.25	-0.50	

Table 4.18: Sensitivity Analysis of chloride concentrations for Neogene Aquifer versus aquifer dispersivity.

Chapter 5

Management Alternatives

The supply of adequate amount of suitable water for a long term can be achieved by formulizing management strategies to optimize the utilization of groundwater resources without causing further deterioration. The management techniques are used to predict the expected changes in the piezometric heads and salinity patterns as a result of anticipated groundwater development. After calibration, the model was used to predict the future water levels and the chloride distribution patterns. The three development strategies were proposed to simulate the effects of projected pumping rates on the water levels and chloride distribution patterns in Khobar, Alat and Neogene aquifers. These alternatives are highly simplified and subjected to a number of constraints. The main purpose of the management alternatives was to evaluate the general trends of water levels and chloride distributions that might be expected during a planning period. A planning horizon of 16 years (1994-2010) was

selected for the alternatives with January 1995 as a starting point. Results were analyzed and explained by developing drawdown contour maps for each aquifer at the end of the year 2010. The drawdown contour maps were obtained by subtracting the water levels resulting from each alternative at the end of 2010 from the water levels at the year of 1994. Therefore, they represent the predicted drawdown by the model for the period of 16 years (1994-2010). Temporal variations in drawdowns at some selected nodes from each aquifer were selected to display the "time versus drawdown" hydrographs for various development alternatives. The proposed management alternatives are as follows:

5.1 Alternative I : Continuous Increase in Pumping Rate Trends.

The Eastern province will be an area of sustained economic development in the future with a high growth rate. First, it was assumed that the present water extraction rate trends observed during 1967-1994 period would continue for the planning period of 16 years (1994-2010). Thus, projections of extraction rates for the selected planning period were made by extrapolating the pumping trends of the year 1967-1994. A series of simulations using the best estimated future pumpage were carried out to simulate the effects on the regional groundwater flow and salinity distributions. The locations of wells and well fields that existed during the transient calibration,

i.e by the end of 1994, were kept unchanged for the whole planning period. The projected pumping rates of Khobar, Alat and Neogene aquifers are shown in Figures 5.1, 5.2 and 5.3, respectively. The pumping rates of individual wells and well fields are listed in Appendix-B, (Tables B-4 through B-6). The results of this simulation were demonstrated by the water level surface contour maps of the Khobar, the Alat and the Neogene aquifers, Figures 5.4, 5.5 and 5.6. The chloride concentration distribution maps at the end of year 2010 for alternative I were also prepared to demonstrate the effects of pumping at various locations in the study area, Figures. 5.7, 5.8 and 5.9.

The corresponding predicted water level declines were illustrated in Figures 5.10 through 5.12, from 1994 to 2010 in Khobar, Alat and Neogene aquifers, respectively. The results are consistent with the head decline measured during the year of 1994. Continuation of present increasing pumping trends indicated that water level decline would vary from place to place and would be maximum near Abuhadriya area in Khobar and Alat aquifers. All water level declines have regional effects instead of local drawdowns around or within the individual pumping wells.

The drawdown contour maps demonstrated that there is a large cone of depression near Abuhadriyah area in Khobar aquifer. The piezometric heads dropped to 4.6 meters, with a maximum drawdown of 8.5 meters. The cone of depression decreases elsewhere in the Khobar aquifer, causing a drawdown of less than 2 meters.

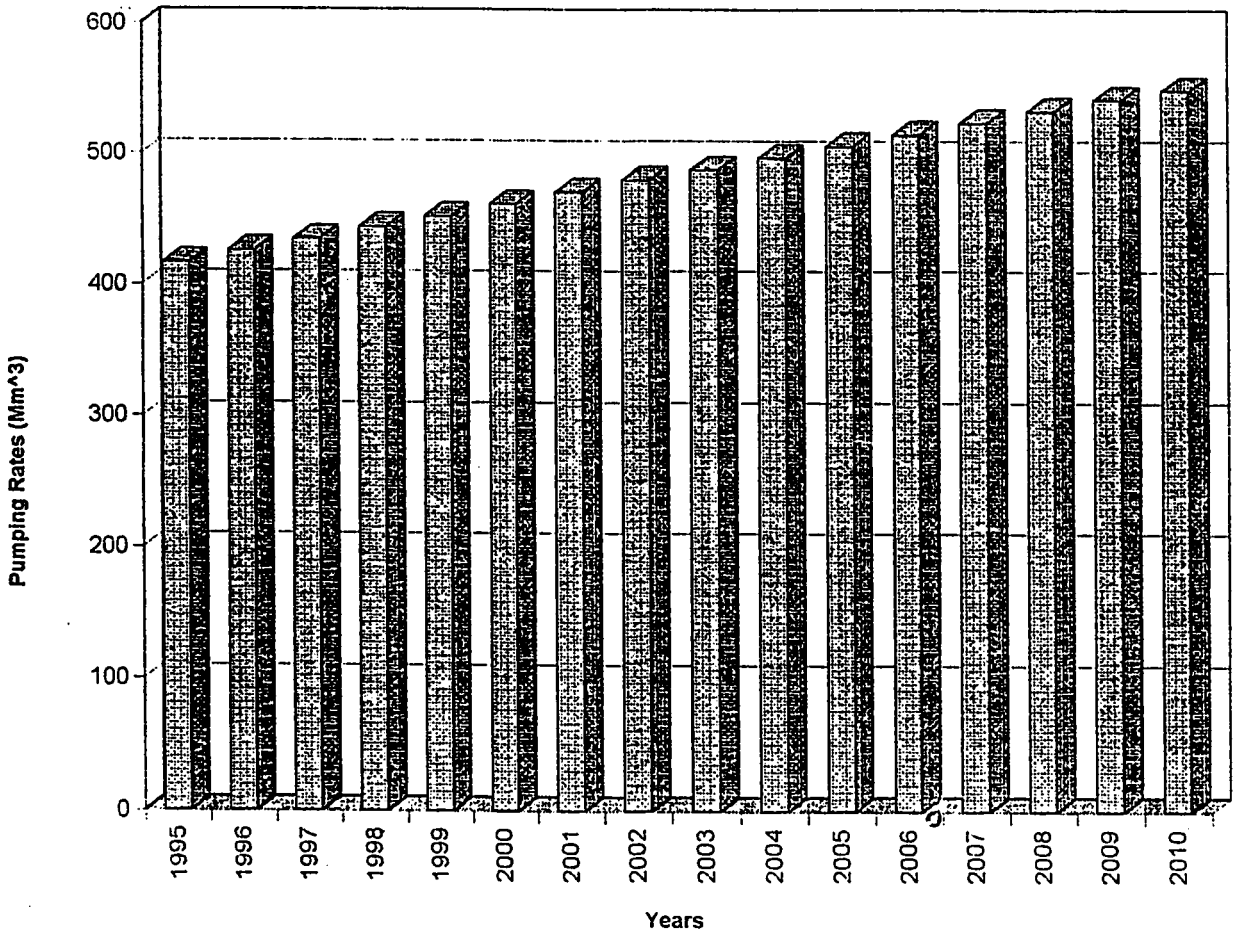

Figure 5.1: The projected pumping rates for Khobar aquifer for the planning period (1995-2010). Alternative I).

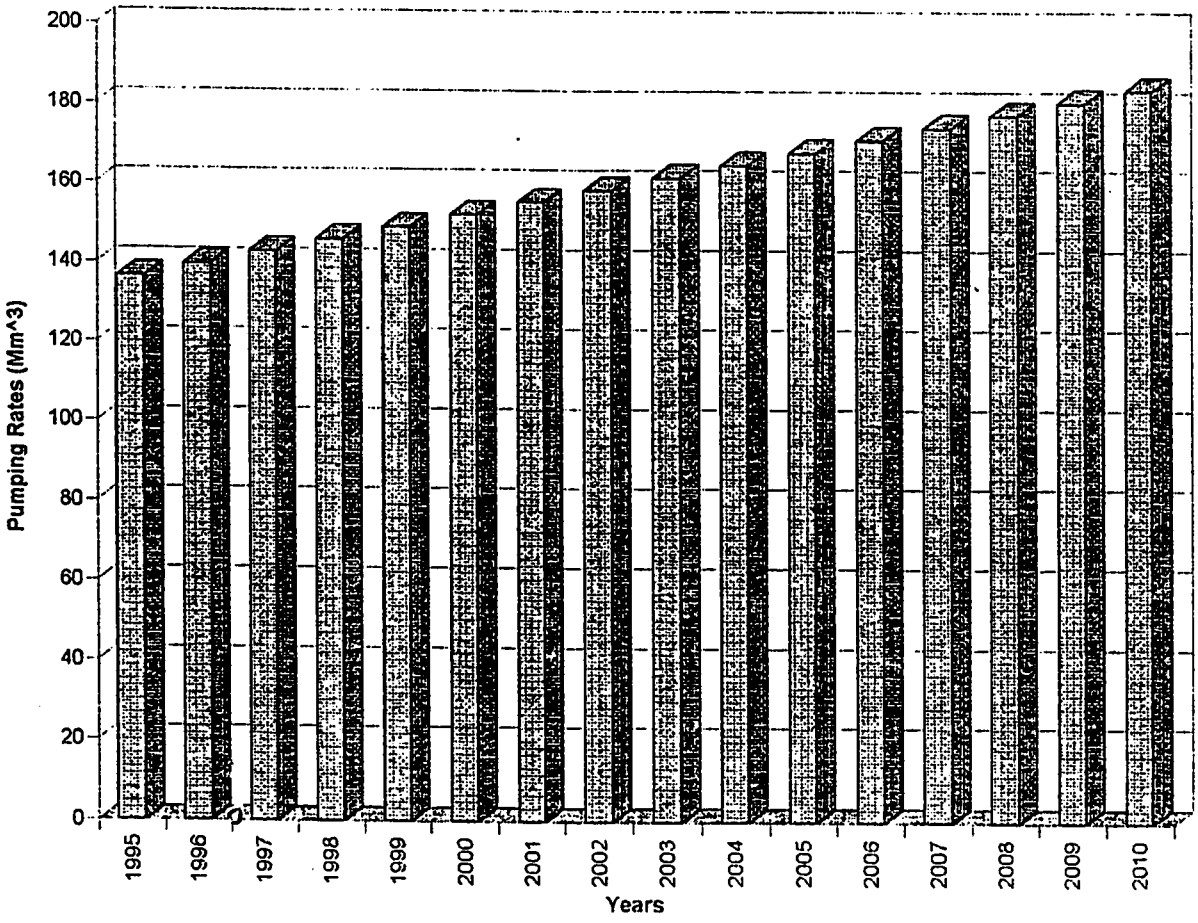

Figure 5.2: The projected pumping rates for Alat aquifer for the planning period (1995-2010), Alternative I).

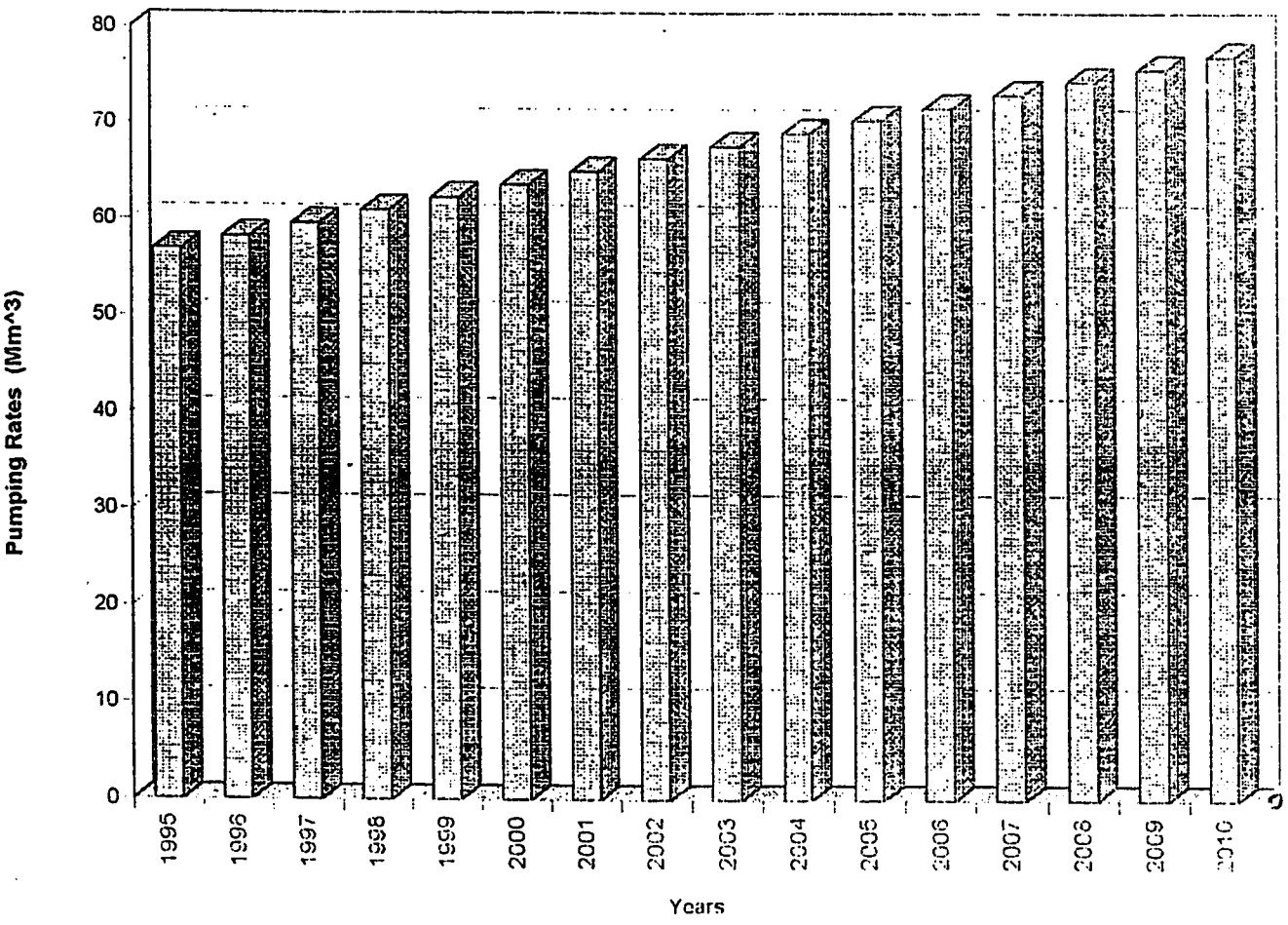

Figure 5.3: The projected pumping rates for Neogene aquifer for the planning period (1995-2010), Alternative I).

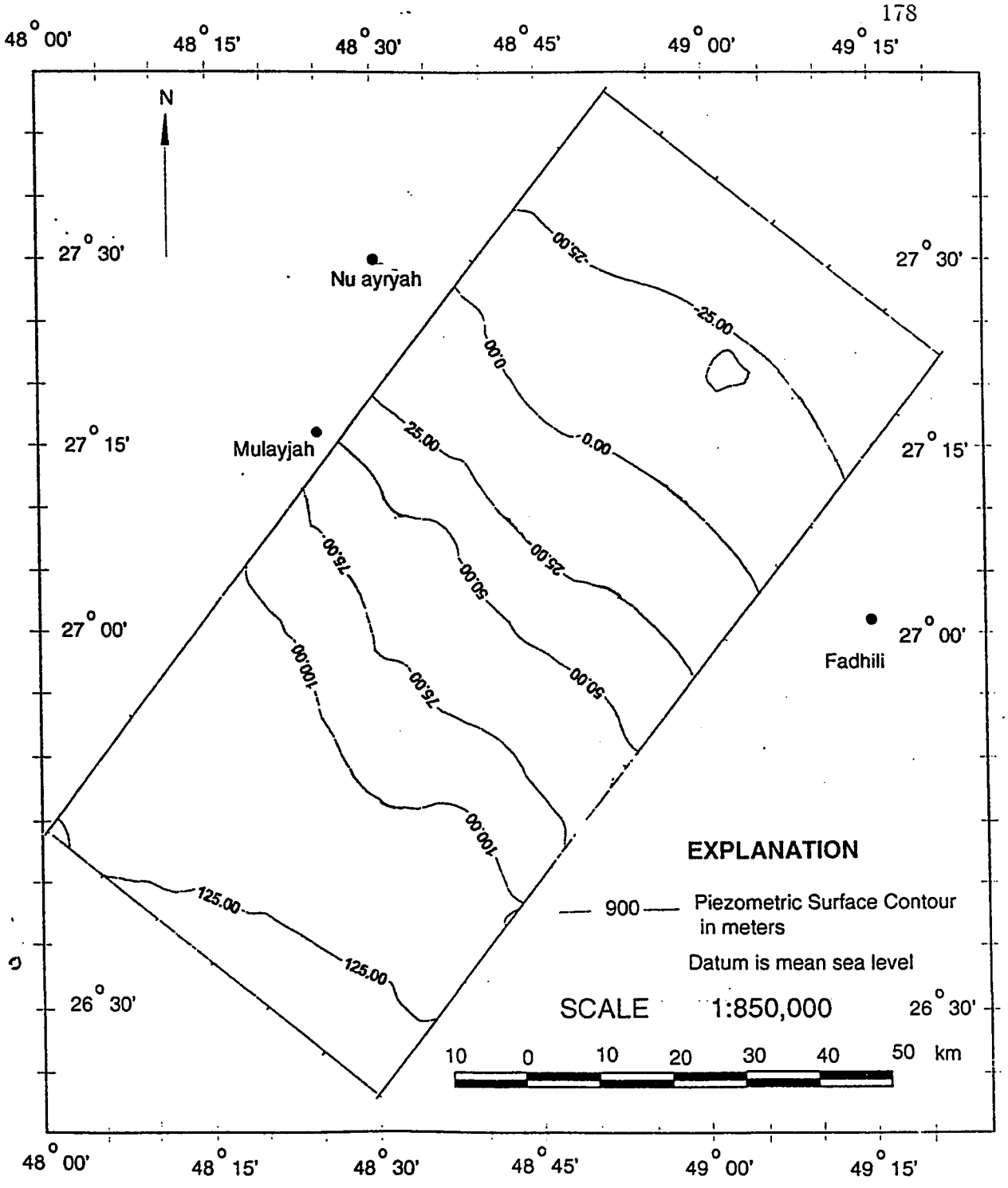

Figure 5.4: Simulated Piezometric Surface Map of Khobar Aquifer for the year 2010, Alternative I).

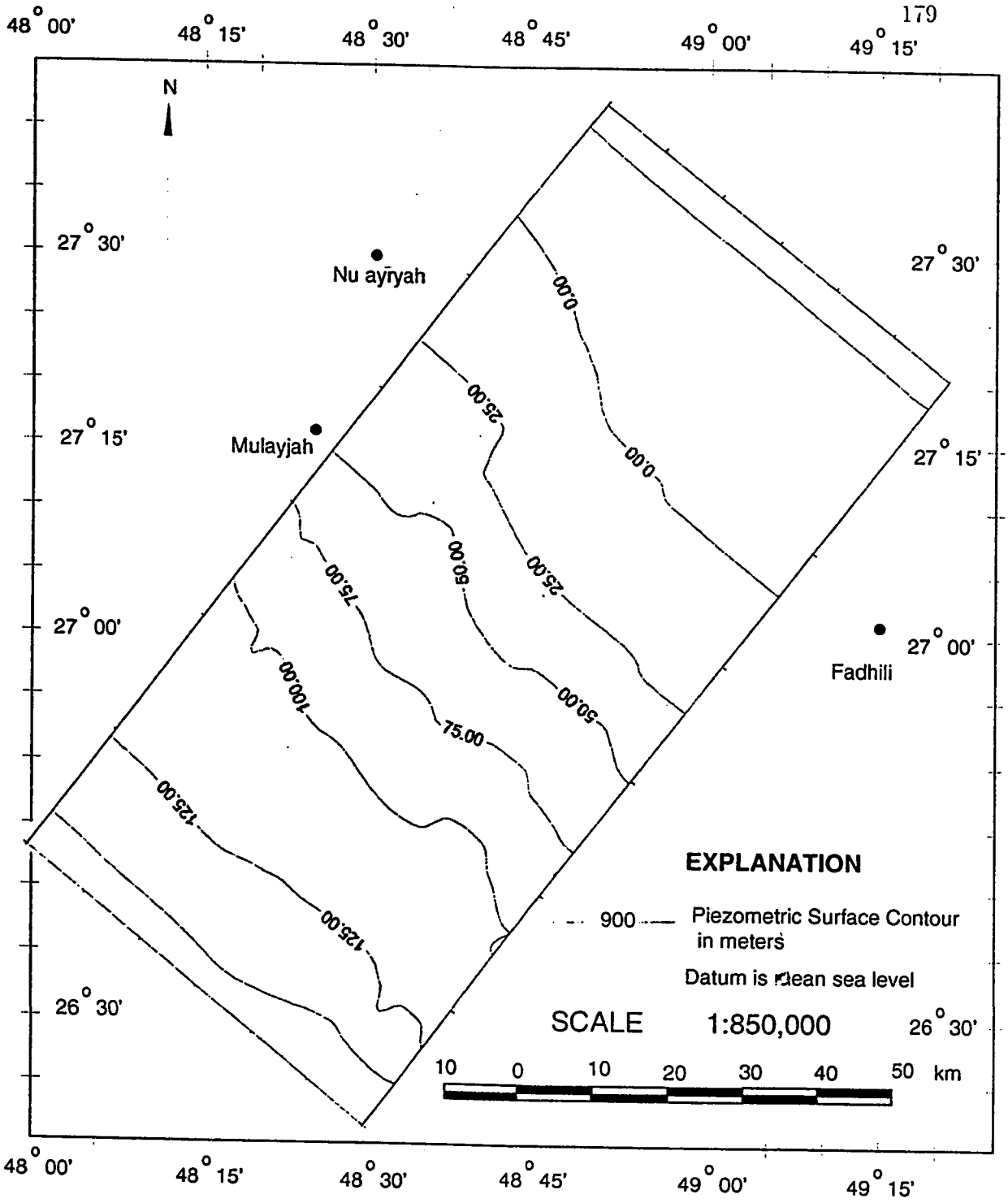

Figure 5.5: Simulated Piezometric Surface Map of Alat Aquifer for the year 2010, Alternative I).

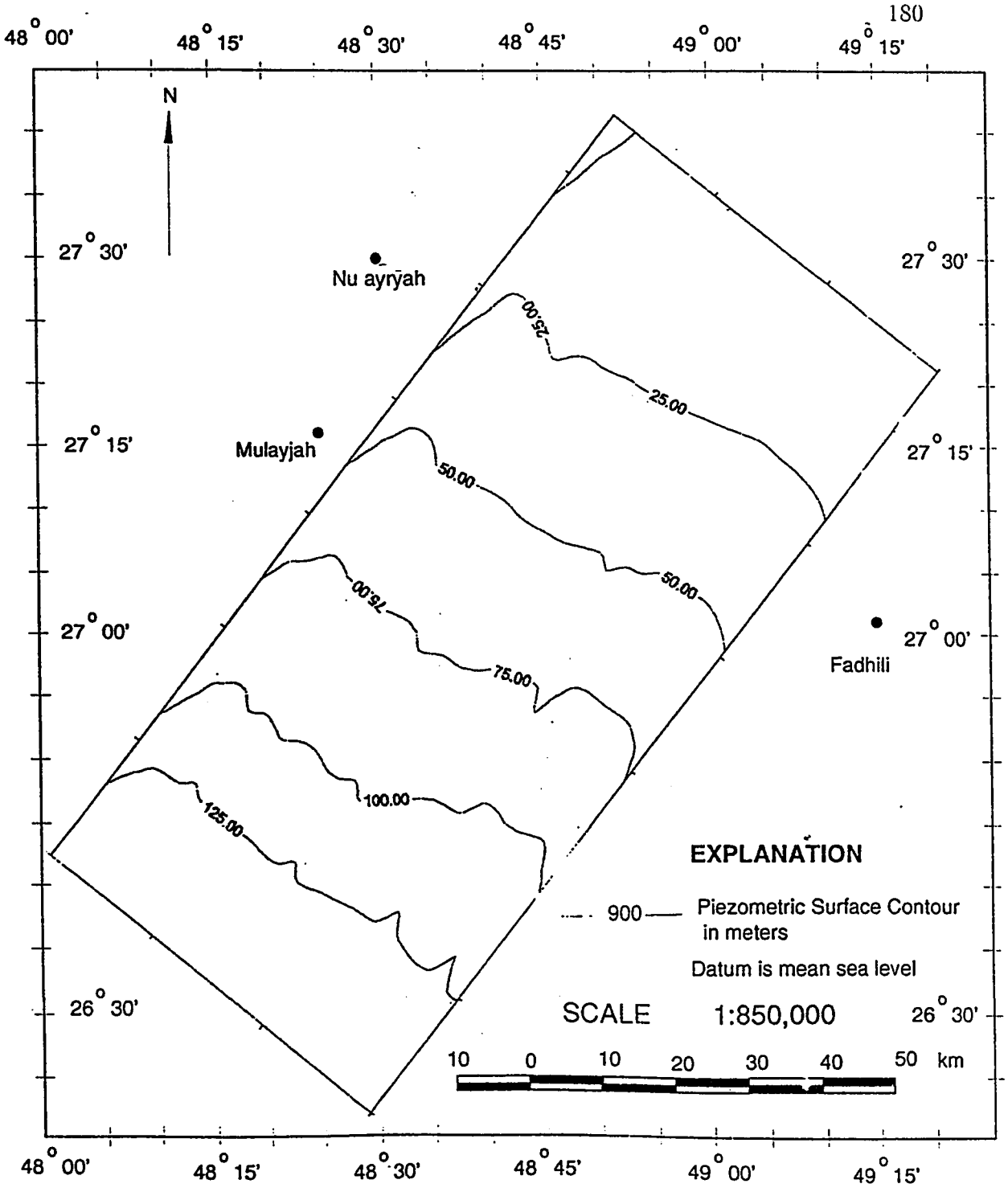

Figure 5.6: Simulated Waterlevel Contour Map of Neogene Aquifer for the year 2010, Alternative I).

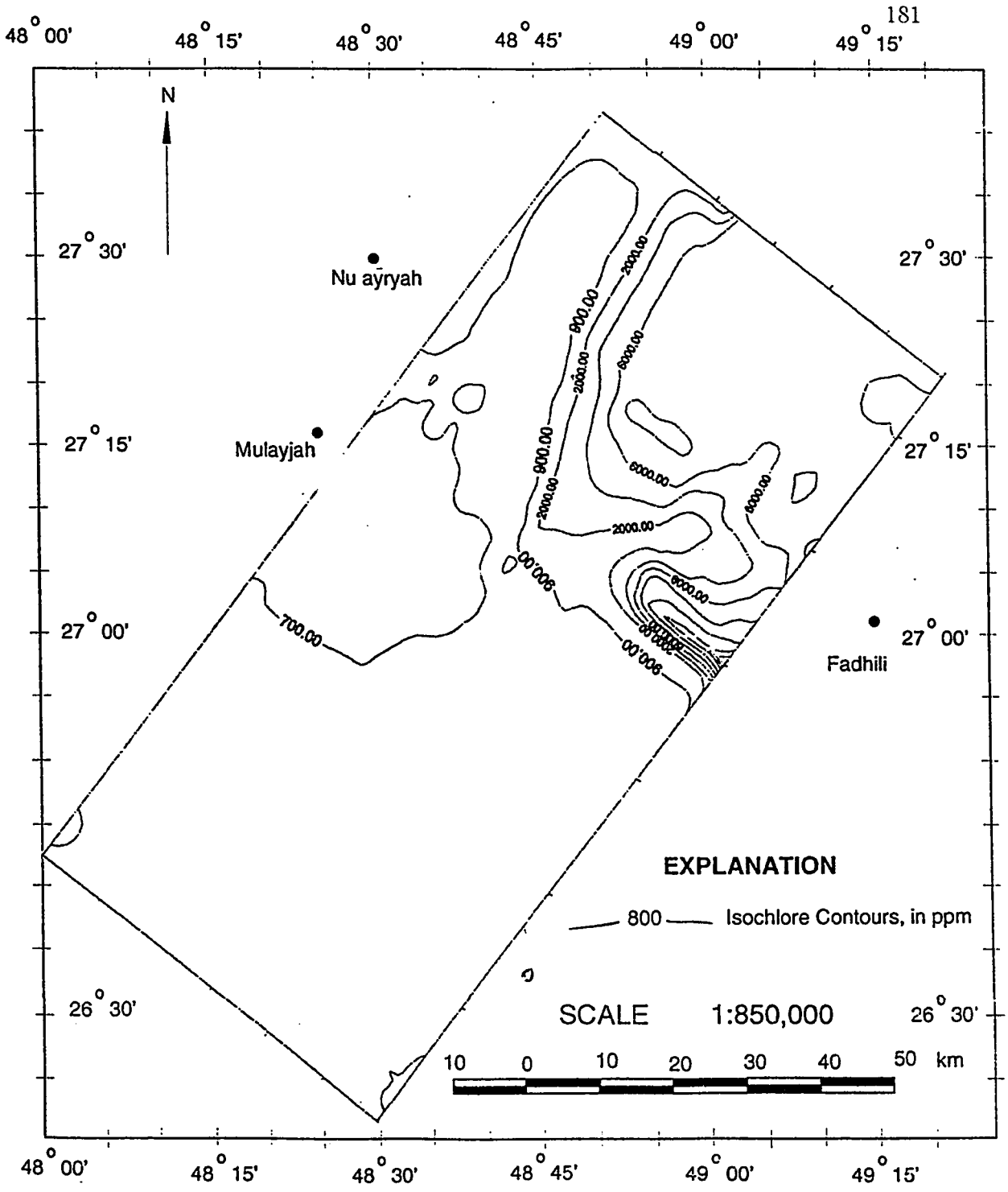

Figure 5.7: Simulated Isochlore Map of Khobar Aquifer for the year 2010, Alternative I).

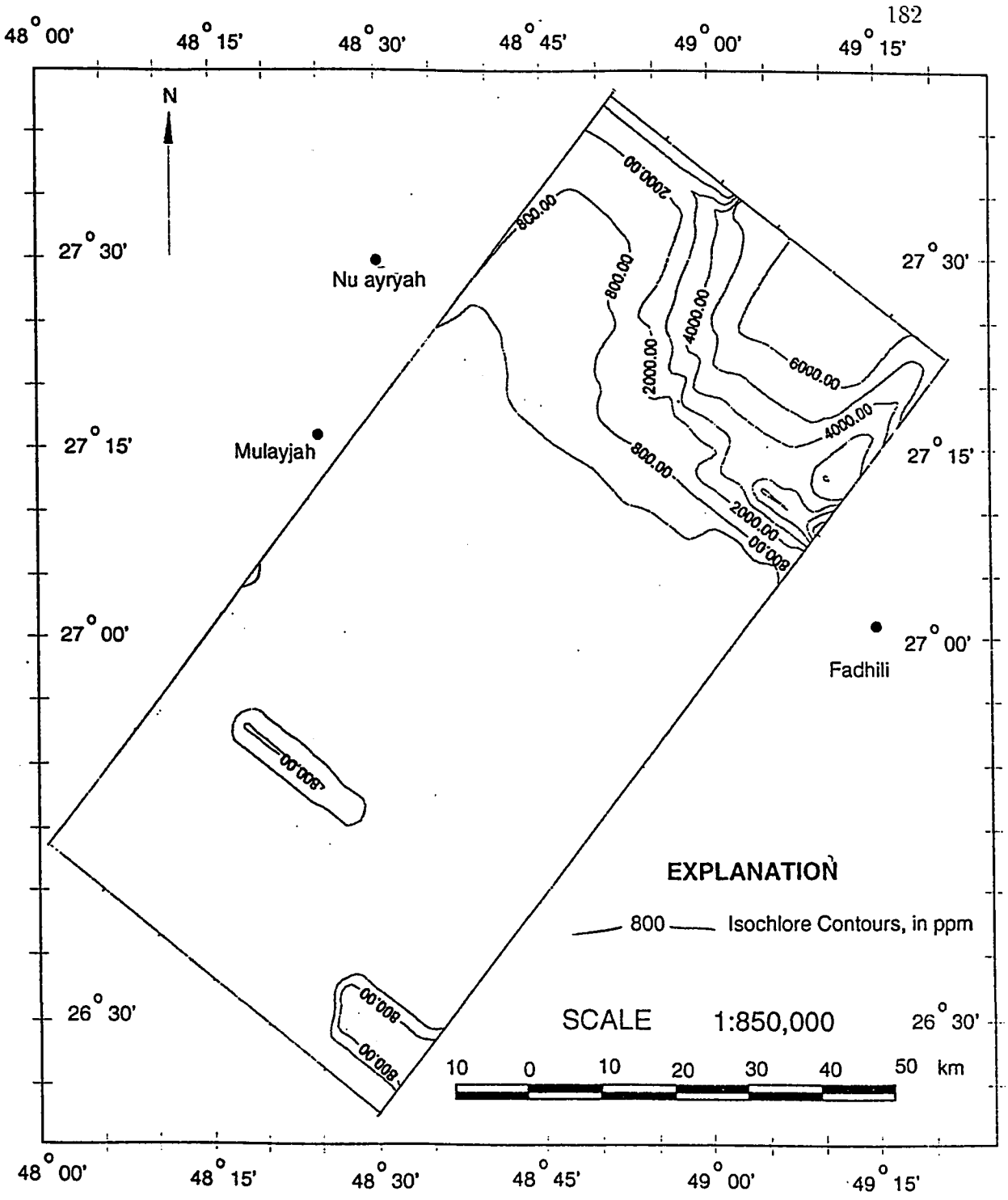

Figure 5.8: Simulated Isochlore Map of Alat Aquifer for the year 2010, Alternative I).

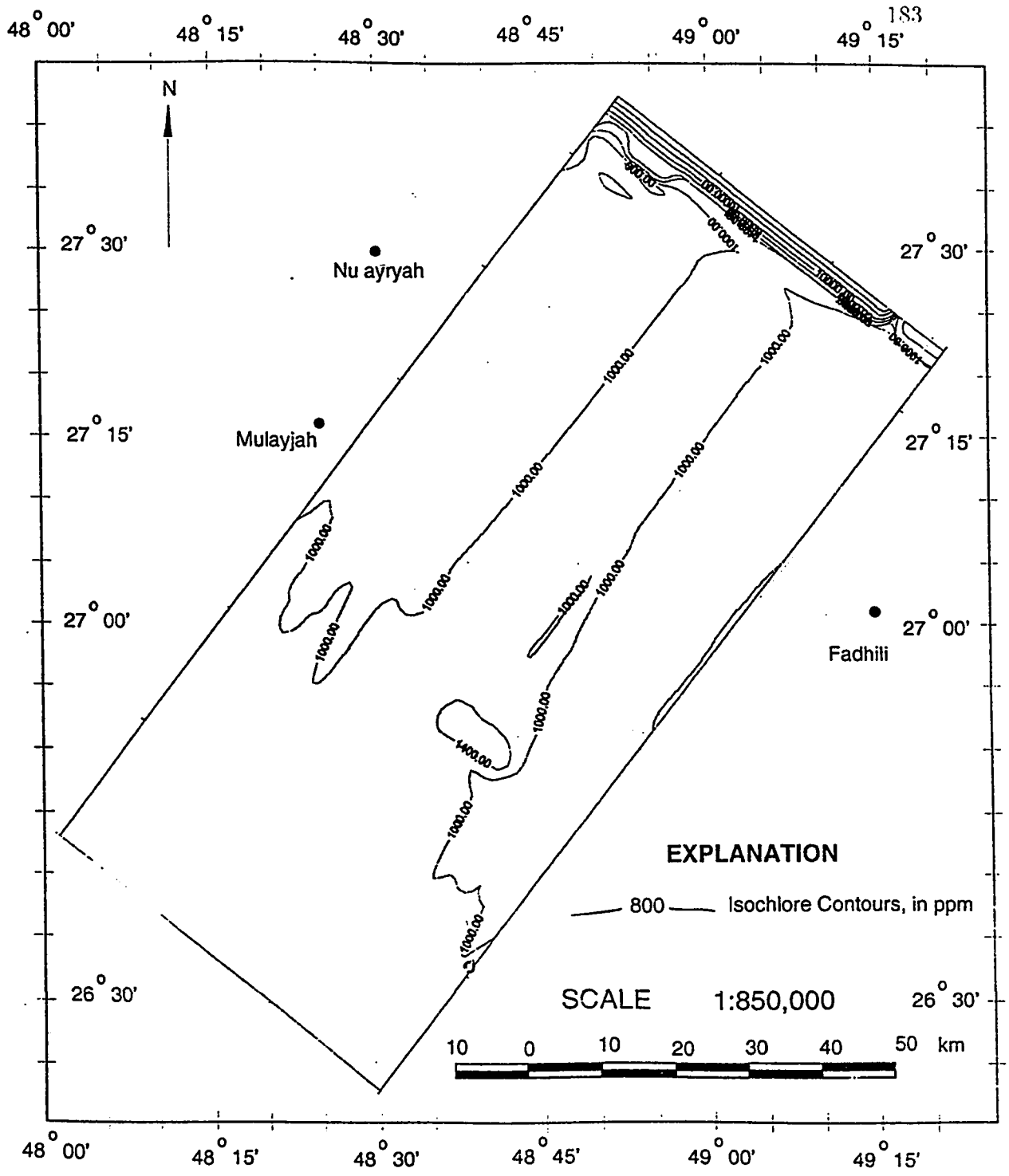

Figure 5.9: Simulated Isochlore Map of Neogene Aquifer for the year 2010. Alternative I).

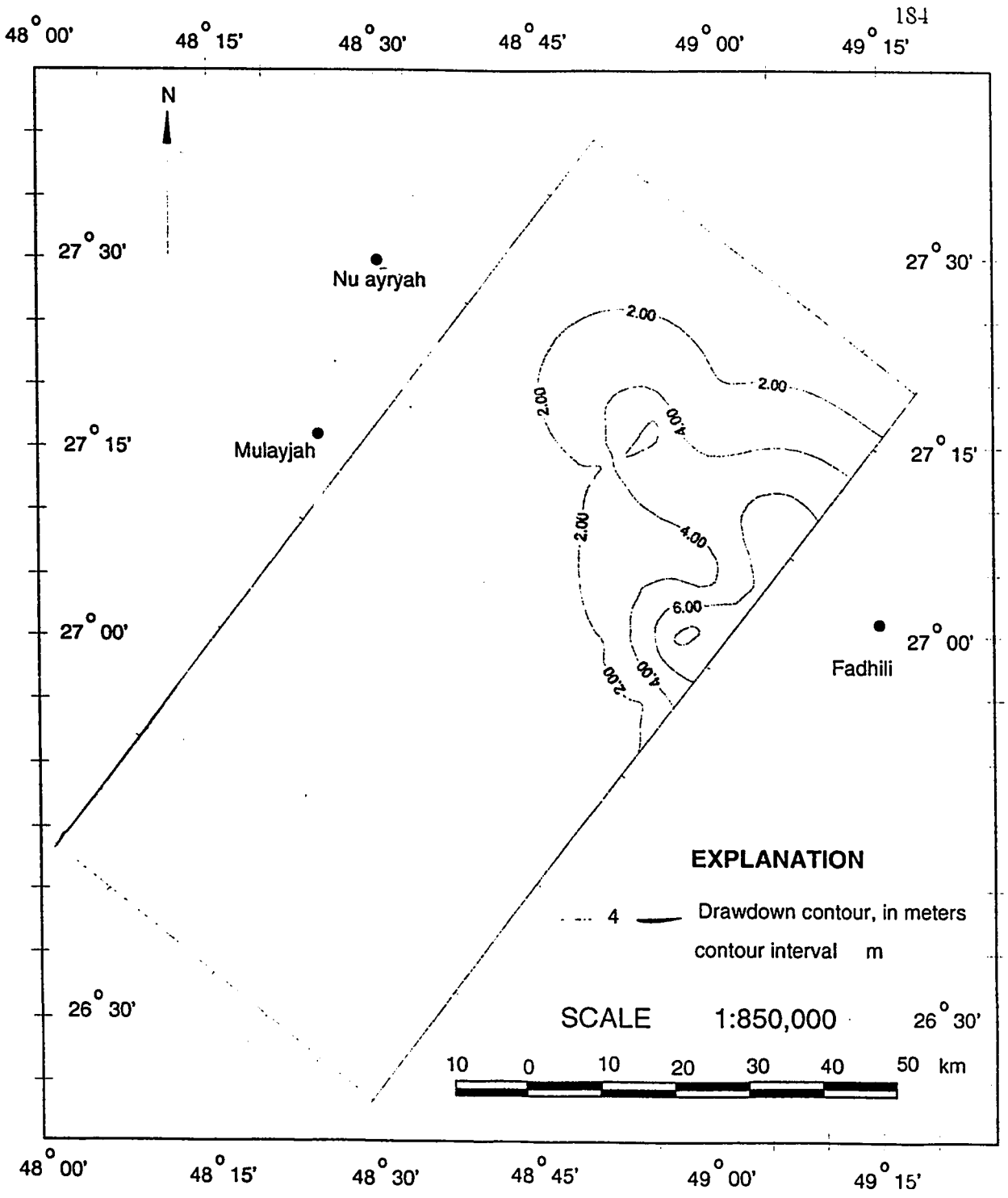

Figure 5.10: Drawdown Map of Khobar Aquifer for the period 1994-2010. Alternative I).

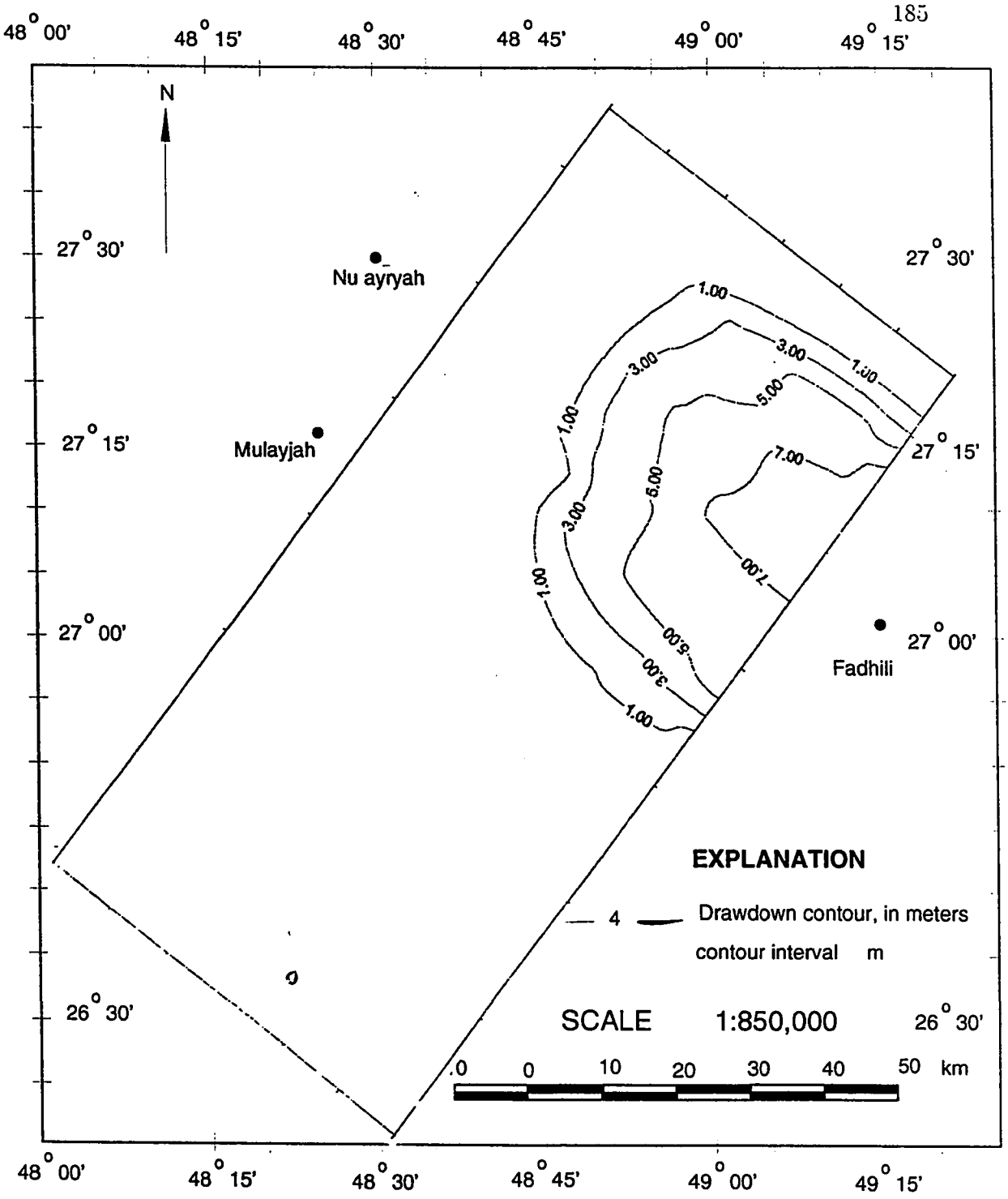

Figure 5.11: Drawdown Map of Alat Aquifer for the period 1994-2010. Alternative I).

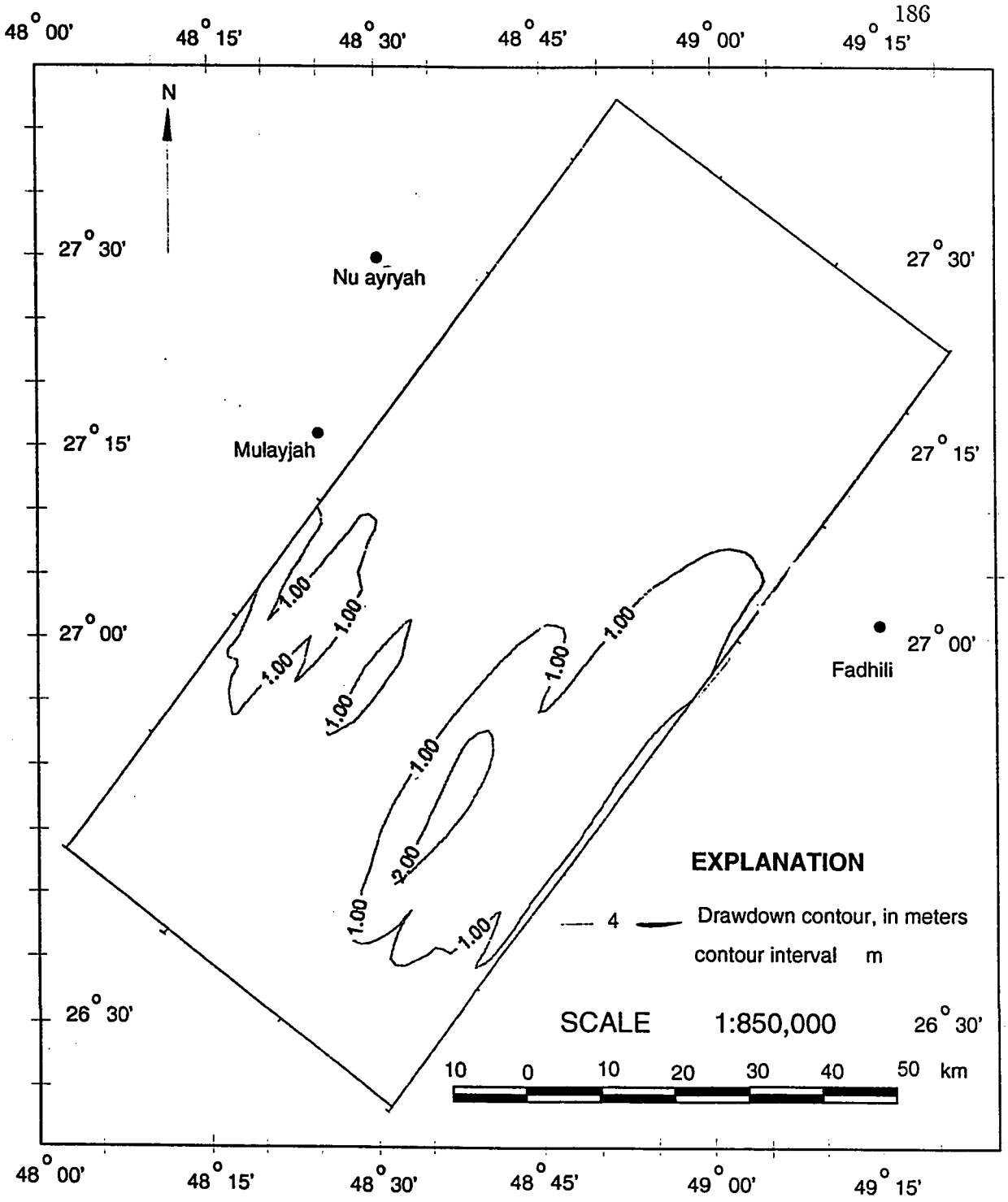

Figure 5.12: Drawdown Map of Neogene Aquifer for the period 1994-2010, Alternative I).

The time versus drawdown graph illustrates a gradual decline in water levels, depicted from an increase in drawdown up to 8.5 meters at south of Abuhadriya area, (nodes 746, 932), Figure, 5.13. An increase of 800-2000 ppm in chloride concentrations has been found at south of Abuhadriya (nodes 746, 932), Figure, 5.16. This increase in chloride concentration corresponds to a marked drop of heads at south of Abuhadriya area. The high pumping may enhance the vertical leakage from Umm Er Radhuma aquifer. As a result, the high concentration zone will increase in size and concentrations, causing a widespread deterioration of the aquifer around Abuhadriya area.

A similar cone of depression was also observed in Alat aquifer at south of Abuhadriya. The head drops down to -10.5 meters at the end of 2010 and the maximum drawdown will be 8.1 meters in this region, Figure 5.14. Elsewhere the drawdown is less than 1 meters. The time versus drawdown graphs illustrate a gradual increase in drawdowns up to 8.1 meters at south of Abuhadriya (node 932). The effects of pumping on the chloride concentration distribution pattern are evident from the simulation results at different places. Time versus concentration graphs demonstate an increase of about 1800 ppm at south of Abuhadriya area, Figure, 5.17. The outcome of this alternative indicates the interconnection of Alat and Khobar aquifers near this region. The high rate of pumping may cause an upward migration of highly saline water into the Alat aquifer.

No significant cone of depression is seen in the Neogene aquifer. The maximum

drawdown is noted about 2.3 meters near south of as-Sarrar area (node 507). Elsewhere the drawdown is less than 1 meter, Figure, 5.15. This is probably due to scattered well fields with low pumping rates. The wells are mainly hand-dug with low productivity. Recharge is high in Neogene aquifer due of large amount of infiltrated water from rainfall and also due to return flow from agricultural farms. The return flow is estimated to reach about 55 % of the extraction in the study area. The increase in chloride concentration is about 60 to 200 ppm at east of Qullayib village, node(507), Figure, 5.18. The cone of depressions and increasing high concentrations at Abuhadriya area in Khobar and Alat aquifers confirmed the hydraulic interaction between them.

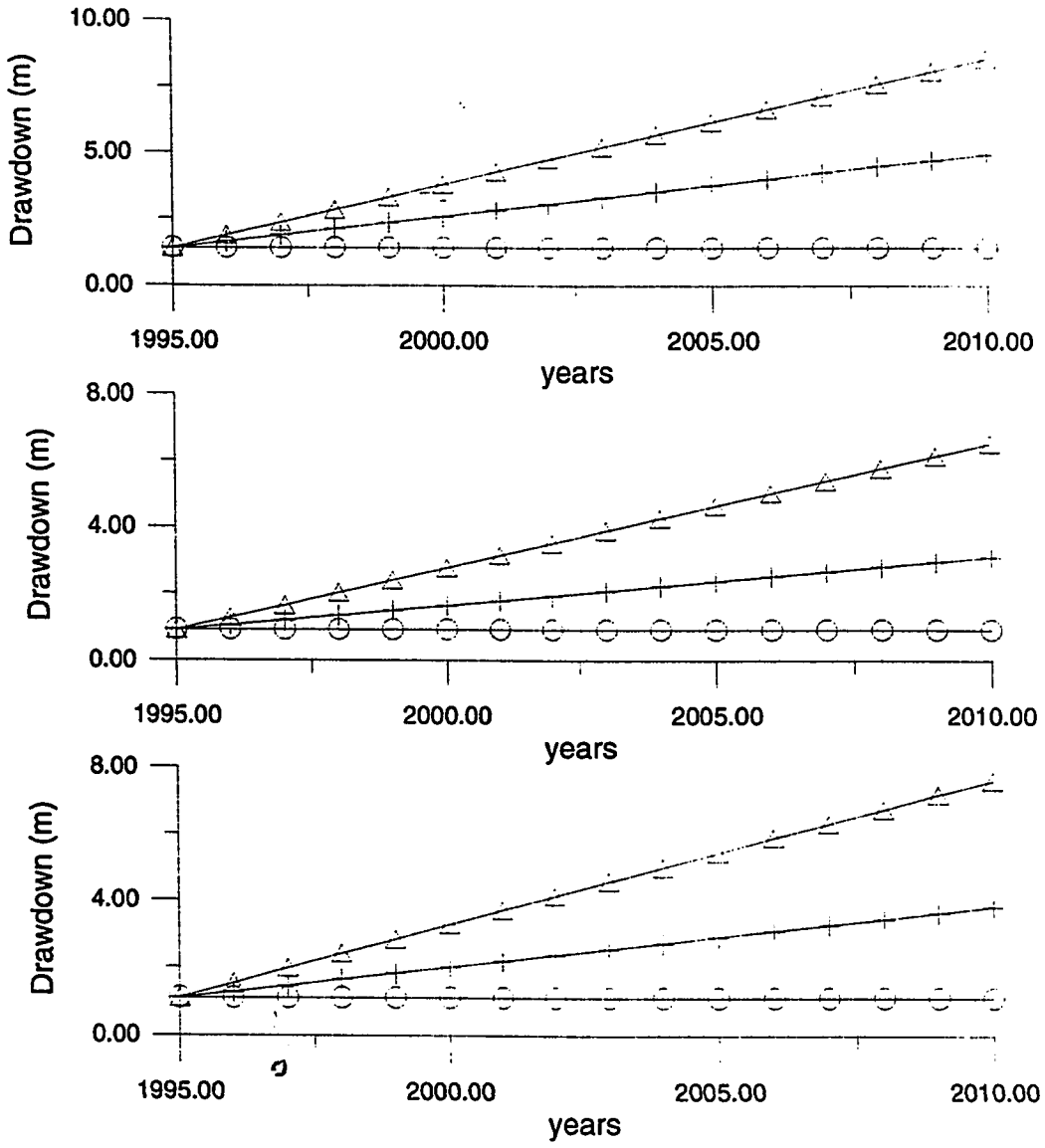

Figure 5.13: Drawdown vs Time graphs for Khobar Aquifer near Abuhadriya at nodes, (746, 912, 932).

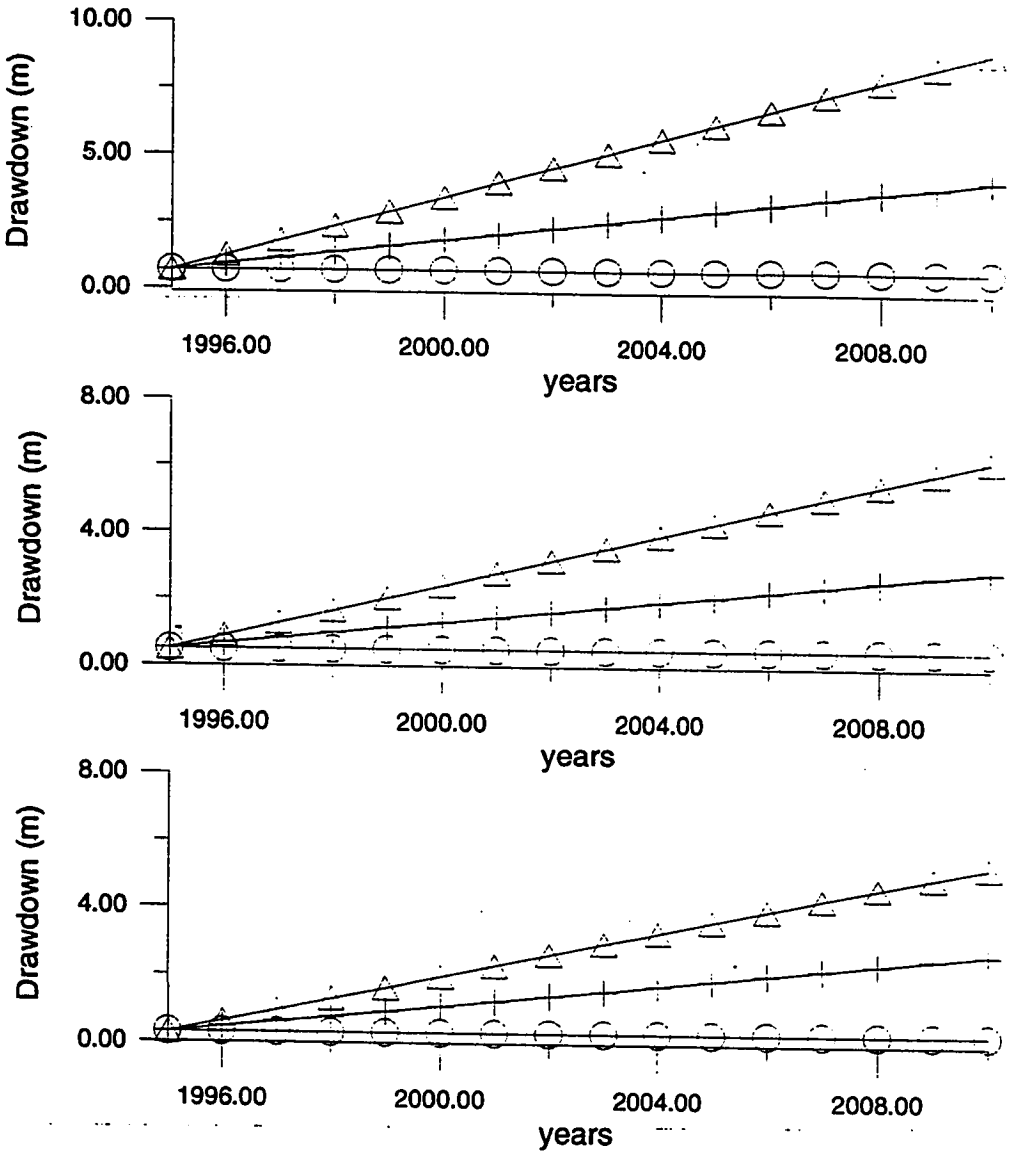

Figure 5.14: Drawdown vs Time graphs for Alat Aquifer near Abuhadriya at nodes. (932, 914, 848)

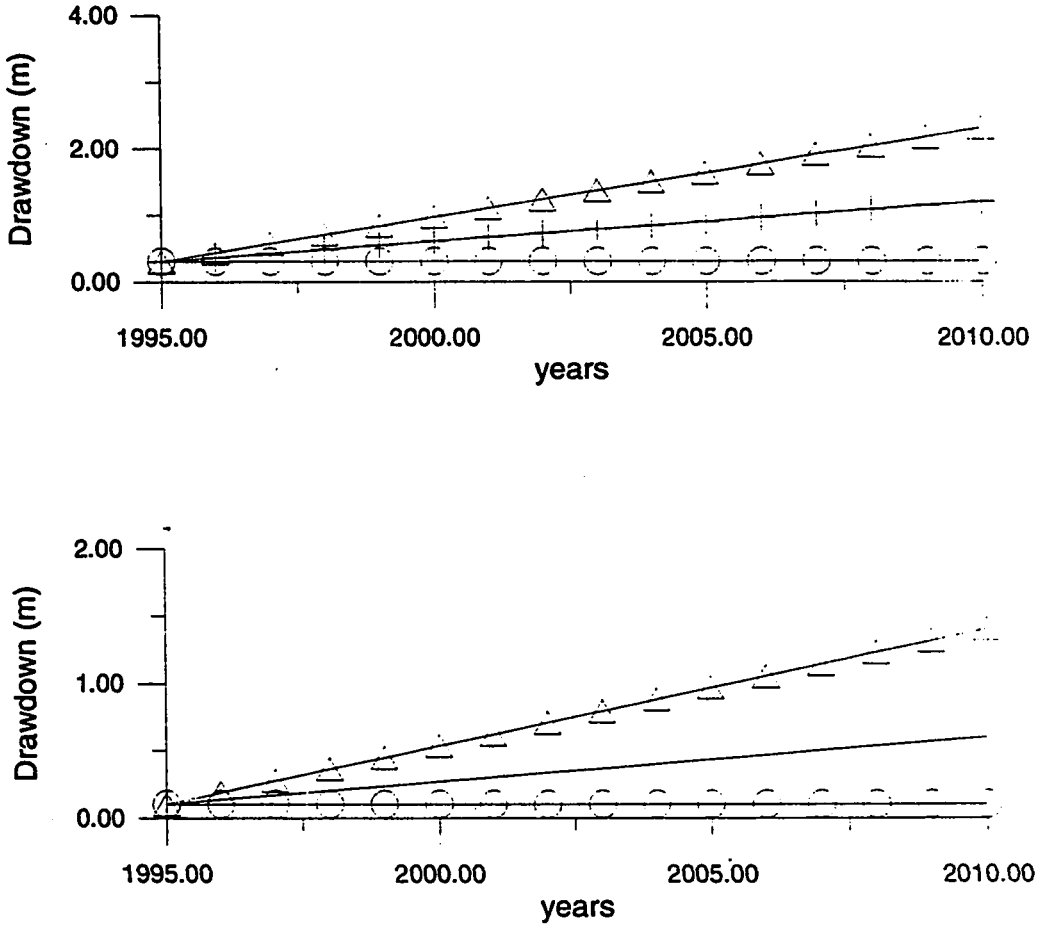

Figure 5.15: Drawdown vs Time graphs for Neogene Aquifer near As-Sarrar at nodes, (457, 507)

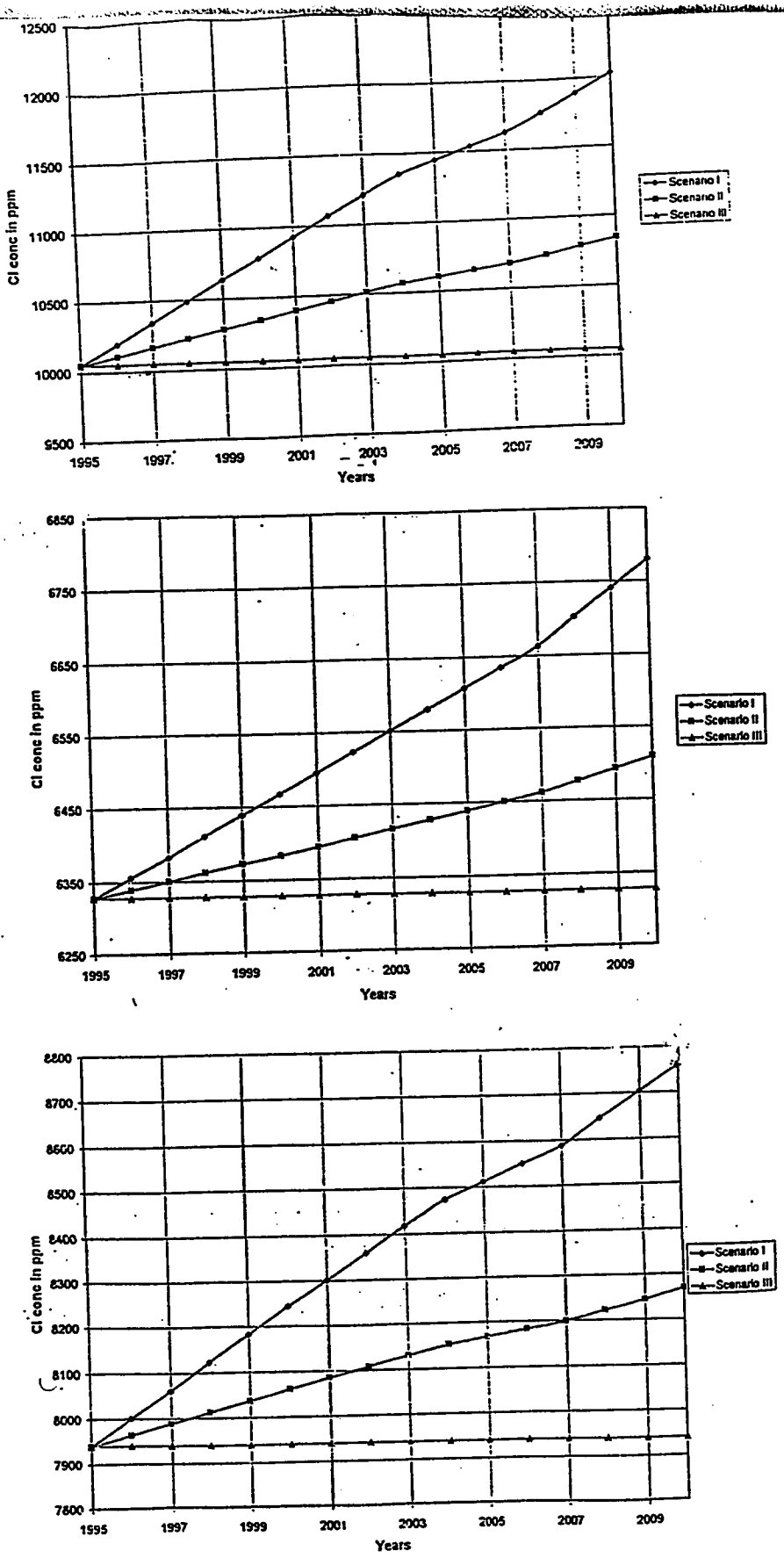

Figure 5.16: Time versus Chloride Concentration graphs for Khobar Aquifer near Abuhadriya area at nodes, (746, 912, 932).

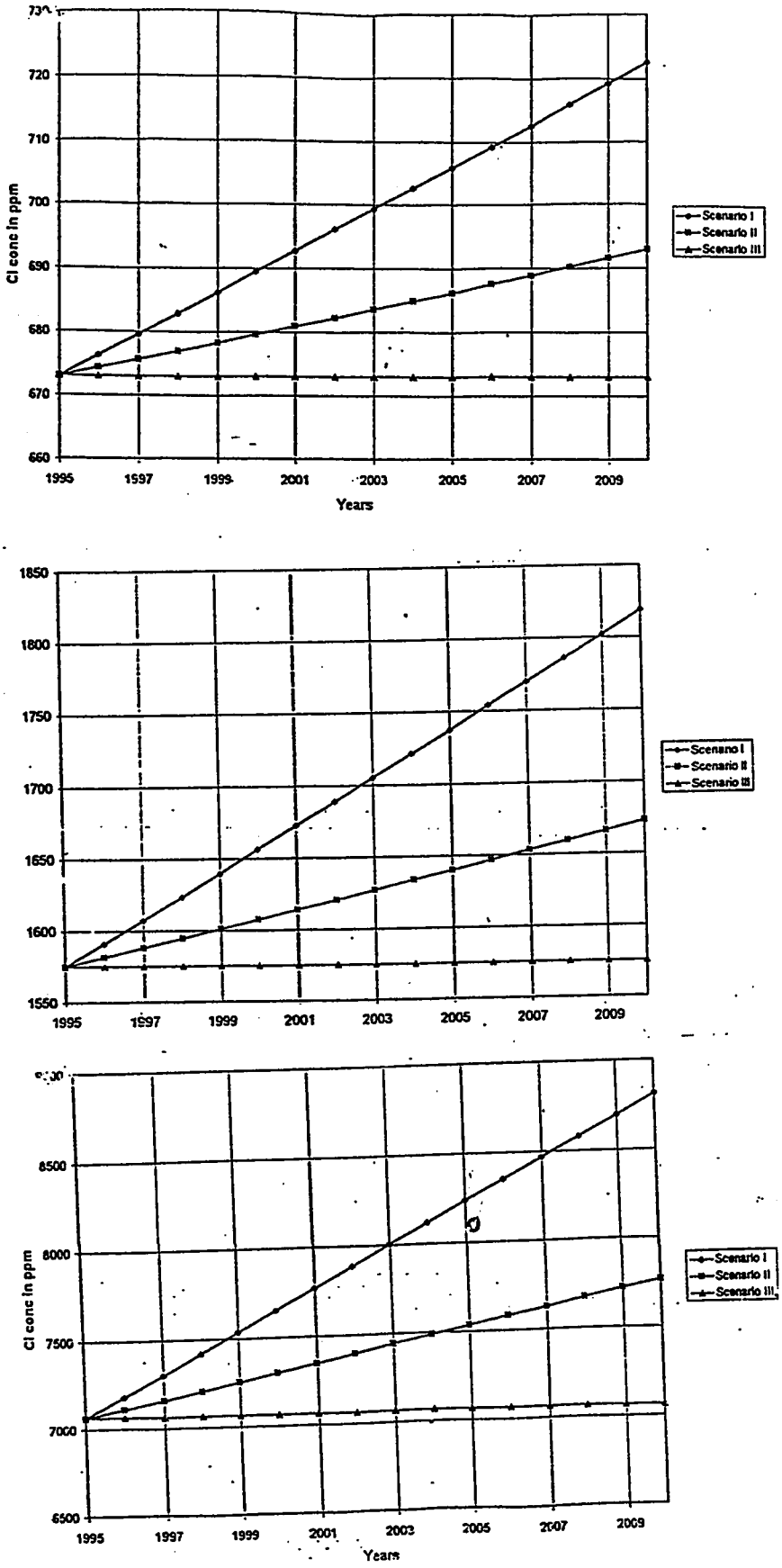

Figure 5.17: Time versus Chloride Concentration graphs for Alat Aquifer near Abuhadriya area at nodes, (848, 914, 932).

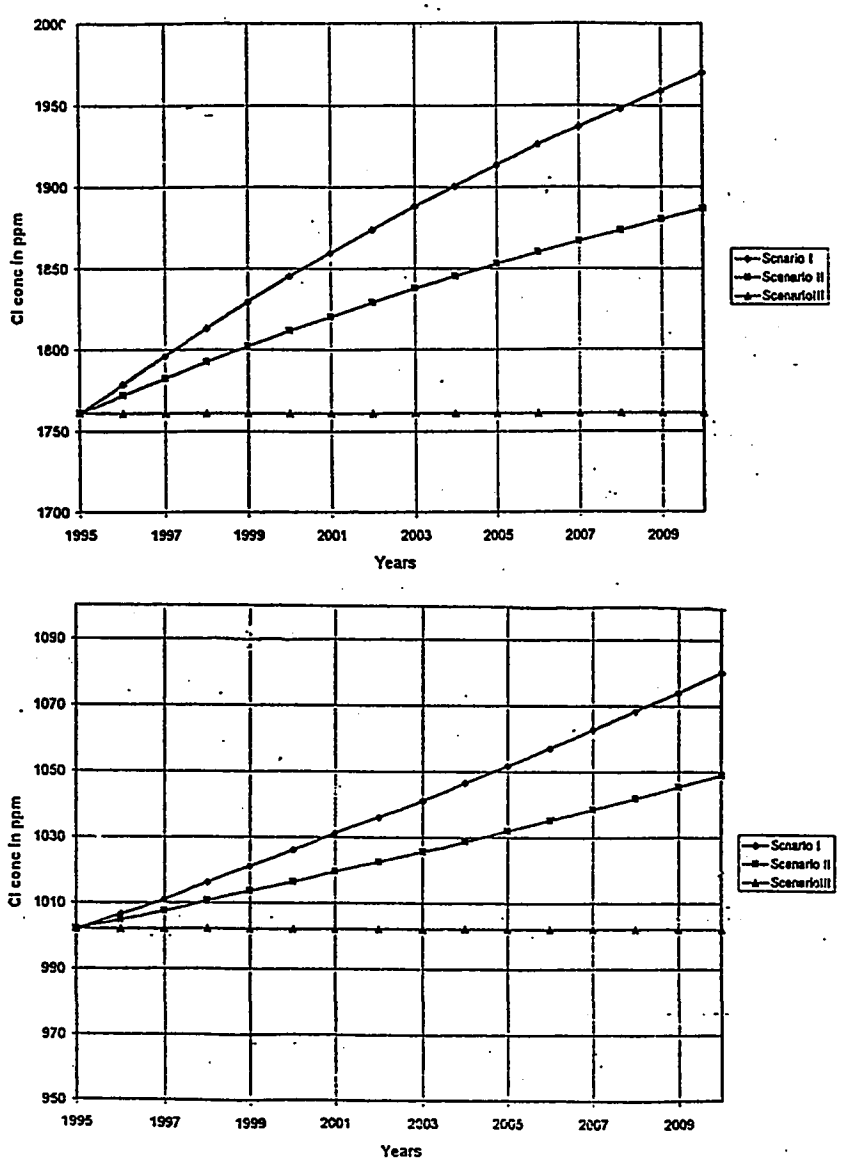

Figure 5.18: Time versus Chloride Concentration graphs for Neogene Aquifer near As-Sarrar area at nodes, (457, 507).

5.2 Alternative II: Conservation : Reduction of 50% in Pumping Rates for the Planning Period:

Water conservation is likely to play an important role in the arid and semi arid regions, where scarcity of water is the major constraint in the development of sound economical and social structures. Due to the self-sufficiency in many water intensive crops in the Kingdom which may cause no further expansion in agricultural activities and also by adopting various water conservation techniques to reduce the municipal demand by the Government, it is reasonable to assume that the expected pumping during this planning period would be reduced by 50% of Alternative I. The pumping rates of individual well fields are given in Appendix-B, (Table B-7 through B-9). Figures 5.19, 5.20 and 5.21 illustrate the water level contour maps at alternative II for Khobar, Alat and Neogene aquifers, respectively. The effects of reducing 50% of pumping rates on the chloride concentration distribution are illustrated in Figures, 5.22, 5.23 and 5.24. Computed drawdown maps for the period 1994-2010 are shown in Figures 5.25 and 5.26 for the Khobar and Alat aquifers, respectively. The drawdown for the Neogene aquifer is insignigicant.

A cone of depression is seen in the Khobar aquifer at south of Abuhadriya with a maximum drawdown of 4.5 meters, Figure 5.25. Drawdown elsewhere in the study

area is less than 1 meter. The isochlore map of the Khobar aquifer demonstrates an increase in the chloride concentration from 500 to 1,000 ppm at south of Abuhadriya, Figure, 5.22.

Figure 5.26 shows a cone of depression in the Alat aquifer south of Abuhadriya, with a maximum drawdown of 5 meters. Drawdown elsewhere is approximately one meter. A marked increase of 800 ppm in chloride concentration at south of Abuhadriya area is noted by adopting alternative II, Figure, 5.23. The Neogene aquifer generally may exhibit insignificant drawdowns. The chloride concentration in Khobar, Alat and Neogene decrease at various places due to reduction in pumping rates.

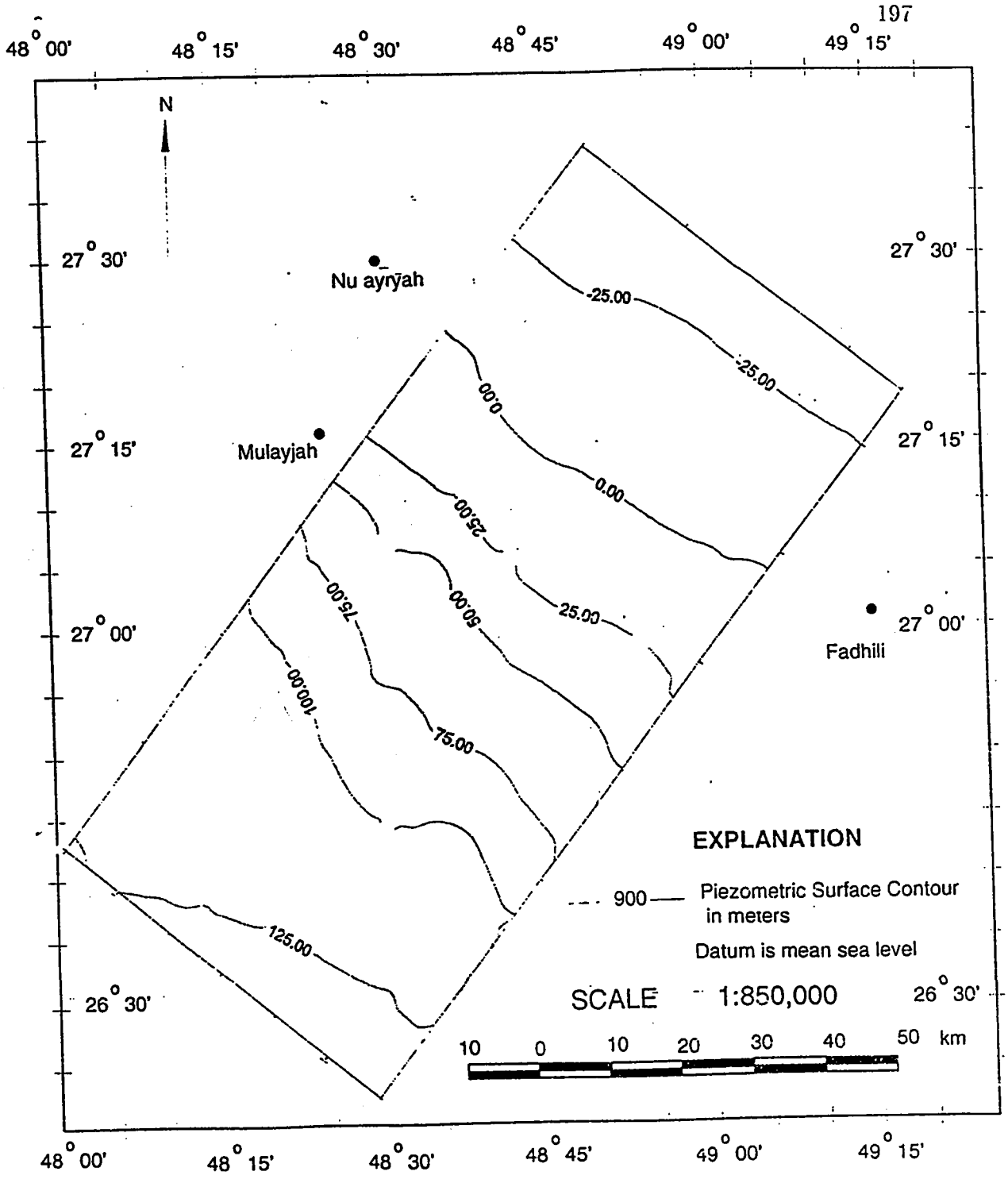

Figure 5.19: Simulated Piezometric Surface Map of Khobar Aquifer for the year 2010, Alternative II).

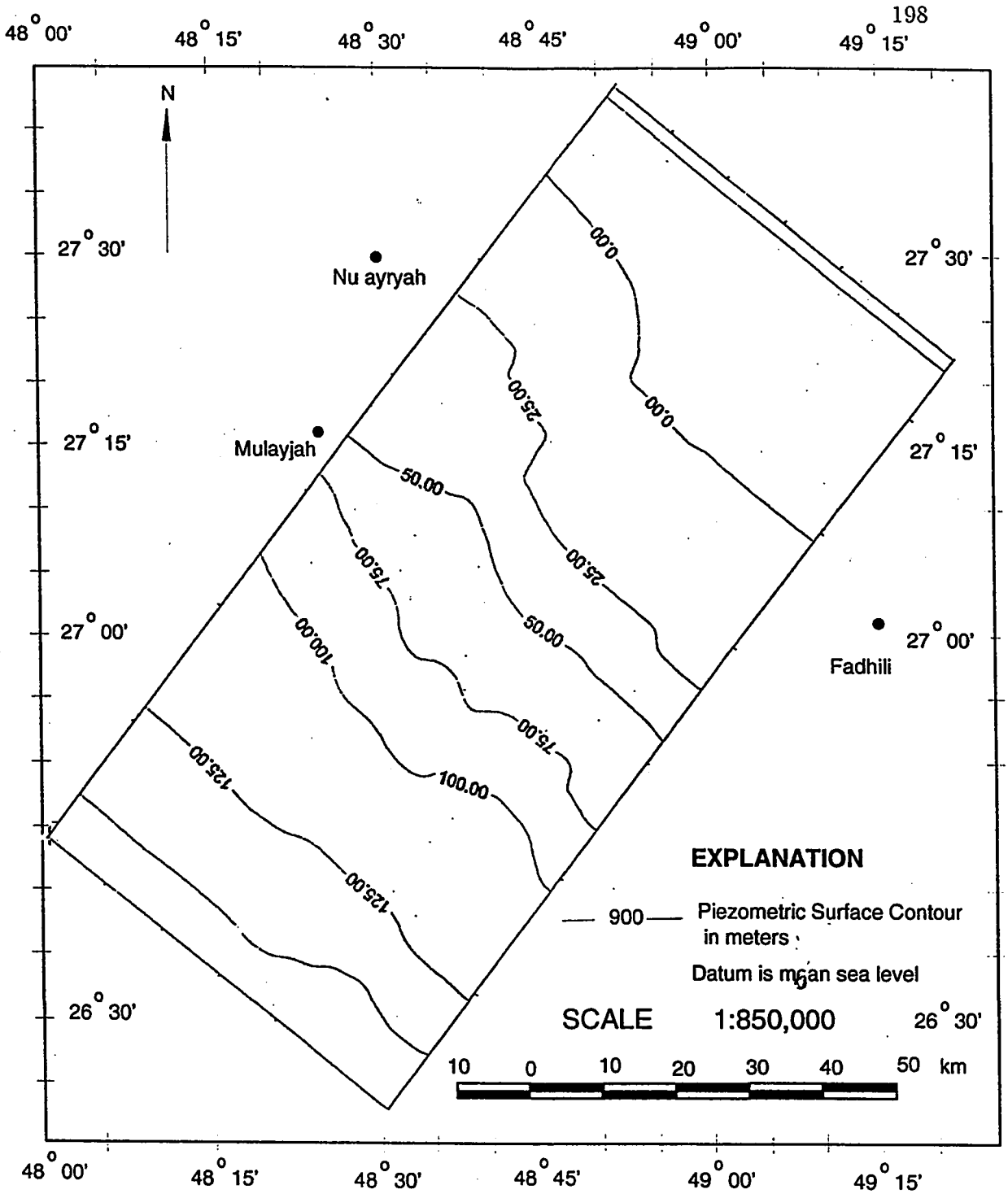

Figure 5.20: Simulated Piezometric Surface Map of Alat Aquifer for the year 2010, Alternative II).

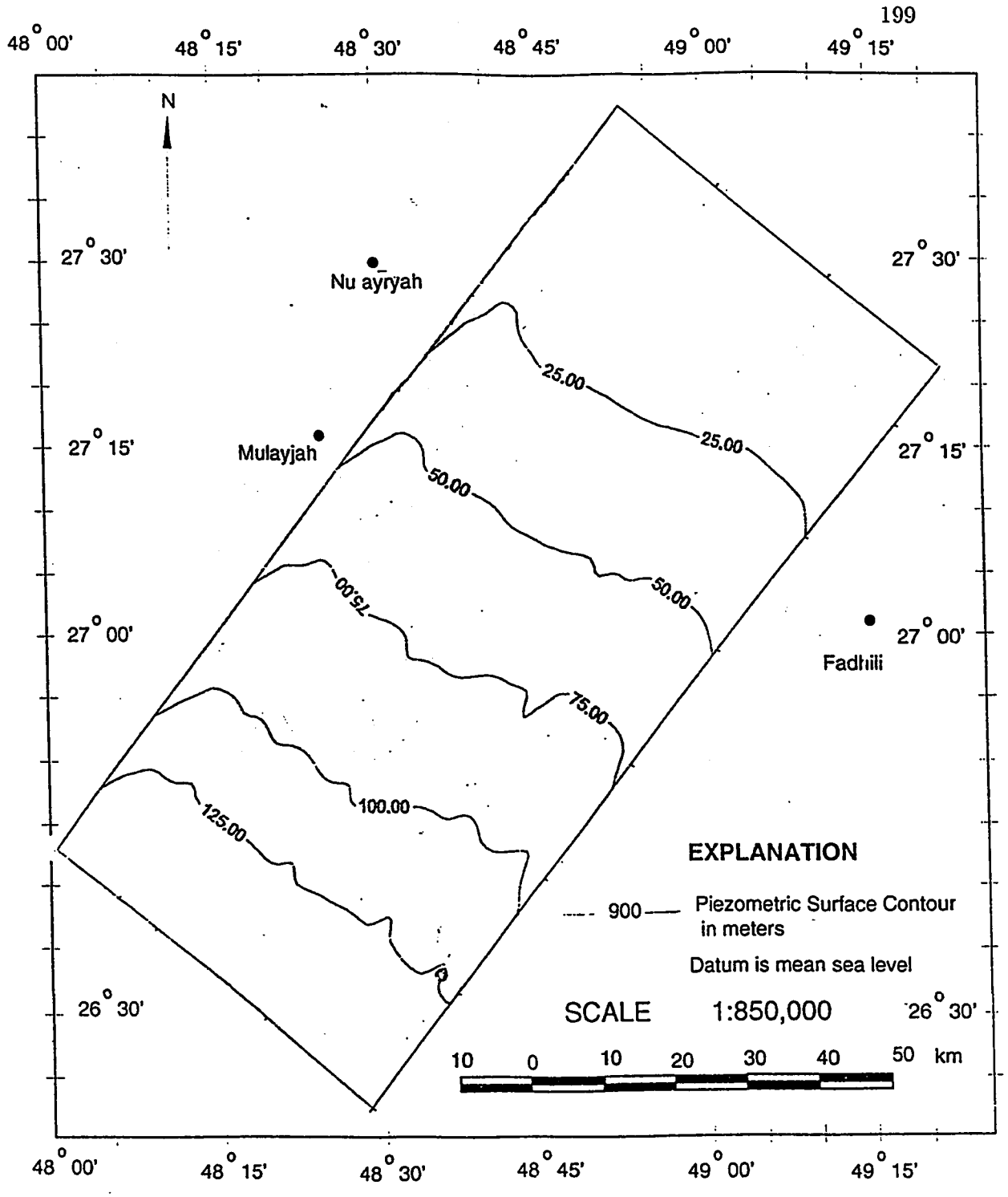

Figure 5.21: Simulated Water level Contour Map of Neogene Aquifer for the year 2010. Alternative II)

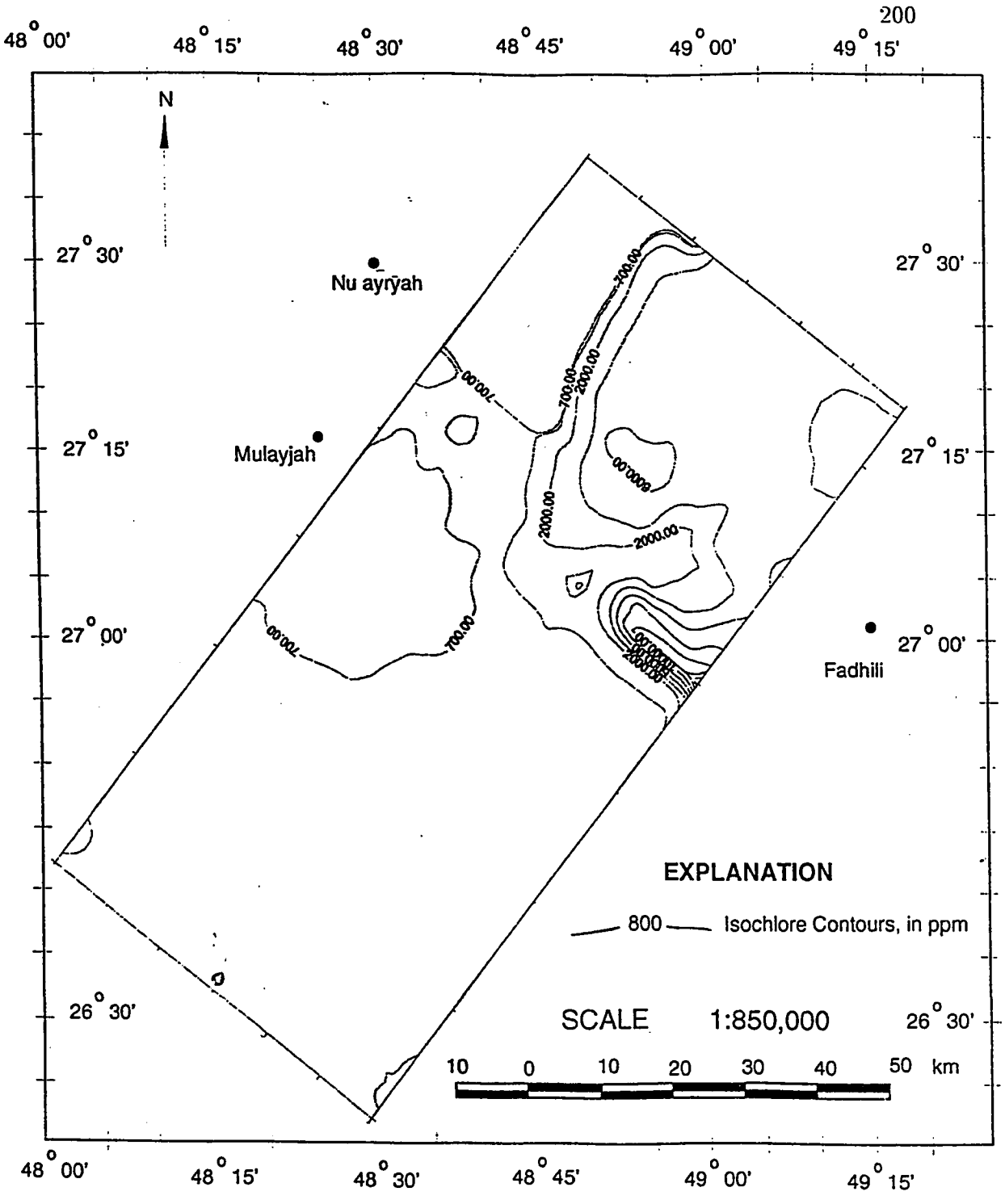

Figure 5.22: Simulated Isochlore Map of Khobar Aquifer for the year 2010. Alternative II).

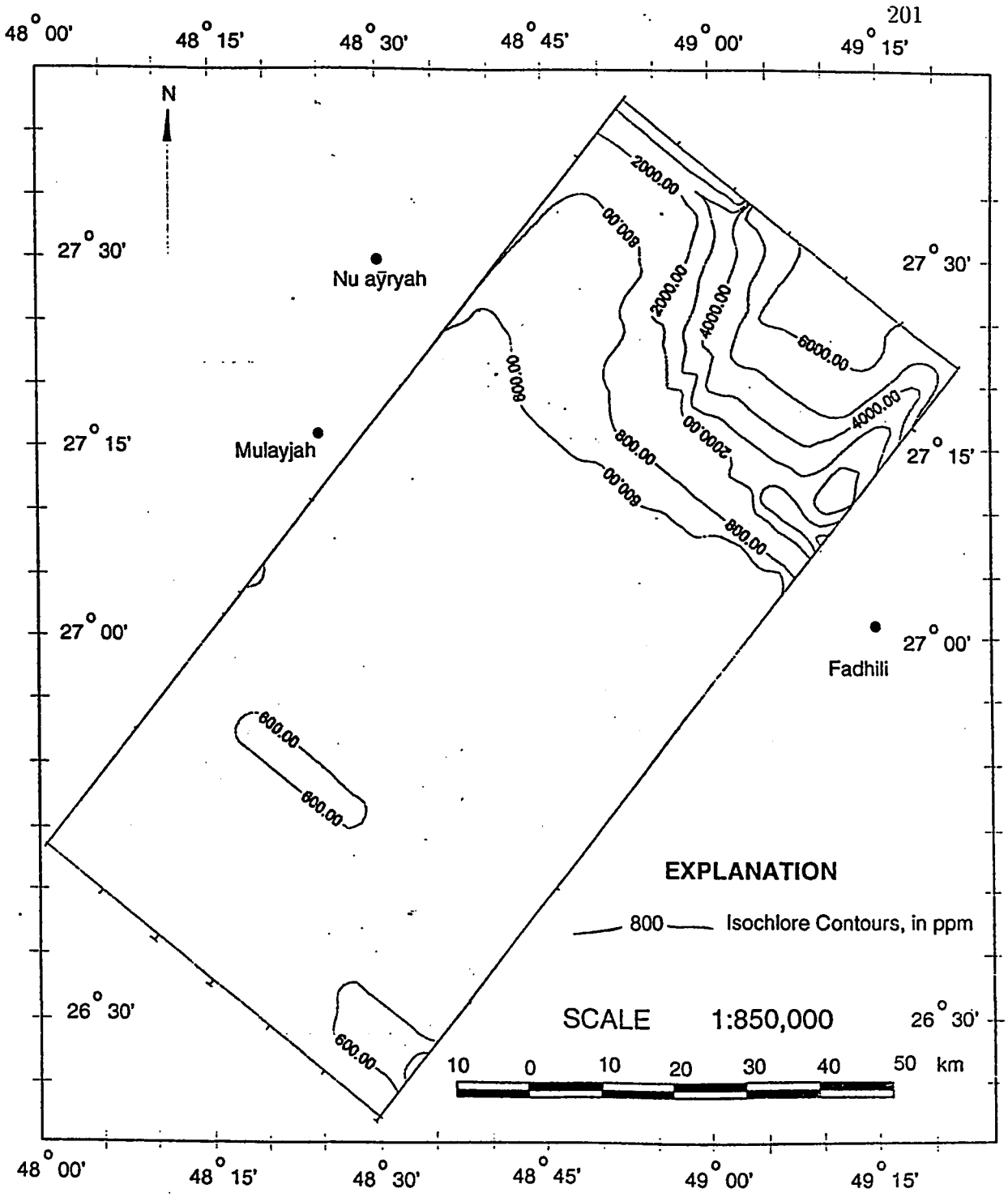

Figure 5.23: Simulated Isochlore Map of Alat Aquifer for the year 2010, Alternative II).

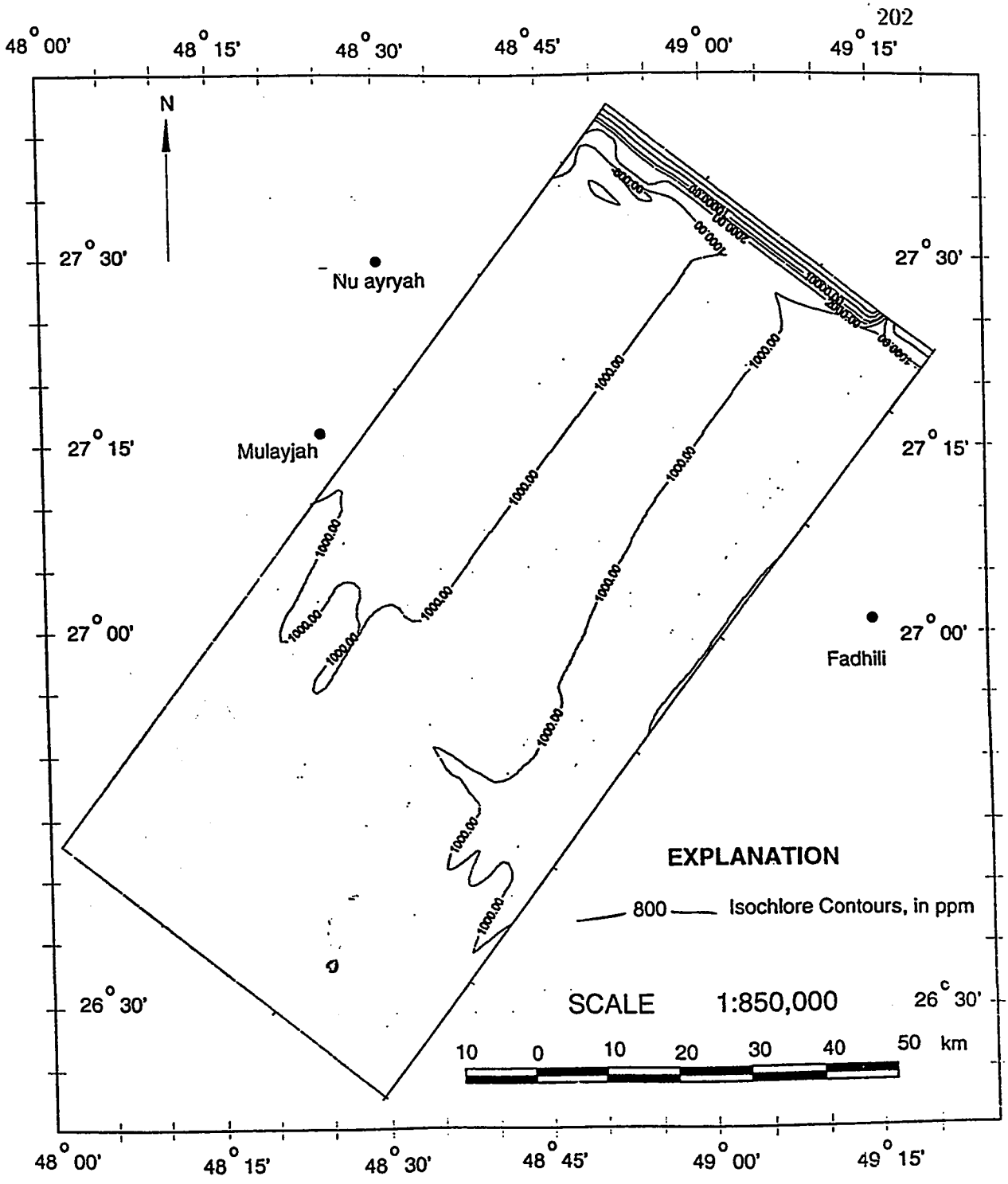

Figure 5.24: Simulated Isochlore Map of Neogene Aquifer for the year 2010, Alternative II).

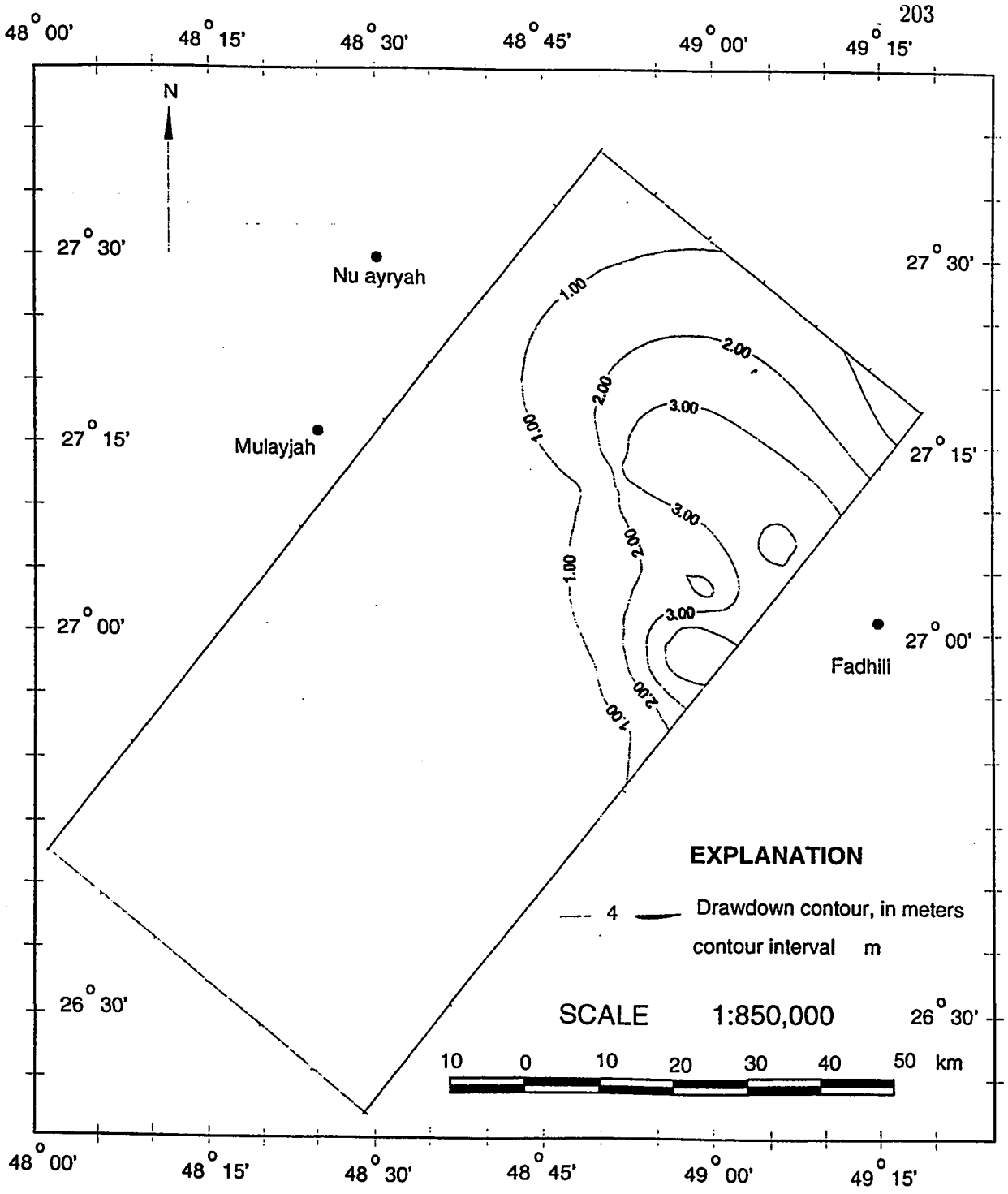

Figure 5.25: Drawdown Map of Khobar Aquifer for the period 1994-2010, Alternative II).

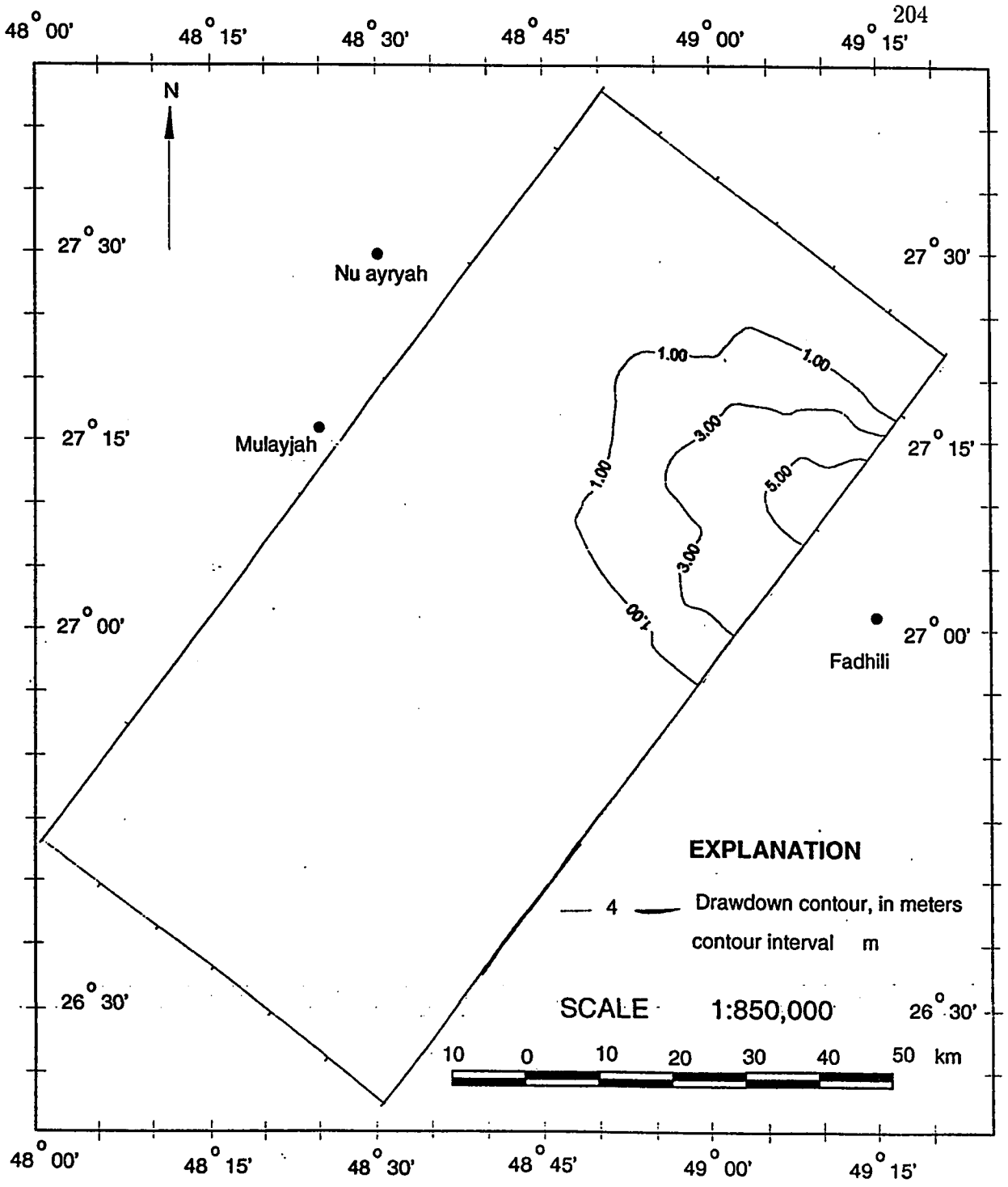

Figure 5.26: Drawdown Map of Alat Aquifer for the period 1994-2010, Alternative II).

5.3 Alternative III No-growth

As a slight decline in agricultural activities has occurred due to economical constraints from 1990 to 1994, it was reasonable to propose a no-growth alternative with a constant pumping rate equivalent to that of 1994. i.e. with zero pumping rate increase. Results of simulation indicated no significant change in water levels and chloride concentration patterns from those of 1994.

Chapter 5

Conclusions and Recommendations

5.1 Conclusions

1. A surface geological map was prepared on the basis of LANDSAT-TM image. It indicates that the study area comprises mainly of Neogene formations (Dam, Hadrukh, Hafuf), scattered large sabkhahs, and sand dunes .

2. Results of geophysical resistivity modeling display a possible occurrence of a collapse structure in the Rus formation which enhanced the vertical connection between the Umm Er Radhuma and the upper shallow aquifers.

3. Comparison of piezometric surface contour maps shows a vertical flow between adjacent aquifers, depending on the vertical hydraulic gradient and the conductivities of different aquifers. Vertical leakage occurs mostly from Umm Er Radhuma and the upper shallow aquifers. Vertical leakage between Khobar, Alat and Neogene aquifers varies from place to place depending upon the vertical hydrualic gradients. Chloride distribution pattern in the aquifers also confirmed the interaction between adjacent aquifers.

4. The groundwater flow and solute transport simulation model constructed, using the SUTRA model, has proved the existence of a vertical connection between adjacent aquifers, mainly from Umm Er Radhuma and the upper shallow aquifers.

5. During transient simulation, a maximum of 1.5 meters drawdown in Khobar aquifer was noted in Abuhadriyah area due to local pumping during the period of 1967 to 1994. Alat aquifer drawdown is 1 to 0.5 meters as compared to 0.5 to 0.2 meters in Neogene aquifer at different places during this period.

6. The transient simulation results have shown zones of low salinity due to vertical leakage. Salinity gradients vary from 800 ppm to 8000 ppm for Khobar aquifer, 600 ppm to 6000 ppm for Alat aquifer, and 1,200 ppm to 19,000 ppm for Neogene aquifer.

(S.P-1)

7. The transient simulation results also indicated local variations of chloride concentration at Abuhadriya area, which varies from 4500 ppm to 8,000 ppm in Khobar and 3500 ppm to 6500 ppm in Alat aquifer during the 1967-1994 period. The variations in chloride concentration for Neogene aquifer are uniform with a low rate of increase, generally from 600 ppm to 1000 ppm.

8. The sensitivity analysis indicated that the model is highly sensitive in terms of head and chloride distribution to changes in lateral permeability.

9. The distribution of calibrated aquifer parameters obtained after transient calibration defined the vertical leakage zones in the study area. The transmissivity values range from 100 to 10,000 m/d for Khobar aquifer, 200 to 15,000 m/d for Alat aquifer and 2000 to 16,000 m/d for Neogene aquifer. The calibrated vertical leakage varies from 5 to 6,000 m^3/d for Khobar aquifer, 1 to 8,000 m^3/d for Alat aquifer and 1 to 1000 m^3/d for Neogene aquifer.

10. Predictive runs of the flow and transport model indicated the following:

    (a) If the 1967-1994 period extraction trend continues to increase at a constant rate until the year 2010, then the continuous decline in water level would vary from 1 to 2 meters, 8.0 to 1 meters, and 8.5 to 2 meters in the Neogene, Alat and Khobar aquifers, respectively. The chloride concentrations continue to increase with the same rate as during the period (1967-1994). Near Abuhadriya area, it varies from 6500 ppm to 12,000

ppm in Alat aquifer.

(b) If the present extraction remains unchanged until the year 2010, there would be no significant changes in water level and chloride concentration distribution in the three aquifers.

5.2 Recommendations

1. The present study used a two-dimensional model in which each aquifer was simulated individually. A three-dimensional model, simulating the interaction of the aquifers at the same time, is highly recommended.

2. Using the simulation results of the present study, an optimization model can be developed for efficient management of the groundwater resources in the study area.

3. Continued model development and more field data aquisition for aquifer parameters will reduce the uncertainty in spatial distribution of aquifer parameters and also improve the understanding of the hydrologic system in the Wadi Al-Miyah area.

4. The projections of starting extractions rates were based on a little discontinueous data. Thus, the extractions rates used in this model were the best possible estimates. They do not represent the actual pumpage. Therefore,

as detailed upto-date information on pumping rates becomes available, the constructed model should be varified with the new data.

5. A detailed and continuous monitoring of water levels and salinity in the study area is strongly recommended to take preventive measures by which quality and water levels of different aquifers can be controlled.

Appendix A

Resistivity Interpretation Results

A.1 VES Data with Apparant Resistivity Curve and Interpreted Model

DATA SET: THESIS-1

CLIENT: M.S.Thesis
LOCATION: Wadi Al-Miyah
COUNTY: Eastern province K.S.A.
PROJECT: Resistivity/IP Sounding

DATE: 14-may-93
SOUNDING: 000N1
EQUIPMENT:

SOUNDING COORDINATES: X: 48 17 17E Y: 26 45 15N.

Schlumberger Configuration

FITTING ERROR: 8.435 PERCENT

L #	RESISTIVITY (ohm-m)	CHARGEABILITY (pfe)	THICKNESS (m)	ELEVATION (m)	CONDUCTANCE (Siemens)
				0.0	
1	2.10		3.00	-3.00	1.42
2	8.30		60.85	-63.85	7.33
3	16.84		20.15	-84.01	1.19
4	200.*				

"*" INDICATES FIXED PARAMETER

PARAMETER BOUNDS FROM EQUIVALENCE ANALYSIS

	LAYER	MINIMUM	BEST	MAXIMUM
RHO	1	0.007	2.100	4.994
	2	4.333	8.300	9.028
	3	5.141	16.842	119.903
	4	200.000	200.000	200.000
THICK	1	0.003	3.000	7.927
	2	36.808	60.854	82.250
	3	6.375	20.158	207.697
DEPTH	1	0.003	3.000	7.927
	2	36.811	63.854	85.113
	3	73.643	84.013	244.508

No.	Spacing (m)	PA (ohm-m) DATA	SYNTHETIC	DIFFERENCE (percent)
1	10.0000	1.0000	4.21	-321.9
2	20.0000	2.8000	5.86	-109.5
3	30.0000	5.6000	6.77	-21.02
4	40.0000	6.7000	7.39	-10.42
5	50.0000	9.6000	7.91	17.53
6	60.0000	9.8000	8.41	14.11
7	70.0000	8.3000	8.93	-7.68
8	80.0000	9.5000	9.49	0.0292
9	90.0000	9.6000	10.10	-5.23
10	100.0000	10.3000	10.75	-4.38
11	110.0000	11.6000	11.44	1.35
12	120.0000	10.7000	12.16	-13.71
13	130.0000	10.9000	12.92	-18.54
14	140.0000	14.0000	13.69	2.15
15	150.0000	12.8000	14.49	-13.21
16	160.0000	20.3000	15.29	24.64
17	170.0000	18.9000	16.11	14.74
18	180.0000	17.6000	16.93	3.79
19	190.0000	18.4000	17.75	3.50
20	200.0000	20.6000	18.57	9.81

PARAMETER RESOLUTION MATRIX:
"F" INDICATES FIXED PARAMETER

P 1	0.64						
P 2	-0.01	1.00					
P 3	0.02	0.00	0.03				
F 4	0.00	0.00	0.00	0.00			
T 1	-0.40	-0.02	0.02	0.00	0.55		
T 2	0.00	0.00	-0.15	0.00	0.00	0.95	
T 3	0.02	0.01	-0.01	0.00	0.03	0.16	0.04
	P 1	P 2	P 3	P 4	T 1	T 2	T 3

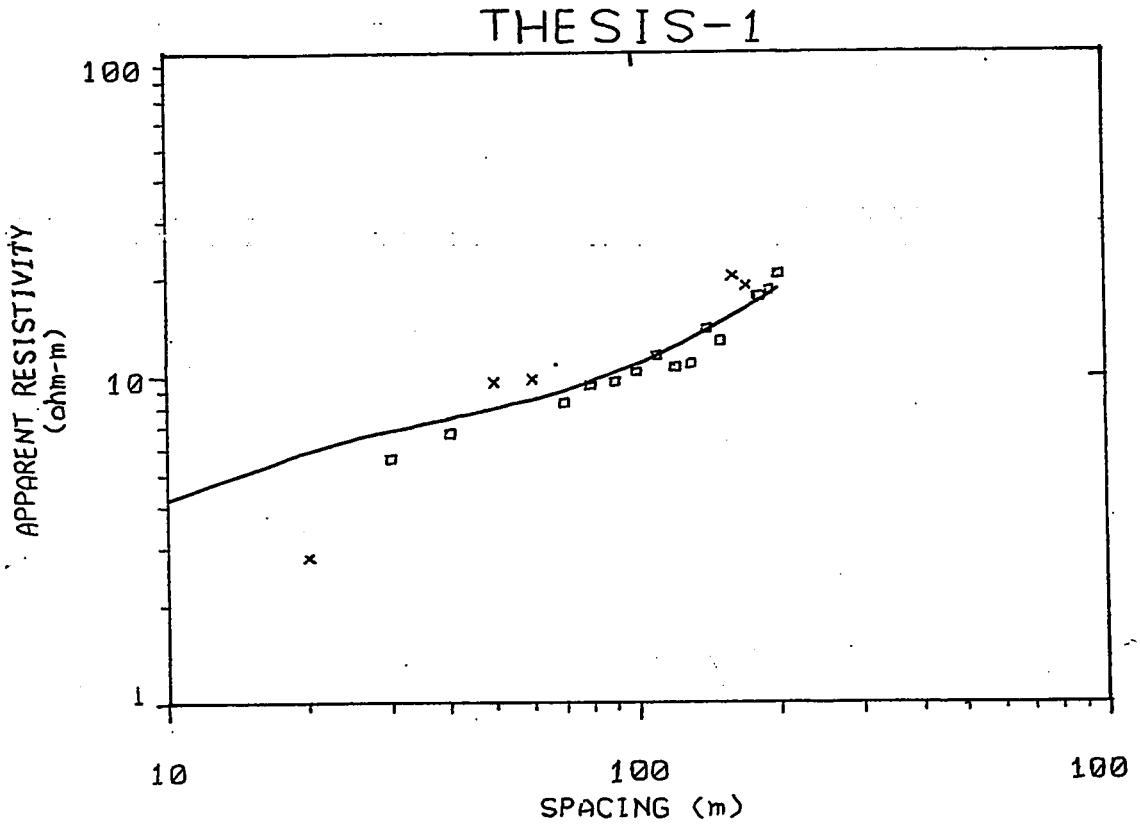
THESIS-1
100
10
1
APPARENT RESISTIVITY (ohm-m)
10
100
100
SPACING (m)

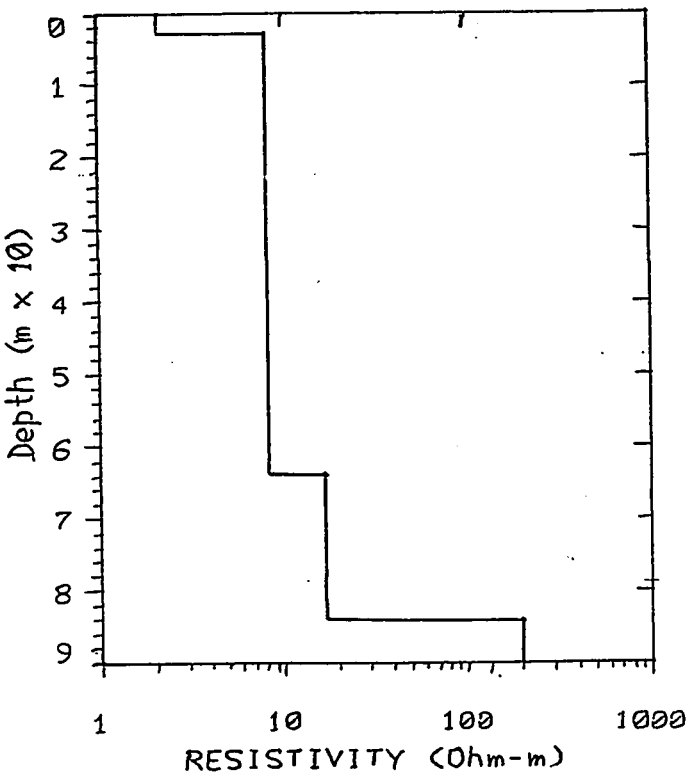
0
1
2
3
4
5
6
7
8
9
Depth (m x 10)
1
10
100
1000
RESISTIVITY (Ohm-m)

A.2 VES Data with Apparant Resistivity Curve and Interpreted Model (S.P-2)

DATA SET: THESIS-2

CLIENT: m.s.thesis
LOCATION: wadi al-miyah
COUNTY: eastern province k.s.a.
PROJECT: Resistivity/IP Sounding
ELEVATION: 0.00
SOUNDING COORDINATES: X: 48 23 17E Y: 27 00 42N

DATE: 3-11-93
SOUNDING: 000N2
AZIMUTH: 0.00 Deg NORTH
EQUIPMENT: resix

Schlumberger Configuration

FITTING ERROR: 19.251 PERCENT

L #	RESISTIVITY (ohm-m)	CHARGEABILITY (pfe)	THICKNESS (m)	ELEVATION (m)	CONDUCTANCE (Siemens)
				0.0	
1	3.37		3.*0	-3.50	1.03
2	8.*0		70.*0	-74.00	8.10
3	19.*0		24.*0	-98.00	1.21
4	265783.2				

"*" INDICATES FIXED PARAMETER

PARAMETER BOUNDS FROM EQUIVALENCE ANALYSIS

	LAYER	MINIMUM	BEST	MAXIMUM
RHO	1	2.811	3.378	4.048
	2	8.700	8.700	8.700
	3	19.700	19.700	19.700
	4	1000000.060	265783.250	**********
THICK	1	3.500	3.500	3.500
	2	70.500	70.500	70.500
	3	24.000	24.000	24.000
DEPTH	1	1.000	3.500	0.000
	2	0.000	74.000	0.000
	3	0.000	98.000	0.000

No.	Spacing (m)	PA (ohm-m) DATA	SYNTHETIC	DIFFERENCE (percent)
1	5.00	5.00	4.02	19.56

No.	Spacing (m)	PA (ohm-m) DATA	SYNTHETIC	DIFFERENCE (percent)
2	10.00	4.70	5.33	-13.45
3	15.00	5.50	6.26	-13.89
4	20.00	6.50	6.88	-5.95
5	25.00	8.20	7.32	10.65
6	30.00	6.90	7.65	-10.98
7	35.00	7.30	7.92	-8.55
8	50.00	6.20	8.56	-38.19
9	100.0	14.20	11.10	21.78
10	175.0	46.60	17.09	62.50
11	200.0	101.1	19.38	80.82
12	225.0	169.0	21.73	87.13
13	250.0	164.0	24.10	85.29

PARAMETER RESOLUTION MATRIX:
"F" INDICATES FIXED PARAMETER

P 1	1.00						
F 2	0.00	0.00					
F 3	0.00	0.00	0.00				
P 4	0.00	0.00	0.00	0.00			
F 1	0.00	0.00	0.00	0.00	0.00		
F 2	0.00	0.00	0.00	0.00	0.00	0.00	
F 3	0.00	0.00	0.00	0.00	0.00	0.00	0.00
	P 1	F 2	F 3	P 4	F 1	F 2	F 3

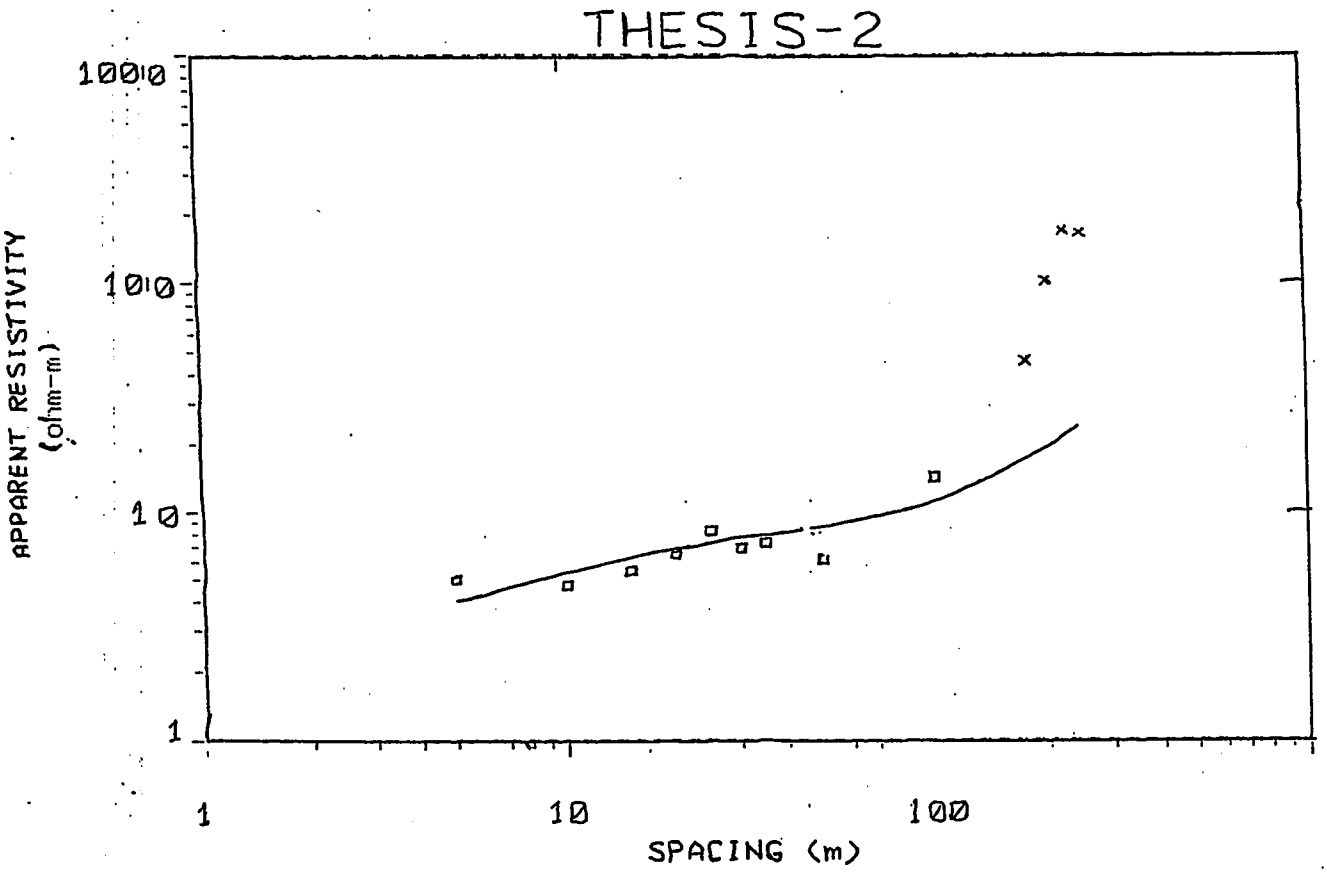
THESIS-2
APPARENT RESISTIVITY (ohm-m)
1000
100
10
1
1
10
100
SPACING (m)

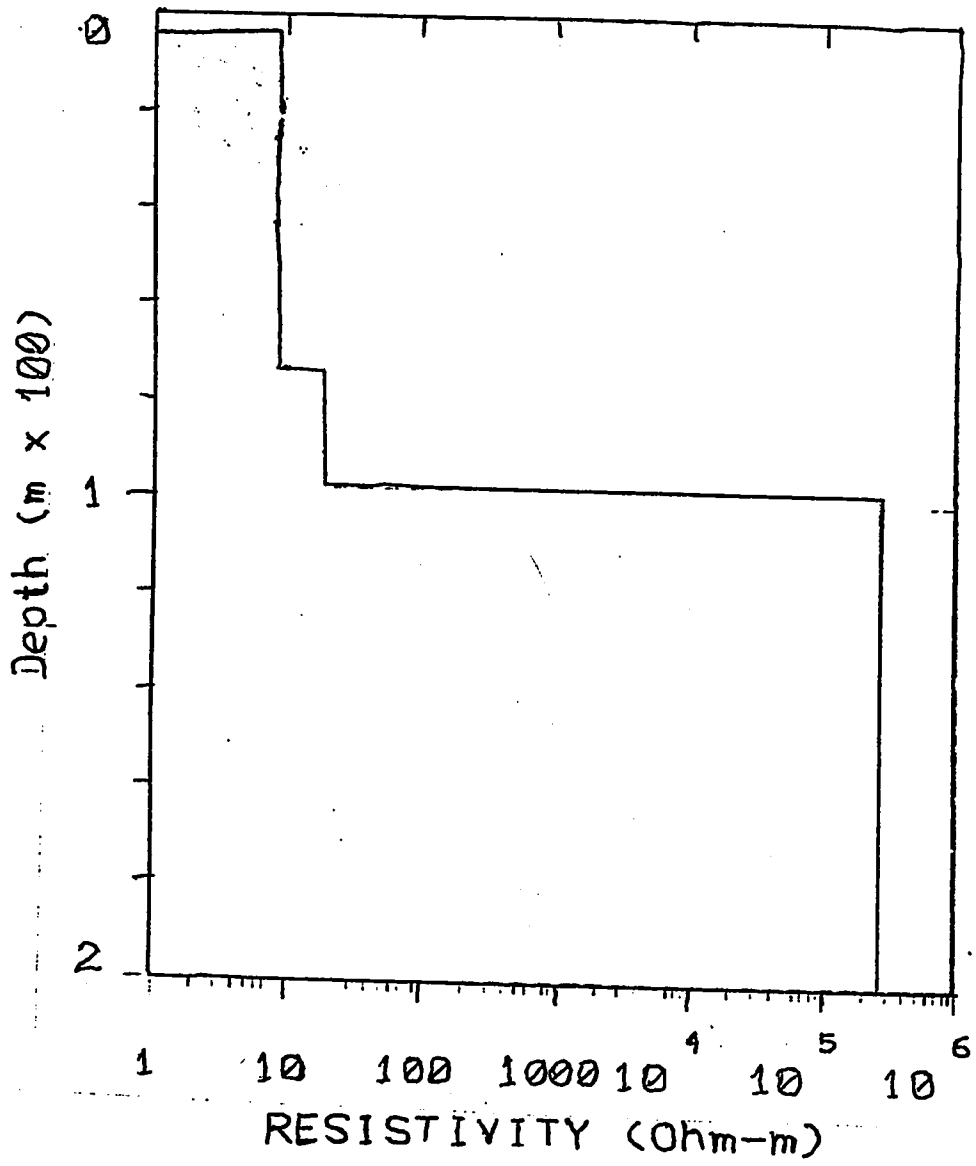
0
1
2
Depth (m x 100)
1
10
100
1000
10^4
10^5
10^6
RESISTIVITY (Ohm-m)

A.3 VES Data with Apparant Resistivity Curve and Interpreted Model (S.P-3)

DATA SET: THESIS-3

CLIENT: m.s.thesis
LOCATION: wadi al-miyah
COUNTY: eastern province k.s.a.
PROJECT: Resistivity/IP Sounding
ELEVATION: 0.00
SOUNDING COORDINATES: X: 48 24 29E Y: 26 56 46N

DATE: 18-11-93
SOUNDING: 000N3
AZIMUTH: 0.00 Deg NORTH
EQUIPMENT: resix

Schlumberger Configuration

FITTING ERROR: 12.040 PERCENT

L #	RESISTIVITY (ohm-m)	CHARGEABILITY (pfe)	THICKNESS (m)	ELEVATION (m)	CONDUCTANCE (Siemens)
				0.0	
1	0.0525		1.24	-1.24	23.63
2	8.*7		95.*6	-96.70	10.64
3	18.*7		32.*7	-129.0	1.74
4	3808.4				

"*" INDICATES FIXED PARAMETER

PARAMETER BOUNDS FROM EQUIVALENCE ANALYSIS

	LAYER	MINIMUM	BEST	MAXIMUM
RHO	1	0.006	0.053	0.428
	2	8.970	8.970	8.970
	3	18.570	18.570	18.570
	4	380.848	3808.482	38084.809
THICK	1	0.163	1.243	9.503
	2	95.461	95.461	95.461
	3	32.375	32.375	32.375
DEPTH	1	0.163	1.243	9.503
	2	95.623	96.704	104.964
	3	127.999	129.079	137.339

No.	Spacing (m)	PA (ohm-m) DATA	SYNTHETIC	DIFFERENCE (percent)
1	25.00	0.500	0.954	-90.99

No.	Spacing (m)	PA (ohm-m) DATA	SYNTHETIC	DIFFERENCE (percent)
2	50.00	1.30	1.76	-35.85
3	75.00	2.50	2.48	0.419
4	100.0	3.60	3.16	12.14
5	125.0	3.60	3.81	-5.85
6	150.0	4.70	4.44	5.34
7	175.0	4.90	5.08	-3.79
8	200.0	6.40	5.72	10.50
9	225.0	5.70	6.37	-11.85
10	250.0	7.30	7.03	3.68
11	275.0	7.60	7.69	-1.21
12	300.0	9.50	8.36	11.99
13	310.0	9.50	8.62	9.17
14	320.0	9.10	8.89	2.22
15	330.0	9.80	9.16	6.45
16	340.0	8.30	9.43	-13.70
17	350.0	9.00	9.70	-7.87
18	360.0	10.00	9.98	0.199
19	370.0	9.90	10.25	-3.55
20	375.0	11.00	10.38	5.56
21	380.0	10.10	10.52	-4.19
22	385.0	13.80	10.66	22.75
23	390.0	13.60	10.79	20.61
24	395.0	11.60	10.93	5.75
25	400.0	9.50	11.06	-16.51

PARAMETER RESOLUTION MATRIX:
"F" INDICATES FIXED PARAMETER

P 1	0.50						
F 2	0.00	0.00					
F 3	0.00	0.00	0.00				
P 4	-0.01	0.00	0.00	0.00			
T 1	-0.48	0.00	0.00	-0.01	0.53		
F 2	0.00	0.00	0.00	0.00	0.00	0.00	
F 3	0.00	0.00	0.00	0.00	0.00	0.00	0.00
	P 1	F 2	F 3	P 4	T 1	F 2	F 3

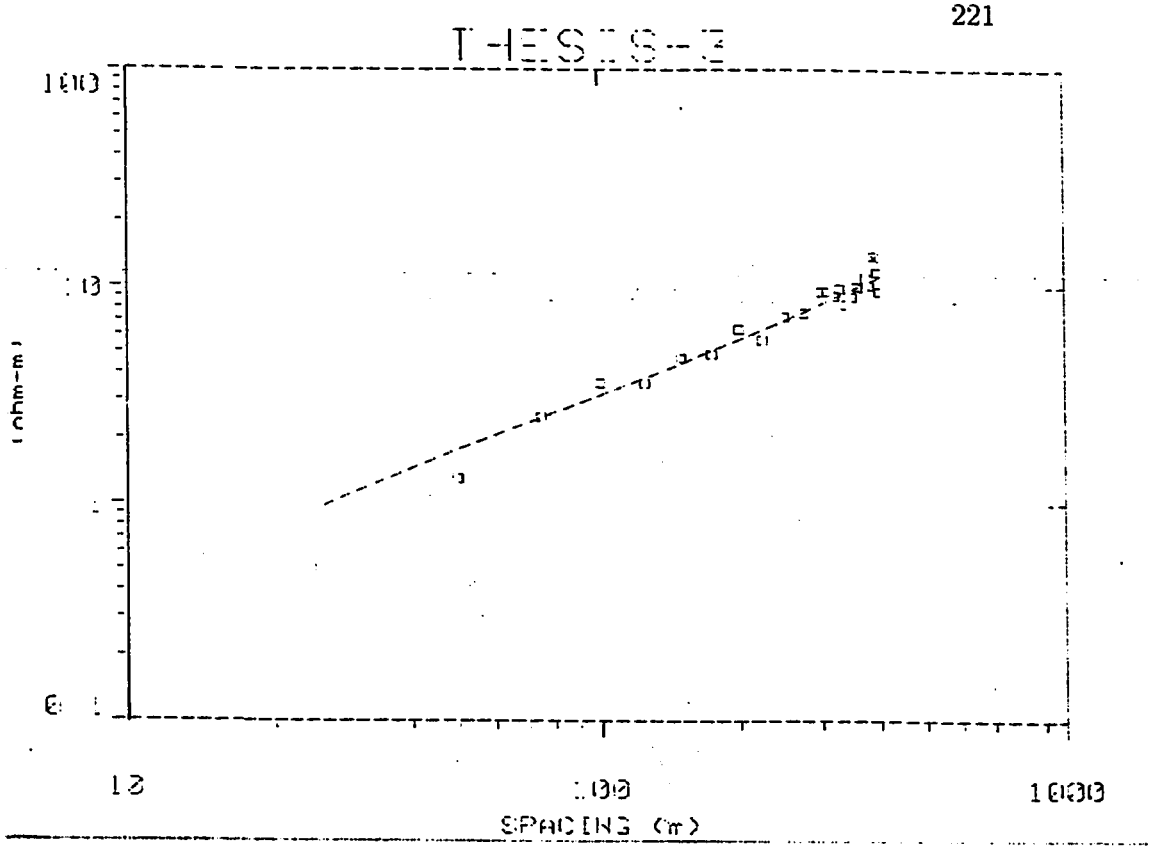
THESIS-2
1000
100
10
1
10
100
10000
SPACING (m)

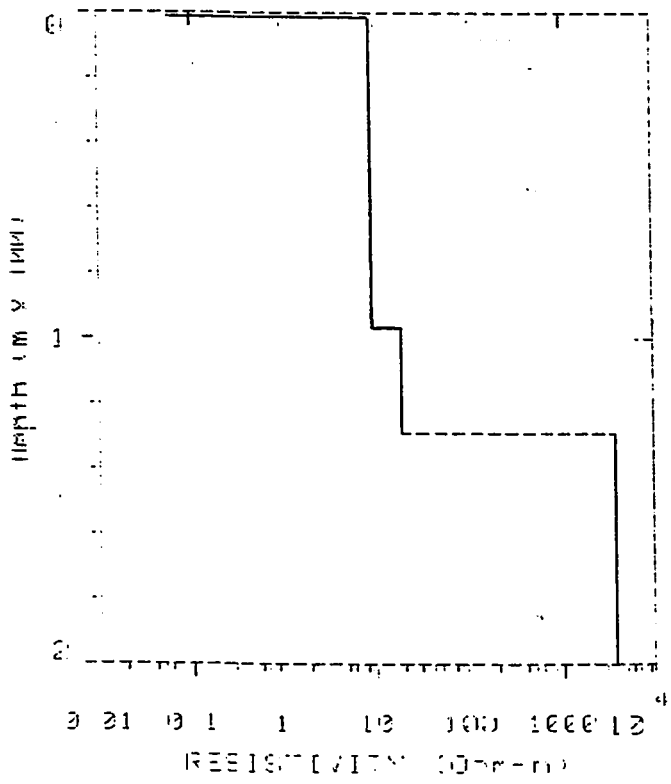
1
2
3 21 3 1 1 10 100 1000 2
RESISTIVITY

A.4 VES Data with Apparant Resistivity Curve and Interpreted Model (S.P-4)

DATA SET: THESIS-4

CLIENT: MS. THESIS FIELD SURVEY DATE: --
LOCATION: SOUTH OF SARRAR, AT SABKHAH. SOUNDING: N4
COUNTY: WADI AL-MIYAH,EASTERN PROVINCE AZIMUTH: N 16 E
PROJECT: Resistivity/IP Sounding EQUIPMENT: RESIX-IP
ELEVATION: 0.00
SOUNDING COORDINATES: X: 48 19 49E Y: 26 58 03N

Schlumberger Configuration

FITTING ERROR: 16.013 PERCENT

L #	RESISTIVITY (ohm-m)	CHARGEABILITY (pfe)	THICKNESS (m)	ELEVATION (m)	CONDUCTANCE (Siemens)
				0.0	
1	1.39		40.64	-40.64	29.16
2	8.*6		69.*0	-109.6	7.70
3	18.*9		30.*0	-139.6	1.59
4	197.*		45.*5	-185.4	0.232
5	5.905E+06				

"*" INDICATES FIXED PARAMETER

PARAMETER BOUNDS FROM EQUIVALENCE ANALYSIS

	LAYER	MINIMUM	BEST	MAXIMUM
RHO	1	0.968	1.393	1.672
	2	8.960	8.960	8.960
	3	18.790	18.790	18.790
	4	197.560	197.560	197.560
	5	59045.504	590450.000	**********
THICK	1	27.469	40.641	49.433
	2	69.000	69.000	69.000
	3	30.000	30.000	30.000
	4	45.857	45.857	45.857
DEPTH	1	27.469	40.641	49.433
	2	96.469	109.641	118.433
	3	126.469	139.641	148.433
	4	172.326	185.497	194.290

No.	Spacing (m)	PA (ohm-m) DATA	SYNTHETIC	DIFFERENCE (percent)
1	25.00	1.40	1.45	-3.83
2	50.00	2.00	1.75	12.01
3	75.00	2.00	2.25	-12.86
4	100.0	1.90	2.82	-48.83
5	125.0	3.10	3.41	-10.30
6	195.0	0.900	5.11	-468.6
7	205.0	5.20	5.36	-3.17
8	215.0	7.40	5.61	24.14
9	245.0	5.50	6.36	-15.70
10	250.0	5.10	6.48	-27.24
11	255.0	6.50	6.61	-1.77
12	260.0	7.70	6.74	12.44
13	265.0	8.10	6.86	15.21
14	270.0	9.20	6.99	23.97
15	275.0	44.00	7.12	83.81

PARAMETER RESOLUTION MATRIX:
"F" INDICATES FIXED PARAMETER

P 1	1.00								
F 2	0.00	0.00							
F 3	0.00	0.00	0.00						
F 4	0.00	0.00	0.00	0.00					
P 5	0.00	0.00	0.00	0.00	0.00				
T 1	0.00	0.00	0.00	0.00	0.00	1.00			
F 2	0.00	0.00	0.00	0.00	0.00	0.00	0.00		
F 3	0.00	0.00	0.00	0.00	0.00	0.00	0.00	0.00	
F 4	0.00	0.00	0.00	0.00	0.00	0.00	0.00	0.00	0.00
	P 1	F 2	F 3	F 4	P 5	T 1	F 2	F 3	F 4

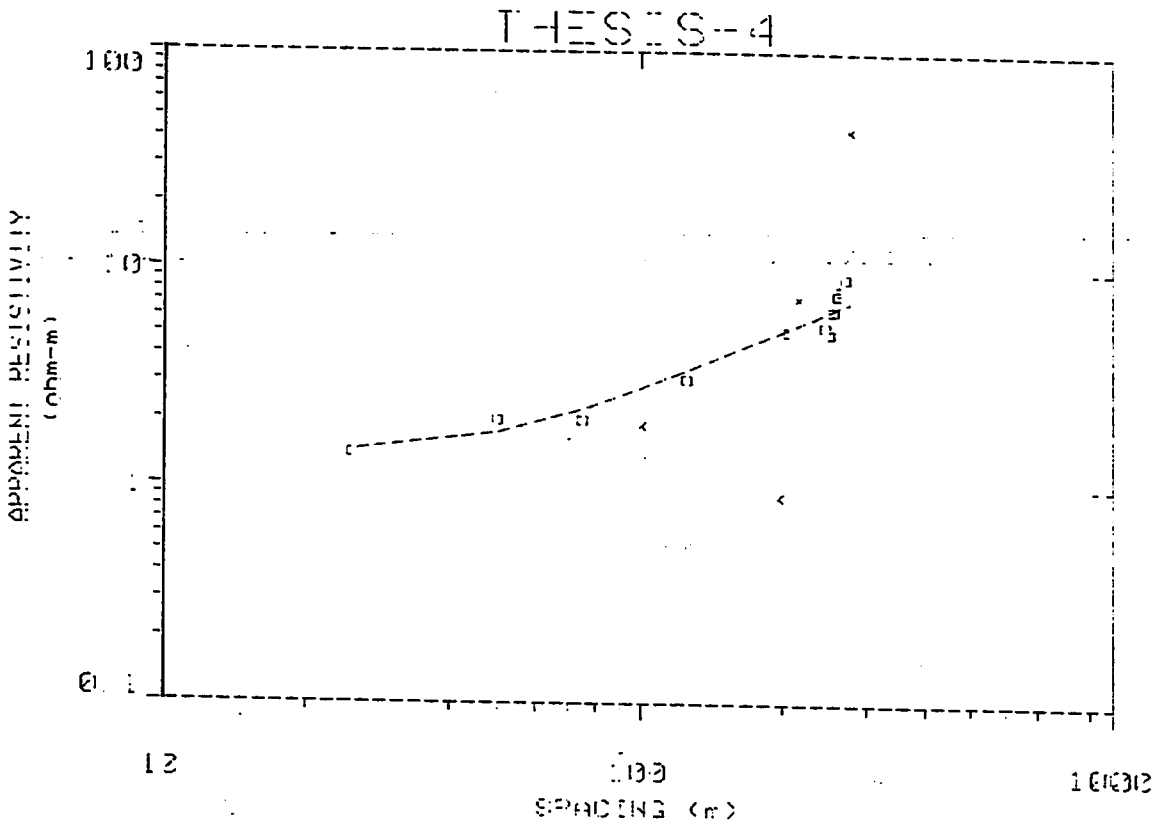
THESIS-4
1000
10
1
0.1
APPARENT RESISTIVITY (ohm-m)
1.2
100
10000
SPACING (m)

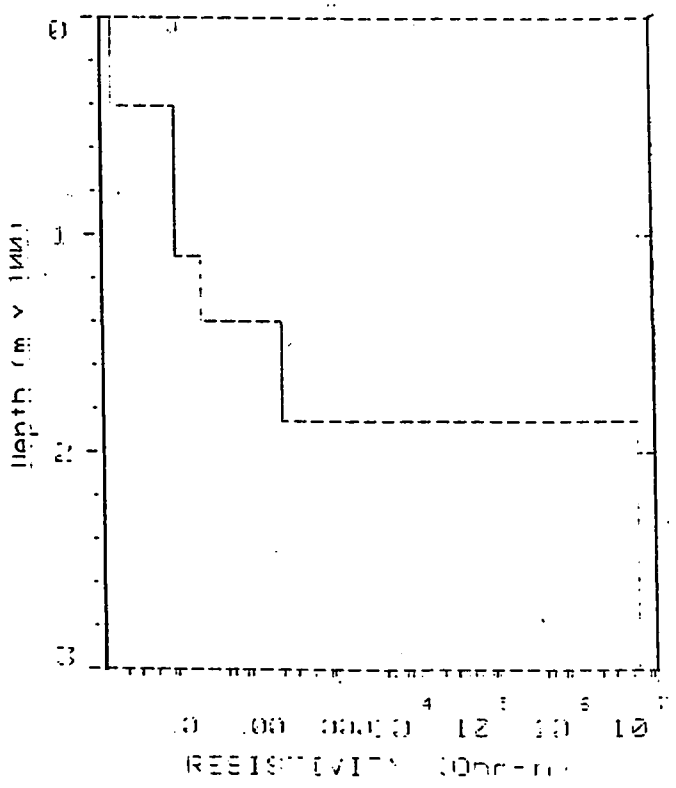
0
1
2
3
Depth (m x 1000)
RESISTIVITY (Ohm-m)

A.5 VES Data with Apparant Resistivity Curve and Interpreted Model (S.P-5)

DATA SET: THESIS-5

CLIENT: thesis
LOCATION: wadialmiyah
COUNTY: eastern province
PROJECT: Resistivity/IP Sounding
ELEVATION: 0.00
SOUNDING COORDINATES: X: 48 24 50E Y: 26 53 54N

DATE: 30-JUN-93
SOUNDING: 000n5
AZIMUTH: 0.00 Deg NORTH
EQUIPMENT: resix

Schlumberger Configuration

FITTING ERROR: 19.876 PERCENT

L #	RESISTIVITY (ohm-m)	CHARGEABILITY (pfe)	THICKNESS (m)	ELEVATION (m)	CONDUCTANCE (Siemens)
				0.0	
1	7.17		100.9	-100.9	14.06
2	19.*6		52.*5	-153.9	2.66
3	179.*		43.*9	-197.2	0.241
4	2.808E+06				

"*" INDICATES FIXED PARAMETER

PARAMETER BOUNDS FROM EQUIVALENCE ANALYSIS

	LAYER	MINIMUM	BEST	MAXIMUM
RHO	1	5.983	7.179	8.615
	2	19.860	19.860	19.860
	3	179.000	179.000	179.000
	4	28082.38	92808238.750	**********
THICK	1	79.573	100.991	128.173
	2	52.954	52.954	52.954
	3	43.293	43.293	43.293
DEPTH	1	79.573	100.991	128.173
	2	132.527	153.945	181.127
	3	175.820	197.237	224.419

No.	Spacing (m)	PA (ohm-m) DATA	SYNTHETIC	DIFFERENCE (percent)
1	25.00	8.00	7.19	10.04
2	50.00	8.70	7.32	15.77
3	75.00	7.20	7.65	-6.29
4	100.0	7.10	8.20	-15.58
5	125.0	7.80	8.97	-15.12
6	150.0	11.20	9.93	11.25
7	175.0	10.30	11.04	-7.24
8	200.0	10.70	12.26	-14.61
9	225.0	10.40	13.56	-30.40
10	250.0	12.80	14.91	-16.52
11	275.0	16.10	16.30	-1.28
12	310.0	28.50	18.29	35.79
13	320.0	48.30	18.87	60.92

PARAMETER RESOLUTION MATRIX:
"F" INDICATES FIXED PARAMETER

P 1	1.00						
F 2	0.00	0.00					
F 3	0.00	0.00	0.00				
P 4	0.00	0.00	0.00	0.00			
T 1	0.00	0.00	0.00	0.00	1.00		
F 2	0.00	0.00	0.00	0.00	0.00	0.00	
F 3	0.00	0.00	0.00	0.00	0.00	0.00	0.00
	P 1	F 2	F 3	P 4	T 1	F 2	F 3

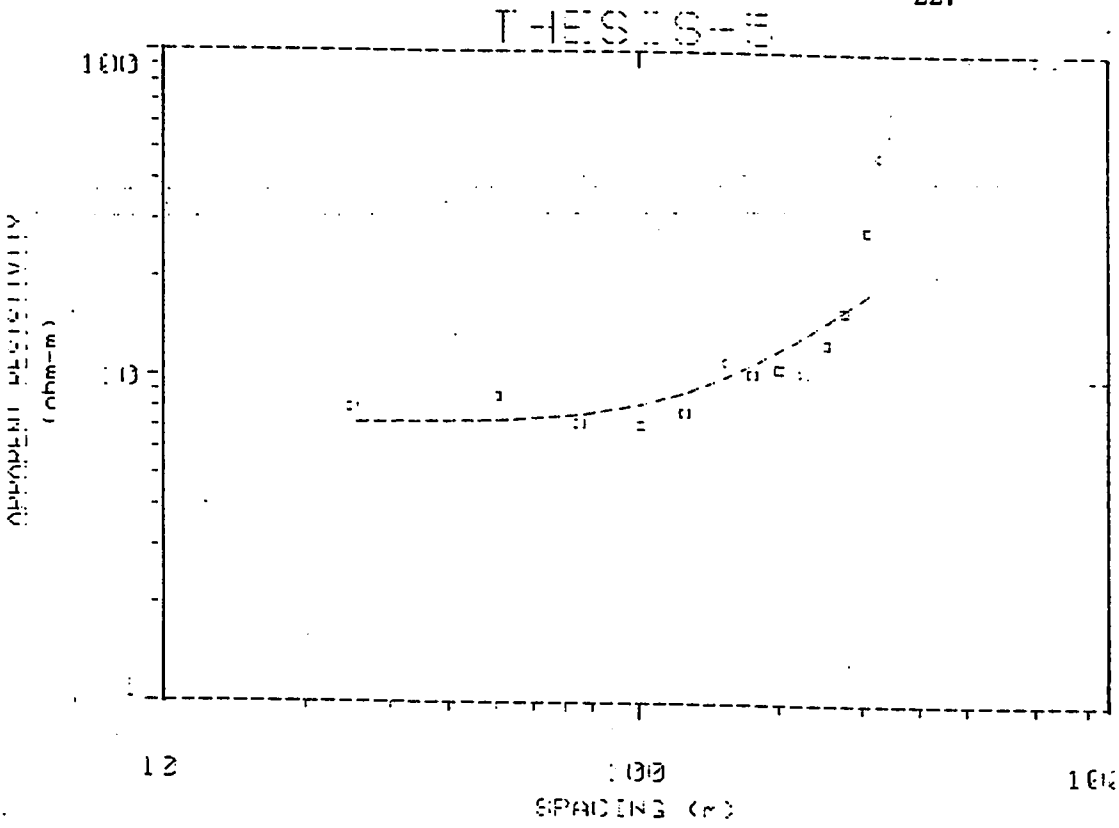
THESIS-E
1000
10
1
APPARENT RESISTIVITY
(ohm-m)
1
100
1000
SPACING (m)

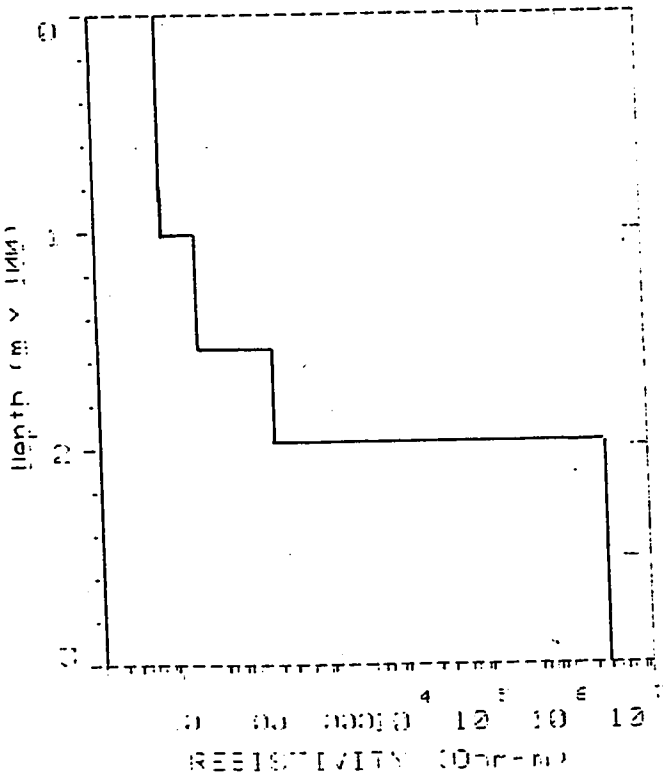
0
2
3
Depth (m x 1000)
1
10
100
1000
RESISTIVITY (Ohm-m)

A.6 VES Data with Apparant Resistivity Curve and Interpreted Model (S.P-6)

DATA SET: THESIS-6

CLIENT: MS. THESIS FIELD SURVEY
LOCATION: WADI AL-MIYAH
COUNTY: EASTERN PROVINCE, K.S.A.
PROJECT: Resistivity/IP Sounding
ELEVATION: 0.00
SOUNDING COORDINATES: X: 48 21 26E Y: 26 52 27N

DATE: 17-DEC-93
SOUNDING: S6
AZIMUTH: 0.00 Deg
EQUIPMENT: RESIX-IP

Schlumberger Configuration

FITTING ERROR: 19.231 PERCENT

L =	RESISTIVITY (ohm-m)	CHARGEABILITY (pfe)	THICKNESS (m)	ELEVATION (m)	CONDUCTANCE (Siemens)
1	0.100			0.0	
2	9.*5		1.51	-1.51	15.05
3	19.*5		68.*9	-70.41	6.92
4	9.894E+06		27.*4	-98.36	1.41

"*" INDICATES FIXED PARAMETER

No.	Spacing (m)	PA (ohm-m) DATA	PA (ohm-m) SYNTHETIC	DIFFERENCE (Percent)
1	25.00	0.600	1.44	-141.3
2	50.00	2.10	2.62	-25.03
3	75.00	6.70	3.67	45.20
4	100.0	3.90	4.66	-19.56
5	125.0	5.10	5.64	-10.61
6	150.0	7.50	6.62	11.63
7	175.0	4.30	7.62	-[illegible]
8	225.0	1.60	9.67	-[illegible]
9	250.0	1.70	10.71	-530.2
10	285.0	19.10	12.18	36.20

PARAMETER RESOLUTION MATRIX:
"F" INDICATES FIXED PARAMETER
P 1 0.16
P 2 0.00 0.06
P 3 [illegible]

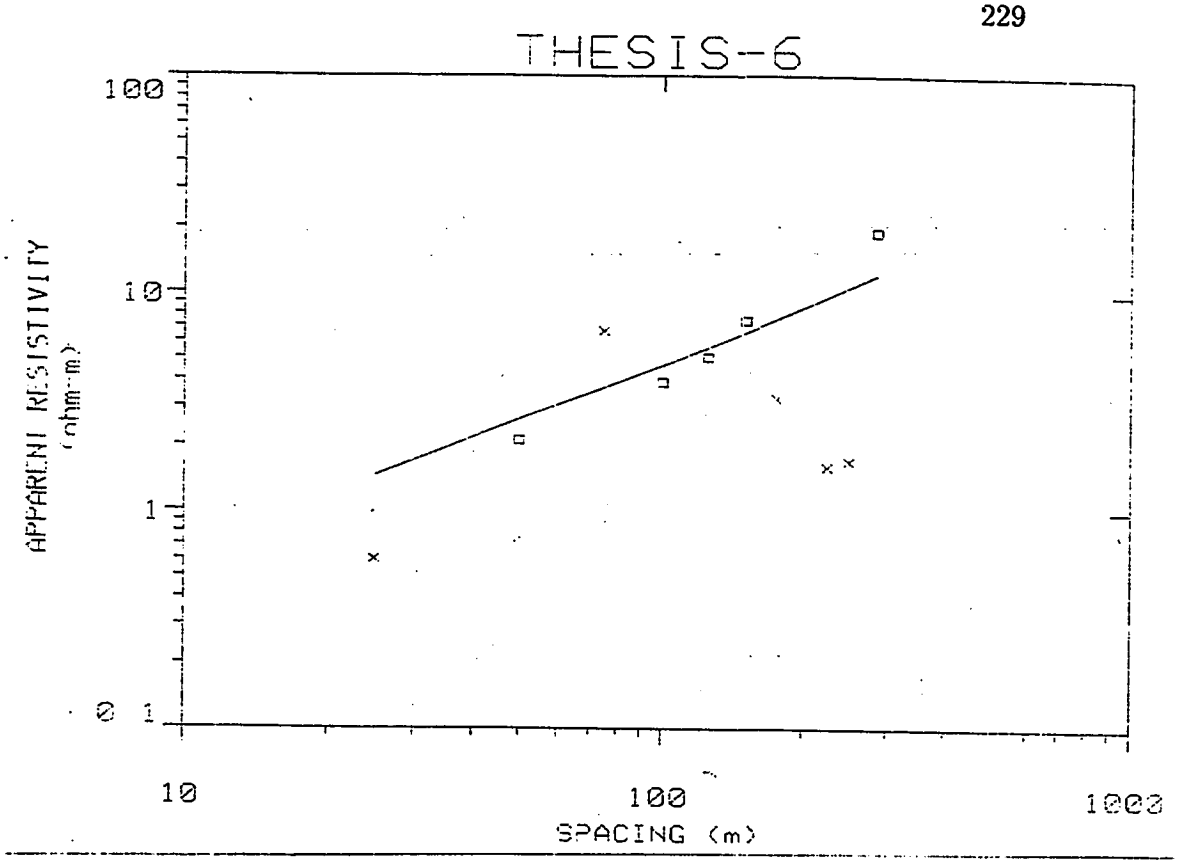
THESIS-6
100
10
1
0
1
APPARENT RESISTIVITY
(ohm-m)
10
100
1000
SPACING (m)

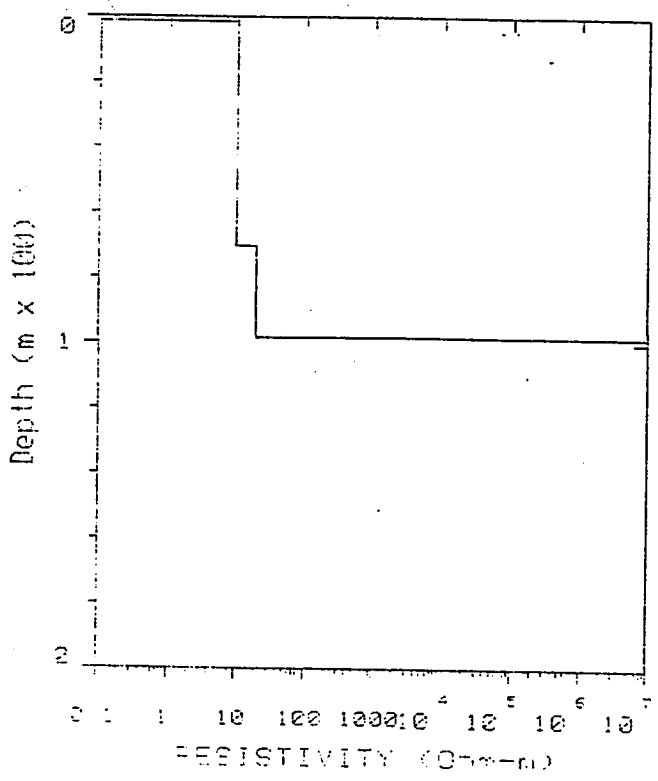
0
1
2
Depth (m x 100)
0 1 1 10 100 1000 10 10 10 10
RESISTIVITY (Ohm-m)

A.7 VES Data with Apparant Resistivity Curve and Interpreted Model (S.P-7)

DATA SET: THESIS-7

CLIENT: MS THESIS FIELD SURVEY
LOCATION: WADIAL-MIYAH
COUNTY: EASTERN PROVINCE
PROJECT: Resistivity/IP Sounding
ELEVATION: 0.00
SOUNDING COORDINATES: X: 48 19 01E Y: 26 49 34N

DATE: 17-DEC-93
SOUNDING: N7
AZIMUTH: 0.00 Deg NORT
EQUIPMENT: RESIX-IP

Schlumberger Configuration
FITTING ERROR: 16.707 PERCENT

L #	RESISTIVITY (ohm-m)	CHARGEABILITY (pfe)	THICKNESS (m)	ELEVATION (m)	CONDUCTANCE (Siemens)
				0.0	
1	1.*0		5.54	-5.54	3.26
2	5.*2		35.*2	-40.87	7.03
3	19.*8		44.*7	-85.74	2.24
4	9.69*E+09				

"*" INDICATES FIXED PARAMETER

PARAMETER BOUNDS FROM EQUIVALENCE ANALYSIS

	LAYER	MINIMUM	BEST	MAXIMUM
RHO	1	1.700	1.700	1.700
	2	5.020	5.020	5.020
	3	19.980	19.980	19.980
	4	**********	**********	**********
THICK	1	5.547	5.547	5.547
	2	35.326	35.326	35.326
	3	44.871	44.871	44.871
DEPTH	1	5.547	5.547	5.547
	2	40.874	40.874	40.874
	3	85.745	85.745	85.745

No.	Spacing (m)	PA (ohm-m) DATA	SYNTHETIC	DIFFERENCE (percent)
1	25.00	3.00	3.57	-19.01
2	50.00	5.90	5.03	14.58
3	75.00	5.60	6.57	-17.39
4	100.0	5.30	8.28	-56.41
5	225.0	21.50	17.90	16.72
6	300.0	47.80	23.85	50.08
7	375.0	32.00	29.81	6.81

PARAMETER RESOLUTION MATRIX:
"F" INDICATES FIXED PARAMETER

F 1	0.00						
F 2	0.00	0.00					
F 3	0.00	0.00	0.00				
F 4	0.00	0.00	0.00	0.00			
T 1	0.00	0.00	0.00	0.00	1.00		
F 2	0.00	0.00	0.00	0.00	0.00	0.00	
F 3	0.00	0.00	0.00	0.00	0.00	0.00	0.00
	F 1	F 2	F 3	F 4	T 1	F 2	F 3

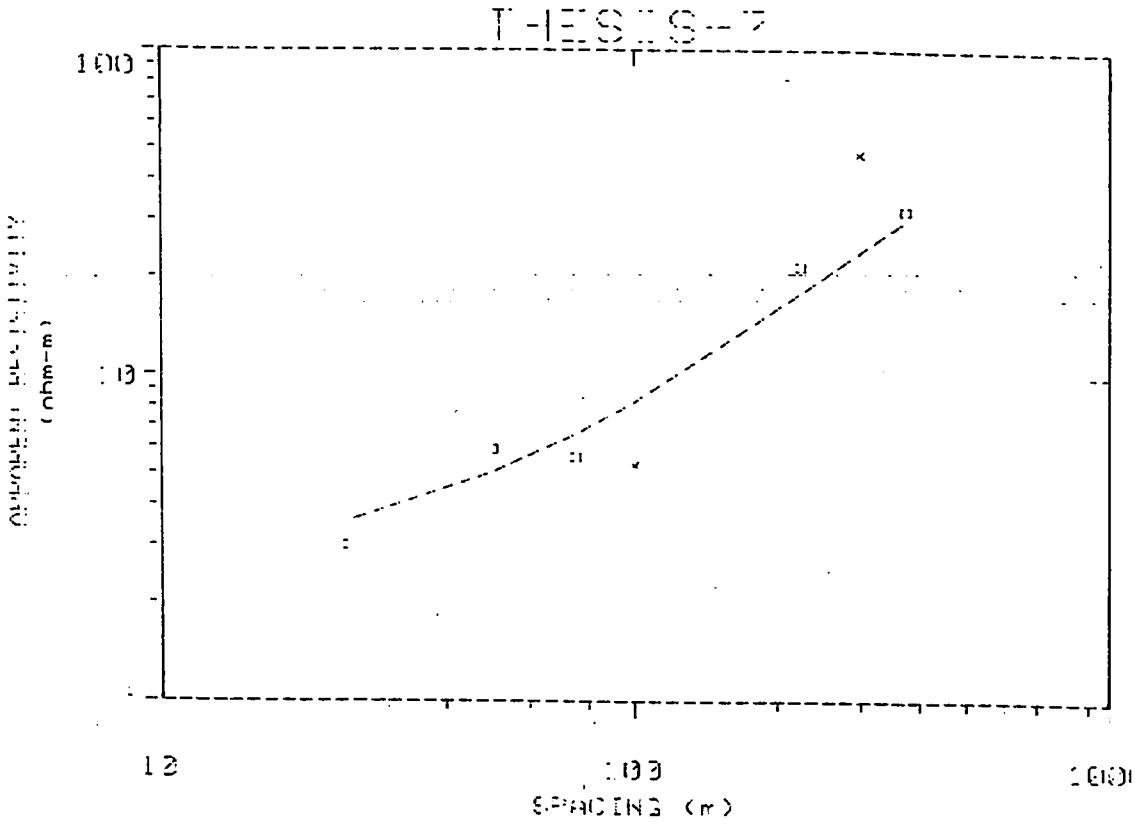
1000
10
1 0
100
1000
SPACING (m)

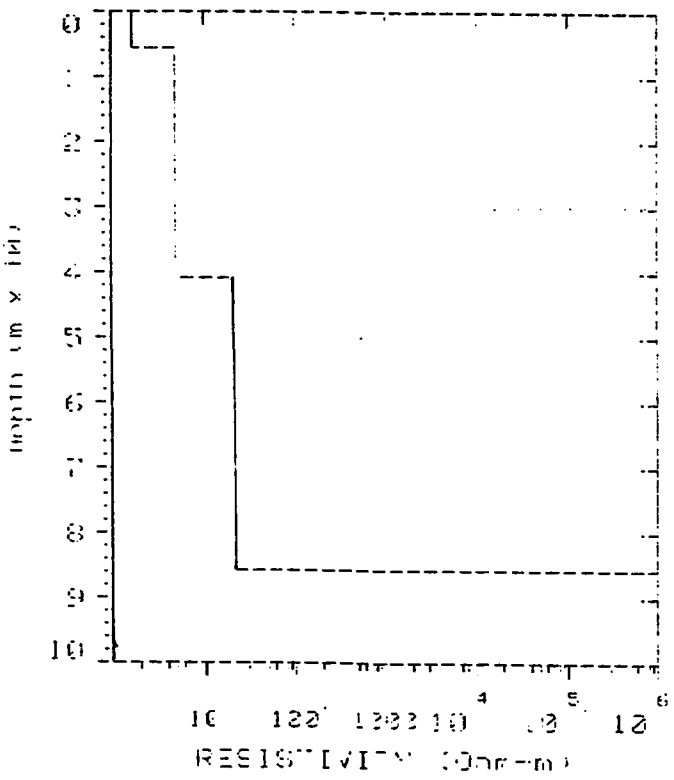
0
1
2
3
4
5
6
7
8
9
10
10
100
1000
10000
RESISTIVITY (Ohm-m)

Appendix B

Extraction Rates of Individual Wells/Wellfields

Well Fields			Recent Abstractions (in m^3/sec)																											
No	Name	Node #	1967	1968	1969	1970	1971	1972	1973	1974	1975	1976	1977	1978	1979	1980	1981	1982	1983	1984	1985	1986	1987	1988	1989	1990	1991	1992	1993	1994
1	Oulayyib	116	0 02	0 032	0 044	0 056	0.068	0 08	0 092	0 104	0.116	0 128	0 14	0.152	0 164	0 176	0.188	0.2	0 212	0.224	0.236	0.248	0 26	0 272	0 284	0 296	0.308	0.32	0 332	0 344
2	Oulayyib	120	0 04	0 05	0.06	0 07	0.08	0.09	0.1	0.11	0.12	0.13	0.14	0.15	0.16	0.17	0.18	0.19	0.2	0 21	0.24	0 25	0.26	0.27	0.28	0 29	0 3	0 31	0 32	0 33
3	Sarrar	301	0 01	0 02	0.03	0.04	0.05	0.06	0.07	0 08	0.09	0 1	0.11	0.12	0 18	0 17	0.18	0.27	0 28	0 29	0.3	0 31	0 32	0.35	0.36	0 37	0.38	0 39	0 4	0 41
4	Sarrar	493	0 05	0 06	0.07	0 08	0 09	0.1	0.11	0.12	0.13	0.14	0.15	0.16	0.18	0.2	0.21	0.22	0.23	0 24	0.26	0.27	0 28	0.29	0.3	0 31	0.32	0 33	0 34	0.35
5	Al Hinnah	506	0.71	0.72	0.73	0.74	0.75	0.76	0.77	0 78	0 79	0 8	0.81	0 82	0.85	0 86	0.87	0 9	0 91	0.92	0.93	0.94	0.95	0.98	0 99	1	1.01	1 02	1 03	1 04
6	Al-Hinnah	883	0 1	0.11	0.12	0 13	0.14	0 15	0.16	0.17	0.18	0.19	0.2	0.21	0.25	0 26	0.27	0.28	0.29	0 3	0.31	0 32	0 33	0.34	0.35	0.36	0.37	0 38	0 39	0 4
7	Manifah	1018	0.18	0 19	0.2	0.21	0.22	0.23	0.24	0.25	0.26	0.27	0 28	0.29	0.34	0.35	0.36	0.36	0.37	0.38	0 4	0.41	0.42	0.43	0.44	0.45	0.46	0.47	0.48	0.49
8	Abuhadriya	747	0.17	0 19	0.2	0.22	0.23	0.25	0.26	0 28	0.29	0.31	0.32	0.34	0.35	0 37	0 38	0 4	0.41	0.43	0 44	0 48	0.47	0.5	0 51	0.53	0.54	0 56	0 57	0 59
9	Abuhadriya	912	0 12	0 13	0.14	0.15	0.16	0.17	0.18	0 19	0.2	0.21	0 22	0.23	0 27	0 28	0.29	0 29	0 3	0.31	0.32	0 33	0.34	0 35	0 36	0 37	0.38	0 39	0 4	0 41
10	Abuhadriya	913	0.09	0.1	0.11	0.12	0.14	0.15	0.16	0.17	0.18	0 2	0 21	0.22	0.23	0.24	0.26	0.27	0.28	0 29	0.32	0.32	0 33	0.38	0 39	0 4	0 38	0 39	0 4	0 41
11	Abuhadriya	914	0.02	0 04	0.05	0.07	0 09	0.11	0.12	0.14	0.16	0.17	0 19	0.21	0.22	0 24	0.26	0.28	0.29	0 31	0.33	0.34	0.36	0.38	0.39	0.41	0.43	0.45	0.46	0.48
12	Abuhadriya	932	0.18	0.19	0.2	0 21	0.22	0 23	0.24	0.25	0.26	0.27	0 28	0.29	0 3	0.31	0.32	0 35	0.36	0.37	0 4	0.41	0 42	0.44	0 45	0.48	0.47	0.48	0.49	0 5
13	Abuhadriya	933	0.21	0 22	0.23	0.25	0 26	0 27	0 28	0 29	0 31	0 32	0.33	0 33	0 36	0.37	0 38	0.39	0 4	0.41	0.43	0.44	0.46	0.46	0.47	0.49	0 5	0 51	0 52	0 53
14	Abuhadriya	943	0.12	0.15	0.17	0 2	0.22	0.25	0.27	0 3	0.32	0.35	0.37	0 4	0.42	0.45	0.47	0 5	0 52	0.55	0.57	0 6	0 62	0.67	0.69	0 72	0.74	0 77	0 79	0 82
15	Abuhadriya	746	0 97	0.98	0.99	1	1.01	1.02	1.03	1.04	1.05	1.06	1.07	1.08	1.09	1.1	1 11	1 14	1 15	1.16	1 2	1.21	1.22	1.23	1.24	1.25	1.26	1 27	1.28	1 29
16	Abuhadriya	902	0.18	0.19	0.21	0.22	0.24	0.25	0.27	0.28	0.3	0.31	0 33	0.36	0.38	0 39	0.41	0.42	0.44	0.45	0.47	0.48	0.5	0.53	0.55	0.58	0.58	0.59	0 61	0 62
17	Abuhadriya	1071	0.12	0.13	0.14	0 15	0.16	0.17	0 18	0.19	0.2	0.21	0.22	0.23	0.24	0.25	0.26	0.27	0.28	0.29	0.3	0.31	0.32	0.33	0.34	0 35	0.36	0.37	0 38	0 39
18	Abuhadriya	1043	0 12	0.13	0.14	0.15	0.16	0.17	0.18	0.19	0.2	0.21	0.22	0.24	0.25	0.26	0.27	0.28	0 29	0 3	0.33	0.34	0 35	0 36	0.37	0 38	0.39	0 4	0 41	0 42
19	Manifah	1081	0 12	0 13	0.14	0.15	0.16	0.17	0.18	0 19	0 2	0.21	0 22	0.23	0.25	0.26	0.27	0 29	0.3	0 31	0.32	0.33	0.34	0 35	0 36	0.37	0 38	0 39	0 4	0 41
20	Manifah	1087	0 22	0 23	0.24	0.25	0.26	0.27	0 28	0.28	0 3	0.31	0.32	0.33	0.34	0.35	0.36	0.37	0 38	0 39	0.4	0.41	0.42	0.45	0.46	0.47	0.48	0.49	0 5	0 51
21	Manifah	1008	0.2	0.21	0.22	0.23	0.24	0.25	0.26	0 27	0.28	0.29	0 3	0.31	0.33	0 34	0 35	0 36	0.37	0.38	0.39	0 4	0.41	0.42	0.43	0.44	0.45	0.46	0.47	0.48
22	Manifah	1160	0.2	0 21	0.22	0.23	0.24	0.25	0.26	0.27	0 28	0.29	0 3	0.31	0.32	0 33	0.34	0 35	0.36	0.37	0 4	0.41	0.42	0.43	0.44	0.45	0.46	0.47	0.48	0.49
23	Manifah	1079	0 22	0 23	0.24	0 25	0.26	0.27	0.28	0 29	0 3	0 31	0.32	0.33	0.36	0 37	0.38	0 39	0 4	0.41	0.42	0.43	0.44	0.45	0.46	0.47	0.48	0.49	0 5	0 51
24	Abuhadriya	770	0 12	0 14	0.16	0.18	0.2	0.22	0.24	0 26	0.28	0 3	0 32	0.34	0.36	0.38	0 4	0.45	0.47	0.49	0.51	0.53	0.55	0.57	0.59	0.61	0.63	0 65	0.67	0.69
	Total in m^3/sec		4 49	4 782	5.054	5 356	5.648	5.94	6.212	6 504	6.796	7.088	7.37	7.682	8.184	8 476	8.768	9 22	9 492	9.784	10 23	10.5	10 78	11.23	11.5	11 81	12.08	12 35	12 62	12 91
	Total in Mm^3/Year		141.7	150 9	159.5	169	178.2	187 5	196	205 3	214.5	223 7	232 6	242 4	258.3	267.5	276.7	291	299 5	308 0	322 7	331.3	340.2	354.5	363	372 6	380.5	389.7	398 3	407 5

B-1 : Extraction Rates in Khobar Aquifer for the period (1967-1994).

Recent Extractions (m^3/sec)

SR	Name	NODE WELL #	1967	1968	1969	1970	1971	1972	1973	1974	1975	1976	1977	1978	1979	1980	1981	1982	1983	1984	1985	1986	1987	1988	1989	1990	1991	1992	1993	1994
1		1135 S-414	0.02	0.02	0.02	0.02	0.02	0.02	0.02	0.02	0.02	0.02	0.02	0.02	0.04	0.04	0.05	0.06	0.07	0.08	0.08	0.08	0.08	0.08	0.08	0.08	0.08	0.08	0.08	0.08
2	Sarrar	298 WA-242	0.041	0.046	0.051	0.056	0.061	0.066	0.071	0.076	0.081	0.086	0.091	0.096	0.101	0.106	0.111	0.116	0.121	0.126	0.131	0.136	0.141	0.146	0.151	0.156	0.161	0.16	0.16	0.165
3	Sarrar	301 MI-3A	0.08	0.083	0.086	0.089	0.071	0.074	0.077	0.08	0.082	0.085	0.089	0.091	0.094	0.093	0.099	0.102	0.105	0.102	0.4	0.403	0.406	0.409	0.412	0.42	0.423	0.4	0.4	0.403
4	East of Sarrar	493 MI-25A	0.01	0.01	0.01	0.011	0.01	0.01	0.01	0.01	0.01	0.01	0.01	0.01	0.01	0.02	0.02	0.02	0.02	0.02	0.02	0.005	0.005	0.005	0.005	0.005	0.006	0.006	0.006	0.006
5	Qulayyt	95 B17	0.01	0.011	0.012	0.013	0.01	0.011	0.012	0.013	0.014	0.007	0.005	0.009	0.02	0.021	0.011	0.012	0.03	0.031	0.032	0.015	0.016	0.017	0.018	0.019	0.019	0.02	0.02	0.021
6		747 MI-35-A	0.007	0.008	0.013	0.018	0.023	0.028	0.033	0.039	0.043	0.048	0.053	0.058	0.063	0.068	0.073	0.078	0.083	0.088	0.093	0.098	0.103	0.108	0.113	0.118	0.123	0.128	0.133	0.136
7	Abuhadriya	902	0.01	0.012	0.014	0.016	0.018	0.02	0.022	0.024	0.026	0.028	0.03	0.032	0.034	0.036	0.038	0.04	0.04	0.042	0.044	0.046	0.048	0.05	0.052	0.054	0.056	0.058	0.05	0.052
8	Abuhadriya	1087 S-407	0.47	0.483	0.509	0.524	0.542	0.56	0.578	0.596	0.614	0.632	0.65	0.668	0.686	0.704	0.722	0.74	0.758	0.776	0.704	0.812	0.83	0.848	0.866	0.884	0.902	0.9	0.9	0.918
9	Abuhadriya	912 AHW-B08	0.042	0.057	0.072	0.087	0.102	0.117	0.132	0.147	0.162	0.177	0.192	0.207	0.222	0.237	0.252	0.267	0.282	0.297	0.312	0.327	0.342	0.357	0.372	0.387	0.402	0.41	0.422	0.447
10	Abuhadriya	933	0.201	0.211	0.221	0.231	0.241	0.251	0.261	0.271	0.281	0.291	0.301	0.311	0.321	0.331	0.341	0.351	0.361	0.371	0.381	0.391	0.401	0.411	0.421	0.431	0.441	0.451	0.45	0.46
11	Abuhadriya	963 B-11	0.051	0.061	0.071	0.091	0.091	0.101	0.111	0.121	0.131	0.141	0.151	0.161	0.171	0.181	0.191	0.201	0.211	0.221	0.231	0.241	0.251	0.261	0.271	0.281	0.291	0.301	0.311	0.321
12	Abuhadriya	944 B-9	0.029	0.039	0.049	0.059	0.068	0.078	0.089	0.099	0.109	0.118	0.128	0.138	0.148	0.158	0.168	0.178	0.188	0.198	0.208	0.218	0.228	0.238	0.248	0.259	0.269	0.278	0.288	0.299
13	Abuhadriya	842 S-222	0.048	0.058	0.068	0.078	0.088	0.098	0.108	0.118	0.129	0.138	0.149	0.158	0.168	0.179	0.188	0.199	0.208	0.218	0.228	0.238	0.248	0.258	0.268	0.278	0.288	0.299	0.308	0.318
14	Abuhadriya	1047 WA-504	0	0.001	0.002	0.003	0.004	0.005	0.006	0.007	0.008	0.009	0.01	0.011	0.012	0.013	0.014	0.015	0.016	0.017	0.018	0.019	0.02	0.021	0.022	0.023	0.024	0.025	0.026	0.027
15	Abuhadriya	932 B-18	0.321	0.331	0.341	0.351	0.361	0.371	0.381	0.391	0.401	0.411	0.421	0.431	0.441	0.451	0.461	0.471	0.481	0.491	0.501	0.511	0.521	0.531	0.541	0.551	0.561	0.571	0.581	0.591
16		1071 S-505	0.001	0.001	0.001	0.001	0.001	0.001	0.002	0.002	0.002	0.002	0.002	0.002	0.002	0.002	0.002	0.002	0.003	0.003	0.003	0.003	0.003	0.003	0.003	0.003	0.003	0.003	0.004	0.004
			1.518	1.416	1.518	1.615	1.711	1.811	1.912	2.012	2.111	2.207	2.303	2.403	2.533	2.644	2.751	2.851	2.987	3.087	3.456	3.523	3.623	3.723	3.823	3.928	4.028	4.068	4.119	4.219
			41.53	44.69	47.84	50.97	54	57.15	60.34	63.49	66.62	69.52	72.68	75.83	79.94	83.44	86.81	89.97	93.83	96.79	109.1	111.2	114.3	117.5	120.6	124	127.1	129.9	133	133.1

B-2 : Extraction Rates in Alat Aquifer for the period (1967-1994).

Well Fields No	Name	Node	Well #	Recent Extractions (Mm^3/sec) 1967	1968	1969	1970	1971	1972	1973	1974	1975	1976	1977	1978	1979	1980	1981	1982	1983	1984	1985	1986	1987	1988	1989	1990	1991	1992	1993	1994
1		176	WA-347	0.09	0.091	0.092	0.093	0.094	0.095	0.096	0.097	0.098	0.099	0.1	0.101	0.102	0.103	0.104	0.105	0.106	0.107	0.108	0.109	0.11	0.111	0.112	0.113	0.114	0.115	0.116	0.117
2	North of Hanidh	188	WA-323	0.0306	0.0316	0.0326	0.0336	0.0346	0.036	0.037	0.038	0.039	0.04	0.041	0.042	0.043	0.044	0.049	0.05	0.052	0.06	0.061	0.062	0.063	0.064	0.065	0.066	0.067	0.068	0.069	0.07
3	North of Hanidh	219	WA-327	0.0403	0.0404	0.0405	0.0406	0.0407	0.041	0.041	0.041	0.041	0.041	0.041	0.041	0.042	0.042	0.043	0.043	0.046	0.046	0.046	0.046	0.046	0.046	0.048	0.048	0.048	0.048	0.049	0.049
4	North of Hanidh	284	WA-313	0.028	0.0284	0.0288	0.0292	0.0296	0.03	0.03	0.031	0.031	0.032	0.032	0.032	0.034	0.034	0.035	0.036	0.036	0.037	0.037	0.038	0.038	0.038	0.039	0.039	0.04	0.04	0.04	0.041
5	Sarrar	301	MW-1 N	0.039	0.04	0.041	0.042	0.043	0.044	0.045	0.046	0.047	0.048	0.049	0.05	0.051	0.052	0.053	0.054	0.06	0.064	0.065	0.066	0.067	0.068	0.069	0.07	0.071	0.072	0.073	0.074
6	Al-Wannan	320	WA-337	0.0396	0.0406	0.0416	0.0426	0.0436	0.045	0.046	0.047	0.048	0.049	0.05	0.051	0.06	0.061	0.065	0.068	0.069	0.07	0.071	0.072	0.073	0.078	0.079	0.08	0.081	0.082	0.083	0.084
7	Sarrar	322	WA-329	0.01	0.011	0.012	0.013	0.014	0.015	0.016	0.017	0.018	0.019	0.02	0.021	0.022	0.023	0.024	0.025	0.026	0.027	0.028	0.029	0.03	0.031	0.032	0.033	0.034	0.035	0.036	0.037
8	Sarrar	370		0.003	0.005	0.007	0.009	0.011	0.013	0.015	0.017	0.019	0.021	0.023	0.025	0.028	0.03	0.035	0.038	0.04	0.044	0.046	0.048	0.05	0.06	0.062	0.064	0.066	0.068	0.07	0.072
9	North of Hanidh	382	WA-331	0.004	0.005	0.006	0.007	0.008	0.009	0.01	0.011	0.012	0.013	0.014	0.015	0.016	0.017	0.018	0.019	0.02	0.021	0.022	0.023	0.024	0.026	0.029	0.03	0.031	0.032	0.033	0.034
10	Sarrar	398	WA-251	0.04	0.046	0.052	0.058	0.064	0.07	0.076	0.082	0.088	0.094	0.1	0.106	0.114	0.12	0.13	0.15	0.16	0.17	0.178	0.182	0.188	0.194	0.2	0.206	0.212	0.218	0.224	0.23
11	Al-Wannan	417	WA-240	0.00072	0.00132	0.00232	0.0033	0.00432	0.005	0.006	0.007	0.008	0.009	0.01	0.011	0.012	0.013	0.014	0.017	0.018	0.019	0.02	0.021	0.022	0.023	0.024	0.025	0.026	0.027	0.028	0.029
12	Ghanwa	547	WA-293	0.042	0.048	0.056	0.063	0.07	0.077	0.084	0.091	0.098	0.105	0.112	0.119	0.126	0.133	0.14	0.147	0.154	0.161	0.168	0.175	0.182	0.189	0.196	0.203	0.21	0.217	0.224	0.231
13	Ghanwa	551	WA-279	0.0528	0.0608	0.0688	0.0768	0.0848	0.093	0.101	0.109	0.117	0.125	0.133	0.141	0.15	0.158	0.17	0.178	0.188	0.196	0.204	0.212	0.22	0.24	0.248	0.256	0.264	0.272	0.28	0.288
14	East of Hanidh	580		0.0182	0.0222	0.0262	0.0302	0.0342	0.038	0.042	0.046	0.05	0.054	0.058	0.062	0.066	0.07	0.074	0.078	0.082	0.086	0.092	0.098	0.1	0.104	0.108	0.112	0.116	0.12	0.124	0.128
15	Al Hinnah	677	WA-496	0.009	0.01	0.011	0.012	0.013	0.014	0.015	0.016	0.017	0.018	0.019	0.02	0.023	0.024	0.028	0.03	0.031	0.032	0.033	0.034	0.035	0.036	0.037	0.038	0.039	0.04	0.041	0.042
16		702	WA-277	0.006	0.008	0.01	0.012	0.014	0.016	0.018	0.02	0.022	0.024	0.026	0.028	0.03	0.032	0.038	0.04	0.047	0.049	0.051	0.053	0.055	0.08	0.062	0.064	0.066	0.068	0.07	0.072
17	Abuhadriya	745	WA-344	0.018	0.019	0.02	0.021	0.022	0.023	0.024	0.025	0.026	0.027	0.028	0.029	0.03	0.031	0.032	0.033	0.034	0.038	0.039	0.04	0.041	0.045	0.046	0.047	0.048	0.049	0.05	0.051
18		789	WA-314	0.0003	0.0013	0.0023	0.0033	0.0043	0.005	0.006	0.007	0.008	0.009	0.01	0.011	0.012	0.013	0.015	0.016	0.017	0.018	0.019	0.02	0.021	0.022	0.023	0.024	0.025	0.026	0.027	0.028
19		853	WA-310	0.0001	0.0011	0.0021	0.0031	0.0041	0.005	0.006	0.007	0.008	0.009	0.01	0.011	0.012	0.013	0.014	0.015	0.017	0.018	0.019	0.02	0.021	0.022	0.023	0.024	0.025	0.026	0.027	0.028
20	Abuhadriya	967	WA-315	0.00005	0.00205	0.00405	0.0061	0.00805	0.01	0.012	0.014	0.016	0.018	0.02	0.022	0.024	0.026	0.028	0.03	0.032	0.034	0.036	0.038	0.04	0.045	0.047	0.049	0.051	0.053	0.055	0.057
	Total in m^3/sec			0.47127	0.51377	0.55627	0.5988	0.64127	0.684	0.726	0.769	0.811	0.854	0.896	0.939	0.997	1.04	1.108	1.172	1.235	1.298	1.341	1.383	1.426	1.508	1.548	1.591	1.633	1.676	1.718	1.761
	Total in Mm^3/year			14.8722	16.2133	17.5545	18.896	20.2368	21.58	22.92	24.26	25.6	26.94	28.28	29.63	31.47	32.81	34.97	36.98	38.97	40.97	42.31	43.65	44.99	47.52	48.86	50.2	51.54	52.88	54.22	55.56

B-3 : Extraction Rates in Neogene Aquifer for the period (1967-1994).

Well Fields			Projected Extractions in m^3/sec														
No.	Name	Node #	1995	1996	1997	1998	1999	2000	2001	2002	2003	2004	2005	2006	2007	2008	2009	2010
1	Qulayyib	116	0.356	0.368	0.38	0.392	0.404	0.416	0.428	0.44	0.452	0.464	0.476	0.488	0.5	0.512	0.524	0.536
2	Qulayyib	120	0.34	0.35	0.36	0.37	0.38	0.39	0.4	0.41	0.42	0.43	0.44	0.45	0.46	0.47	0.48	0.49
3	Sarrar	301	0.42	0.43	0.44	0.45	0.46	0.47	0.48	0.49	0.5	0.51	0.52	0.53	0.54	0.55	0.56	0.57
4	Sarrar	493	0.36	0.37	0.38	0.39	0.4	0.41	0.42	0.43	0.44	0.45	0.46	0.47	0.48	0.49	0.5	0.51
5	Al-Hinnah	506	1.05	1.06	1.07	1.08	1.09	1.1	1.11	1.12	1.13	1.14	1.15	1.16	1.17	1.18	1.19	1.2
6	Al-Hinnah	883	0.41	0.42	0.43	0.44	0.45	0.46	0.47	0.48	0.49	0.5	0.51	0.52	0.53	0.54	0.55	0.56
7	Manifah	1018	0.5	0.51	0.52	0.53	0.54	0.55	0.56	0.57	0.58	0.59	0.6	0.61	0.62	0.63	0.64	0.65
8	Abuhadriya	747	0.6	0.62	0.63	0.65	0.66	0.68	0.69	0.71	0.72	0.74	0.75	0.77	0.78	0.8	0.81	0.82
9	Abuhadriya	912	0.42	0.43	0.44	0.45	0.46	0.47	0.48	0.49	0.5	0.51	0.52	0.53	0.54	0.55	0.56	0.57
10	Abuhadriya	913	0.42	0.44	0.45	0.46	0.47	0.48	0.5	0.51	0.52	0.53	0.54	0.56	0.57	0.58	0.59	0.6
11	Abuhadriya	914	0.5	0.51	0.53	0.55	0.56	0.58	0.6	0.62	0.61	0.63	0.65	0.66	0.68	0.7	0.71	0.73
12	Abuhadriya	932	0.51	0.52	0.53	0.54	0.55	0.56	0.57	0.58	0.59	0.6	0.61	0.62	0.63	0.64	0.65	0.66
13	Abuhadriya	933	0.54	0.55	0.56	0.57	0.58	0.59	0.6	0.61	0.62	0.63	0.64	0.65	0.66	0.67	0.68	0.69
14	Abuhadriya	943	0.84	0.87	0.89	0.92	0.94	0.97	0.99	1.02	1.04	1.07	1.09	1.12	1.14	1.17	1.19	1.2
15	Abuhadriya	746	1.3	1.31	1.32	1.33	1.34	1.35	1.36	1.37	1.38	1.39	1.4	1.41	1.42	1.43	1.44	1.45
16	Abuhadriya	902	0.64	0.65	0.67	0.68	0.7	0.71	0.73	0.74	0.76	0.77	0.79	0.8	0.82	0.83	0.85	0.82
17	Abuhadriya	1071	0.4	0.41	0.42	0.43	0.44	0.45	0.46	0.47	0.48	0.49	0.5	0.51	0.52	0.53	0.54	0.55
18	Abuhadriya	1043	0.43	0.44	0.45	0.46	0.47	0.48	0.49	0.5	0.51	0.52	0.53	0.54	0.55	0.56	0.57	0.58
19	Manifah	1081	0.42	0.43	0.44	0.45	0.46	0.47	0.48	0.49	0.5	0.51	0.52	0.53	0.54	0.55	0.56	0.57
20	Manifah	1087	0.52	0.53	0.54	0.55	0.56	0.57	0.58	0.59	0.6	0.61	0.62	0.63	0.64	0.65	0.66	0.67
21	Manifah	1008	0.49	0.5	0.51	0.52	0.53	0.54	0.55	0.56	0.57	0.58	0.59	0.6	0.61	0.62	0.63	0.64
22	Manifah	1160	0.5	0.51	0.52	0.53	0.54	0.55	0.56	0.57	0.58	0.59	0.6	0.61	0.62	0.63	0.64	0.65
23	Manifah	1079	0.52	0.53	0.54	0.55	0.56	0.57	0.58	0.59	0.6	0.61	0.62	0.63	0.64	0.65	0.66	0.67
24	Abuhadriya	778	0.71	0.73	0.75	0.77	0.79	0.81	0.83	0.85	0.87	0.89	0.91	0.93	0.95	0.97	0.99	1.01
Total in m^3/sec			13.2	13.49	13.77	14.06	14.33	14.63	14.92	15.21	15.46	15.75	16.04	16.33	16.61	16.9	17.17	17.4
Total in Mm^3/Year			416.4	425.6	434.5	443.8	452.3	461.6	470.8	480	487.9	497.2	506.1	515.3	524.2	533.4	542	549

B-4 : Extraction Rates in Khobar Aquifer - Alternative I (1995-2010).

SR. N	Name	NODES	WELL #	Projected Extraction 1995	1996	1997	1998	1999	2000	2001	2002	2003	2004	2005	2006	2007	2008	2009	2010
1		1135	S-414	0.05	0.05	0.05	0.05	0.05	0.05	0.05	0.05	0.05	0.05	0.05	0.05	0.05	0.05	0.05	0.05
2	Sarrar	396	WA-242	0.17	0.175	0.18	0.185	0.19	0.195	0.2	0.205	0.21	0.215	0.22	0.225	0.23	0.235	0.24	0.245
3	Sarrar	301	MI-3A	0.406	0.409	0.412	0.415	0.418	0.421	0.424	0.427	0.43	0.433	0.436	0.439	0.442	0.445	0.448	0.451
4	East of Sarrar	493	MI-25A	0.006	0.007	0.007	0.007	0.007	0.007	0.008	0.008	0.008	0.008	0.008	0.009	0.009	0.009	0.009	0.009
5	Qulayyib	95	B17	0.022	0.023	0.024	0.025	0.026	0.027	0.027	0.028	0.029	0.03	0.031	0.031	0.032	0.033	0.034	0.035
6		747	Hu-35-A	0.143	0.148	0.153	0.158	0.163	0.168	0.173	0.178	0.183	0.188	0.193	0.198	0.203	0.208	0.213	0.218
7	Abuhadriya	902		0.054	0.056	0.058	0.06	0.062	0.064	0.066	0.068	0.07	0.072	0.074	0.076	0.078	0.08	0.082	0.084
8	Abuhadriya	1087	S-407	0.936	0.954	0.972	0.99	1.008	1.026	1.044	1.062	1.08	1.098	1.116	1.134	1.152	1.17	1.188	1.206
9	Abuhadriya	912	AHW-B08	0.462	0.477	0.492	0.507	0.522	0.537	0.552	0.567	0.582	0.597	0.612	0.627	0.642	0.657	0.672	0.687
10	Abuhadriya	933		0.47	0.48	0.49	0.5	0.51	0.52	0.53	0.54	0.55	0.56	0.57	0.58	0.59	0.6	0.61	0.62
11	Abuhadriya	963	B-11	0.331	0.341	0.351	0.361	0.371	0.381	0.391	0.401	0.411	0.421	0.431	0.441	0.451	0.461	0.471	0.481
12	Abuhadriya	944	B-9	0.308	0.318	0.328	0.338	0.348	0.358	0.368	0.378	0.388	0.398	0.408	0.418	0.428	0.438	0.448	0.458
13	Abuhadriya	848	S-222	0.328	0.338	0.348	0.358	0.368	0.378	0.388	0.398	0.408	0.418	0.428	0.438	0.448	0.458	0.468	0.478
14	Abuhadriya	1047	WA-504	0.028	0.029	0.03	0.031	0.032	0.033	0.034	0.035	0.036	0.037	0.038	0.039	0.04	0.041	0.042	0.043
15	Abuhadriya	932	B-18	0.601	0.611	0.621	0.631	0.641	0.651	0.661	0.671	0.681	0.691	0.701	0.711	0.721	0.731	0.741	0.751
16		1071	S-505	0.004	0.004	0.004	0.004	0.004	0.004	0.004	0.004	0.005	0.005	0.005	0.005	0.005	0.005	0.005	0.005
				4.319	4.42	4.52	4.62	4.72	4.82	4.92	5.02	5.121	5.221	5.321	5.421	5.521	5.621	5.721	5.821
				136.3	139.48	142.64	145.8	148.95	152.11	155.26	158.42	161.61	164.76	167.92	171.07	174.23	177.39	180.54	183.7

B-5 : Extraction Rates in Alat Aquifer - Alternative I (1995-2010).

No.	Well Fields Name	Node	Well #	Projected Extraction Rates (m^3/sec) 1995	1996	1997	1998	1999	2000	2001	2002	2003	2004	2005	2006	2007	2008	2009	2010
1		176	WA-347	0.118	0.119	0.12	0.121	0.122	0.123	0.124	0.125	0.126	0.127	0.128	0.129	0.13	0.131	0.132	0.133
2	North of Hanidh	188	WA-323	0.071	0.072	0.073	0.074	0.075	0.076	0.077	0.078	0.079	0.08	0.081	0.082	0.083	0.084	0.085	0.086
3	North of Hanidh	219	WA-327	0.049	0.049	0.049	0.049	0.049	0.049	0.049	0.049	0.05	0.05	0.05	0.05	0.05	0.05	0.05	0.05
4	North of Hanidh	284	WA-313	0.041	0.042	0.042	0.042	0.043	0.043	0.044	0.044	0.044	0.045	0.045	0.046	0.046	0.046	0.047	0.047
5	Sarrar	301	MI-4-N	0.075	0.076	0.077	0.078	0.079	0.08	0.081	0.082	0.083	0.084	0.085	0.086	0.087	0.088	0.089	0.09
6	Al-Wannan	320	WA-337	0.085	0.086	0.087	0.088	0.089	0.09	0.091	0.092	0.093	0.094	0.095	0.096	0.097	0.098	0.099	0.1
7	Sarrar	322	WA-329	0.038	0.039	0.04	0.041	0.042	0.043	0.044	0.045	0.046	0.047	0.048	0.049	0.05	0.051	0.052	0.053
8	Sarrar	370		0.074	0.076	0.078	0.08	0.082	0.084	0.086	0.088	0.09	0.092	0.094	0.096	0.098	0.1	0.102	0.104
9	North of Hanidh	382	WA-391	0.035	0.036	0.037	0.038	0.039	0.04	0.041	0.042	0.043	0.044	0.045	0.046	0.047	0.048	0.049	0.05
10	Sarrar	398	WA-251	0.236	0.242	0.248	0.254	0.26	0.266	0.272	0.278	0.284	0.29	0.296	0.302	0.308	0.314	0.32	0.326
11	Al-Wannan	417	WA-240	0.03	0.031	0.032	0.033	0.034	0.035	0.036	0.037	0.038	0.039	0.04	0.041	0.042	0.043	0.044	0.045
12	Ghanwa	547	WA-293	0.238	0.245	0.252	0.259	0.266	0.273	0.28	0.287	0.294	0.301	0.308	0.315	0.322	0.329	0.336	0.343
13	Ghanwa	551	WA-233	0.296	0.304	0.312	0.32	0.328	0.336	0.344	0.352	0.36	0.368	0.376	0.384	0.392	0.4	0.408	0.416
14	East of Hanidh	589		0.132	0.136	0.14	0.144	0.148	0.152	0.156	0.16	0.164	0.168	0.172	0.176	0.18	0.184	0.188	0.192
15	Al-Hinnah	677	WA-496	0.043	0.044	0.045	0.046	0.047	0.048	0.049	0.05	0.051	0.052	0.053	0.054	0.055	0.056	0.057	0.058
16		702	WA-277	0.074	0.076	0.078	0.08	0.082	0.084	0.086	0.088	0.09	0.092	0.094	0.096	0.098	0.1	0.102	0.104
17	Abuhadriya	745	HU-34-N	0.052	0.053	0.054	0.055	0.056	0.057	0.058	0.059	0.06	0.061	0.062	0.063	0.064	0.065	0.066	0.067
18		789	WA-314	0.029	0.03	0.031	0.032	0.033	0.034	0.035	0.036	0.037	0.038	0.039	0.04	0.041	0.042	0.043	0.044
19		953	WA-310	0.029	0.03	0.031	0.032	0.033	0.034	0.035	0.036	0.037	0.038	0.039	0.04	0.041	0.042	0.043	0.044
20	Abuhadriya	967	WA-315	0.059	0.061	0.063	0.065	0.067	0.069	0.071	0.073	0.075	0.077	0.079	0.081	0.083	0.085	0.087	0.089
	'Total in m^3/sec			1.803	1.846	1.888	1.931	1.973	2.016	2.058	2.101	2.143	2.186	2.228	2.271	2.313	2.356	2.398	2.441
	Total in Mm^3/year			56.9	58.25	59.59	60.93	62.27	63.61	64.95	66.29	67.63	68.98	70.32	71.66	73	74.34	75.68	77.02

B-6 : Extraction Rates in Neogene Aquifer - Alternative I (1995-2010).

	Well Fields					Projected Extractions in m^3/sec												
No.	Name	Node #	1995	1996	1997	1998	1999	2000	2001	2002	2003	2004	2005	2006	2007	2008	2009	2010
1	Qulayyib	116	0.175	0.177	0.179	0.181	0.183	0.185	0.187	0.189	0.191	0.193	0.202	0.211	0.22	0.229	0.238	0.247
2	Qulayyib	120	0.17	0.177	0.179	0.181	0.183	0.185	0.187	0.189	0.191	0.193	0.199	0.205	0.211	0.217	0.223	0.229
3	Sarrar	301	0.21	0.213	0.215	0.217	0.219	0.221	0.223	0.225	0.227	0.229	0.238	0.247	0.256	0.265	0.274	0.283
4	Sarrar	493	0.18	0.182	0.184	0.186	0.188	0.19	0.192	0.194	0.196	0.198	0.207	0.216	0.225	0.234	0.243	0.252
5	Al-Hinnah	506	0.51	0.512	0.514	0.516	0.518	0.52	0.522	0.524	0.526	0.528	0.537	0.546	0.555	0.564	0.573	0.582
6	Al-Hinnah	883	0.22	0.222	0.224	0.226	0.228	0.23	0.232	0.234	0.236	0.246	0.256	0.266	0.276	0.286	0.296	0.306
7	Manifah	1018	0.5	0.506	0.508	0.51	0.512	0.514	0.516	0.518	0.52	0.529	0.538	0.547	0.556	0.565	0.574	0.583
8	Abuhadriya	747	0.35	0.352	0.354	0.356	0.358	0.36	0.362	0.364	0.366	0.368	0.376	0.378	0.38	0.382	0.384	0.386
9	Abuhadriya	912	0.21	0.213	0.215	0.217	0.219	0.221	0.223	0.225	0.227	0.236	0.245	0.254	0.263	0.272	0.281	0.29
10	Abuhadriya	913	0.21	0.212	0.214	0.216	0.218	0.22	0.222	0.224	0.226	0.233	0.24	0.247	0.254	0.261	0.268	0.275
11	Abuhadriya	914	0.3	0.31	0.312	0.314	0.316	0.318	0.32	0.322	0.324	0.332	0.34	0.348	0.356	0.364	0.372	0.38
12	Abuhadriya	932	0.24	0.252	0.254	0.256	0.258	0.261	0.264	0.267	0.27	0.28	0.29	0.3	0.31	0.32	0.33	0.34
13	Abuhadriya	933	0.27	0.335	0.337	0.339	0.341	0.343	0.345	0.347	0.349	0.358	0.367	0.376	0.385	0.394	0.403	0.412
14	Abuhadriya	943	0.42	0.424	0.426	0.428	0.43	0.434	0.438	0.442	0.446	0.456	0.466	0.476	0.486	0.496	0.506	0.516
15	Abuhadriya	746	0.47	0.473	0.475	0.477	0.479	0.484	0.489	0.494	0.499	0.504	0.509	0.514	0.519	0.524	0.529	0.534
16	Abuhadriya	902	0.32	0.335	0.35	0.365	0.38	0.395	0.41	0.425	0.44	0.455	0.47	0.485	0.5	0.515	0.53	0.545
17	Abuhadriya	1071	0.2	0.25	0.252	0.254	0.256	0.263	0.27	0.277	0.284	0.291	0.298	0.305	0.312	0.319	0.326	0.333
18	Abuhadriya	1043	0.21	0.212	0.214	0.216	0.218	0.22	0.222	0.224	0.231	0.241	0.251	0.261	0.271	0.281	0.291	0.301
19	Manifah	1081	0.22	0.23	0.232	0.234	0.236	0.238	0.24	0.242	0.244	0.253	0.262	0.271	0.28	0.289	0.298	0.307
20	Manifah	1087	0.26	0.262	0.264	0.266	0.268	0.27	0.272	0.274	0.276	0.284	0.292	0.3	0.308	0.316	0.324	0.332
21	Manifah	1008	0.24	0.242	0.244	0.246	0.248	0.25	0.252	0.254	0.256	0.262	0.268	0.274	0.28	0.286	0.292	0.298
22	Manifah	1160	0.25	0.253	0.255	0.257	0.259	0.261	0.263	0.265	0.267	0.269	0.271	0.279	0.287	0.295	0.303	0.311
23	Manifah	1079	0.26	0.263	0.265	0.267	0.269	0.271	0.273	0.275	0.277	0.279	0.281	0.29	0.299	0.308	0.317	0.326
24	Abuhadriya	778	0.21	0.216	0.218	0.22	0.222	0.224	0.226	0.228	0.23	0.232	0.242	0.252	0.262	0.272	0.282	0.292
	Total in m^3/sec		6.605	6.823	6.884	6.945	7.006	7.078	7.15	7.222	7.299	7.449	7.645	7.848	8.051	8.254	8.457	8.66
	Total in Mm^3/Year		208.4	215.3	217.2	219.2	221.1	223.4	225.6	227.9	230.3	235.1	241.3	247.7	254.1	260.5	266.9	273.3

B.7: Extraction Rates in Khobar Aquifer for the Period (1995-2010) - Alternative II.

				Projected Extraction Rates (m^3/sec)															
SR	Name	NOD	WELL #	1995	1996	1997	1998	1999	2000	2001	2002	2003	2004	2005	2006	2007	2008	2009	2010
1		1135	S-414	0.05	0.05	0.05	0.05	0.05	0.05	0.05	0.05	0.05	0.05	0.05	0.05	0.05	0.05	0.05	0.05
2	Sarrar	396	WA-242	0.08	0.085	0.09	0.095	0.1	0.105	0.11	0.115	0.12	0.125	0.13	0.135	0.14	0.145	0.15	0.155
3	Sarrar	301	MI-3A	0.255	0.258	0.261	0.264	0.267	0.27	0.273	0.276	0.279	0.282	0.285	0.288	0.291	0.294	0.297	0.3
4	East of Sarr	493	MI-25A	0.006	0.007	0.007	0.007	0.007	0.007	0.008	0.008	0.008	0.008	0.008	0.009	0.009	0.009	0.009	0.009
5	Qulayyib	95	B17	0.022	0.023	0.024	0.025	0.026	0.027	0.027	0.028	0.029	0.03	0.031	0.031	0.032	0.033	0.034	0.035
6		747	Hu-35-A	0.067	0.072	0.077	0.082	0.087	0.092	0.097	0.102	0.107	0.112	0.117	0.122	0.127	0.132	0.137	0.142
7	Abuhadriya	902		0.054	0.056	0.058	0.06	0.062	0.064	0.066	0.068	0.07	0.072	0.074	0.076	0.078	0.08	0.082	0.084
8	Abuhadriya	1087	S-407	0.34	0.358	0.376	0.394	0.412	0.43	0.448	0.466	0.484	0.502	0.52	0.538	0.556	0.574	0.592	0.61
9	Abuhadriya	912	AHW-B08	0.33	0.345	0.36	0.375	0.39	0.405	0.42	0.435	0.45	0.465	0.48	0.495	0.51	0.525	0.54	0.555
10	Abuhadriya	933		0.12	0.13	0.14	0.15	0.16	0.17	0.18	0.19	0.2	0.21	0.22	0.23	0.24	0.25	0.26	0.27
11	Abuhadriya	963	B-11	0.22	0.23	0.24	0.25	0.26	0.27	0.28	0.29	0.3	0.31	0.32	0.33	0.34	0.35	0.36	0.37
12	Abuhadriya	944	B-9	0.12	0.13	0.14	0.15	0.16	0.17	0.18	0.19	0.2	0.21	0.22	0.23	0.24	0.25	0.26	0.27
13	Abuhadriya	848	S-222	0.26	0.27	0.28	0.29	0.3	0.31	0.32	0.33	0.34	0.35	0.36	0.37	0.38	0.39	0.4	0.41
14	Abuhadriya	1047	WA-504	0.054	0.055	0.056	0.057	0.058	0.059	0.06	0.061	0.062	0.063	0.064	0.065	0.066	0.067	0.068	0.069
15	Abuhadriya	932	B-18	0.2	0.21	0.22	0.23	0.24	0.25	0.26	0.27	0.28	0.29	0.3	0.31	0.32	0.33	0.34	0.35
16		1071	S-505	0.004	0.004	0.004	0.004	0.004	0.004	0.004	0.004	0.005	0.005	0.005	0.005	0.005	0.005	0.005	0.005
		Total in m^3/sec		2.182	2.283	2.383	2.483	2.583	2.683	2.783	2.883	2.984	3.084	3.184	3.284	3.384	3.484	3.584	3.684
		Total i	in Mm^3/year	68.86	72.05	75.2	78.36	81.51	84.67	87.82	90.98	94.17	97.32	100.5	103.6	106.8	109.9	113.1	116.3

B.8: Extraction Rates in Alat Aquifer for the Period (1995-2010) - Alternative II.

	Well Fields			Projected Extraction Rates (m^3/sec)															
No.	Name	Node	Well #	1995	1996	1997	1998	1999	2000	2001	2002	2003	2004	2005	2006	2007	2008	2009	2010
1		176	WA-347	0.055	0.056	0.057	0.058	0.059	0.06	0.061	0.062	0.063	0.064	0.065	0.066	0.067	0.068	0.069	0.07
2	North of Hanidh	188	WA-323	0.03	0.031	0.032	0.033	0.034	0.035	0.036	0.037	0.038	0.039	0.04	0.041	0.042	0.043	0.044	0.045
3	North of Hanidh	219	WA-327	0.02	0.02	0.02	0.02	0.02	0.021	0.021	0.021	0.021	0.021	0.021	0.021	0.021	0.021	0.021	0.022
4	North of Hanidh	284	WA-313	0.041	0.041	0.042	0.042	0.043	0.043	0.043	0.044	0.044	0.045	0.045	0.045	0.046	0.046	0.047	0.047
5	Sarrar	301	MI-4-N	0.021	0.022	0.023	0.024	0.025	0.026	0.027	0.028	0.029	0.03	0.031	0.032	0.033	0.034	0.035	0.036
6	Al-Wannan	320	WA-337	0.033	0.034	0.035	0.036	0.037	0.038	0.039	0.04	0.041	0.042	0.043	0.044	0.045	0.046	0.047	0.048
7	Sarrar	322	WA-329	0.02	0.021	0.022	0.023	0.024	0.025	0.026	0.027	0.028	0.029	0.03	0.031	0.032	0.033	0.034	0.035
8	Sarrar	370		0.033	0.035	0.037	0.039	0.041	0.043	0.045	0.047	0.049	0.051	0.053	0.055	0.057	0.059	0.061	0.063
9	North of Hanidh	382	WA-391	0.018	0.019	0.02	0.021	0.022	0.023	0.024	0.025	0.026	0.027	0.028	0.029	0.03	0.031	0.032	0.033
10	Sarrar	398	WA-251	0.087	0.093	0.099	0.105	0.111	0.117	0.123	0.129	0.135	0.141	0.147	0.153	0.159	0.165	0.171	0.177
11	Al-Wannan	417	WA-240	0.015	0.016	0.017	0.018	0.019	0.02	0.021	0.022	0.023	0.024	0.025	0.026	0.027	0.028	0.029	0.03
12	Ghanwa	547	WA-293	0.088	0.095	0.102	0.109	0.116	0.123	0.13	0.137	0.144	0.151	0.158	0.165	0.172	0.179	0.186	0.193
13	Ghanwa	551	WA-233	0.18	0.188	0.196	0.204	0.212	0.22	0.228	0.236	0.244	0.252	0.26	0.268	0.276	0.284	0.292	0.3
14	East of Hanidh	589		0.08	0.084	0.088	0.092	0.096	0.1	0.104	0.108	0.112	0.116	0.12	0.124	0.128	0.132	0.136	0.14
15	Al-Hinnah	677	WA-496	0.043	0.044	0.045	0.046	0.047	0.048	0.049	0.05	0.051	0.052	0.053	0.054	0.055	0.056	0.057	0.058
16		702	WA-277	0.033	0.035	0.037	0.039	0.041	0.043	0.045	0.047	0.049	0.051	0.053	0.055	0.057	0.059	0.061	0.063
17	Abuhadriya	745	HU-34-N	0.03	0.031	0.032	0.033	0.034	0.035	0.036	0.037	0.038	0.039	0.04	0.041	0.042	0.043	0.044	0.045
18		789	WA-314	0.029	0.03	0.031	0.032	0.033	0.034	0.035	0.036	0.037	0.038	0.039	0.04	0.041	0.042	0.043	0.044
19		953	WA-310	0.029	0.03	0.031	0.032	0.033	0.034	0.035	0.036	0.037	0.038	0.039	0.04	0.041	0.042	0.043	0.044
20	Abuhadriya	967	WA-315	0.02	0.022	0.024	0.026	0.028	0.03	0.032	0.034	0.036	0.038	0.04	0.042	0.044	0.046	0.048	0.05
	Total in m^3/sec			0.904	0.947	0.989	1.032	1.074	1.117	1.159	1.202	1.244	1.287	1.329	1.372	1.414	1.457	1.499	1.542
	Total in Mm^3/year			28.54	29.88	31.22	32.56	33.91	35.25	36.59	37.93	39.27	40.61	41.95	43.29	44.64	45.98	47.32	48.66

B.9: Extraction Rates in Neogene Aquifer for the Period (1995-2010) - Alternative II.

Bibliography

[1] Hasan M.H. Hydrogeochemistry of Alat and Khobar Aquifers in Eastern Saudi Arabia. Master's thesis, K.F.U.P.M, Dhahran, Saudi Arabia, December 1992.

[2] Evans. Hydrochemical investigation in the areas of Al-Qatif and Al-Hasa with some remarks on water samples from Wadi Al-Miyah and Wadi As Sah'ba near Haradh. In Al-Sayyari and Zottle, editors, *Quaternary Period in Saudi Arabia,*, 1978.

[3] Burdon D.J and Otkun G. Hydrogeological control of development in Saudi Arabia. *XXIII International Geological Congress.*, 12:145–153, 1968.

[4] Mercer J.W and Faust CR. Groundwater Modeling - an Overview. *Groundwater*, 18:267–296, 1980.

[5] Prickett T.A. Groundwater Computer Models - State of the Art. *Groundwater*, 16:167–173, 1979.

[6] Piggot A.R., Bobba A.G, and Xiang J. Inverse analysis implementation of the SUTRA groundwater model. *Groundwater*, 32:829–836, 1994.

[7] Naimi A.I. The groundwater of Northeastern Saudi Arabia. In Arabian American Oil Company, editor, *Fifth Arab Petroleum Congress*, Cairo, March 1965.

[8] Italconsult. Water and agricultural development studies for area IV, Eastern Province, Saudi Arabia. Technical report, Ministry of Agriculture and Water, Riyadh, Kingdom of Saudi Arabia, 1969.

[9] Bureau De Recherches Geologiques et Mineres (BRGM). Al-Hassa Development Project: Groundwater resources study and management program. Technical report, Ministry of Agriculture and Water, Riyadh, Kingdom of Saudi Arabia, 1977.

[10] Groundwater Development Consultants (G.D.C). Umm Er Radhuma Study: Bahrain Assignment. Technical report, Ministry of Agriculture and Water., Riyadh, Saudi Arabia, 1980.

[11] Bakiewicz W, Milne D.M, and Noori M. Hydrogeology of the Umm Er Radhuma Aquifer, Saudi Arabia, with reference to fossil gradients. *Q. J. Eng. Geol. London*, 15:105–126, 1982.

[12] ARAMCO Hydrology Division. Aramco Aquifer observation program in the Eastern Province. In *Development and Uses of Water Resources*, Riyadh, march 1982.

[13] Shampine W., Dincer T., and Noory M. An evaluation of isotope concentrations in the groundwater of Saudi Arabia. *International Journal of Water Resources Research.*, 1:22, 1982.

[14] Pike J.G. Groundwater resources development and the environment in the Central Region of the Arabian Gulf. *International Journal of Water Resources Research.*, 1:22, 1982.

[15] Al-layla R.I, Yazicigil H., and dejong R.L. Optimum development of Dammam aquifer in the Eastern province of Saudi Arabia. Technical report, General Directorate of Research Grants Programs, King Abdul Aziz City of Science and Technology. Riyadh, 1992.

[16] deJong R.L. Water balance of the Eastern Segment of the Arabian Peninsula. In *Problems of regional hydrology*, Germany, August 1984.

[17] Abderrahman W.A. Effect of groundwater use on the chemistry of spring water in Al-Hassa oasis. *J.K..A.U.: Earth Sci.*, 3:259–265, 1990.

[18] dejong R.L Al-layla R.I, Yazicigil H. Optimum development of Dammam aquifer in the Eastern province of Saudi arabia. Technical report, General directorate

of research grants programs, King Abdul Aziz city of Science and Technology. Riyadh, 1992.

[19] Rashiduddin M. Numerical modelling of Alat, Khobar and Umm Er Radhuma Aquifer System in Eastern Saudi Arabia. Master's thesis, K.F.U.P.M., Dhahran., 1988.

[20] Edgell H.S. Geological Framework of Saudi Arabia Groundwater Resources. In J.K.A.U: Earth Science, editor, *1st Saudi Symposium on Earth Science*, Jeddah, 1989.

[21] Abderrahman W.A and Rashiduddin M. Groundwater budgeting for a multi-aquifer system using numerical techniques. *Arab Gulf Journal Scientist Resources*, 12(1):29–40, 1994.

[22] Rajai S.A.A. Numerical simulation of groundwater in the Umm Er Radhuma Aquifer at SHADCO Project, Eastern Province. Master's thesis, K.F.U.P.M., Dhahran, 1992.

[23] Voss C.I. *Saturated-Unsaturated Transport: A finite-element simulation model for saturated-unsaturated, fluid density-dependent groundwater flow with energy transport or chemically reactive single-species solute transport.* National Center, Reston, Virginia, 1984.

[24] Job C. Hydrochemical investigation in the areas of Al-Qatif and Al-Hasa with some remarks on water samples from Wadi Al-Miyah and Wadi As Sah'ba near Haradh. In Al-Sayyari and Zottle, editors, *Quaternary Period in Saudi Arabia,*, 1978.

[25] Powers et.al. Sedimentary geology of Saudi Arabia. *USGS Prof. Paper*, 560-D, 1966.

[26] Seara J.L and Granda A. Interpretation of IP time domain/resistivity soundings for delineating saltwater intrusion in some coastal areas of the Northeast of Spain. *Geoexploration*, 24:153–167, 1987.

[27] Inman J.R. Resistivity inversion with ridge regression. *Geophysics*, 40:798–817, 1975.

[28] Burdon D.J. Hydrogeological conditions in the Middle East. *Q. J. Eng. Geol. London*, 15:71–82, 1982.

[29] Hem J.D. Study and interpretation of the chemical characteristics of natural water. Water-supply paper 1473, U.S.G.S, Reston, U.S.A, 1970. 2nd edition.

[30] Lohman S.W. Groundwater hydraulics. Geol. Survey Prof. paper 708, U.S.G.S, Washigton, U.S.A, 1972.

[31] Matthess G and Harvey JC. *The properties of groundwater.* John Wiley and Sons, Prentice-Hall, Inc.,, Englewood Cliffs, N.J. U.S.A., 1982.

Vita

- Ayaz Hasan
- Born in Karachi, Pakistan
- Received Master's degree in Geology from University of Karachi, Karachi, Pakistan in 1989.
- Completed Master's degree in Geology at King Fahd University of Petroleum and Minerals, Dhahran, Saudi Arabia in April, 1995.